CIGARETTE SMOKE EXPOSURE AND ITS IMPACT ON OVARIAN FOLLICLES

EXPOSURE TO CIGARETTE SMOKE AND ITS IMPACT ON THE OVARIAN FOLLICLE POPULATION: MECHANISMS OF FOLLICLE LOSS

By ANNE MARIE GANNON, B.Sc., M.Sc.

A Thesis Submitted to the School of Graduate Studies in Partial Fulfillment of the Requirements for the Degree of Doctor of Philosophy

DOCTOR OF PHILOSOPHY (2013) McMaster University
(Medical Sciences) Hamilton, Ontario

TITLE: Exposure to Cigarette Smoke and its Impact on the Ovarian Follicle Population: Mechanisms of Follicle Loss.

AUTHOR: Anne Marie Gannon, B.Sc., M.Sc., (University of Waterloo)

SUPERVISOR: Dr. Warren G. Foster

SUPERVISORY COMMITTEE: Dr. Martin R. Stämpfli
Dr. Charu Kaushic

NUMBER OF PAGES: xxiv, 278

Abstract

Cigarette smoking is a lifestyle behaviour associated with adverse reproductive health effects including premature exhaustion of the follicle population and premature menopause; however, the mechanisms mediating its effects on follicle loss are largely unexplored. Therefore, this thesis was undertaken to examine the effect of cigarette smoke, at concentrations representative of human exposure, on follicle loss in mouse ovaries and determine the underlying mechanisms mediating their loss. Cigarette smoke contains over 4,000 chemicals, many of which are involved in reactive oxygen species (ROS) generation and oxidative stress, which can lead to cell death. In the first study, we hypothesized that follicles exposed to cigarette smoke would be lost via apoptosis in a selective stage-dependent manner. Although apoptosis is a cell death pathway through which follicles are thought to die, the studies herein found no changes in apoptosis markers, despite increased follicle loss. Given these findings, we hypothesized that an alternative cell death mechanism was responsible for cigarette smoke-induced follicle loss. At the time, the relevance of autophagy, a novel ovarian cell death pathway, to granulosa cell death and toxicant-induced changes in ovarian function were unknown. Consistent with our earlier findings, we confirmed that apoptosis was not increased in treated ovaries, and further demonstrated increased oxidative stress, decreased antioxidant expression, and autophagy in treated ovaries. Finally, to further explore the mechanism controlling smoke-induced ovarian follicle loss, we tested the hypothesis that cigarette smoke exposure results in dysregulation of mitochondrial repair mechanisms, leading to follicle loss via autophagy-mediated granulosa cell death. Indeed, we

demonstrated that cigarette smoke exposure activates the autophagy cascade and alters mitochondrial dynamics. Taken together, these studies provide evidence that cigarette smoke causes significant follicle loss, a decrease in the cell's ability to cope with the production of ROS causing mitochondrial repair mechanisms to dysfunction, leading to autophagy-mediated follicle loss.

Acknowledgements

There are few who can count themselves as lucky as I am to have so many truly wonderful and supportive people in my life. First and foremost, I'd like to thank my supervisor and mentor, Dr. Warren Foster for affording me the opportunity to pursue my PhD and for believing in my abilities, even when I had my doubts. Like many in my shoes, I often questioned whether I belonged in research, especially when seemingly nothing went according to plan, but Warren always encouraged me to persevere and seek out alternative possibilities than the seemingly obvious ones. The day my project really took flight is a day I will always remember – it was like Christmas morning...but for scientists. We'd run into yet another brick wall and had decided to try one more experiment to see if we were missing something subtle. I expected yet another disappointing negative result. Boy was I wrong! I ran down the hall to Warren's office to drag him to see the images I was seeing and, to my delight, he was as excited as I was. It was the kind of day every researcher should have – the kind of day that reminds you of why you went into research in the first place and why you'll endure the countless disappointments of failed experiments and negative results for just one more day like this one. It was glorious!

I'd also like to thank my excellent committee members, Drs. Charu Kaushic, Martin Stämpfli and David Andrews for their counsel and suggestions throughout my studies. Dr. Kaushic's questions during committee meetings were always thought-provoking and challenging and I often left these meetings with new insight. I would especially like to thank Dr. Stämpfli for being so compassionate and supportive, and to whom I always felt

I could turn for advice. His love of life and science are infectious. Although not a member of my committee, Dr. Alison Holloway deserves a big thank you for her advice and support.

This thesis is not the result of a singular effort; I owe many thanks to the people who assisted me in the course of my PhD. I would especially like to acknowledge the technical expertise of Joanna Kasinska, Sussan Kianpour, and Dr. Bing Zhang.

I am forever indebted to my friends and colleagues who made my time at McMaster so enjoyable and made reproductive biology entertaining. A special thank you to Drs. Heather Cameron, Rocio Monroy, Kyle Stephenson, and JC Sadeu for their support and friendship over the years. I would also like to thank my partner in crime, Jocelyn Wessels for enduring the last year of my PhD with grace and good humour and for keeping me sane while writing. Glad I could repay you with a coffee addiction!

Finally, I would like to thank my family and my wonderful friends, who have always been there encouraging me and supporting my dreams. Mom and Dad, thank you for instilling in me the confidence to shoot for the moon and believing that I could reach it. Your support gave me the confidence and strength that I alone could never have hoped for. To my sisters – my lifelong allies and friends – thank you for being my personal cheerleaders. Lisa Marie and Kerin, thank you for your endless love and support. Last, but not least, Todd and Aidan, without your love and support, I could never have done this – you two are my true north. Thank you.

Table of Contents

List of Figures

Chapter 1

Chapter 2

Chapter 3

Chapter 4

Appendix I

Appendix II

List of Tables

Chapter 1

Chapter 3

List of Abbreviations and Symbols

3,4-DMF	3,4-dimethoxy flavone
3-MA	3-methyladenine
8-OHdG	8-hydroxydeoxyguanosine
ACTB	beta actin
AFC	antral follicle count
ADP	adenosine diphosphate
AhR	aryl hydrocarbon receptor
AhR^d	AhR deletion mutant
AIF	apoptosis inducing factor
AMH	anti-Müllerian hormone
ANOVA	analysis of variance
Apaf1	apoptosis protease activating factor 1
ARKO	aryl hydrocarbon receptor knockout
ARNT	aryl hydrocarbon receptor nuclear translocator
As_2O_3	arsenic trioxide
Atg	autophagy
ATP	adenosine triphosphate
BAK	bcl2-antagonist/killer
BaP	benzo(a)pyrene
BAX	bcl2-associated x
BCL2	B cell leukemia/lymphoma 2
BCL2L1	B cell leukemia/lymphoma 2 like protein 1 (BCLXL)
BECN1	beclin 1
BH	bcl2 homology
bHLH-PAS	basic helix-loop-helix-Per-Arnt-Sim
BID	BH3 interacting domain
BIR	baculovirus inhibitor of apoptosis repeat
BMI	body mass index
BMP	bone morphogenetic protein
BMPRIB	bone morphogenetic protein receptor I B

BMPRII	bone morphogenetic protein receptor II
BPDE	benzo(a)pyrene diol epoxide
BSA	bovine serum albumin
Ca^{2+}	calcium
CASP	caspase
cDNA	complimentary deoxyribonucleic acid
CHOP	CCAAT/enhancer binding protein-homologous protein
cIAP	cellular inhibitor of apoptosis
CO	carbon monoxide
CO_2	carbon dioxide
COC	cumulus oocyte complex
COX	cyclooxygenase
CS	cigarette smoke
CSC	cigarette smoke condensate
CSE	cigarette smoke extract
CT	crossing threshold
CYP	cytochrome p450
DAB	diaminobenzidine
DED	death effector domain
DMBA	7,12-dimethylbenzanthracene
DRE	dioxin response element
Drp-1	dynamin related protein 1
E_2	estradiol
EDTA	ethylenediaminetetraacetic acid
ELISA	enzyme linked immunosorbent assay
ER	endoplasmic reticulum
ET	environmental toxicant
ETC	electron transport chain
FADD	fas-associated death domain
FasL	fas ligand
FLIP	FLICE- inhibitory protein
FSH	follicle stimulating hormone

G_1	gap 1
G_2	gap 2
GAPDH	glyceraldehyde 3-phosphate dehydrogenase
GDF	growth and differentiation factor
GFP	green fluorescent protein
GFP-LC3	GFP fused to LC3
Gn	gonadotropin
GnRH	gonadotropin releasing hormone
GSH	glutathione
GST	glutathione S-transferase
GTP	guanosine triphosphate
GTPase	guanosine triphosphatase
H&E	haematoxylin and eosin
H_2O_2	hydrogen peroxide
HBSS	Hank's balanced salt solution
hCG	human chorionic gonadotropin
Hrk	*harakiri*
HSE	heat shock element
HSF	heat shock factor
HSP	heat shock protein
IAP	inhibitor of apoptosis
ICAD	inhibitor of caspase-activated DNase
IgG	immunoglobulin G
IHC	immunohistochemistry
IM	inner membrane
IP_3	inositol 1,4,5-triphosphate
IP_3R	IP_3 receptor
IVF	*in vitro* fertilization
JNK	jun kinase
KCl	potassium chloride
KDEL	Lys-Asp-Glu-Leu
KH_2PO_4	potassium hydrogen phosphate

KitL	kit ligand
LCM	laser capture microdissection
LH	luteinizing hormone
Lox1	lectin-like oxidized low-density receptor
M	metaphase
Map1lc3	microtubule-associated protein 1 light chain 3
MEF	mouse embryonic fibroblast
MES	2-(N-morpholino)ethanesulphonic acid
MFFR	MitoFluor far red
MFN	mitofusin
MMP	mitochondrial membrane potential
Mn	manganese
MPA	metaphosphoric acid
mRNA	messenger ribonucleic acid
mtDNA	mitochondrial deoxyribonucleic acid
mTOR	mammalian target of rapamycin
Na^+/K^+ ATPase	sodium/potassium adenosine triphosphatase
Na_3PO_4	sodium phosphate
NaCl	sodium chloride
NOBOX	newborn ovary homeobox
$O_2^{\bullet-}$	superoxide
$OH^{\bullet-}$	hydroxyl free radical
OM	outer membrane
OOSP	oocyte specific protein
OPA1	optic atrophy 1
OXPHOS	oxidative phosphorylation
PAH	polycyclic aromatic hydrocarbon
PARK2	parkin
PCB	polychlorinated biphenyl
PCD	programmed cell death
PCOS	polycystic ovarian syndrome
PCR	polymerase chain reaction

PE	phosphatidylethanolamine
PI3K	class III phosphatidylinositol 3-kinase
PID	pelvic inflammatory disease
PINK1	PTEN-induced kinase 1
PKA	protein kinase A
PMSF	phenylmethanesulphonyl fluoride
POF	premature ovarian failure
PVDF	polyvinylidene difluoride
RFP	red fluorescent protein
RFP-ER	RFP tagged with calreticulin and KDEL sequences
RIPA	radioimmunoprecipitation assay
ROS	reactive oxygen species
RT	room temperature
RT-PCR	reverse transcriptase-polymerase chain reaction
S	synthesis
SDS	sodium dodecyl sulphate
SDS-PAGE	sodium dodecyl sulphate polyacrylamide gel electrophoresis
SEM	standard error of the mean
sHSP	small heat shock protein
siRNA	small interfering ribonucleic acid
SOD	superoxide dismutase
STI	sexually transmitted infection
TAE	Tris-acetic acid-EDTA
tBID	truncated bid
TBS	tris buffered saline
TBST	tris buffered saline with Tween 20
TCDD	2,3,7,8-tetrachlorodibenzo-*p*-dioxin
TCE	trichloroethylene
TEM	transmission electron microscopy
TGFβ	transforming growth factor beta
TMRM	tetramethylrhodamine methylester
TNF	tumor necrosis factor

TNFR	tumor necrosis factor receptor
TRAF	tumor necrosis factor receptor associated factor
TUNEL	terminal deoxynucleotidyl transferase dUTP nick end labelling
UPR	unfolded protein response
UV	ultraviolet
VCD	4-vinylcyclohexene diepoxide
VCH	4-vinylcyclohexene
WT	wild type
XIAP	X-linked inhibitor of apoptosis
XRE	xenobiotic response element

Format and Organization of Thesis

This thesis was prepared in the sandwich thesis format as described in the School of Graduate Studies' Guide for the Preparation of Master's and Doctoral Theses. This thesis is comprised of three original research papers (Chapters 2-4), preceded by a general introduction and followed by a general discussion. All papers have been previously published in peer reviewed journals with the candidate as first author.

Declaration of Academic Achievement

Chapter 2

Publication:

Mulligan Tuttle A, Stämpfli M, Foster WG. Cigarette smoke causes follicle loss in mice ovaries at concentrations representative of human exposure. *Human Reproduction*. 2009. 1(1):1-8.

Contribution:

This study was designed by WG Foster and MR Stämpfli. Animal experiments were coordinated by AM Gannon. *In vivo* cigarette smoke exposure was conducted by Dr. Stämpfli's technician. *In vitro* experiments were coordinated and conducted by AM Gannon. All tissue collection, preparation and analyses were conducted by AM Gannon. Manuscript preparation was completed by AM Gannon.

Chapter 3

Publication:

Gannon AM, Stämpfli MR, Foster WG. Cigarette smoke exposure leads to follicle loss via an alternative ovarian cell death pathway in a mouse model. *Toxicological Sciences*. 2012. 125(1):274-284.

Contribution:

This study was designed by WG Foster and AM Gannon. Animal experiments were coordinated by AM Gannon and carried out by Dr. Stämpfli's technician. All tissue collection, preparation and analyses were conducted by AM Gannon. Laboratory

experiments were designed and carried out by AM Gannon. Manuscript preparation was completed by AM Gannon.

Chapter 4

Publication:

Gannon AM, Stämpfli MR, Foster WG. Cigarette smoke exposure elicits increased autophagy and dysregulation of mitochondrial dynamics in murine granulosa cells. *Biology of Reproduction*. 2013. 88(3):63, 1-11.

Contribution:

This study was designed by WG Foster and AM Gannon. Animal experiments were coordinated by AM Gannon and carried out by Dr. Stämpfli's technician. All tissue collection, preparation and analyses were conducted by AM Gannon. Laboratory experiments were designed and carried out by AM Gannon. Manuscript preparation was completed by AM Gannon.

Chapter 1

Introduction

Infertility affects millions worldwide. Although numerous sources of infertility have been identified, many otherwise healthy couples of childbearing age experience infertility for unknown reasons. Infertility is defined as the inability to achieve a clinical pregnancy following 12 or more months of regular unprotected sexual intercourse [1;2]. Premature follicle loss has been identified as a possible causative factor for infertility, which has been linked with exposure to environmental toxicants. However, the mechanisms of action are not known. Cigarette smoke, in particular, has been found to affect both male and female fertility via adverse effects on testicular function, uterine receptivity and ovarian function. In women, cigarette smoke is a documented reproductive toxicant that depletes ovarian follicle reserve and impairs uterine receptivity [3]. Delayed conception [4;5], decreased success in assisted reproductive technologies [6;7] and premature ovarian failure [8] have all been reported in female smokers compared with non-smokers. Smoking cessation programs have proven ineffective for some and damage may already be done in those that begin smoking as teenagers and young adults. Therefore, it is imperative that the mechanisms of action underlying the toxic effects of cigarette smoke on fertility are elucidated.

1.1 Infertility

1.1.1 Prevalence

Worldwide, infertility touches the lives of approximately 15% of reproductive-aged couples [9;10]. In the United States alone, approximately 6.1 million (~10%) American women between the ages of 15 and 44 experience infertility (Centers for Disease Control and Prevention). Similar numbers are seen in Canada, where the prevalence of women experiencing infertility is on the rise, up from 7% in 1992 to 13.7% in 2010 [10].

1.1.2 Impact

Infertility can have multiple health effects on a couple. The emotional, psychological, financial and health consequences of infertility are well-documented. According to the Harvard Mental Health Letter [11], the grief associated with infertility exacts a psychological toll, often similar to that of a person mourning the loss of a family member. For women, the inability to become pregnant is often coupled with feelings of guilt and inadequacy given the "natural" role of woman as child-bearer instilled at an early age [1]. Couples experiencing infertility often withdraw from social situations involving children and/or friends with children to insulate themselves from the heartache associated with remaining childless [11]. Additionally, the financial burden that fertility treatments place on a couple is significant. In the US, between $4 and 6 billion is spent annually on infertility treatments (extrapolated from data obtained in [12]).

1.1.3 Aetiology

Infertility is rooted in a number of different causes, many of which are physiological or due to lifestyle factors but others remain unexplained. Of the many different aetiologies of infertility, male factor infertility is indicated in approximately one third of cases, the remaining two thirds being diagnosed as female factor or unexplained infertility [2]. In ten to twenty percent of cases, both male and female factors are identified [2]. In 30% of cases where female infertility is the cause, anovulation (where the oocyte is not released from the ovary) is the underlying cause. In the remaining cases, tubal obstruction, pelvic pathologies and immunologic factors make up the majority of cases with unexplained infertility accounting for between 10 and 20% of cases [2;11].

The physiological factors implicated in infertility include disorders of the ovary, thyroid and pituitary glands, and various pathologies of the pelvic region. Ovarian disorders contributing to infertility include polycystic ovary syndrome (PCOS), advanced maternal age and premature ovarian failure (POF). PCOS is a condition that typically presents with multiple small cysts in the ovaries, abnormally high levels of androgens, irregular menstrual cycles and hirsutism (excessive hair growth in areas where hair growth does not normally occur) [13]. It is the most common cause of anovulatory infertility.

Although there is no strict definition of what constitutes advanced maternal age, it is generally accepted that infertility becomes more pronounced after age 35. The ovary is

endowed with a finite number of eggs at birth and this number gradually declines during the reproductive lifespan of every woman. As a woman ages, the number of eggs she possesses declines at a predictable rate (Figure 1) and after age 35, this rate accelerates until the pool of quiescent follicles (those housing the least developed oocytes) is exhausted at menopause [14]. As such, the older the woman, the fewer follicles left in the ovary and therefore the lower the chance of becoming pregnant. Conversely, POF refers to the exhaustion of the ovarian reserve of follicles coupled with elevated gonadotropin (Gn) levels earlier than would be expected based on chronological age [15;16]. POF can occur as a result of a number of insults to the body including chromosomal disorders, autoimmune disorders, radiation or chemotherapy and a number of chemical exposures, including cigarette smoke [15-19].

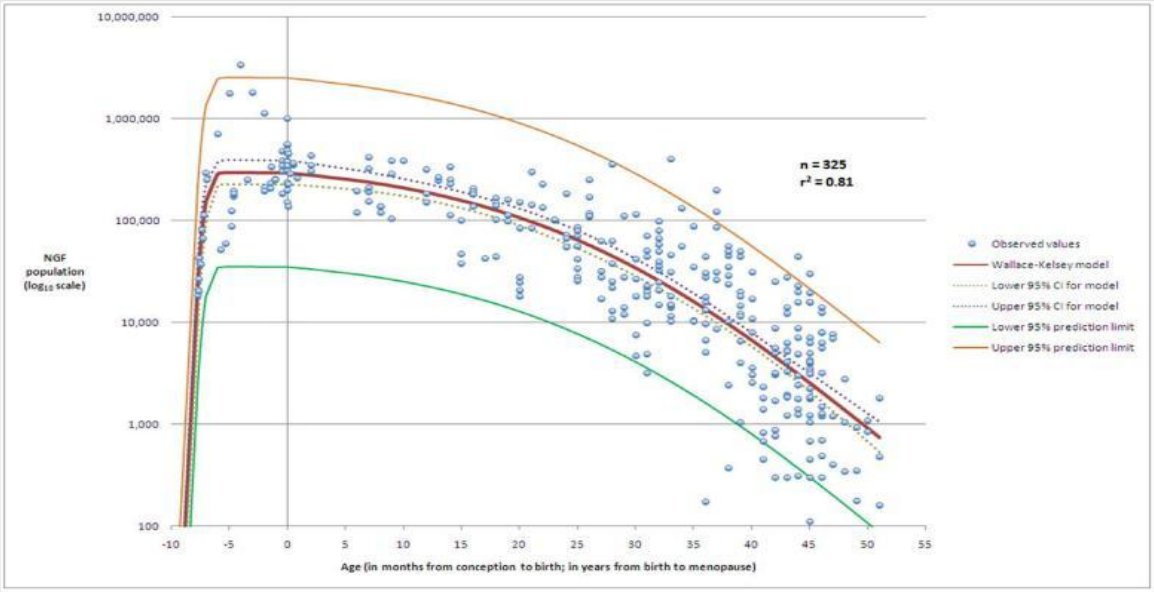

Figure 1: The Wallace-Kelsey model of ovarian reserve.
The model for the establishment of the non-growing follicle population from conception through the subsequent decline until age at menopause. The figure shows the dataset (n = 325), the model, the 95% prediction limits of the model, and the 95% confidence interval for the model. Adapted from [14].

Finally, lifestyle factors affecting fertility include, but are not restricted to, delayed family planning for the pursuit of education and career ambitions, obesity, excessive exercise, caffeine and alcohol consumption, exposure to environmental toxicants, and cigarette smoking. In recent decades, couples have been opting to postpone starting a family until later in their reproductive years, a time when natural fertility is in a steady decline. Increasing numbers of women pursuing higher education and career ambitions are common reasons in women's decision to delay starting a family [19;20]. The association between the exhaustion of ovarian follicle reserve and age has been well-documented. Consequently, many of these women are faced with unexpected problems related to a reduced ovarian reserve, often resulting in the need to employ the use of artificial reproductive technologies. Obesity has also been linked to infertility irrespective of ovulatory function; although its role in infertility has not been clearly elucidated. At the other end of the spectrum, excessive exercise and weight loss has been suggested to alter the height to weight ratio and the critical fat mass necessary to initiate ovulatory cycles is not met in women who engage in strenuous exercise and maintain a low body mass index (BMI) [21-26]. Finally, excessive caffeine and alcohol consumption as well as drug use and exposure to cigarette smoke have also been linked with decreased rates of pregnancy and increased adverse fetal effects [27;28]. Of the documented causes of infertility, I have chosen cigarette smoke as the model toxicant for my studies in part because it is associated with dysfunction of every part of the female reproductive tract but also because there is an element of choice and thus it is a potentially modifiable cause of infertility.

1.2 Cigarette Smoking

Cigarette smoking is the single most preventable cause of death in our society. The adverse health effects of smoking are vast and include aneurysm, cardiovascular disease, stroke, cancer, and chronic obstructive pulmonary disease, to name but a few. Of the top ten leading causes of death in high income countries worldwide, smoking-related diseases occupy the top three spots [29]. This is true in both the US and Canada, according to the Centers for Disease Control and Prevention and Statistics Canada, respectively [30;31].

1.2.1 Prevalence

Although fewer Canadians are smoking today, a survey on tobacco use in Canada revealed that 14% of households reported that at least one person smoked inside the home daily [32]. In the Canadian Tobacco Use Monitoring Survey, 17% of female respondents report being current smokers, consuming an average of 13.8 cigarettes/day [32]. Alarmingly young women in their reproductive prime are the fastest growing population of smokers. In Canada, 18.5% of girls aged 18-19 smoke [33] and in southwestern Ontario, 36.2% of teenage girls smoke [34]. This population has historically been the most at risk for taking up smoking and the number of active smokers in this age group continues to be high despite aggressive anti-smoking campaigns and implementation of warning label legislation, suggesting that our current approaches are not effective in this population. What is perhaps most troubling about this is that these are the women who, in ten to fifteen years, will be populating fertility clinics.

1.2.2 Impact on Fertility

Cigarette smoking is a documented reproductive toxicant that has been correlated with earlier age at menopause and ovarian follicle loss. It is well documented that smoking depletes ovarian follicle reserve and impairs uterine receptivity [3]. Smokers report a longer time to pregnancy, often require higher doses of Gn during ovarian stimulation protocols, have fewer oocytes retrieved, lower implantation rates and undergo on average twice as many *in vitro* fertilization (IVF) cycles before conceiving than do non-smokers [3;35-37]. Table 1 summarizes many of the adverse effects that have been reported in female smokers compared with non-smokers. While most of these adverse effects have been confirmed by multiple studies, others report conflicting outcomes with respect to fertilization. Based on population studies, there is a significant correlation between number of cigarettes smoked daily and decreased fertility, and ex-smokers have similar levels of fertility relative to non-smokers [37;38]. While cigarette smoking has been attributed to causing adverse effects on female reproductive function, including ovarian follicle loss, the underlying mechanisms regulating these phenomena are unknown.

Table 1: Clinical effects of cigarette smoke on reproductive function.

Adverse Effects Reported by Smokers	Reference
Fewer healthy oocytes retrieved	[39-41]
↓ Fecundability	[42]
↓ Ovarian sensitivity	[43]
↓ Ovarian reserve	[44;45]
↓ Implantation rates	[28]
Delayed conception	[46]
↑ Ectopic pregnancy	[47;48]
↑,↓or ↔ Fertilization	[40;41;47;48]
↓ Pregnancy rates	[28;47]
↓ Uterine receptivity	[3]
Early placentation defects	[46;49]
↑ Spontaneous abortion	[47]
In utero growth restriction	[50]
↑ Still birth	[51]
↑ Preterm birth	[46]
↓ Live birth rate	[39;47]
Low birth weight	[46;51]
↑ Infant death	[51]
Shorter menstrual cycle	[52]
Premature ovarian failure	[53]

Young women in their reproductive prime are the fastest growing population of smokers. This trend, coupled with the fact that many women are choosing to postpone starting their families until after education and career ambitions are achieved [54], an increased demand for IVF services is occurring. In earlier animal studies, benzo(a)pyrene (BaP), a constituent of cigarette smoke, was found to selectively destroy the follicles in the resting pool [55]. This finding led the researchers to hypothesize that a similar exhaustion of the resting pool was occurring in women who smoke, leading to premature menopause. Studies have revealed that women exposed to cigarette smoke (whether it was mainstream or sidestream smoke) had greatly decreased implantation rates (12-12.6% for those exposed to cigarette smoke vs. 25% for non-smokers) and pregnancy rates (19.4-

20% for those exposed to cigarette smoke vs. 48.3% for non-smokers) [28]. Our laboratory has also found that BaP is detectable in the serum and follicular fluid of women who smoke or are exposed to cigarette smoke and that treatment with BaP impairs cumulus expansion in isolated rat and mouse follicle culture experiments [56-58].

Cigarette smoking is widely accepted to have a negative effect on fertility and is associated with decreased fecundity. The cause of this decreased fertility and shortened reproductive lifespan, however, is not known. The fundamentally accepted dogma is that cigarette smoke exposure causes the production of reactive oxygen species (ROS), leading to mitochondrial stress and ultimately cell death via apoptosis. It is thought that a stage-dependent destruction of primordial follicles occurs thereby decreasing the ovarian reserve, ultimately shortening reproductive life [3;59]. Targeted primordial follicle destruction is considered to be the most devastating effect of cigarette smoking on reproductive function, the effects of which are not detected until years after the exposure, often after ovarian failure is well established [60]. Numerous studies have shown that exposure to environmental toxicants results in the destruction of the follicle population in a stage-specific manner [56;61-68]. While premature follicle loss has been identified as a causative factor for infertility, the mechanisms underlying this follicle loss are not well-understood. Of the numerous environmental toxicants and lifestyle factors known to affect fertility and ovarian function studied to date, cigarette smoking may perhaps be the single most clinically-relevant and preventable toxic exposure in women, making it an ideal target for infertility prevention [27].

1.3 The Ovary

The ovary is a complex and plastic organ whose function is to produce fertilizable oocytes and to produce and secrete the steroid hormones required to ready the female reproductive tract for fertilization of an oocyte and the establishment of a successful pregnancy [69;70]. During fetal development (in humans), or shortly after birth (in mice), the ovaries are endowed with millions of germ cells enveloped by pre-granulosa cells. Barring the existence of ovarian stem cells [71-79], the existence of which is hotly debated, this finite number of primordial follicles is the entire complement of gametes the ovaries will ever possess. By birth, only about 1 million of these follicles remain [80], the vast majority of which will be lost through a process known as atresia. This number will gradually decrease during childhood until the onset of puberty, when approximately 500,000 follicles remain in the primordial follicle pool. Of the estimated 500,000 follicles present at menarche, only about 400 of these will reach the pre-ovulatory stage and be ovulated [70;81] prior to exhaustion of the ovarian follicle reserve and menopause. The ovarian reserve is the number of primordial follicles remaining in the ovary that have not yet been selected to mature [54;80;82]. This process is tightly regulated and can easily be disrupted by outside influences.

1.3.1 Function

The ovary is a dynamic organ that, with each cycle, undergoes extensive cell proliferation, inflammation, tissue remodelling, angiogenesis, and removal of damaged cells or cells whose function is no longer needed. During each cycle, follicles are selected

to leave the resting pool and enter the growing pool of follicles through the process of folliculogenesis (Figure 2). A follicle consists of a meiotically-arrested oocyte surrounded by one or more layers of somatic cells called granulosa cells whose function is to support the growth of the oocyte throughout its development. Follicles progress through development from the primordial follicle stage, the most immature stage, through to the Graafian follicle, resulting in ovulation. At ovulation, the oocyte is released from the follicle into the Fallopian tube where it will make its way into the uterus. Following ovulation, the granulosa cells remaining in the ovary will form the corpus luteum, a structure of luteinized cells that produce progesterone and, in the event of fertilization and implantation, will nourish the embryo until the placenta is fully functional. In the absence of fertilization, the corpus luteum regresses and is reabsorbed by the ovarian stroma and another cycle of follicle maturation will ensue. The process of follicular maturation, ovulation and resorption occurs up to 400 times in a woman's reproductive lifespan prior to the cessation of ovarian function at menopause [70;81]. In the ovary, tightly controlled follicle development is essential in maintaining fertility.

1.3.2 Ovarian Failure

Ovarian failure, or menopause, begins 5-10 years prior to the onset of amenorrhea or cessation of menses and typically occurs when there are fewer than 1,000 follicles remaining in the ovary. In the years leading up to the menopause (typically defined as 12 months of anovulation), changes in numerous parameters make it possible to identify when menopause is imminent. First, menstrual cycle length, although already variable

within healthy young women with demonstrated fertility varies dramatically with bleeding irregularities and wide ranges in the length of the follicular phase [83]. Additional measures currently used to identify impending ovarian failure include the biophysical parameter, antral follicle count (AFC), and biochemical parameters, which include serum follicle stimulating hormone (FSH), estradiol (E_2), luteinizing hormone (LH) and inhibin B levels [61;84-90]. These markers are cycle-dependent and subject to variability depending on the stage of the cycle in which they are measured [90]. In recent years, another hormone, anti-Müllerian hormone (AMH) has been correlated with predicting impending ovarian failure. Unlike other markers of reproductive aging, AMH shows a decline in circulating levels long before there are other signs of impending ovarian failure [61;85;86;88;91]. According to some, AMH concentration is a reliable indicator of the ovarian reserve in aging women, correlating positively with AFC and inhibin B levels [86;87;91-93]; however, changes in serum AMH concentration are not a direct measure of the ovarian reserve but are reflective of the number of follicles in the growing pool.

1.3.3 Folliculogenesis

The basic functional unit of the ovary is the follicle. It consists of an oocyte surrounded by granulosa and theca cells. Follicular growth, or folliculogenesis, can be divided into three discrete stages based chiefly on follicle maturity and its responsiveness to gonadotropins: 1) Gn-independent (primordial, primary, and small secondary stage follicles), 2) Gn-responsive (pre-antral to early antral stage follicles), and 3) Gn-

dependent (large antral stage follicles) [94;95]. The selection of primordial follicles for recruitment into the growing pool of follicles is not well-understood owing primarily to the fact that isolation of these very small follicles is technically difficult. What is known is that primordial follicle initiation is under inhibitory control from larger follicles, although it is as yet unclear whether there is one or multiple factors acting in an inhibitory fashion to control follicle recruitment [95]. One of the most likely candidates for this factor is AMH, which is expressed in early stage follicles and has been identified as an inhibitory factor in follicle recruitment [96]. Like other members of the transforming growth factor beta (TGFβ) superfamily, AMH acts through a signalling pathway consisting of two serine/threonine kinase single membrane spanning receptors, type I and type II. The type II receptor imparts ligand binding specificity, while the type I receptor is activated upon binding with the type II receptor and subsequently mediates the downstream signalling of Smad proteins. AMH plays an inhibitory role in two critical selection stages of follicle development: it prevents recruitment of primordial follicles from the resting pool [97] and it decreases the responsiveness of preantral follicles to FSH [69;82;89;93;96;98-100]. AMH administration *in vitro* reduces the number of growing follicles by a factor of two [97], while deletion of the *Amh* gene results in premature depletion of the primordial follicle pool altogether [101]. AMH is expressed in follicles that have been selected for development from the primordial follicle pool and continues to be expressed in healthy growing follicles until such time as they are large enough to be selected for dominance by FSH. Expression of AMH in granulosa cells decreases the sensitivity of the follicle to FSH stimulation such that healthy growing

follicles expressing less AMH are more responsive to FSH stimulation and become selected for dominance [99].

Once they have entered the growing pool, follicles begin to express and respond to a variety of growth factors, most of which are intraovarian regulators including growth factors, cytokines and steroids. Each individual component of the follicle, the oocyte, granulosa and theca cells all express and respond to different factors, which can act in an autocrine and/or paracrine fashion, depending on the expression of receptors present in the cell membrane. Table 2 summarizes the growth factors involved in follicle recruitment, development and ovulation and the species in which they have been identified and characterized. Beginning at the primary follicle stage, the oocyte begins to express and secrete growth and differentiation factor (GDF) 9, bone morphogenetic protein (BMP) 6, BMP15, and oocyte specific protein (OOSP) 1 [98]. GDF9 is a member of the TGFβ superfamily, as are BMP15 (GDF9B) and activin. GDF9 is only expressed in the oocytes of follicles [102-104] in mammalian ovaries. GDF9 mRNA and protein are detectable in the oocyte at all stages of folliculogenesis, with the exception of primordial follicles [103;105;106]. Like AMH, GDF9 signals through a serine/threonine kinase signalling cascade that is mediated by type I and type II receptors. GDF9 is known to signal through the BMP/GDF pathway, binding to bone morphogenetic protein receptor II (BMPRII) [104]. BMPRII, along with a number of type I receptors, are present in the cell membranes of granulosa cells. The known functions of GDF9 are many: promotion of granulosa cell proliferation [104;107], cumulus expansion [102;104;107], preantral

follicle growth [104;106;107], and suppression of FSH-induced LH receptor content [102;107]. While GDF9 is expressed in and secreted by the oocyte, its actions are on the granulosa cells surrounding the oocyte. GDF9 has been implicated in stimulating the growth of granulosa cells [105;108], particularly in establishing the characteristic properties of cumulus and mural granulosa cells dependent upon their distance from the oocyte [109]. It has been shown to be essential in the development of follicles past the primordial stage. Mice lacking the gene are sterile and have ovaries that contain follicles arrested at the primary stage [102;104-107;110], often with oocytes that are much larger than those normally found in the primary follicles of wild type (WT) mice [106]. Despite knowing what processes GDF9 is involved in, few downstream targets of GDF9 have been elucidated. To date, GDF9 is known to regulate *Has2* and *Cox2*, genes involved in late follicle development and ovulation [106]. It is unlikely that these are the only targets of GDF9 function. Numerous studies have shown that communication between the oocyte and granulosa cells is important for the proper growth of the follicle. Cumulus expansion, for example, will not occur in the absence of an oocyte. Another study points to the oocyte as a regulator of *Amh* expression in granulosa cells [98]. In this study, the oocyte was required to enhance expression of *Amh*, suggesting that the oocyte must secrete a factor that works to regulate *Amh* gene expression. In fetal ovaries exposed to gamma radiation, most of the follicles present were at the primary stage lacking any *Amh* or *BmprII* gene expression, but with robust *Gdf9* expression [111], suggesting a lack of communication between the oocyte and granulosa cells.

BMP15 is also expressed by the oocyte and is a potent regulator of granulosa cell proliferation and differentiation and a modulator of FSH action [112], although BMP15 itself is FSH-independent. BMP15, like GDF9, has been detected in the oocytes of all stages of follicle development; but unlike GDF9, its expression is detectable in primordial follicles, suggesting a role in inhibition of follicle recruitment as well as in growth and development [112]. As with most members of the TGFβ superfamily, BMP15 also signals through the serine/threonine kinase receptor complex. In the case of BMP15, it has been shown to signal through the BMPRIB type I receptor [113], which is found on both oocyte and granulosa cell membranes [114]. Studies in sheep and mice have helped to elucidate the role of BMP15 in the ovary and regulation of fertility. While both BMP15 and GDF9 have been identified as being essential for normal follicular development in numerous lines of sheep [110;112;115], BMP15 was shown not to be essential in mice, as knockout mice are fertile only exhibiting signs of subfertility with ovulation and oocyte fertilization being impaired [116;117]. It has been further shown that terminal oocyte-cumulus maturation is impaired in these mice, thus impairing fertilization [116;117]. In sheep, inactivation of both *Bmp15* genes results in sterility and primary ovarian insufficiency [115;118]; however, when only one *Bmp15* gene is mutated, ewes are fertile and have increased ovulation rates leading to accelerated ovarian follicle depletion and a higher incidence of twin and triplet births [118]. Finally, BMP15 appears to act along with GDF9 in promoting granulosa cell proliferation [112;119] and regulating steroidogenesis, with GDF9 interfering with human chorionic gonadotropin binding [102] and BMP15 suppressing the gene expression of the FSH receptor [120].

The transition from pre-antral to early antral follicle marks the Gn-responsive stage [94]. At this stage of development, the follicle does not require the presence of gonadotropins to grow but the presence of FSH is stimulatory [94] and influences the rate of pre-antral follicle development [95]. The pituitary gonadotropins, FSH and LH, are released and exert their effects on ovarian somatic cells via their respective cell membrane-bound receptors. FSH receptors are expressed in the membranes of granulosa cells of growing follicles beginning at the primary stage and continue through to the pre-ovulatory follicle [121]. Meanwhile, LH receptors can be found in the membranes of theca interna cells of antral through pre-ovulatory follicles and in the membranes of granulosa cells of large estrogenic antral follicles [122;123]. The transition from Gn-responsive to Gn-dependent occurs somewhere during antral follicle growth; however, definitive evidence of when this occurs is not available and the mechanistic steps involved is unresolved. *In vitro* studies showed that sheep antral follicles with larger diameters are more capable of growth in the presence of physiological FSH concentrations than are smaller diameter follicles [124], a time corresponding to the detection of LH receptor expression in these follicles [121].

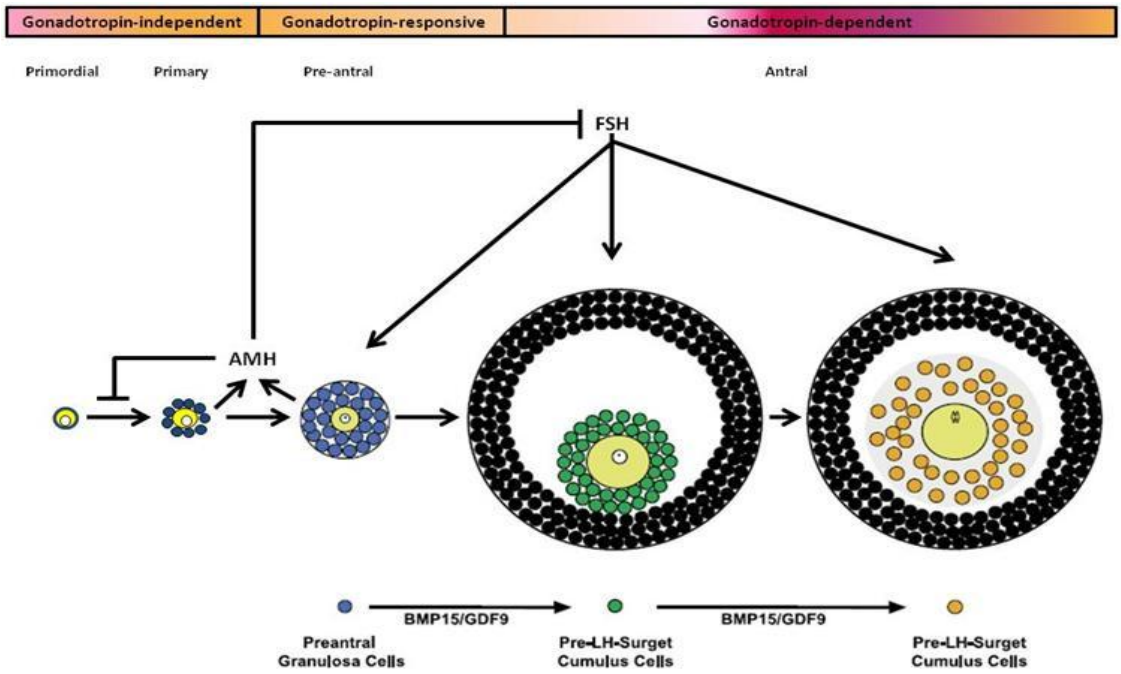

Figure 2: Folliculogenesis.
Primordial follicles are recruited from the resting pool of follicles into the growing pool to become primary follicles. At this stage, the follicles are in the Gn-independent stage of development. Growing follicles require the presence of various growth factors (many of which they themselves produce) to stimulate proliferation of granulosa cells. These growth factors include GDF9, BMP15, and OOSP1. Once a follicle develops into a pre-antral follicle, it becomes Gn-responsive, and one follicle is selected for dominance by FSH. Finally, at the antral follicle stage, the Gn-dependent stage of follicle development, the follicle continues its development becoming a pre-ovulatory follicle. AMH is expressed by follicles selected for development and continues to be expressed by healthy growing follicles until they are large enough to be selected for dominance or become atretic. AMH plays a critical role at two stages of folliculogenesis: at the primordial stage, it inhibits follicle recruitment and at the pre-antral stage, inhibits FSH-responsiveness. Thus, pre-antral follicles expressing less AMH are more responsive to FSH and more likely to be selected for dominance over ones expressing more AMH. Reprinted and modified from **[125]**, with permission from Elsevier.

Finally, the Gn-dependent stage of folliculogenesis indicates the stage of development controlled primarily by the pituitary hormones combined with the expression of the

growth factors that modulate their action. FSH acts to stimulate follicle growth and differentiation while pulsatile secretion of LH is crucial in the final maturation and ovulation of oocytes from antral follicles [81]. In studies where FSH expression was suppressed, the rapid atresia of ovulatory sized follicles was evident irrespective of the method through which FSH was suppressed [126-128]. Conversely, when FSH was present, follicle growth could be stimulated in hypogonadotropic ewes and GnRH-agonist suppressed cattle infused with FSH saw an increase in mRNA expression of developmental markers for follicle development seen in normal animals [95]. Studies using transgenic mice showed that LH is important in antral follicle development [129] but that too much LH is deleterious to their development [130]. Additionally, LH indirectly exerts control over follicle development by directing estrogen secretion in the ovary and thereby influencing the level of pituitary FSH release [127]. As a whole, these studies suggest that the selection and development of ovulatory follicles is governed by both FSH and LH.

As with early follicle developmental stages, the Gn-dependent stage relies on oocyte- and granulosa cell-secreted growth factors, expressed at specific times of folliculogenesis to bring the follicle to an ovulatory size. These are the same factors that are important in early follicle development and include inhibin, activin, GDF9, BMP15, BMP6, and newborn ovary homeobox (NOBOX). Both inhibins A and B are produced and secreted by the dominant follicle and work to inhibit FSH secretion by the pituitary [83]. In humans, inhibin A is secreted in the follicular phase and is LH-dependent and positively

correlated with estradiol, inhibin B peaks five days post menses onset and thus reflects the growing follicles in response to FSH [83]. Consequently, inhibin B is often used as a marker for the number and health of Gn-dependent follicles; however, since its expression is cycle-stage dependent, it is not an ideal marker for ovarian follicle estimates [90]. Activin, on the other hand, works to stimulate FSH secretion by the pituitary [131]. The oocyte and surrounding granulosa cells rely on an intricate network of intracellular gap junctions, both between granulosa cells and the oocyte and between adjacent granulosa cells, to link these cells to one another during development and allow for the passage of signals to and from the oocyte. Numerous studies have shown that intact gap junctions between the oocyte and granulosa cells are essential for oocyte growth and importantly, that intact gap junctions between granulosa cells are equally important in producing ovulation sized oocytes capable of fertilization [109;132-138]. While cigarette smoke has been found to affect the expression of a number of the growth factors discussed above and summarized in table 2, the canonical pathway through which follicles have been shown to be lost is apoptosis-mediated atresia. Therefore, follicle loss was examined in our mice.

Table 2: Growth factors needed for folliculogenesis.

Growth Factor	Cell Type Produced By	Function	Species Studied In To Date	Reference
Activins	Granulosa and theca cells	Granulosa cell proliferation, follicle survival and prevention of premature luteinisation, promote pituitary FSH release, ovarian steroidogenesis	Mouse, zebrafish, cattle, human, rat, sheep, goat, chicken	[131;139-146]
AMH	Granulosa cells of healthy growing follicles	Inhibits follicle recruitment from resting pool, decreases responsiveness of preantral follicles to FSH	Mouse, human, cattle, rat, goat, sheep, chicken	[69;70;80;91;93;96;97;99;100;147-151]
BMP15	Oocyte	Granulosa cell proliferation, COC integrity	Mouse, sheep, goat, zebrafish, cattle, pig, chicken	[70;105;106;110;112-117;120;125;152-159]
BMP2	Granulosa cells	Granulosa cell proliferation, follicle survival and prevention of premature luteinisation	Mouse, pigs, chicken, cattle, sheep, rat, human	[160-167]
BMP4	Oocytes, granulosa and theca cells	Primordial to primary follicle recruitment; suppresses progesterone production in granulosa cells	Mouse, zebrafish, cattle, rat, sheep, human	[160;161;168-172]
BMP5	Granulosa cells	Granulosa cell proliferation, follicle survival and prevention of premature luteinisation	Rat	[173]
BMP6	Oocyte, Granulosa cells	Granulosa cell proliferation, follicle survival and prevention of premature luteinisation, alters AMH gene expression	Mouse, pig, chicken, zebrafish, cattle, sheep, human, rat	[153;160;161;163;165;174-178]
BMP7	Granulosa and theca cells	Primordial to primary follicle recruitment, granulosa cell proliferation, follicle survival and prevention of premature luteinisation	Mouse, human, rat, sheep, cattle	[161;170;178-181]
Estrogen (Estradiol)	Granulosa cells	Antrum formation, AMH repression, follicle maturation and rupture during ovulation	Mouse, chicken, human, reptile, rat, cattle, sheep, goat, pig	[123;151;182-193]
GDF9	Oocyte	Proliferation of granulosa cells, COC integrity and expansion, preantral follicle growth, suppression of FSH-induced LH receptor content	Mouse, sheep, rat, goat, zebrafish, buffalo, cattle, pig, chicken	[70;106;108;116;119;125;152;153;155-160;194;195]
Inhibins	Granulosa and theca cells	Inhibit pituitary FSH release, ovarian steroidogenesis	Mouse, goat, sheep, cattle, zebrafish, human, chicken	[126;140;141;143;144;194;196;197]
KIT	Oocyte, stromal cells	Primordial follicle recruitment (some species), follicle growth and survival, theca cell development	Mouse, pig, rat, cattle, humans, rabbit	[152;198-202]
KITL	Oocyte, stromal cells	Primordial follicle recruitment (some species), follicle growth and survival	Mouse, pig, rat, humans, cattle, rabbit	[151;152;198;199;202-204]
NOBOX	Oocyte	Transcription factor that regulates numerous germ-cell specific genes, Inhibits primordial recruitment	Mouse, human, cattle	[205-208]

1.3.4 Follicle Atresia

Given that the ovary begins with several million follicles, only approximately 400 of which will be ovulated in the reproductive lifespan of a woman, the vast majority of follicles will undergo atresia, a process of follicle loss, most often through a form of programmed cell death called apoptosis. Like all somatic cells, granulosa cells must progress through the phases of the cell cycle in order to proliferate. The cell cycle is comprised of four distinct phases: gap 1 (G_1), synthesis (S), gap 2 (G_2) and mitosis (M) [209]. When cells are not dividing, they are found in a quiescent state known as G_0, and are not considered a part of the cell cycle (Figure 3). During the first gap phase, the cell readies itself for replication. During S phase, DNA replication occurs. During the second gap phase, the cell ensures that there is no DNA damage and that it is fully replicated prior to entering M phase, progression into this phase is dependent upon cyclin B-dependent kinase [209]. During M phase, nuclear chromosomal separation and cytokinesis (cytoplasmic division) occur. M phase is further broken down into four phases: prophase, metaphase, anaphase and telophase. During prophase, chromatin begins to condense and centrioles begin migrating to opposite ends of the cell and send out spindle fibres that will attach to the centromeres of the chromosomes. In metaphase, chromosomes begin to align themselves along the midline of the cell nucleus (metaphase plate); helping to ensure each daughter cell will receive an equal number of chromosomes. During anaphase, paired chromosomes separate at the kinetochores and move to opposite ends of the nucleus. Finally, in telophase, new membranes form around the two daughter nuclei and the partitioning of the cell begins, chromosomes de-condense

and cytokinesis occurs [210;211]. DNA damage checkpoints exist within G_1, S and G_2 phases while G_2 possesses additional unreplicated DNA checkpoint and M phase possesses both a spindle assembly and chromosome segregation checkpoint. At any of these checkpoints, if there is damage detected, or if the environment does not favour replication, the cell can halt its progress through the cell cycle. The G_1/S boundary however, appears to be the point particularly susceptible to apoptosis and this checkpoint is often referred to as the restriction point and cells exposed prior to this checkpoint are vulnerable to perturbation while cells exposed after this checkpoint are not susceptible in that particular division [209]. Of the cells present in the follicle, granulosa cells, specifically those proliferating and in the G_1/S phase transition, have been shown to be more susceptible to apoptosis than those that are resting in early G_1 phase [183;212]. This finding would help to explain why many reproductive toxicants have been found to selectively target growing follicles and why their method of follicle loss is apoptosis. However, the vast majority of these studies have utilized animal models with doses far higher than would be considered environmentally relevant to humans outside of occupational exposures. Therefore, studies are necessary to determine if these toxicants, at concentrations representative of human exposure, activate the apoptotic pathway of programmed cell death or if other mechanisms are responsible for follicle loss.

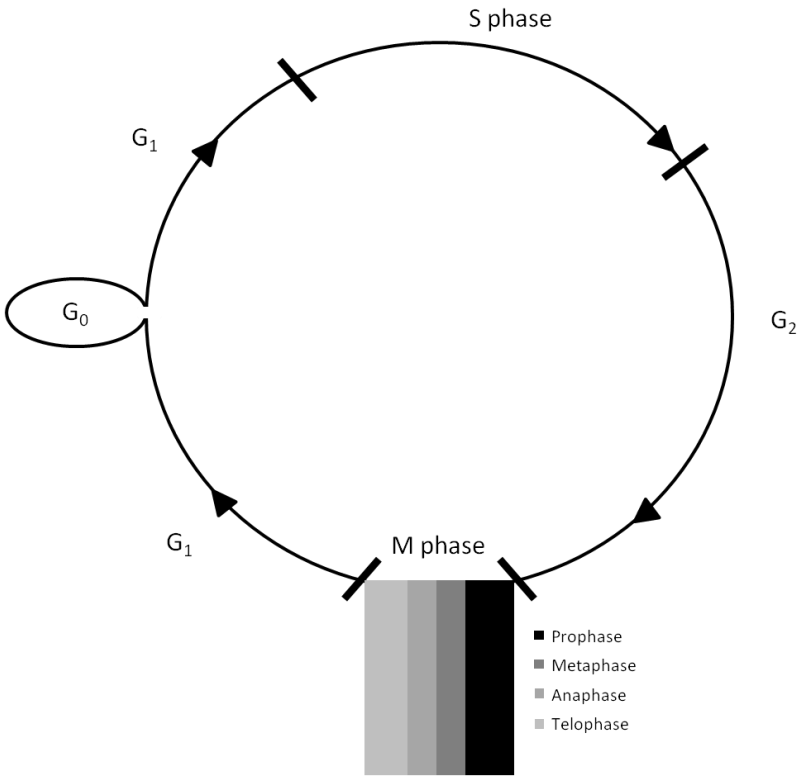

Figure 3: The cell cycle.
The cell cycle is comprised of four distinct phases: gap 1 (G_1), synthesis (S), gap 2 (G_2) and mitosis (M). Non-dividing cells are outside the cell cycle in what is referred to as G_0. During G_1, the cell readies itself for replication and ensures that the environment in which the cell is currently is suitable for cell division. During S phase, DNA replication occurs. During G_2, the cell ensures that it is fully replicated and that it is free of DNA damage. During M phase, chromosomal separation and cytokinesis (cytoplasmic division) occur. M phase is further divided into four stages: prophase, metaphase, anaphase and telophase.

1.4 Lessons Learned from Environmental Toxicants

A variety of toxicants increase follicle loss and are lethal to embryos; however, the mechanism of action is unknown. In women, menopause represents the end of reproductive life [69;80], and exposure to chemicals that have the capacity to shorten that window are of particular interest. Postmenopausal women are at greater risk for developing cardiovascular disease, Alzheimer's disease and osteoporosis [18]; thus,

chemicals that have the capacity to exhaust the ovarian reserve and induce early menopause can have serious health consequences. The association between the exhaustion of the ovarian follicle reserve and environmental toxicant exposure has been well-documented. A variety of environmental toxicants have a negative effect on fertility and ovarian function. A literature search of environmental toxicants and the ovary quickly reveals that the mode of toxicant-induced infertility varies depending on the environmental toxicant studied; while some disrupt signalling, others increase follicle atresia thereby depleting the follicle pool prematurely. Animal models have confirmed that environmental toxicants destroy follicles in a stage-specific manner. For example, exposure to certain polychlorinated biphenyls (PCBs) results in the destruction of growing follicles [213;214]. Phthalates, used as plasticisers and known endocrine disruptors, have been linked with antral follicle atresia in rodents [212;215], while 4-vinylcyclohexene diepoxide (VCD), a metabolite of 4-vinylcyclohexene (VCH) and a solvent used in industry, induces apoptosis in primordial and primary follicles [19;62;63]. Trichloroethylene (TCE), a chlorinated hydrocarbon used in industrial solvents, decreases oocyte fertilizability in mice and increases protein carbonyl formation in rats [18]. When testing whether the ovary was capable of metabolizing TCE or if the parent compound was responsible for adverse outcomes, investigators found that *in vitro* treatment with the metabolite of TCE elicited the same response as the parent compound did *in vivo* [216]. This finding indicated that the reproductive toxicity of TCE is due to its metabolism and bioactivation within the ovary. 7,12-dimethylbenz[a]anthracene (DMBA), a member of the polycyclic aromatic hydrocarbon (PAH) group and constituent of cigarette smoke,

destroys all follicle types in the ovaries of mice and rats dose-dependently [217], while another PAH and cigarette smoke constituent, BaP selectively targets and depletes the primordial follicle pool [218;219]. As these studies illustrate, each chemical elicits a distinct response from the ovary. Additionally, some toxicants may be bioactivated by an enzyme (i.e.: whereas glutathione (GSH) conjugation catalyzed by glutathione S-transferase (GST) represents bioactivation in the presence of VCH, detoxification occurs when VCD or DMBA is the toxicant encountered [18]). Despite the diversity of environmental toxicants that have been shown to elicit adverse effects on ovarian function in animal models, there are few studies that show effects on the human population. Moreover, the decrease in fertility seen in these animal studies was due to toxicological levels of these toxicants [62-66;220;221], high dose exposures that have debatable relevance to human exposure. Therefore, more studies evaluating lower doses and more sensitive end points are needed to determine if these toxicants induce selective stage-dependent destruction of ovarian follicles at concentrations representative of human exposure.

1.5 Apoptosis

Cells generally die through one of at least three distinct processes, those being necrosis, terminal differentiation leading to cell death, and apoptosis. Although all three mechanisms are important, apoptosis is thought to be the main route of follicle atresia in the mammalian ovary [222-228]. Apoptosis is a genetically determined and biologically functional means of cell death and is essential under both normal and pathologic

conditions. It depletes the resting pool of follicles by roughly two thirds before birth [229] and is the primary mechanism through which atretic follicles die. Given that the majority of environmental toxicant studies to date showed apoptosis as the mechanism of cell death and that Mattison and colleagues [230] found that the primordial and primary follicles of mice exposed to aryl hydrocarbon receptor (AhR) ligands (several of which are found in cigarette smoke) were rapidly depleted and that these ovotoxic effects could be prevented in the presence of AhR antagonists [231], we hypothesized that a similar phenomenon was occurring in cigarette smoke-exposed ovaries.

The morphological manifestations of programmed cell death are distinct from those of necrosis, the passive death of a cell brought on by infection, injury or disease. Necrotic cells exhibit signs of inflammation, cell and organelle swelling, adenosine triphosphate (ATP) loss, membrane damage and ultimately cell lysis [232]. Apoptotic cells have hallmark features distinct from necrosis which include nuclear chromatin condensation, formation of apoptotic bodies, DNA fragmentation (detectable by gel electrophoresis as a classical laddering pattern or by TUNEL staining) and cytoplasmic vacuolization [233]. Apoptosis is a non-traumatic mechanism of removing unneeded cells and occurs in all tissues of the body. Unlike necrosis, apoptosis is a “silent” form of cell death, being physiologically undetected by the organism but requires energy from the cell and results in changes in biochemical and molecular markers that can be measured to assess the degree and location of apoptosis occurring in response to a cellular assault [19].

Apoptosis can occur via two major mechanistic pathways, the extrinsic death receptor pathway or the intrinsic mitochondrial pathway (Figure 4). Each pathway involves the activation and recruitment of different factors, but both ultimately involve the mitochondria in the execution of cell death. While the extrinsic pathway relies on the binding of a death ligand to a death receptor to produce caspase 8 and begin the cascade of events that lead to cell death, the intrinsic pathway, as its name suggests, is initiated by internal signals such as DNA damage, defective cell cycles, hypoxia, loss of cell survival factors or other types of cellular stress [234]. The release of pro-apoptotic proteins results in activation of caspases from within the mitochondria, triggering apoptosis. The intrinsic pathway hinges on a delicate balance of pro-apoptotic and pro-survival members of the BCL2 family whose role is to regulate the permeability of the mitochondrial membrane [235].

In mammals, the BCL2 family of proto-oncogenes is associated with apoptosis. The BCL2 family, which contains multiple α–helical segments known as BCL2 homology domains (BH1-4) [236-238], contain several proteins that are pro-apoptotic and others that are anti-apoptotic. The pro-survival proteins of the BCL2 family contain all 4 BH domains, while the death-inducing members only contain 2 or 3 of the domains (BH1-3). The mammalian pro-apoptotic proteins are: BAX, BAK, BOK/MTD, and $BCLX_S$. There is a sub-group of pro-apoptotic proteins which contain only the BH3 domain; they are: BID, BAD, BIK/NBK, BLK, HRK, BIM/BOD, NIP3, and NIX/BNIP3 [239;240]. To date, the mammalian pro-survival proteins identified in the BCL2 family are: BCL2,

BCL2L1, BCLW, MCL-1, A1/BFL-1, BOO/DIVA, and NR-13 [241;242]. This family of proteins function upstream of irreparable cellular damage with much of their function focused on the mitochondria. Apoptosis occurs via two pathways (the extrinsic, or death receptor-mediated, and the intrinsic, or mitochondrial), that ultimately converge, resulting in the death of the cell. BAX, BAK, BCL2, BCL2L1 (BCLXL), MCL1 and BAD have all been detected in the ovary.

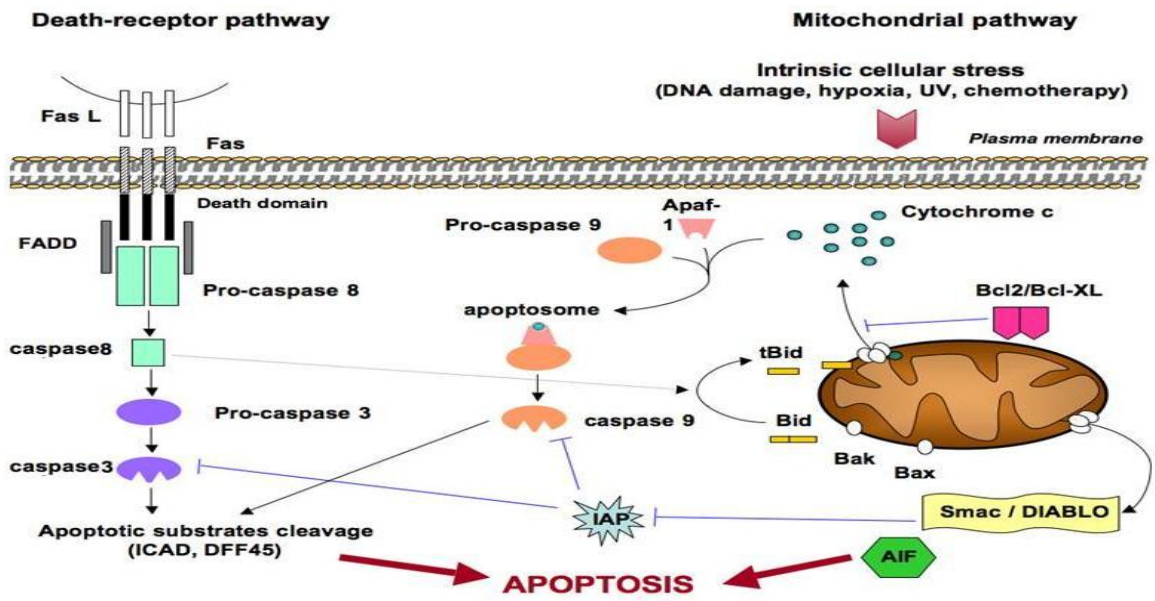

Figure 4: The apoptosis pathways.
Cells can undergo apoptosis via two discrete pathways: the extrinsic (death-receptor) pathway or the intrinsic (mitochondrial) pathway. In the extrinsic pathway, death can be induced by the binding of ligands to their receptors on the cell surface. The receptor's death domain is then bound by an adaptor, which serves to recruit the pro form of the initiator caspase for subsequent activation. This induces caspase 3 activation. Caspase 3 cleaves its substrate, the inhibitor of caspase-activated DNase (ICAD), which is released to enter the nucleus and cleaves DNA resulting in apoptosis of the cell. Caspase 8 cleaves BID, resulting in a truncated form (tBID) that, upon dimerization of BAX or BAD, causes the release of cytochrome *c* from mitochondria through the potential alteration of mitochondrial membrane permeability. BCL2 inhibits the release of cytochrome *c* and AIF into the cytoplasm. In the cytosol, cytochrome *c* binds to apoptosis protease activating factor (APAF1), forming the apoptosome, which converts pro-caspase 9 to caspase 9. This results in activation of downstream effector caspases. Smac/DIABLO binds to inhibitors of apoptosis proteins (IAPs) and prevents them from inhibiting the activation of caspases 3 and 9. In the intrinsic pathway, death is induced by direct signals from within the cell, bypassing the need to activate membrane-bound death receptors. These signals alter the balance of pro-apoptotic and anti-apoptotic signalling molecules (namely BAX, BID, and BCL2) in favour of apoptosis. Mitochondrial membrane permeability is altered when BAX and BID insert themselves into the membrane pores, leading to cytochrome *c* release and subsequent activation of caspase 9 and death. This figure was reprinted from **[243]** and used with permission.

Inhibitor of apoptosis proteins (IAPs) are a conserved family of proteins, which have been found in yeast, insects, worms, viruses and vertebrates that, as their name suggests, protect against apoptosis [244]. IAPs contain one or more baculovirus IAP repeat (BIR) domains, zinc-binding folds, and are involved in various cellular functions, including regulation of cell cycle and intracellular signal transduction [244-246]. IAPs are known to regulate apoptosis, being induced by an assortment of death-inducing stimuli. To date, the known members of the mammalian IAP family are X-linked IAP (XIAP), cellular IAP 1 (cIAP1), cIAP2, Apollon, neuronal apoptosis inhibitory protein (NAIP), BIR repeat containing ubiquitin-conjugating enzyme (BRUCE), Livin and Survivin (also known as mouse TIAP) [247-250]. The predominant function of several IAPs is the regulation of apoptosis. Survivin, which is a nuclear protein expressed primarily during the G_2-M phase of the cell cycle [244;250], attenuates the activity of caspase 3, while XIAP, a mainly cytoplasmic protein, is a potent and direct inhibitor of caspases 3, 7 and 9 [251] and is involved in the prevention of Fas-mediated apoptosis [244;248] (part of the extrinsic or receptor-mediated apoptotic pathway). cIAP1 and cIAP2 which have also been implicated in the extrinsic apoptotic pathway, bind to and inhibit the function of tumor necrosis factor receptor (TNFR) 1 and 2 through their interaction with TNF Receptor Associated Factors (TRAFs) [244].

Several IAP family members are expressed in the ovary. These include Survivin [250;252;253], XIAP [246], cIAP1 [250] and cIAP2 [254]. cIAP1 is thought to play a role in the cell cycle, along with Survivin, based on its being found in concentrations at

the midbody of cells in telophase [244]. Survivin, likewise, is hypothesized to inhibit a default apoptotic cascade initiated during mitosis by means of its α-helix coiled-coil domain binding to mitotic spindle microtubules [250]. From previous studies, we know that Survivin acts as a bifunctional protein regulating both the cell cycle and inhibition of apoptosis in granulosa cells [252]. Similarly, mRNA and protein expression of XIAP is reduced to trace or negative levels in the granulosa cells of atretic follicles but has a robust expression in healthy follicles [246]. cIAP1 [250], cIAP2 [255] and BCLXL [255] have all been identified as playing a role in the suppression of granulosa cell death in the mammalian ovary.

1.5.1 The Extrinsic Pathway

The death receptor pathway involves signals arising from outside the cell. Death receptors (FAS, TNF-R1 or TNF-R2) bind their ligand (FASL or TNFα), initiating the transmission of death signals via cytoplasmic death domains (FADD) [233;256;257]. Death domains in turn recruit the pro form of the initiator caspase 8 for subsequent activation. This induces activation of pro-caspase 3, initiating the caspase cascade, leading to cell death. This process is regulated by FLICE-inhibitory protein (FLIP), which contains two death effector domains (DED) and an inactive caspase domain, which binds FADD and caspase 8, preventing death receptor-mediated apoptosis [258]. Caspase 3 (CASP3) cleaves its substrate, the inhibitor of caspase-activated DNase (ICAD), which is released to enter the nucleus and cleaves DNA resulting in apoptosis of the cell. In addition caspase 8 cleaves BID protein, resulting in a truncated BID (tBID) that, upon

dimerization with BAX or BAD, causes the release of cytochrome *c* from mitochondria through the potential alteration of mitochondrial membrane permeability. Anti-apoptotic BCL2, on the other hand, inhibits the release of cytochrome *c* and AIF into the cytoplasm by binding to BAX and preventing it from inserting itself into the mitochondrial membrane. The presence of cytochrome *c* in the cytosol causes apoptotic protease activating factor-1 (APAF1) to release HSP90 and bind to cytochrome *c*, forming the apoptosome. Binding in the presence of ATP induces the oligomerization of APAF1 and the subsequent recruitment and activation of pro-Caspase 9 [233]. This results in activation of downstream effector caspases. Smac/DIABLO, which is also released from the mitochondria upon membrane permeability changes, binds to inhibitors of apoptosis proteins and prevents them from inhibiting the activation of caspases 3 and 9.

1.5.2 The Intrinsic Pathway

As previously explained and shown in figure 4, the intrinsic or mitochondrial pathway of apoptosis begins with death signals arising from within the cell which signal the pro-apoptotic BCL2 proteins (especially BAX or BID) to translocate to the mitochondrial membrane, where they insert themselves into the pores of the mitochondrial membrane, altering its permeability via changes in membrane potential thereby allowing the release of cytochrome *c* into the cytosol [233;259;260], resulting in a collapse of the mitochondrial membrane potential and halting of ATP synthesis, thus initiating the apoptosome, which mediates the activation of the caspase cascade via CASP3 activation. The mitochondrial membrane potential (MMP) is generated by the respiratory chain as it

pumps protons to the intermembrane space and must be maintained within a relatively narrow range (150-180 mV) to maintain ATP production and mitochondrial energetic capacity [261]. Because the pumping of protons to the intermembrane space and their subsequent re-entry into the inner membrane energizes the conversion of adenosine diphosphate (ADP) to ATP, even small changes in MMP can have dramatic effects on the energy-producing capacity of the mitochondrion. For example, a 14 mV decrease in MMP results in a 10-fold decrease in the ATP/ADP ratio [261].

1.5.3 Apoptosis in the Ovary

Numerous animal studies have employed the use of environmental toxicants from different chemical families to induce ovarian follicle loss and the overwhelming majority of these studies have concluded that the mechanism by which follicles are lost is via apoptosis irrespective of the follicle population specifically targeted [53;62;63;66;213;214;217-219;229;231;262-268]. Primordial follicle destruction is considered to be the most disastrous, as the effects of which are not detected until years after the exposure, often after ovarian failure is well established. The loss of follicles appears to be primarily due to apoptosis of the granulosa cells of the follicles. The mechanisms of follicular apoptosis are not completely understood and appear to involve both intrinsic and extrinsic pathways, depending on the apoptotic stimulus received.

In mice, maternal exposure to high doses of the PAHs, BaP and 7,12-dimethylbenz[a]anthracene (DMBA;1 mg/Kg each/week for six weeks) significantly

depleted primordial follicle numbers via increased expression of BAX which, in a subsequent experiment was shown to involve induction of the *harakiri* gene, which codes for a BCL2 interacting protein [269]. Unlike the results above, treatment of pregnant mice with high concentrations of BaP and DMBA (1 mg/Kg each/week for six weeks) inhibited apoptosis in the murine placenta [270]. In this study, treatments increased FASL and XIAP expression but decreased BAX and apoptosis in the placenta, suggesting tissue specificity. Therefore, the AhR mediated effects on apoptosis are also target tissue-dependent. Others still have found that the dose and duration of exposure play a part in follicle demise. In a time-course study in rats, it was found that an acute exposure of a high dose of VCD was not sufficient to elicit follicle death but was in fact protective against atresia while repeated daily doses of a lower dose resulted in significant atresia and activation of the oxidative stress response as measured by superoxide dismutase (SOD) 2 expression in small but not large follicles demonstrating that not only do toxicants specifically target follicle populations, but do so in a dose- and time-dependent manner [19].

1.5.4 Oxidative Stress

Mitochondria are the powerhouse of the cell. They are the organelle in which cellular respiration, the Krebs cycle and fatty acid oxidation occur. The transformation of energy from glucose to ATP is achieved through a series of redox reactions. During cellular respiration, mitochondria produce ROS in the form of superoxide ($O2^{\bullet-}$), hydrogen peroxide (H_2O_2) and hydroxyl free radicals ($OH^{\bullet-}$) (Figure 5). Under physiological

conditions, these by-products serve as signals in such processes as growth, hormone synthesis and inflammation. However, their overproduction is deleterious to cells leading to DNA, protein and lipid damage that ultimately result in pathological processes and death, if unmitigated. The cell possesses several defense mechanisms capable of mediating ROS to prevent cellular damage. These include the mitochondrial ROS-detoxifying enzymes superoxide dismutase, glutathione peroxidase, glutathione reductase, and catalase. In healthy cells, ROS oxidize factors in numerous pathways. For example, certain genes such as p53, serve to aide in upregulation of antioxidant genes to reduce ROS levels [271].

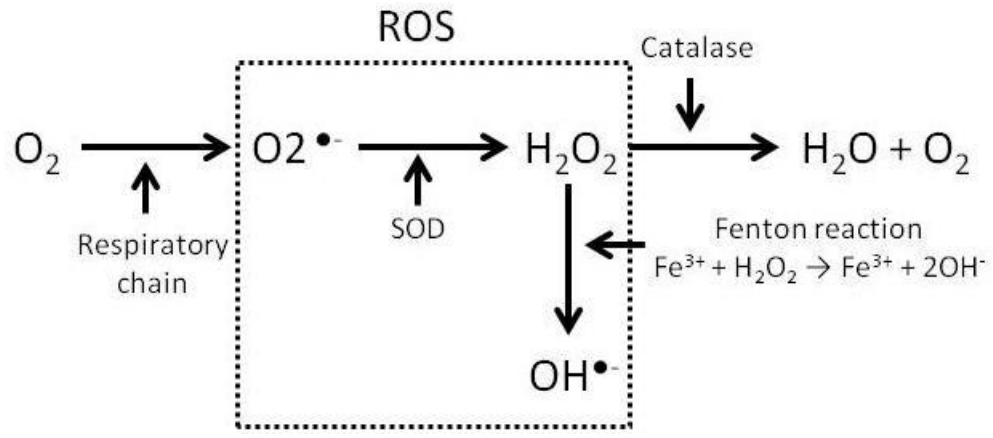

Figure 5: Endogenous ROS generation.
During normal cellular respiration, ROS are generated in the form of superoxide ($O2^{\bullet -}$), hydrogen peroxide (H_2O_2) and hydroxyl free radicals ($OH^{\bullet -}$). In small concentrations, they play various roles in physiological processes and their detoxification is mediated by antioxidant enzymes (superoxide dismutase, catalase, glutathione peroxidase, and glutathione reductase). When produced in excess, however, ROS can interfere with normal cell function and potentially lead to cell death.

Reactive oxygen species have been found to be important in many physiological processes in the female reproductive tract: playing roles in hormone signalling,

steroidogenesis, ovulation and pregnancy. When produced in physiological concentrations, ROS are beneficial to follicle development and ovulation, as evidenced by the changes in $O_2^{\bullet-}$ levels leading up to ovulation where it is thought to play a role in the breakdown of follicular walls allowing for the extrusion of the cumulus-oocyte complex at ovulation [272]. Additionally, oxidant production rises as the number of granulosa cells increases in the growing follicle, owing to the increased cell metabolism associated with differentiation [273]. Moreover, during embryonic development, ROS act in a physiological manner in the activation of apoptotic cell death in interdigital regions, leading to appropriate digit formation [274]. Oocytes possess the most mitochondria of all the cells in the body due to their high energy demands [275]. As such, they are capable of producing a large amount of ROS as a by-product of mitochondrial electron transport chain (ETC) function. They also produce the requisite ROS detoxifying enzymes to counterbalance this production. If this delicate balance is disrupted, oxidative stress results in the oocyte and can lead to the death of the oocyte [275].

Oxidative stress is the term used to describe what happens when ROS generation overwhelms the *in situ* antioxidant mechanisms. Studies have identified caspase activation and catalase activity as being essential to ROS mediation, the blockage of which leads to accumulation of ROS, oxidative stress and ultimately cell death [276-278]. Occasionally, mitochondrial proteins can become misfolded or damaged resulting in aggregates [275;279]. Under homeostatic conditions, the mitochondria have the ability to identify and remove these aggregated proteins; however, under cell stress conditions, they

accumulate and the mitochondrion must fuse with healthy mitochondria to maintain mitochondrial DNA (mtDNA) integrity and repair, the failure of which results in mitochondrial degradation. Excessive mitochondrial degradation has been linked to a number of neurodegenerative [275;280] and metabolic [261;281-284] diseases.

In addition to physiological sources, several environmental contaminants can induce ROS production and oxidative stress (Figure 6) including carbon monoxide (CO), arsenic, dioxins, VCH and its metabolite, ultraviolet (UV) radiation, pesticides and cigarette smoke, many of its constituents being oxidants and free radicals which result in the formation of oxidized bases including 8-hydroxy-2'-deoxyguanosine (8-OHdG), an oxidized nucleoside of DNA and a classical biomarker of oxidative DNA damage [285-292]. CO results in the production of superoxide and the hydroxyl radical, even at low concentrations. However, these low concentrations have a physiological role to play in multiple signalling pathways including angiogenesis, heme oxidation, and vascular remodelling, whereas in high concentrations or following accidental exposure, CO can have detrimental effects on the mitochondrial ETC [285] culminating in death of the cell. Studies in multiple cell lines have shown that arsenic can induce superoxide and H_2O_2 production as well as increase the expression of antioxidant enzymes including SOD and catalase [289]. Similarly, UV radiation, especially UVB, has been associated with inducing lipid and protein oxidation in the plasma membrane of epidermal cells and in the production of H_2O_2 which can indirectly activate cell growth pathways leading to the tumor process [287]. Exposure to cigarette smoke, which contains a number of oxidants

and free radicals, induces oxidative stress [40;292-296]. In addition, many of these studies point to the importance of cigarette smoking, its constituents, the production of ROS and oxidative stress in the reproductive tract [3;40;44;292;297]. Specifically, exposure to cigarette smoke resulted in significant oxidative damage in oocytes and decreased blastocyst formation [298]. While BaP results in smaller ovaries [297] in addition to retarding the development of follicles *in vitro* [57;58;299;300].

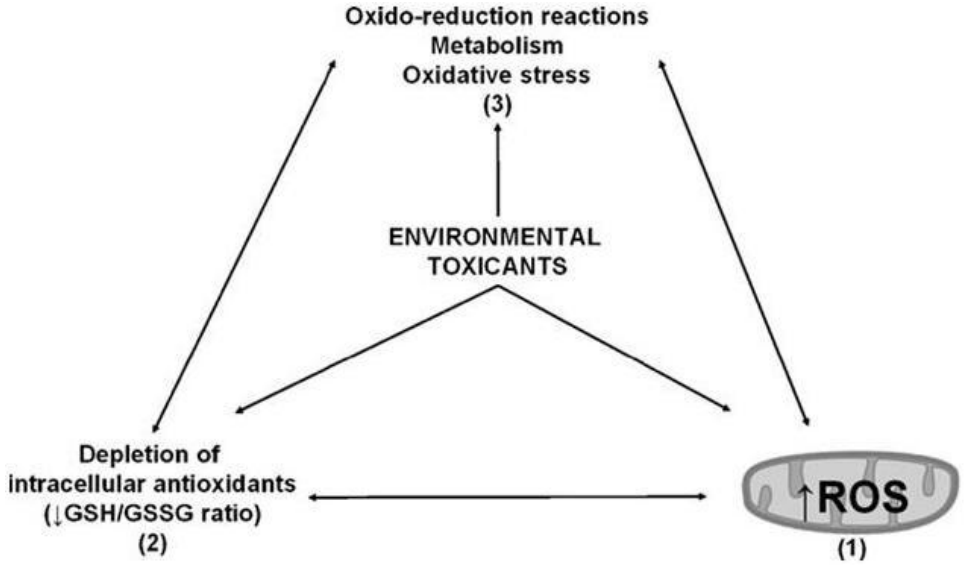

Figure 6: Mechanisms of ROS generation by environmental toxicants.
Exposure to environmental toxicants (i.e.: BaP) induces changes in the equilibrium of the cell's anti-oxidants and reactive oxygen species by different interconnected mechanisms. (1) Environmental toxicants can generate ROS directly via targeting of the mitochondria. ROS can further deplete antioxidant defenses leading to increased oxidative stress. (2) Environmental toxicants can directly deplete the cellular antioxidant defenses (i.e.: vinylcyclohexidene induces the depletion of intracellular GSH via direct conjugation catalyzed by GST). Depletion of these antioxidant defenses facilitates the accumulation of ROS. (3) Environmental toxicants have also been reported to induce oxidative stress by mediating a variety of redox reactions and/or through different metabolic pathways (i.e.: CYP1A1-mediated metabolism of BaP), which can in turn promote mitochondrial damage, ROS formation and depletion of antioxidant molecules in the cell. Reprinted from [301] with permission from Elsevier.

1.6 Adaptive Responses to Stress

Organisms react to changes in their environment by either increasing or decreasing protein production. Although the systematic mechanisms of adaptation to changes in an organism's environment are well-known [302], the molecular and genetic mechanisms are less well-known.

1.6.1 Heat Shock Proteins

The heat shock response, one mechanism of stress adaption employed by living organisms is mediated by a common set of proteins known as heat shock proteins (HSPs) whose expression pattern is conserved almost universally [302]. Heat shock proteins are cellular components that have been found in nearly all organisms studied to date, both prokaryotic and eukaryotic alike [303;304]. However, despite extensive research, the functional significance of heat shock proteins is not wholly understood. Heat shock proteins, first discovered in chromosomal puffs of salivary glands of *Drosophila* in 1962, are involved in a complex cascade of events that make up the heat shock response, a cellular survival mechanism important for cells to survive the onslaught of environmental stresses in the course of an organism's lifespan.

Although some HSPs are expressed constitutively within the cell under normal physiological conditions, others are only expressed upon stress conditions [302;305]. Those expressed under normal conditions in the cell are differentially expressed both spatially and temporally and are mediated at the level of mRNA synthesis, stability and

translational efficiency and posttranslational modifications [302]. It is generally accepted that these proteins act as molecular chaperones, maintaining other proteins in a folding-competent state and preventing the aggregation of damaged or denatured proteins [306], while remaining separate from the final functional structures they help to form [305;307]. Heat shock proteins are key participants in RNA translation, DNA replication, protein folding and translocation through the endoplasmic reticulum (ER) and mitochondrial membranes, cell signalling and protection at higher temperatures [302;307;308].

To date, nearly every organism studied has been found to possess HSP genes that are expressed in response to elevated temperature or other stressors such as exposure to ethanol, heavy metal ions or cigarette smoke [309-311]. Certain physiological stresses such as oxidative stress, fever, and inflammation can induce hsp gene expression as can non-pathological conditions such as growth factors, development, and differentiation [309;312;313]. HSPs are classified based on their molecular weights and comprise three main families: the high molecular weight HSP90s, the HSP70s and the small HSPs (sHSPs). Transcription of hsp genes is mediated by the heat shock element (HSE) found in the 5' upstream region of these genes and interacts with a transcription activating factor termed a heat shock factor (HSF). Members of the sHSPs, the least conserved of the heat shock protein families, are stress-inducible molecular chaperones that range in size from 12 to 43 kDa [314-317]. In their role as molecular chaperones, sHSPs bind to unfolded proteins and maintain their target protein in a soluble and folding-competent state so that once the stressor is removed, they can be refolded to their native state by other

chaperones, including HSP40 and HSP70 [315-317]. sHSPs aid in a number of biological processes including modulation of redox parameters, cell proliferation and differentiation, and actin polymerization [314;316;317]. Additionally, it has been demonstrated in a number of cultured cell systems that a sub-lethal heat shock can confer tolerance to other stresses that would otherwise prove to be toxic [318;319]. Finally, sHSP synthesis or mutations have been associated with a variety of diseases including estrogen-dependent cancers (i.e.: breast), muscle myopathy, multiple sclerosis, and various neuropathologies [315;320-323].

HSP25, a member of the sHSP family, was first discovered as HSP27 in the cytosol of human breast cancer cells following estradiol stimulation [324]. In this context, it plays a role as an estrogen-regulated protein. Murine HSP25 is related to human HSP27. In normal adult mice, *Hsp25* and its protein occur in various organs including the skeletal muscle, heart, aorta, stomach, intestine, lung, urinary bladder, eye, pancreas, kidney, thymus, testis, uterus and ovary [320;325-330]. In the ovary, it is constitutively present in unfertilized eggs, coinciding with its housekeeping role, and induced by zygotic gene activation at the 2-cell stage, a stage critical for embryonic development. Mouse *Hsp25* is seen in post-implantation embryo back muscles, neurons of the spinal cord and purkinje cells during embryogenesis [331]. The expression pattern indicates that *Hsp25* is involved in development and differentiation of pre-implantation embryos and oocyte maturation [332]. Additionally, HSP25 protein is translocated to the nucleus upon chronic heat shock, the functional significance of this translocation is not known at

present. Work conducted by Arrigo suggests that disruption of sodium active transport, resulting in the failure of HSP25 to be redistributed following the return to physiologic conditions, may be the underlying cause of oocyte death following chronic heat shock [333]. In addition to heat shock experiments, it has been shown that HSP25 expression patterns are affected by exposure to toxicants including acetaminophen [334], arsenic [335], cadmium [335], cisplatin [336], schisandrin B [337] and trichloroethylene [338]. HSP25 is both constitutively present and heat-inducible in the mouse oocyte. The presence of HSP25 in the ovary, its role in protecting tissues under stress, and its response to toxicant exposure make it a good candidate protein for study in the context of cigarette smoke-induced ovarian follicle loss.

1.6.2 Autophagy

Autophagy is an evolutionarily conserved mechanism in eukaryotes through which damaged organelles and long-lived proteins are degraded by lysosomal enzymes [339-341]. Autophagy literally translates to "self-eating" and was first discovered over half a century ago. Since then, 35 autophagy-related (Atg) genes have been identified in yeast, many of which have homologues in humans. Classically considered a mechanism of survival, autophagy involves the cytoplasmic sequestering of cellular debris, long-lived proteins and superfluous organelles in double-membrane vesicles termed autophagosomes which then fuse with lysosomes, becoming autophagolysosomes, for degradation of their contents and release into the cytoplasm for the building of new macromolecules and for energy production.

Autophagy is characterized into three types based on morphological characteristics exhibited: macroautophagy, microautophagy, and chaperone-mediated autophagy. During macroautophagy (the focus of our study and hereafter referred to as simply autophagy), damaged proteins and organelles are engulfed in double membrane-bound vesicles (autophagosomes) and delivered to lysosomes for constitutive degradation within the autophagolysosome. Autophagy can be either bulk (non-specific) or selective. Selective autophagy occurs when specific cargo is targeted for autophagosomal degradation. To date, there have been five different types of selective autophagy identified: xenophagy (pathogens), aggrephagy (protein aggregates), pexophagy (peroxisomes), glycophagy (glycogen) and mitophagy (mitochondria) [342]; each of these employing the use of a subset of Atg genes, some of them unique only to that type of autophagy.

Autophagy can be broken down into four distinct steps: initiation, nucleation, elongation and closing, and degradation [343], each of which involves different molecular mediators. Briefly, autophagy is induced in response to various stresses, including nutrient starvation, oxidative stress or genotoxic agents, leading to initiation which depends on the ULK1 complex, followed by activation of the Beclin 1-Vps34/15-Atg14L complex and membrane nucleation [341-346]. Although a number of additional proteins are involved in the autophagy cascade, the Atg genes comprise the core machinery for membrane nucleation and expansion (Figure 7). Beclin 1 (BECN1/Atg6) is essential for the progression of membrane nucleation but is inhibited by BCL2 [345;347]. Following

nucleation, two ubiquitin-like proteins, Atg12 and microtubule-associated protein 1 light chain 3 (Map1lc3), along with their conjugation complexes, help to form the autophagosomes [342;343;347]. Specifically, Atg12 is activated by Atg7 and conjugated to Atg5 by Atg10 while Map1lc3 (hereafter referred to as LC3), which is present in its inactive form in the cytoplasm as LC3-I, is activated by Atg7 and conjugated to phosphatidylethanolamine (PE) by Atg3 with the help of the Atg12-Atg5 complex [342;343]. Once LC3 has been activated to LC3-II, it is recruited to the membrane of the autophagosome and facilitates transport to and organelle sequestration within the autophagosome. LC3-II can be localised to the autophagosome membrane and therefore serves as a marker for autophagosome formation and degradation [345].

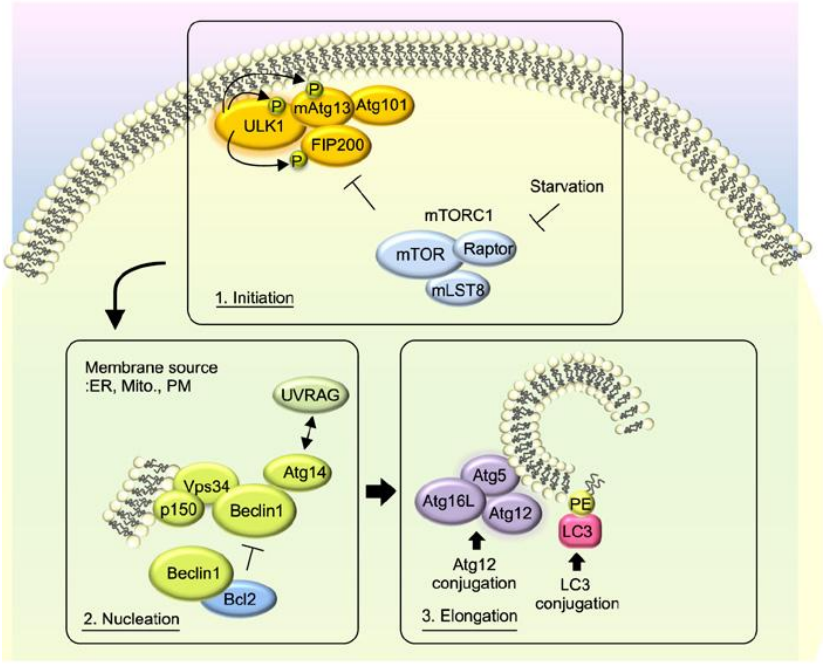

Figure 7: The autophagy pathway.
Initiation, nucleation and elongation steps of the autophagy cascade are shown in this schematic. During the initiation step, the ULK1 complex is required and is negatively regulated by the mammalian target of rapamycin (mTOR) which is in turn inhibited by nutrient starvation. Following initiation, membrane nucleation occurs via the activation and concerted actions of the Beclin1-Vps34/15-Atg14L complex. This step can be inhibited by the binding of Bcl2 to Beclin1, preventing it from forming the complex necessary to initiate nucleation. Finally, membrane elongation occurs following Atg12-Atg5 complex conjugation and subsequent conjugation and activation of LC3 by phosphatidylethanolamine. This figure was reprinted from **[346]** with permission.

1.6.2.1 Autophagy as a Cell Survival Mechanism

Autophagy is widely accepted as a survival mechanism employed by cells under unfavourable conditions, most notably nutrient and oxygen deprivation, to supply the cell with much-needed energy to survive in the absence of external nutrient or oxygen availability. Autophagy occurs at a basal level in the cell but is stress-inducible. As such, autophagy operates as a bulk degradation system where autophagosomes form around a

portion of the cytoplasm and enclose contents which can be used as energy sources until the stressor is removed. Under starvation conditions, H_2O_2 was found to be critical for formation of autophagosomes and subsequent autophagic degradation, a process central to survival of cells experiencing nutrient deprivation [278]. Despite the fact that the origin of the autophagosomal membrane is as yet unidentified, multiple groups have argued that it originates from a variety of candidates including the ER, plasma membrane, mitochondria and lastly *de novo* formation [346;348]; however, the origin (or origins) remains unresolved.

1.6.2.2 Autophagy as a Cell Death Response

Autophagy has conventionally been recognized as a cell survival mechanism, designed to protect the cell from assaults on homeostasis, but recent evidence has implicated autophagy in cell death. The role of autophagy in cell death is controversial, but several lines of evidence point to its being central to inducing cell death under certain conditions including, but not exclusive to, arsenic trioxide (As_2O_3) treatment [349;350], inhibition of mitochondrial ETC in transformed and cancer cell lines [276], and inhibition of apoptosis in mouse embryonic fibroblasts (MEFs) by knockout of central pro-apoptosis genes *Bax* and *Bak* [351]. In the case of apoptosis inhibition, prolonged autophagy can lead to cell death [352]. Specifically, mice deficient in both *Bax* and *Bak*, pro-apoptosis genes, are completely resistant to apoptosis yet programmed cell death proceeds in a normal manner with the appearance of autophagosomes and autolysosomes [351]. Non-apoptotic cell death in these mice was dependent on the autophagic proteins ATG5 and BECN1.

Mechanisms regulating cross-talk between apoptosis and autophagy are unclear; however, emerging studies have identified autophagy as an important alternative cell death pathway in mammalian cells, including human and rodent granulosa cells [353;354]. Despite this, the relevance of autophagy to granulosa cell death and toxicant-induced changes in ovarian function are unexplored. It is noteworthy that BCL2 appears at the interface between apoptosis and autophagy. BCL2 is a key regulatory protein common to both apoptosis and autophagy pathways that inhibits apoptosis via blocking of BAX in apoptosis and Beclin 1 in autophagy. Disassociation of Beclin 1 from BCL2/BCL2L1 in the ER but not mitochondria is a key driver of autophagy. In human granulosa cells, unchecked oxidative stress led to increased expression of lectin-like oxidized low-density receptor (Lox1), a scavenger receptor and membrane glycoprotein that is activated by oxidized low-density lipoprotein [353]. Treatment of malignant gliomas with low levels of As_2O_3, a metabolic toxin, resulted in BNIP3-regulated autophagic cell death [349;350]. Likewise, treatment of either transformed or cancer cell lines with the mitochondrial ETC inhibitors, rotenone or trifluoroacetone, induced expression of several autophagy genes and increased autophagic cell death which could be inhibited by overexpression of SOD2 [276].

Several distinct lines of evidence lead us to believe that cigarette smoke exposure can activate the autophagic pathway of cell death and play an important role in primordial follicle loss. Specifically, recent studies have demonstrated that cigarette smoke increases

autophagy-mediated cell death in lung cells from patients with chronic obstructive pulmonary disease [355;356]. Moreover, cigarette smoke extract (CSE) increased processing of LC3-I to LC3-II and increased autophagy in cultures of human bronchial epithelial cells [357]. Likewise, CSE treatment induced autophagy in lung epithelial cells, macrophages and fibroblasts [355]. Cigarette smoke is a complex mixture of several thousand chemical compounds, many of which are oxidants or free radicals that are inducers of oxidative stress. Cigarette smoke also contains a number of AhR agonists, the activation of which leads to induction of cytochrome P450, which is involved in the generation of ROS [294]. Oxidative stress and the production of ROS can lead to apoptosis and autophagy [294], both processes which are mitochondrially-mediated.

1.6.3 Mitochondria

Mitochondria are organelles that arose from an alpha-proteobacterium engulfed by a eukaryotic ancestor [358;359]. Mitochondria have retained some of their bacterial predecessor's characteristics, including a circular genome that through evolution has been reduced via gene transfer to the nucleus [359] and loss of redundant genes and is now the mtDNA seen in extant mitochondria. Although much of the DNA encoding mitochondrial proteins is actually found in the cell nucleus where it is transcribed and translated and only transported to the mitochondria post-translationally, the mitochondrial genome codes for a number of genes essential for the machinery of cell respiration, including ATPases and cyclooxygenase (COX) enzymes [243]. Mitochondria are also endowed with two functionally discrete lipid bilayer membranes: the inner (IM) and outer

(OM) membranes. These membranes encapsulate the inner membrane space and the matrix [359-361]. Mitochondria were first described in the 1840s, and between then and the early 1980s, mitochondria were thought to be independent structures randomly distributed throughout the cytosol whose primary role was to provide energy in the form of ATP to the cell. However, the advancement of live cell imaging allowed researchers to observe mitochondria in a completely new way which led to the discovery that mitochondria are in fact dynamic organelles which not only communicate extensively with one another, but actually exist within an interconnected reticulum or network that is continually reshaped through the tightly orchestrated and ongoing process of fission and fusion [362-364]. This state of change allows the mitochondria to move, enlarge and contract in response to the ever-changing energy requirements of the cell.

Mitochondria are essential to survival. Their primary function is that of supplying metabolic energy through oxidative phosphorylation (OXPHOS) [363]. In addition, mitochondria are key regulators of catabolic and anabolic reactions including the Krebs cycle and fatty acid oxidation as well as of apoptosis and aging [359-361;363;365]. Because every cell differs in its energy requirements, the state of the mitochondrial network is highly variable and critically depends on the individual physiological status of the cell. Consequently, metabolically active cells favour the generation of interconnected mitochondria while inactive cells possess multiple morphologically and functionally distinct small, short rods [363]. In healthy cells, mitochondria are found in a variety of shapes ranging from the classically-conveyed solitary bean-shaped organelle to long,

interconnected tubules depending on the energy requirements of the cell. Their morphology is reliant upon the balance between the diametrically opposed apparatuses responsible for the fission and fusion of mitochondrial membranes.

Fission and fusion are opposing processes whose strict balance is essential for maintaining proper mitochondrial content in daughter cells and as a mitochondrial quality control mechanism by allowing repair of damaged mitochondria [261;281;282;358;366]. Thus unbalanced fission leads to mitochondrial fragmentation and abundance of individual mitochondria while unbalanced fusion leads to tubulation. Fission and fusion are regulated by a family of evolutionarily conserved large multi-domain guanosine triphosphatases (GTPases): two outer and one inner membrane proteins, mitofusins 1 and 2 (MFN1 and 2) and optic atrophy protein 1 (OPA1), respectively [280;367] (Figure 8). In yeast, there exists only one mitofusin (Mfn), whereas is mammals, there are two. This is due to a suspected gene duplication event somewhere in its evolution [358]. However, studies have shown they are not functionally redundant [368;369].

During fission, protein kinase A activates PTEN-induced kinase-1 (PINK1), a mitochondrially-targeted serine/threonine kinase which contains an N-terminal mitochondrial localization signal [370], which phosphorylates Parkin, an E3 ubiquitin-protein ligase, and causes its translocation from the cytosol to damaged mitochondria where it promotes ubiquitination and degradation of the central fusion proteins MFN1 and MFN2 [371-373]. Numerous studies have been conducted in *Pink1* and P*arkin*

knockout models to determine their role in the fission process. Because loss-of-function mutations in either *Pink1* or *Parkin* are the foremost cause of hereditary early-onset Parkinson's disease, they have generated considerable interest in the research community. As such, it is now known that loss of *Pink1* and P*arkin* results in enlarged and swollen mitochondria and Parkin (at least) is essential for turnover of damaged mitochondria [374], that Parkin acts downstream of PINK1 in a common pathway [280] and that although their mutation results in early-onset Parkinson's, rodent models fail to recapitulate the dramatic phenotype of dopamine neuron loss seen in humans with *Pink1* or *Parkin* mutations [375], suggesting that in rodents at least, another factor plays a compensatory role. In addition to PINK1 and Parkin, dynamin-related protein-1 (Drp-1), a cytosolic GTPase, plays a key role in mitochondrial fission. Drp-1 translocates from the cytosol to mitochondria where it is believed to bind with fission receptors on the outer membrane [376]. Once bound, Drp-1 forms helical structures around the mitochondria resulting in constriction sites at which fragmentation is thought to occur [359]. Unlike *Pink1* and *Parkin*, *Drp-1* appears to be obligatory to proper fission. Viability in *Pink1* or *Parkin* mutants with a single copy of *Drp-1* also removed is dramatically reduced [280]. Further evidence of *Drp-1*'s importance is that, like *Opa1* and *Mfn*, it is conserved from yeast to mammals whereas *Pink1* and *Parkin* are only found in metazoans.

Less is known about the precise mechanics of mitochondrial fusion, but it is proposed that fusion with other mitochondria within the reticulum is vital for exchange of inner membrane space and matrix contents as well as diluting of any mtDNA mutations

between mitochondria [359] and this must be done by joining both the OM and IM of adjacent mitochondria without leakage of their contents into the cytosol. Major fusion events are mediated by OPA1, MFN1 and MFN2, which drive mitochondrial elongation, increased cristae density, and maintenance of ATP output [377;378] to sustain cell viability. OPA1 encodes a 96 amino acid GTPase that is associated with sequestration of cytochrome *c* in the mitochondria and regulation of mitochondrial fusion. OPA1 directs the fusing of the IMs. Additionally, studies have shown that not only is OPA1 required for IM fusion [360], but so is normal membrane potential [283;366;379]. MFN1 and MFN2 are outer membrane proteins that act as anti-apoptotic GTPases to protect the cell from apoptotic stimuli [380;381]. Similar to OPA1, MFN1 and 2 direct the fusion of the OMs. The mitofusins orchestrate both the tethering of adjacent mitochondria (through homo- or hetero-oligomers of their coiled-coiled domains) and the fusing of the membranes with the help of GTP hydrolysis [368;382]. Dysregulation of mitochondrial dynamics and inhibition of mitochondrial fusion has been documented in neurodegenerative diseases [383-387]; however, changes in mitochondrial dynamics have not been explored in granulosa cells previously.

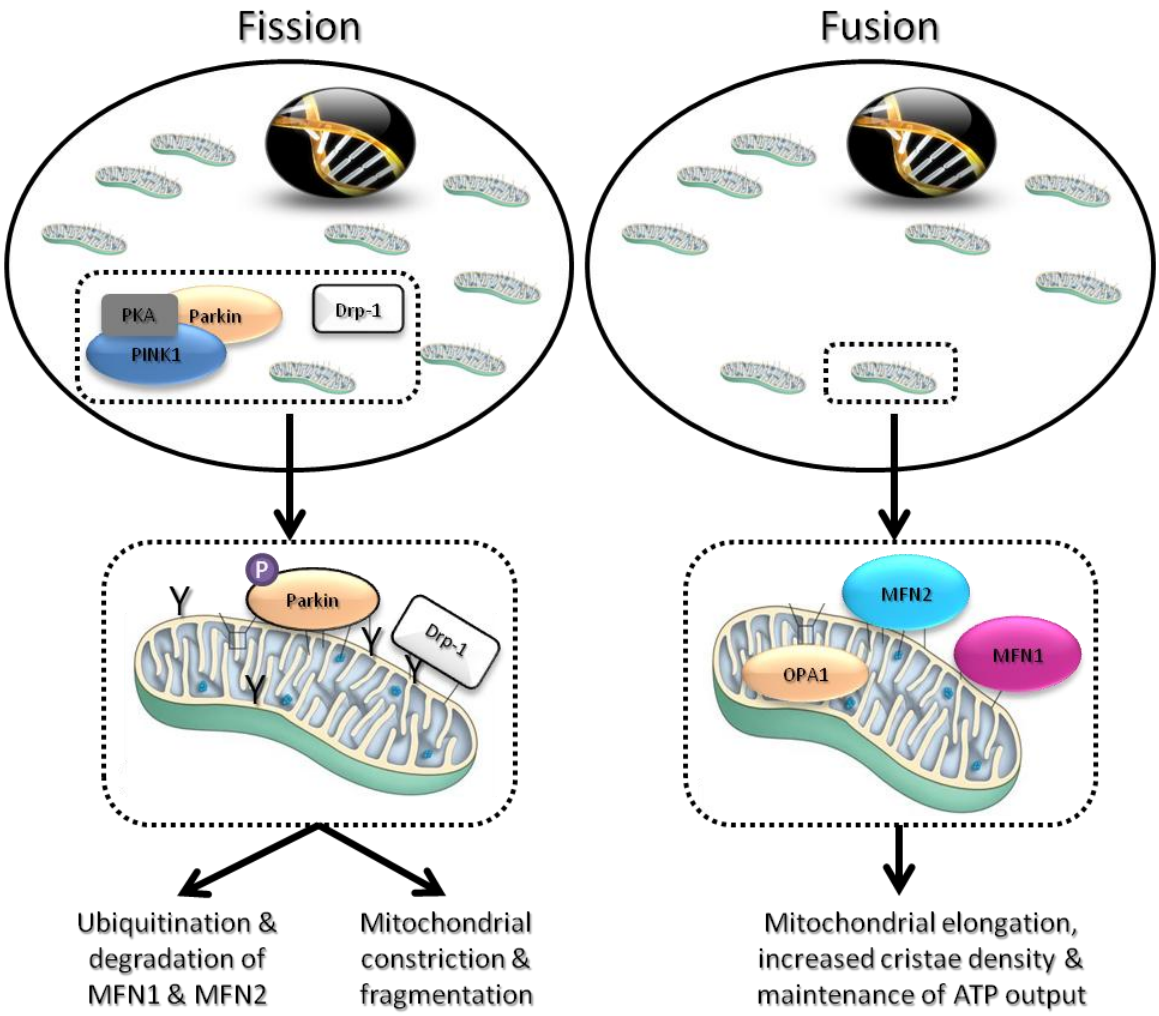

Figure 8: Mitochondrial fission and fusion.
During fission, PKA activates PINK1, which in turn phosphorylates and activates Parkin. Parkin then translocates to the mitochondria where it serves to mediate ubiquitination of the mitofusin proteins, MFN1 and MFN2, targeting them for destruction. At the same time, Drp-1 binds to hFis on the membrane of the mitochondria, forming helical structures around the mitochondria, resulting in constriction and fragmentation. During fusion, the outer membrane proteins MFN1 and MFN2 are required to form connection points between adjacent mitochondria for fusion of those membranes. Similarly, OPA1 on the inner membrane is required for the fusion of the IM, along with normal mitochondrial membrane potential. These factors serve to drive elongation of mitochondria, increase cristae density and maintain ATP output.

In addition to fission and fusion, the mitochondria employ several quality control mechanisms for maintenance of appropriate protein folding and organelle function. First, the proteolytic system within the mitochondrial IM serves to degrade unfolded membrane proteins. Next, the lysosome within the cytosol accepts transport of vesicles containing proteins from the mitochondria for degradation. And finally, the proteasome is used as a processing point for misfolded IM and OM proteins [365]. However, these quality control systems are not adequate for disposal of large cargo, namely entire mitochondria that have been irreparably damaged and cannot fuse with the reticulum to mediate repair. To combat this, a specialized form of autophagy has evolved that targets damaged or superfluous mitochondria for autophagosomal degradation, termed mitophagy [365]. It is believed that the machinery chiefly responsible for fission is also central to tagging mitochondria for mitophagy. Specifically, Parkin, through its ubiquitination of the MFNs could potentially fulfill its role both as an anti-fusion protein (by inactivating the Mfn profusion function) and as a pro-mitophagy protein (by mediating Mfn ubiquitination thereby tagging the mitochondria in which the ubiquitinated Mfn resides for destruction by autophagosomal engulfment and degradation) [388-391].

1.7 Rationale for studies completed herein

1.7.1 Rationale

Cigarette smoke is a documented reproductive toxicant, with women who smoke reporting shorter menstrual cycles, longer times to pregnancy and earlier age at menopause compared to non-smokers, suggesting an adverse effect of cigarette smoke on ovarian follicles. Despite this, the molecular mechanisms regulating its effects on the ovary are ill-defined. Therefore, the purpose of this thesis was to investigate the mechanisms underlying ovarian follicle loss following cigarette smoke exposure. The panoptic hypothesis for the studies contained herein was that cigarette smoke causes primordial follicle death via apoptosis leading to shortened reproductive lifespan. Each of the individual studies had its own specific hypothesis and was conducted in a sequential manner, each building on the outcomes of the former. The specific aims below outline in detail the explicit hypothesis and underlying rationale for each objective. Collectively, these studies enhance our understanding of the molecular mechanisms regulating cigarette smoke-induced ovarian follicle loss and identify a novel mechanism of ovarian follicle loss that may potentially be important in identifying novel therapeutic targets for fertility preservation in women exposed to this and other ovarian toxicants.

1.7.2 Specific Aim 1

The first objective of this PhD was to determine the effects of cigarette smoke exposure on the ovary and the length of exposure necessary to cause significant follicle loss using a mouse model of cigarette smoke exposure. It is well-documented that women who smoke

encounter difficulties achieving and maintaining pregnancy, decreased success with assisted reproductive technologies and experience earlier age at menopause compared to women who have never smoked. Additionally, studies using environmental toxicants have shown that ovarian follicle loss is stage-specific and time- and dose-dependent. Our model of cigarette smoke exposure employs a single dose; however, the duration of exposure is adjustable. Therefore, I hypothesized that cigarette smoke, like other reproductive toxicants, would cause ovarian follicle loss in a stage-specific and time-dependent manner.

1.7.3 Specific Aim 2

The second objective of this PhD was to measure the effects of cigarette smoke exposure on changes in markers of reactive oxygen species and oxidative stress and determine the underlying mechanism driving cigarette smoke-induced ovarian follicle loss. Results from the first study made it clear that cigarette smoke exposure resulted in significant follicle loss. Data from other landmark studies in the field of toxicology pointed to apoptosis as the mechanism by which follicles are lost, preceded by increased oxidative stress and subsequent exhaustion of the follicle pool. Cigarette smoke contains numerous oxidants and free radicals, as well as chemicals capable of inducing oxidative damage. Furthermore, mitochondria are particularly susceptible to damage by reactive oxygen species and can initiate apoptosis following oxidative stress. Therefore, I hypothesized that exposure to cigarette smoke would result in oxidative stress coupled with decreased

growth support for the growing follicles and subsequent activation of the mitochondria-mediated apoptosis pathway.

1.7.4 Specific Aim 3

Results from the first two studies showed that although cigarette smoke exposure causes significant follicle loss and oxidative stress, apoptosis is not the mechanism by which this loss is occurring. One finding in particular pointed to a potential mechanism by which ovarian follicle loss was occurring. Therefore, the third and final objective of this PhD was to measure the effects of cigarette smoke exposure on the expression levels of mitochondrial repair mechanisms and of members of a novel alternative ovarian cell death pathway, the autophagy pathway. I hypothesized that cigarette smoke exposure would result in dysregulation of mitochondrial dynamics leading to an increase in the expression of pro-autophagy cascade members culminating in the death of granulosa cells leading to ovarian follicle loss.

Chapter 2

Cigarette smoke causes follicle loss in mice ovaries at concentrations representative of human exposure

Mulligan Tuttle, AM., Stämpfli, M., and Foster WG.

This article appeared in *Human Reproduction*, 2009; 24: 1452-59.

2.1 Abstract

Background: Cigarette smoke is a documented reproductive toxicant associated with infertility and ovarian failure. However, the underlying mechanism(s) regulating the toxic effects of cigarette smoke are unknown. Therefore, we tested the hypothesis that mainstream cigarette smoke and a cigarette smoke constituent, Benzo(a)pyrene (BaP) induce apoptosis in ovarian follicles.

Methods: Mice were exposed to mainstream cigarette smoke and the ovaries were analysed for follicle loss and markers of apoptosis (TUNEL, CASP3, CASP8, BAX, BCL2, FAS and FASL). Isolated ovaries from female pups were cultured in media containing increasing concentrations of BaP (1-10000 $ng \cdot ml^{-1}$) and markers of apoptosis were quantified.

Results: Cigarette smoke exposure induced a significant reduction in the number of primordial follicles, but not growing or antral follicles compared to controls. Mainstream cigarette smoke exposure had no effect on any marker of apoptosis measured. Exposure

of ovaries to BaP *in vitro* resulted in a decrease in the pro-survival marker BCL2, but no increase in apoptosis.

Conclusions: Our data suggest that cigarette smoke-induced follicle loss is not mediated via BaP-induced apoptosis.

2.2 Introduction

Cigarette smoke is a documented reproductive toxicant that depletes ovarian follicle reserve and impairs uterine receptivity (Soares, Simon *et al.*, 2007). Delayed conception (Jick and Porter, 1977; Hughes and Brennan, 1996), decreased success in assisted reproductive technologies (Neal, Hughes *et al.*, 2005; Klonoff-Cohen, 2005) and premature ovarian failure (Baird, Hooven *et al.*, 2005) have all been reported in female smokers compared to non-smokers. While fewer Canadians are smoking today, a survey on tobacco use in Canada revealed that 14% of households reported at least one person who smoked inside the home daily (Health Canada, 2006). In the Canadian Tobacco Use Monitoring Survey, 17% of female respondents report being current smokers, consuming an average of 13.8 cigarettes/day (Health Canada, 2006). What is perhaps more troubling is that young women, aged 15-19, in their reproductive prime is the fastest growing population of smokers. In south-western Ontario alone, 36.2% of teenage girls smoke (Cohen, Evers *et al.*, 2003) and 33% of girls are regular smokers by the age of 15, according to a British study (Augood, Duckitt *et al.*, 1998). Therefore, it is imperative that we determine the mechanisms of action that explain the toxic effects of cigarette smoke on fertility.

Studies conducted in our laboratory have revealed that women exposed to cigarette smoke had greatly decreased pregnancy rates (Neal, Hughes *et al.*, 2005). We have also found that BaP is detectable in the serum and follicular fluid of women who smoke or are exposed to cigarette smoke and that treatment with BaP impairs cumulus expansion in isolated rat follicle culture experiments (Neal, Zhu *et al.*, 2008; Neal, Zhu *et al.*, 2007).

Targeted primordial follicle destruction is considered to be the most devastating effect of cigarette smoking on reproductive function, the effects of which are not detected until years after the exposure, often after ovarian failure is well established (Cortvrindt and Smitz, 2002). Premature follicle loss has been identified as a possible causative factor for infertility. A variety of toxicants increase follicle loss and are lethal to embryos; however, the mechanism of action is unknown. Previous studies have revealed that of the more than 4000 chemicals present in cigarette smoke, levels of PAHs, especially Benzo(a)pyrene, are present in levels 10-fold higher in sidestream than mainstream smoke (Lodovici, Akpan *et al.*, 2004). Benzo(a)pyrene (BaP), a member of the PAH family, a class of compounds formed by the incomplete combustion of fossil fuels and organic matter (Sagredo, Ovrebo *et al.*, 2006), is a ubiquitous environmental pollutant that possesses potent mutagenic properties. BaP is known to cause the formation of DNA adducts and is primarily activated by P450 enzymes, most notably CYP1A1 and CYP1B1, which are regulated by the Aryl hydrocarbon receptor (AhR) pathway. Upon exposure to BaP, the AhR is bound by BaP and translocates to the nucleus where it binds the aryl hydrocarbon receptor nuclear translocator (ARNT) and transcriptionally activates

genes containing the xenobiotic response element (XRE) in their promoter regions (Sagredo, Ovrebo *et al.*, 2006). Ovarian follicles of women exposed to cigarette smoke have detectable levels of BaP in the serum and follicular fluid (Neal, Zhu *et al.*, 2007). The follicles are also known to express the AhR (Thompson, Bourguet *et al.*, 2005) and are susceptible to BaP exposure.

Numerous studies have shown that exposure to environmental toxicants (ETs) results in the destruction of the follicle population, frequently in a stage-specific manner (Desmeules and Devine, 2006; Devine, Sipes *et al.*, 2004; Devine, Sipes *et al.*, 2002; Mayer, Pearsall *et al.*, 2002;Neal, Zhu *et al.*, 2008;Jurisicova, Taniuchi *et al.*, 2007b). BaP has been shown to selectively target and deplete the primordial follicle pool (Mattison, White *et al.*, 1980; Mattison and Nightingale, 1982). Similarly, VCD, a metabolite of 4-vinylcyclohexene and a solvent used in industry, induces apoptosis in primordial and primary follicles (Devine, Sipes *et al.*, 2004; Devine, Sipes *et al.*, 2002), whereas exposure to dioxin-like PCBs results in the destruction of growing follicles (Muller, Hobson *et al.*, 1978; Pocar, Brevini *et al.*, 2006), and exposure to high concentrations of non-dioxin-like PCBs, namely PCB 126 and PCB 153, results in the increased secretion of estradiol from granulosa cells and the subsequent attenuation of atretic follicle elimination (Gregoraszczuk, Sowa *et al.*, 2003). Despite the diversity of ETs shown to elicit adverse effects on ovarian function in animal models, few studies show effects in the human populations. Moreover, the decreased primary follicle numbers observed have been due to toxicological levels of these toxicants (Devine, Sipes *et al.*,

2004; Devine, Sipes *et al.*, 2002; Mayer, Pearsall *et al.*, 2002; Desmeules and Devine, 2006; Jurisicova, Taniuchi *et al.*, 2007b; Devine, Sipes *et al.*, 2001; Takai, Canning *et al.*, 2003), high dose exposures that have debatable relevance to human exposure. Therefore, experiments were designed to determine if cigarette smoke, at concentrations representative of human exposure, induces selective stage-dependent destruction of primordial and primary follicles in mouse ovaries.

2.3 Materials and Methods

2.3.1 Mice for *in vivo* studies

The ovarian effects of cigarette smoke exposure was studied in female C57BL/6 mice (6-8 weeks old) obtained from Charles River Laboratories (Montreal, PQ, Canada). Mice were maintained in polycarbonate cages with a 12-hour light-dark cycle and unlimited access to food and tap water. All animal work described in this study was conducted using protocols approved by the McMaster University Animal Research Ethics Board and follows CCAC guidelines for the use of animals in research.

2.3.2 Cigarette Smoke Exposure

Mice (n=5) were exposed to nose-only exposure whereby female mice were placed in individual exposure chambers (9 x 3 x 3 cm^3) and were exposed to two cigarettes daily (1R3 reference cigarettes; Tobacco and Health Research Institute, University of Kentucky) as described previously (Hautamaki, Kobayashi *et al.*, 1997). Cigarette smoke was delivered into the exposure chambers at a rate of 0.08 L・min^{-1}, 1 puff (20 mL) per

52 s. In an initial 2 week lead-up period, mice were exposed to one cigarette in the first week and to two cigarettes in the second week. Animals were then exposed 5 days per week for a total of 8 weeks, including the 2 week lead-up period. To control for handling, groups of mice were placed in restrainers only and exposed to room air (sham exposure, n=5). Mice were euthanised at the end of the 8 week exposure by exsanguination and ovaries were collected and placed in Hanks' Balanced Salt Solution (HBSS; Sigma Aldrich) prior to processing.

2.3.3 Histology and Immunohistochemistry

Ovaries were fixed for standard histology. Serial sections, at 4 μm thickness, were stained with haematoxylin and eosin and follicle counts were carried out as outlined below. To determine the cellular localization of the active apoptotic pathways, immunohistochemical staining was performed. Terminal deoxynucleotidyl transferase dUTP nick end labelling (TUNEL) was conducted on serial sections to determine if increased apoptosis occurred in treated versus control ovaries. Immunohistochemical staining for BAX (Santa Cruz Biotechnology, Inc., Santa Cruz, CA), BCL2 (Santa Cruz), CASP3 (Santa Cruz), CASP8 (Abcam, Cambridge, MA), FAS (Santa Cruz) and FASL (Santa Cruz) was carried out. Briefly, following rehydration, endogenous peroxidase activity was quenched and antigen retrieval was carried out using citrate buffer (pH 3.0) at 37^{o}C for 30 minutes. Sections were blocked with goat serum (for rabbit primary antibodies) or horse serum (for mouse primary antibodies). Avidin/biotin blocking was carried out prior to incubation with primary antibody (1:100) for 24h at 4^{o}C.

Immunohistochemical targets were localized using diaminobenzidine (DAB; 0.25 mg • mL^{-1} w/v; Sigma Aldrich) in PBS and counterstained using Harris' haematoxylin (Sigma Aldrich). Sections were dehydrated and cover slips were mounted using Permount. Slides were examined using an Olympus IX81 microscope at 20× and 40× magnification and images were captured using Image Pro AMS (Media Cybernetics, Silver Spring, MD, USA).

2.3.4 Ovarian volume measurements

Ovaries were sectioned and the number of sections recorded. This number was multiplied by the micron thickness of the sections to determine the length of each ovary. Serial sections were then measured at two radius points (width and length) and the mean of each was determined. The mean radii were then used in calculating the volume of the ovary along with half the length using the formula for the volume of an ellipse: $(4/3)\ \pi\ r_1\ r_2\ r_3$.

2.3.5 Follicle counts

Primordial, transitional, growing (primary and secondary) and antral follicles were identified under light microscopy using a modification of Pedersen and Peters' classification system (Pedersen and Peters, 1968). Briefly, primordial follicles were defined as having a single squamous cell layer surrounding the oocyte; transitional follicles as having a single cell layer of granulosa cells surrounding the oocyte whereby half the cells were squamous and half were cuboidal; primary follicles contained a single layer of cuboidal granulosa cells surrounding the oocyte; secondary follicles were any oocyte surrounded by two or more complete layers of granulosa cells but lacking an

antrum; and antral follicles were any oocyte surrounded by two or more complete layers of granulosa cells and having an antrum. Only follicles with a visible nucleus were counted. Every tenth section was counted from serially sectioned ovaries.

2.3.6 TUNEL staining

Serial sections were deparaffinized in xylene and rehydrated in graded ethanol solutions followed by immersion in phosphate buffered saline. An ApopTag® Plus Peroxidase In-situ cell death detection kit (Chemicon International, Temecula, CA, USA) was used. Briefly, samples were treated with proteinase K and 3% H_2O_2, and labelled with digoxygenin in a humidified chamber for 30 minutes at room temperature. Samples were then incubated with POD-horseradish peroxidase, stained with DAB and counterstained with methyl green (0.5% w/v). Ovarian sections were examined using light microscopy as described above.

2.3.7 DNA laddering

DNA was extracted from whole ovaries, from either BaP-exposed or smoke-exposed and control animals, using the QIAamp® DNA Mini kit (Qiagen Sciences, Maryland, USA). Briefly, samples were suspended in PBS, lysed in tissue lysis buffer and proteinase K and passed through a QIAamp® Spin Column to isolate DNA from other cellular components. Samples were then quantified by spectrophotometry at 260 and 280 nm. DNA was electrophoresed on a 2% w/v agarose gel in 1X TAE buffer at 60V for 1 hour. Gels were examined using the Epi Chem II Darkroom (UVP Bioimaging Systems, Upland, CA, USA).

2.3.8 Western blotting

Protein expression was measured in whole ovarian homogenates of either BaP-exposed ovaries or smoke-exposed and control animals. Protein was extracted from the whole ovaries using RIPA lysis buffer (2 mM v/v EDTA, 1% v/v Triton X-100, 0.1% w/v SDS, 150 mM NaCl, 0.5% w/v sodium deoxycholate), with phenylmethanesulphonyl fluoride (PMSF; 1mM; Sigma Aldrich) and Complete Mini EDTA-free protease inhibitors (Roche Applied Science, Laval, PQ). For Western blots, 10-20 μg of protein was loaded. SDS-PAGE was carried out with 12% acrylamide gels using a Mini-Protean II system (BioRad, Mississauga, ON) and then electro-transferred to polyvinylidene difluoride (PVDF) blotting membrane (BioRad Laboratories, Hercules, CA). Membranes were blocked overnight with 5 % w/v skim milk in TBS-T (TBS, 0.5% v/v Tween-20) at 4^{o}C and incubated for 16 h at 4^{o}C in primary antibody on a rocking platform. A loading control antibody was used. The following antibodies were used for this study (all rabbit polyclonal except BCL2, Na^{+}/K^{+}-ATPase and α-Tubulin): BAX (1:800; 23 kDa), BCL2 (1:1000; mouse monoclonal; 26 kDa), Active CASP3 (1:2000; 17 kDa; Abcam), CASP3 (1:1000; antibody reacts with both the inactive [35 kDa] and the active [17 kDa] forms), CASP8 (1:5,000; antibody reacts with both the inactive [55kDa] and the active [17 kDa] forms), FAS (1:200; 50 kDa), FASL (1:1000; antibody reacts with both the membrane bound form [40 kDa] and the soluble form [26 kDa]), Na^{+}/K^{+}-ATPase (1:5000; mouse monoclonal; 112 kDa; Abcam) and α-Tubulin (1:5000; mouse monoclonal; 55 kDa; Abcam). Following washing with TBS-T, blots were incubated with horseradish peroxidase-conjugated secondary anti-rabbit IgG (1:4000; Santa Cruz) or anti-mouse IgG

(1:4000; Amersham Biosciences, Piscataway, NJ) antibodies for 1 h at room temperature on a rocking platform. Blots were washed thoroughly in TBS-T, followed by TBS whereupon reactive protein was detected using ECL-plus chemiluminescence substrate (Amersham Biosciences) and Bioflex X-ray film (Clonex Corporation, Markham, ON). Densitometric analysis of immunoblots was performed using ImageJ 1.37v software; all proteins were quantified relative to the loading control.

2.3.9 Mice for *in vitro* studies

To evaluate the effect of BaP on the mechanisms underlying ovarian follicle loss, cultures of 4 day old ovaries were employed. Briefly, male and female C57BL/6 mice (6 weeks old) were used to generate a breeding colony. A male was placed in the cage with two females for breeding. Vaginal smears were examined daily for the presence of sperm and post coital day one was assigned to the day a sperm plug was detected. Pups at 4 days postpartum were used for the *in vitro* ovarian organ culture studies described below.

2.3.10 Ovarian organ cultures

Newborn mice were collected on post natal day 4. Mice were euthanised by cervical dislocation and ovaries were excised using a dissecting scope to ensure all ovarian tissue was collected. Ovaries were cultured in 2 mL of Waymouth medium 752/1 supplemented with 0.23 mM pyruvic acid, 50 mg・L^{-1} streptomycin sulphate, 75 mg・L^{-1} penicillin G, 3 mg・mL^{-1} BSA, and 10% fetal bovine serum. Treatments with BaP (1-10,000 ng・ml^{-1} w/v; Sigma Aldrich, Oakville, ON; n=5), vehicle control (n=5) or serum-free media (n=5)

were carried out on day 1 of culture for 6, 12 or 24 hours. The ovaries were incubated at 37^{o}C and infused with a 5% CO_2:95% air gas mixture. The media was replaced every two days. Ovaries were collected at the end of day 15 and fixed for IHC, TUNEL or frozen for protein extraction.

2.3.11 Statistical analysis

All statistical analyses were performed using SigmaStat (v.3.1, SPSS, Chicago, IL). Results are expressed as mean ± SEM. Data were checked for normality and equal variance and treatment effects were tested using t-test. A $p \leq 0.05$ was considered significant.

2.4 Results

2.4.1 General health of animals exposed to cigarette smoke

Animals were assessed at necropsy for changes in general health. Treatment had no effect on the general health of the mice, as shown by absence of signs of lacrimation, porphyria, or changes in body weight.

2.4.2 Cotinine levels in cigarette smoke exposed mice

Mice exposed to cigarette smoke for four days had serum cotinine levels that were 220-fold higher compared to controls (Mean control = 0.5 ± 0.1 ng/mL, mean smoke exposed group = 118.9 ± 15.4 ng/mL). Mice normally have a 4-5 day estrus cycle, therefore an 8 week exposure would be the equivalent of approximately 11-14 cycles, the human equivalent of one year of uninterrupted menstrual cycles; in addition, the proposed dose

is representative of a pack a day habit in humans, as previously determined by serum cotinine levels measured in mice exposed to this regimen.

2.4.3 Effects of cigarette smoke exposure on ovarian volume

At necropsy, gross inspection of ovaries revealed a difference in the size of cigarette smoke exposed ovaries compared to those from age-matched sham controls (Fig. 1a). The ovarian volume of exposed mice was 20% smaller compared to sham exposed mice, although the difference was not statistically significant (p = 0.094) (Fig. 1b).

2.4.4 Effects of cigarette smoke exposure on ovarian follicle numbers

Microscopic evaluation of ovarian sections revealed significant reductions in the number of follicles in different stages of development in ovaries of mice exposed to cigarette smoke for 8 weeks compared to the sham exposed mice. Specifically, smoke-exposed ovaries had significantly fewer follicles than sham exposed ovaries (Fig. 2a). When the follicle numbers were further separated into follicle stage, it was evident that the primordial pool of follicles was being selectively targeted for depletion (p=0.01; Fig. 2b). There were also significantly (p=0.04) fewer follicles in the transitional stage (the stage between the resting primordial pool of follicles and the primary follicles in the growing pool) compared to sham exposed mice (Fig. 2b). However, when normalized to the total number of follicles, there was a significantly (p=0.03) greater percentage (7.8%) of follicles in the transitional pool of follicles of cigarette smoke-exposed mice relative to controls (Fig. 2c). Taken together, contrary to the larger proportion of follicles in the

transitional pool of smoke exposed mice compared to controls, there were no significant differences in the number of primary, secondary or antral follicles.

2.4.5 Cell death markers in response to cigarette smoke exposure

Treatment with eight week cigarette smoke exposure did not result in an increase in apoptosis, as determined by TUNEL staining. There was no difference in the number of positively staining follicles between groups (Fig. 3). Positively stained follicles were defined as those with 10% or greater apoptotic granulosa cells. There were also no statistically significant differences in the apoptosis rates for each follicle type studied (data not shown). To further substantiate this finding, DNA gel electrophoresis was conducted to determine if DNA fragmentation could be detected (Fig. 4). There was no difference in DNA fragmentation between ovaries of the cigarette smoke and sham exposed mice. Protein expression was also unchanged for pro-apoptotic markers, BAX and Active CASP3 (Fig. 5a and 5b). Additional markers included FAS, FASL, CASP3 and CASP8; none showed a change in expression between treated and untreated groups (data not shown). However, the pro-survival factor, BCL2, was significantly (p=0.04) decreased in smoke-exposed ovaries compared to sham controls (Fig. 5c).

2.4.6 *In vitro* exposure to Benzo(a)pyrene results in decreased BCL2 expression but not an increase in apoptosis

In vitro treatment of ovaries from 4 day old pups with BaP did not result in an increase in expression of any of the pro-apoptotic markers tested above by Western blot analysis (data not shown). Additionally, DNA fragmentation was not evident in the whole

homogenates from ovaries treated with 1,000 ng · ml^{-1} BaP for 24h (Fig. 6). However, treatment of ovaries with 100 ng · ml^{-1} BaP *in vitro* for 6 h resulted in a decrease in BCL2 expression (Fig. 7a) and no overall change in BAX levels (Fig. 7b). Extending the treatment period to 24 h of culture with increasing concentrations of BaP produced BCL2 and BAX protein level results consistent with the 6 h cultures (data not shown).

2.5 Discussion

The present study was designed to test the hypothesis that cigarette smoke exposure decreases the resting pool of follicles via increased apoptosis involving the BAX/CASP3 pathway. Our study demonstrates that despite significant loss of primordial follicles following exposure to cigarette smoke for 8 weeks, this loss is not attributable to apoptosis. The results of the current study contradict previous studies that have shown that exposure to toxicological levels of PAHs, chemicals present in cigarette smoke, results in follicle loss by apoptosis (Matikainen, Toshitake *et al.*, 2002; Matikainen, Perez *et al.*, 2001b; Matikainen, Perez *et al.*, 2001a; Borman, Christian *et al.*, 2000). Our findings expand the literature by showing that physiologically relevant exposure to cigarette smoke does not increase the rates of apoptosis in the ovary, and by suggesting that there is an increased rate of follicle recruitment.

Serum cotinine, a metabolic breakdown product of nicotine, was significantly higher in mice exposed to cigarette smoke for four days, indicating that the treatment was effective in delivering CS into the systems of our test animals. Similarly, ovarian volume was

visibly decreased in exposed mice and upon measurement, was found to be 20% smaller than sham exposed mice. Although this measurement was not statistically significant, it is similar to the effects of indol-3-carbinol and tamoxifen seen by Gao and colleagues, both of which caused a decrease in ovarian weight gain (Gao, Petroff *et al.*, 2002). Conversely, neither VCD (Flaws, Doerr *et al.*, 1994) nor TCDD (Shirota, Kaneko *et al.*, 2007) treatment result in notable changes in ovarian weight of adult ovaries. This difference could be due to the different test chemicals, doses or exposure times employed.

Despite the decrease in ovarian size, both groups exhibited follicles at all stages of development and had visible degenerating corpora lutea, as seen by microscopic inspection, indicating that ovulation was taking place. However, when individual follicles were counted, there was a significant decrease in the total number of follicles present in ovaries exposed to cigarette smoke. Previous work has attributed toxicant-induced follicle loss to apoptosis (Jurisicova, Taniuchi *et al.*, 2007a; Matikainen, Perez *et al.*, 2001a; Matikainen, Toshitake *et al.*, 2002; Robles, Morita *et al.*, 2000; Kim, Chung *et al.*, 2008). In the study conditions explored here, however, no apparent increase in apoptosis was detected. TUNEL assays revealed that there was an equivalent amount of apoptosis occurring in smoke-exposed ovaries as was taking place in sham ovaries. In addition, electrophoresis gels run to examine the extent of DNA laddering failed to show an increase in apoptosis in any of the treatments administered, *in vivo* or *in vitro*. Finally, Western blot analysis of the expression of proteins previously shown to be up-regulated in ovaries treated with toxicants (active CASP3 (Devine, Sipes *et al.*, 2002; Desmeules

and Devine, 2006), BAX, Caspase 2, CASP3, (Takai, Canning *et al.*, 2003) and BCL2 (Flaws, Marion *et al.*, 2006)) were unaffected by treatments in the current study. Our findings suggest that a decreased growth support leading to an abbreviated estrous cycle and thus an enhanced rate of follicle recruitment may be the underlying cause of follicle demise rather than apoptosis. In previous experiments carried out in our laboratory, inclusion of BaP in the culture medium of *in vitro* isolated rat follicle culture resulted in the inhibition of follicle growth. BaP at 1.5 ng • ml^{-1}, a concentration representative of levels measured in human ovarian follicular fluid, resulted in the failure of cumulus cells to expand compared to controls (Neal, Zhu *et al.*, 2007). Similarly, treatment of isolated follicles *in vitro* with BaP resulted in a concentration-dependent decrease in estradiol (E_2) concentrations in spent media. Disruption of E_2 production may be responsible for the lack of follicle growth contributing to a shorter estrous cycle, allowing more cycles/year thereby aging these ovaries faster than sham ovaries. This hypothesis is supported by the lack of an increase in the number of growing follicles. Further support for this hypothesis is derived from epidemiological studies in women who smoke whose menstrual cycles are also shortened (Windham, Elkin *et al.*, 1999).

Contrary to the *in vivo* studies, *in vitro* dosing of 4 day old ovaries resulted in a change in BCL2 expression. When ovaries were incubated for 6-24h in media containing 100 ng • ml^{-1} of BaP, expression of BCL2 was decreased, although BAX expression went unchanged. Despite the maintenance of BAX expression at control ovary levels, a shift in the BAX:BCL2 ratio was seen, resulting in an environment favouring apoptosis. This

change in the apoptotic ratio may account for some of the loss of these follicles *in vitro*, but it appears to be a concentration-dependent phenomenon and was only detectable at concentrations above 100 ng.ml^{-1}, a concentration we believe to be much greater than those achieved *in vivo*. The concentration of BaP in the serum and follicular fluid of women who smoke (1.32 +/- 0.68 ng・ml^{-1}) or are exposed to second-hand smoke (0.05 +/- 0.01 ng・ml^{-1}) is significantly lower than the concentrations at which we saw effects on follicle apoptosis (100 ng・ml^{-1}) in this experiment. Furthermore, we have shown that concentrations equivalent to the levels measured in human serum and follicular fluid are sufficient to impair follicle expansion and survival in individual follicle culture experiments (Neal, Zhu *et al.*, 2007; Neal, Zhu *et al.*, 2008). However, it is likely that the difference in dose required to detect a response is related to a number of factors. First, individual follicles in culture are surrounded by a thecal cell layer only, whereas follicles in intact ovaries used in our experiments here are surrounded by stroma and other follicles. Additionally, the intact ovaries have a tunica surrounding the ovary, a tough membrane that likely obstructs BaP in the media from reaching the follicles within the ovary. Hence, the actual concentration of BaP capable of exerting an effect on the follicles within the intact ovary may be much lower than 100 ng・ml^{-1}. Follicular fluid measurements of BaP were not conducted in this study, and as such, this hypothesis cannot be tested at present. Future studies will include measurement of BaP in the follicular fluid of intact ovaries cultured in BaP-containing media. To determine if BaP is reaching the ovary, future work conducted will include serum measures of BaP and testing for the formation of DNA adducts in the ovaries of exposed mice.

The findings of our study show that exposure to cigarette smoke, at exposure concentrations representative of human exposure, results in significant primordial follicle loss. This loss, however, does not appear to be due to apoptosis, as has been shown to be the case when toxicological levels were employed. Our data provide further support to a growing body of evidence that cigarette smoke is a reproductive toxicant that results in premature ovarian failure.

2.6 Acknowledgements

Funding support for this study was provided by CIHR operating grant MOP-81178 to WGF. The CIHR and the Ontario Women's Health Council provided salary support for Dr. Foster, and Ms. Anne Mulligan Tuttle is the recipient of a CIHR Strategic Training Program in Tobacco Research (STPTR) scholarship and an Ashley Studentship from the Tobacco Council of Canada.

2.7 Reference List

1. Augood C, Duckitt K, and Templeton AA (1998) Smoking and female infertility: a systematic review and meta-analysis. Hum Reprod, 13, 1532-1539.

2. Baird WM, Hooven LA, and Mahadevan B (2005) Carcinogenic polycyclic aromatic hydrocarbon-DNA adducts and mechanism of action. Environ Mol Mutagen, 45, 106-114.

3. Borman SM, Christian PJ, Sipes IG, and Hoyer PB (2000) Ovotoxicity in female Fischer rats and B6 mice induced by low-dose exposure to three polycyclic aromatic hydrocarbons: comparison through calculation of an ovotoxic index. Toxicol Appl Pharmacol, 167, 191-198.

4. Cohen B, Evers S, Manske S, Bercovitz K, and Edward HG (2003) Smoking, physical activity and breakfast consumption among secondary school students in a southwestern Ontario community. Can J Public Health, 94, 41-44.

5. Cortvrindt RG and Smitz JE (2002) Follicle culture in reproductive toxicology: a tool for in-vitro testing of ovarian function? Hum Reprod Update, 8, 243-254.

6. Desmeules P and Devine PJ (2006) Characterizing the ovotoxicity of cyclophosphamide metabolites on cultured mouse ovaries. Toxicol Sci, 90, 500-509.

7. Devine PJ, Sipes IG, and Hoyer PB (2004) Initiation of delayed ovotoxicity by in vitro and in vivo exposures of rat ovaries to 4-vinylcyclohexene diepoxide. Reprod Toxicol, 19, 71-77.

8. Devine PJ, Sipes IG, and Hoyer PB (2001) Effect of 4-vinylcyclohexene diepoxide dosing in rats on GSH levels in liver and ovaries. Toxicol Sci, 62, 315-320.

9. Devine PJ, Sipes IG, Skinner MK, and Hoyer PB (2002) Characterization of a rat in vitro ovarian culture system to study the ovarian toxicant 4-vinylcyclohexene diepoxide. Toxicol Appl Pharmacol, 184, 107-115.

10. Flaws JA, Doerr JK, Sipes IG, and Hoyer PB (1994) Destruction of preantral follicles in adult rats by 4-vinyl-1-cyclohexene diepoxide. Reprod Toxicol, 8, 509-514.

11. Flaws J, Marion S, Miller K, Christian P, Babus J, and Hoyer P (2006) Effect of bcl-2 overexpression in mice on ovotoxicity caused by 4-vinylcyclohexene. Toxicol Appl Pharmacol, 215, 1, 51-56.

12. Gao X, Petroff B, Oluola O, Georg G, Terranova P, and Rozman K (2002) Endocrine disruption by indole-3-carbinol and tamoxifen: Blockage of ovulation. Toxicol Appl Pharmacol, 183, 3, 179-188.

13. Gregoraszczuk EL, Sowa M, Kajta M, Ptak A, and Wojtowicz A (2003) Effect of PCB 126 and PCB 153 on incidence of apoptosis in cultured theca and granulosa cells collected from small, medium and large preovulatory follicles. Reprod Toxicol, 17, 465-471.

14. Hautamaki RD, Kobayashi DK, Senior RM, and Shapiro SD (1997) Requirement for macrophage elastase for cigarette smoke-induced emphysema in mice. Science, 277, 2002-2004.

15. Health Canada (2006) Canadian Tobacco Use Monitoring Survey.

16. Hughes EG and Brennan BG (1996) Does cigarette smoking impair natural or assisted fecundity? Fertil Steril, 66, 679-689.

17. Jick H and Porter J (1977) Relation between smoking and age of natural menopause. Report from the Boston Collaborative Drug Surveillance Program, Boston University Medical Center. Lancet, 1, 1354-1355.

18. Jurisicova A, Taniuchi A, Li H, Shang Y, Antenos M, Detmar J, Xu J, Matikainen T, Benito HA, Nunez G et al (2007) Maternal exposure to polycyclic aromatic hydrocarbons diminishes murine ovarian reserve via induction of Harakiri. J Clin Invest, 117, 3971-3978.

19. Kim J, Chung J-Y, Park J-E, Lee S, Kim Y-J, Cha M-S, Han M, Lee H-J, Yoo Y, and Kim J-M (2008) Benzo[a]pyrene induces apoptosis in RL95-2 human endometrial cancer cells by cytochrome P450 1A1 activation Endocrinology, 148, 10, 5112-22.

20. Klonoff-Cohen H (2005) Female and male lifestyle habits and IVF: what is known and unknown. Hum Reprod Update, 11, 179-203.

21. Lodovici M, Akpan V, Evangelisti C, and Dolara P (2004) Sidestream tobacco smoke as the main predictor of exposure to polycyclic aromatic hydrocarbons. J Appl Toxicol, 24, 4, 277-281.

22. Matikainen T, Perez G, Jurisicova A, Pru J, Schlezinger J, Ryu H-Y, Laine J, Sakai T, Korsmeyer S, Casper R et al (2001a) Aromatic hydrocarbon receptor-driven *Bax* gene expression is required for premature ovarian failure caused by biohazardous environmental chemicals. Nat Genet, 28, 4, 355-360.

23. Matikainen T, Perez G, Zheng T, Kluzak T, Rueda B, Flavells R, and Tilly J (2001b) Caspase-3 gene knockout defines cell lineage specificity for programmed cell death signaling in the ovary. Endocrinology, 142, 6, 2468-2480.

24. Matikainen T, Toshitake M, Morita Y, Perez G, Korsmeyer S, Sherr D, and Tilly J (2002) Ligand activation of the aromatic hydrocarbon receptor transcription factor drives Bax-dependent apoptosis in developing fetal ovarian germ cells. Endocrinology, 143, 2, 615-620.

25. Mattison DR and Nightingale MS (1982) Oocyte destruction by polycyclic aromatic hydrocarbons is not linked to the inducibility of ovarian aryl hydrocarbon (benzo(a)pyrene) hydroxylase activity in (DBA/2N X C57BL/6N) F1 X DBA/2N backcross mice. Pediatr Pharmacol (New York), 2, 1, 11-21.

26. Mattison DR, White NB, and Nightingale MR (1980) The effect of benzo(a)pyrene on fertility, primordial oocyte number, and ovarian response to pregnant mare's serum gonadotropin. Pediatr Pharmacol (New York), 1, 2, 143-151.

27. Mayer LP, Pearsall NA, Christian PJ, Devine PJ, Payne CM, McCuskey MK, Marion SL, Sipes IG, and Hoyer PB (2002) Long-term effects of ovarian follicular depletion in rats by 4-vinylcyclohexene diepoxide. Reprod Toxicol, 16, 775-781.

28. Muller WF, Hobson W, Fuller GB, Knauf W, Coulston F, and Korte F (1978) Endocrine effects of chlorinated hydrocarbons in rhesus monkeys. Ecotoxicol Environ Saf, 2, 161-172.

29. Neal MS, Hughes EG, Holloway AC, and Foster WG (2005) Sidestream smoking is equally as damaging as mainstream smoking on IVF outcomes. Hum Reprod, 20, 2531-2535.

30. Neal MS, Zhu J, and Foster WG (2008) Quantification of benzo[a]pyrene and other PAHs in the serum and follicular fluid of smokers versus non-smokers. Reprod Toxicol, 25, 100-106.

31. Neal MS, Zhu J, Holloway AC, and Foster WG (2007) Follicle growth is inhibited by benzo-[a]-pyrene, at concentrations representative of human exposure, in an isolated rat follicle culture assay. Hum Reprod, 22, 961-967.

32. Pedersen T and Peters H (1968) Proposal for a classification of oocytes and follicles in the mouse ovary. J Reprod Fertil, 17, 555-557.

33. Pocar P, Brevini TA, Antonini S, and Gandolfi F (2006) Cellular and molecular mechanisms mediating the effect of polychlorinated biphenyls on oocyte in vitro maturation. Reprod Toxicol, 22, 242-249.

34. Robles R, Morita Y, Mann K, Perez G, Yang S, Matikainen T, Sherr D, and Tilly J (2000) The aryl hydrocarbon receptor, a basic helix-loop-helix transcription factor of the PAS gene family, is required for normal ovarian germ cell dynamics in the mouse. Endocrinology, 141, 1, 450-453.

35. Sagredo C, Ovrebo S, Haugen A, Fujii-Kuriyama Y, Baera R, Botnen I, and Mollerup S (2006) Quantitative analysis of benzo[a]pyrene biotransformation and adduct formation in Ahr knockout mice. Toxicol Lett, 167, 3, 173-182.

36. Shirota M, Kaneko T, Okuyama M, Sakurada Y, Shirota K, and Matsuki Y (2007) Internal dose-effects of 2,3,7,8-tetrachlorodibenzo-p-dioxin (TCDD) in gonadotropin-primed weanling rat model. Arch Toxicol, 81, 261-269.

37. Soares SR, Simon C, Remohi J, and Pellicer A (2007) Cigarette smoking affects uterine receptiveness. Hum Reprod, 22, 543-547.

38. Takai Y, Canning J, Perez GI, Pru JK, Schlezinger JJ, Sherr DH, Kolesnick RN, Yuan J, Flavell RA, Korsmeyer SJ et al (2003) Bax, caspase-2, and caspase-3 are required for ovarian follicle loss caused by 4-vinylcyclohexene diepoxide exposure of female mice in vivo. Endocrinology, 144, 69-74.

39. Thompson KE, Bourguet SM, Christian PJ, Benedict JC, Sipes IG, Flaws JA, and Hoyer PB (2005) Differences between rats and mice in the involvement of the aryl hydrocarbon receptor in 4-vinylcyclohexene diepoxide-induced ovarian follicle loss. Toxicol Appl Pharmacol, 203, 114-123.

40. Windham GC, Elkin EP, Swan SH, Waller KO, and Fenster L (1999) Cigarette smoking and effects on menstrual function. Obstet Gynecol, 93, 59-65.

2.8 Figures

A

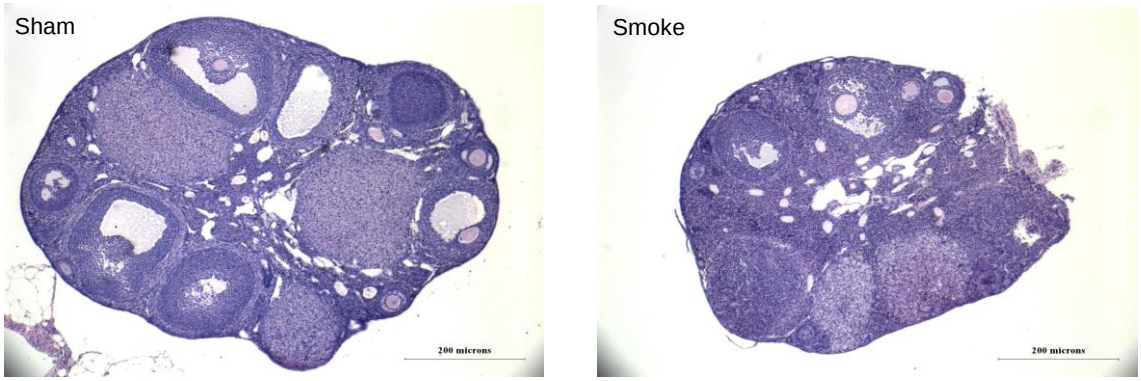

B

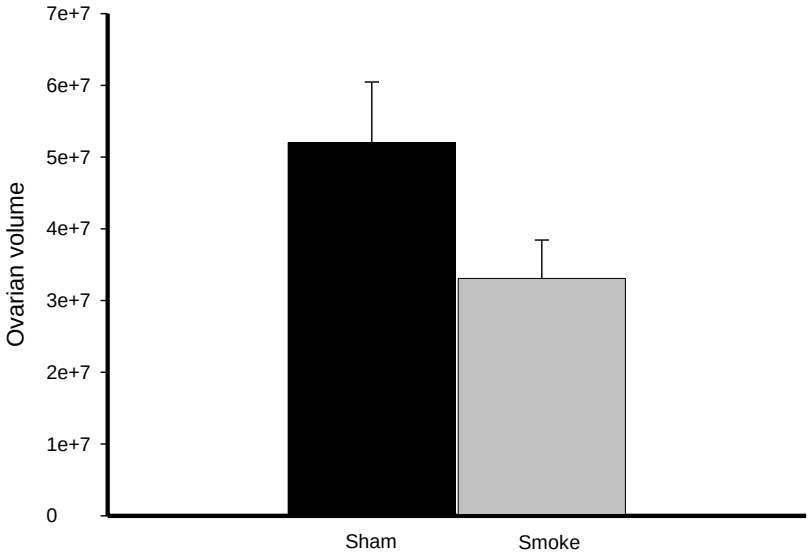

Figure 1.
Representative photomicrographs of H&E stained ovaries showing that **(A)** follicles at all stages of development were present in ovaries from mice with either sham (n=5) or cigarette smoke exposure (n=5). **(B)** Ovarian volume in mice exposed to cigarette smoke was 20% smaller compared to sham-exposed mice although statistical significance could not be shown.

A

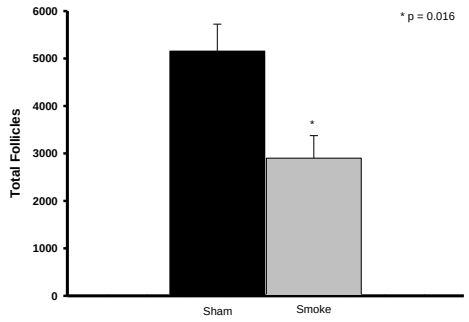
* p = 0.016
Total Follicles
6000
5000
4000
3000
2000
1000
0
*
Sham
Smoke

B

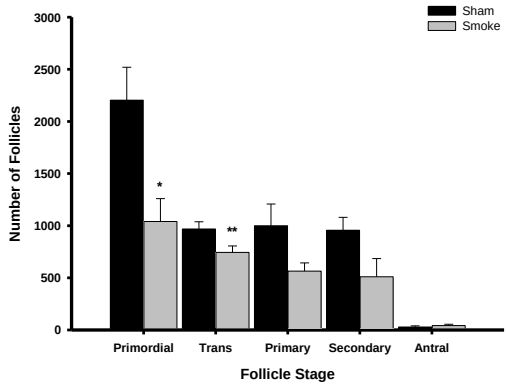
Sham
Smoke
Number of Follicles
3000
2500
2000
1500
1000
500
0
*
**
Primordial
Trans
Primary
Secondary
Antral
Follicle Stage

C

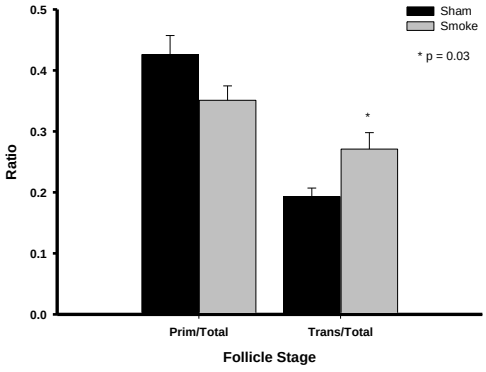
Sham
Smoke
* p = 0.03
Ratio
0.5
0.4
0.3
0.2
0.1
0.0
*
Prim/Total
Trans/Total
Follicle Stage

Figure 2.
The number of follicles was determined in serial sections of ovaries from sham (n=5) and cigarette smoke-exposed (n=5) mice. **(A)** The total follicle number in ovaries from smoke-exposed mice was significantly (* $p < 0.016$) lower than in sham-exposed mice. **(B)** Ovaries from smoke-exposed mice had significantly fewer primordial (* $p = 0.01$) and transitional (** $p = 0.04$) follicles than the sham exposure group. **(C)** Ovaries from smoke-exposed mice had a significantly (* $p = 0.03$) higher percentage of follicles in transition between the resting and growing pools than ovaries from the sham exposure group. Overall treatment effects were determined by t-test.

A

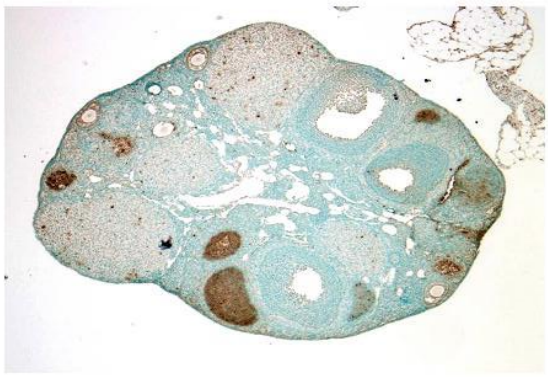

B

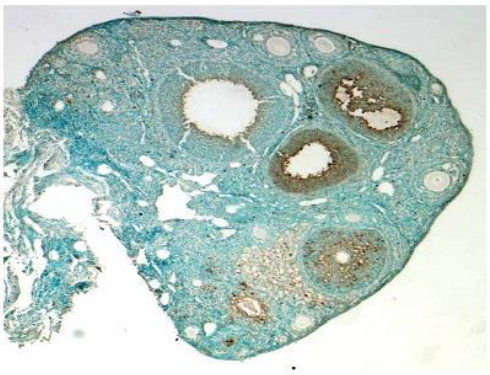

Figure 3.
Representative photomicrographs of TUNEL stained ovarian sections for apoptosis. There was no difference in the number of apoptotic follicles in ovaries from the **(A)** sham (n=5) compared to **(B)** smoke-exposed (n=5) mice.

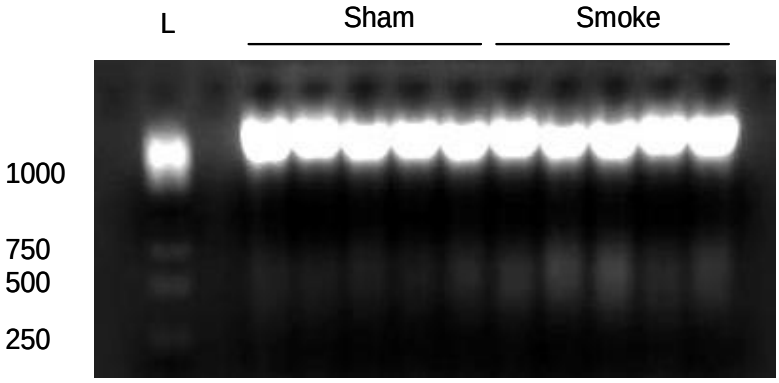
L
Sham
Smoke
1000
750
500
250

Figure 4.
There was no detectable increase in apoptosis as determined by DNA laddering in ovaries from smoke-exposed (n=5) compared to ovaries from sham-exposed mice (n=5). Marker sizes are depicted in base pairs.

A

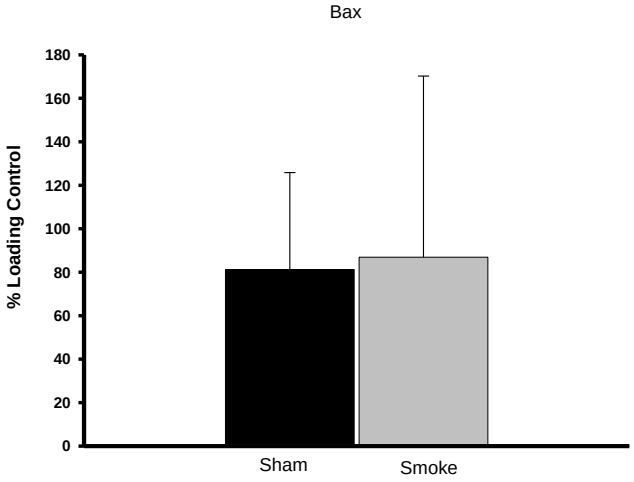
Bax
% Loading Control
180
160
140
120
100
80
60
40
20
0
Sham
Smoke

B

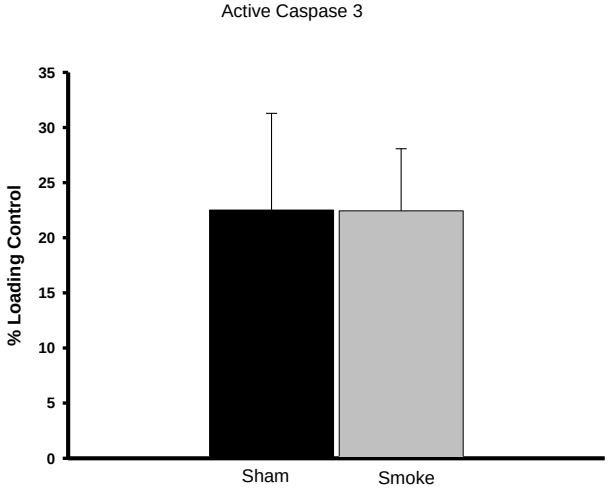
Active Caspase 3
% Loading Control
35
30
25
20
15
10
5
0
Sham
Smoke

C

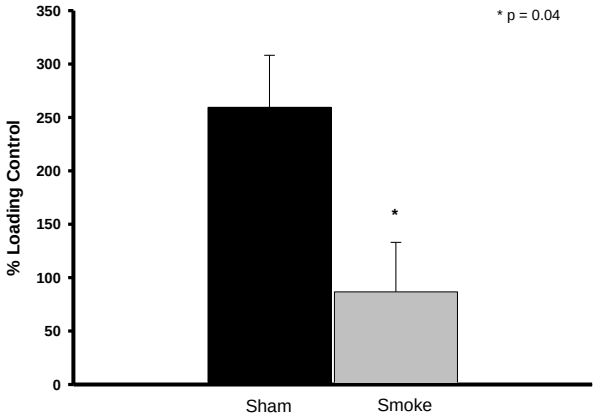
Bcl-2
* p = 0.04
% Loading Control
350
300
250
200
150
100
50
0
*
Sham
Smoke

Figure 5.
Western blot analysis of pro-apoptotic and pro-survival proteins was performed on **w**hole ovary homogenates from sham (n=5) and smoke-exposed mice (n=5). Expression of **(A)** BAX and **(B)** Active CASP3 were unchanged in eight week exposed mice; however, **(C)** BCL2 levels were significantly decreased in exposed mice compared to age-matched controls ($p = 0.04$).

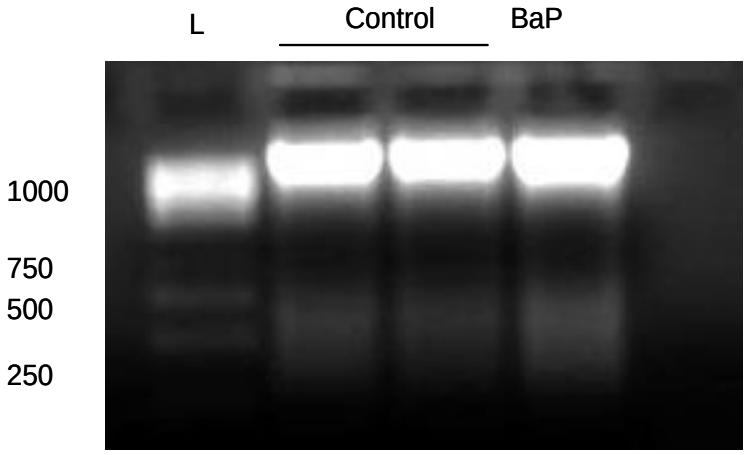
L
Control
BaP
1000
750
500
250

Figure 6.
Representative gel of DNA laddering for apoptosis in *in vitro* studies. There was no change in apoptosis in BaP-treated ovaries (1000 ng · ml^{-1} for 24h; n=5)) compared to control ovaries (n=5). Marker sizes are depicted in base pairs.

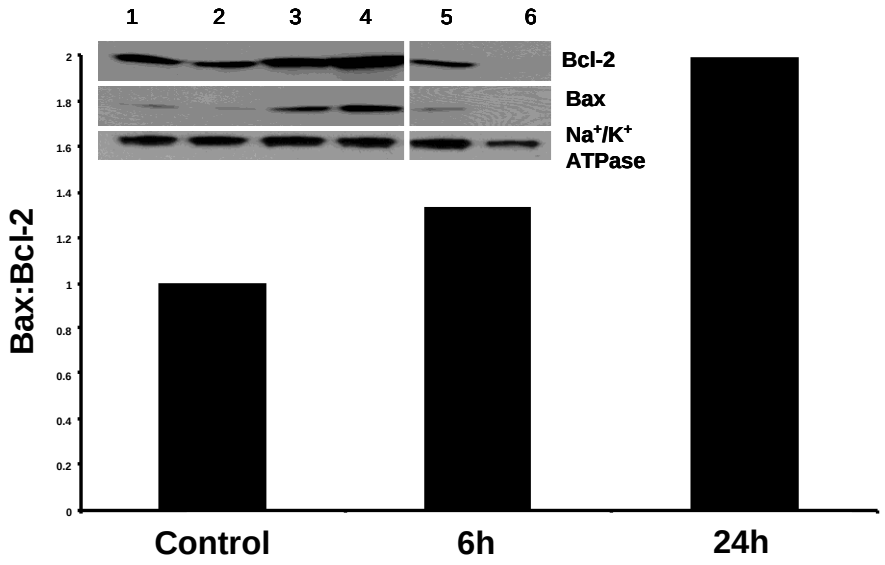
1
2
3
4
5
6
Bcl-2
Bax
Na+/K+
ATPase
Bax:Bcl-2
2
1.8
1.6
1.4
1.2
1
0.8
0.6
0.4
0.2
0
Control
6h
24h

Figure 7.
Representative immunoblots prepared from homogenates of four day old ovaries demonstrating an increase in (a) BCL2 protein levels and (b) no consistent change in BAX protein levels following treatment with increasing concentrations of BaP (lanes 1- 6 are 0, 1, 10, 100, 1,000 and 10,000 ng BaP/ml) for 6 h. Densitometric analysis of immunoblots was performed and BCL2 and BAX protein expression levels were quantified relative to the β-actin loading control with the corresponding results shown in the accompanying graphs.

Chapter 3

Cigarette Smoke Exposure Leads to Follicle Loss via an Alternative Ovarian Cell Death Pathway in a Mouse Model

Gannon, AM., Stämpfli, MR., and Foster, WG.

This article appeared in *Toxicological Sciences*, 2012; 125(1): 274-84.

3.1 Abstract

Cigarette smoking among reproductive-aged women is increasing worldwide. Cigarette smoking is a lifestyle behavior associated with important adverse health effects including subfertility and premature ovarian failure. We previously demonstrated that cigarette smoke (CS) exposure in mice decreases the primordial follicle pool; however, the mechanism of action is largely unknown. Therefore, the present study was designed to elucidate the mechanisms underlying CS exposure–induced ovarian follicle loss. CS exposure induced a significant decrease in the relative ovarian weight and the number of primordial and growing follicles. Oxidative stress, as shown by increased Hsp25 and decreased superoxide dismutase 2 protein expression, was found in mice exposed to CS for 8 weeks. Exposure decreased BCL2 but failed to induce apoptosis. An increased number of autophagosomes in granulosa cells of ovarian follicles together with increased expression of Beclin 1 and microtubule-associated protein light chain 3, key regulatory proteins in the autophagy (Atg) pathway, was found in CS exposed mice compared with the control group. Taken together, our results suggest that CS exposure does not induce apoptosis but rather activates the Atg pathway ultimately leading to ovarian follicle loss.

We further postulate that Atg is a novel mechanism of toxicant-induced ovarian follicle loss.

3.2 Introduction

Of the many environmental toxicants and lifestyle factors known to affect fertility and ovarian function, cigarette smoking is potentially the most clinically relevant and preventable toxic exposure in women (Dechanet et al., 2010; Sadeu et al., 2010). Although cigarette smoking is declining in men, the number of women and teenage girls who smoke is increasing, becoming a global health issue (World Health Organization, 2007, 2008). Approximately 250 million women worldwide are daily smokers (World Health Organization, 2008) and 30% of reproductive age women in the United States are smokers (Woodruff et al., 2011), whereas in Canada, approximately 17% of women are current smokers, smoking an average of 14.0 cigarettes/day (Health Canada, 2003, 2009). Moreover, a survey of high school students in Southwestern Ontario revealed that 36.2% of teenage girls smoke (Cohen et al., 2003). Regrettably, most women remain unaware of the adverse effects of cigarette smoking on fertility (Roth and Taylor, 2001). Our prior studies revealed that women exposed to cigarette smoke (CS) had decreased implantation (12–12.6% for those exposed to CS vs. 25% for nonsmokers) and pregnancy rates (19.4–20% for those exposed to CS vs. 48.3% for nonsmokers) (Neal et al., 2005). Longer time-to-pregnancy, reduced *in vitro* fertilization success rates, altered ovarian steroidogenesis, depleted ovarian reserves, impaired oocyte function and viability, and earlier mean age of menopause have all been documented in women who smoke versus non-smokers (Baird

et al., 2005; Crha et al., 2001; Curtis et al., 1997; El-Nemr et al., 1998; Freour et al., 2008; Fuentes et al., 2010; Hughes and Brennan, 1996; Hughes et al., 1994; Jick and Porter, 1977; Neal et al., 2005; Rosevear et al., 1992; Rowlands et al., 1992; Sharara et al., 1994; Sterzik et al., 1996; Van Voorhis et al., 1996; Waylen et al., 2009; Weigert et al., 1999; Zenzes et al., 1995; Zenzes et al., 1997; Zenzes, 2000), each of which has enormous health, emotional, and financial consequences. Although it is well documented that cigarette smoking depletes the ovarian follicle reserve in women (Soares et al., 2007) and mice (Tuttle et al., 2009), the mechanism underlying ovarian follicle loss in women who smoke remains unknown.

The ovary is a dynamic organ whose main features include steroidogenesis and cyclical recruitment of a cohort of follicles from the primordial pool of follicles (Knight and Glister, 2006; Themmen, 2005). During fetal development (in humans), or shortly after birth (in mice), the total lifetime supply of primordial follicles is established. The primordial follicle pool is gradually depleted through a repetitive process of recruitment, selection of a dominant follicle, and ovulation (Hillier, 2001; Knight and Glister, 2006). Nondominant follicles are lost through atresia, which is thought to be driven by apoptosis (Flaws et al., 2001; Tilly, 1998). This process is tightly regulated and can easily be disrupted by lifestyle and environmental toxicants.

Animal studies have shown that exposure to relatively high concentrations of environmental toxicants, compared with human exposure, results in the destruction of the

follicle population, often in a stage-specific manner (Detmar et al., 2008; Devine et al., 2002; Devine et al., 2004; Jurisicova et al., 2007; Neal et al., 2008; van Beek et al., 2007). Although some environmental toxicants disrupt intra-ovarian signaling, others increase follicle atresia, thereby depleting the follicle pool prematurely. Animal models have confirmed that environmental toxicants destroy follicles in a stage-specific manner. Exposure to polychlorinated biphenyls results in the destruction of growing follicles (Muller et al., 1978; Pocar et al., 2006), whereas 4-vinylcyclohexene diepoxide, a metabolite of 4-vinylcyclohexene and a solvent used in industry, induces apoptosis in primordial and primary follicles (Devine et al., 2002; Devine et al., 2004). Benzo(a)pyrene (BaP), a polycyclic aromatic hydrocarbon (PAH) and constituent of CS, also depletes the primordial follicle pool (Mattison et al., 1980; Mattison and Nightingale, 1982). Primordial follicle destruction is considered to be the most disastrous, as the effects of it are not detected until years after the exposure, often after ovarian failure is well established (Cortvrindt and Smitz, 2002). However, the follicle destruction seen in these animal studies is invariably due to toxicological concentrations (Desmeules and Devine, 2006; Devine et al., 2001, 2002, 2004; Jurisicova et al., 2007; Mayer et al., 2002; Takai et al., 2003) that are not representative of human exposure. In earlier animal studies, BaP exposure was found to selectively destroy the follicles in the resting pool (Mattison and Thorgeirsson, 1978) leading to speculation that a similar exhaustion of the resting pool was occurring in women who smoke, culminating in premature menopause (Mattison and Thorgeirsson, 1978; Westhoff et al., 2000). Moreover, a prior study also demonstrated that a relatively high concentration of BaP (1 mg/Kg/week for 6 weeks)

increased the expression of the *harakiri*, a BCL2 interacting protein (*Hrk*) (Jurisicova et al., 2007). However, we note that aryl hydrocarbon receptor (AhR) ligand–induced apoptosis may be both tissue dependent and concentration dependent. Unlike the results above, treatment of pregnant mice with high concentrations of BaP and 7,12-dimethylbenz[a]anthracene (DMBA) (1 mg/Kg each/week for 6 weeks) inhibited apoptosis in the murine placenta (Detmar et al., 2008). In this study, treatments increased FASL and XIAP expression but decreased BAX and apoptosis in the placenta, suggesting tissue specificity. Moreover, developmental exposure to the AhR ligand 2,3,7,8-tetrachlorodibenzo-*p*-dioxin (TCDD) is associated with vaginal dysmorphogenesis in mice through attenuated apoptosis (Gray and Ostby, 1995).

Therefore, we postulate that AhR-mediated effects on apoptosis are also target tissue dependent. In our studies, we found a significant loss of follicles at all stages of development in mice exposed to CS but exposure did not activate either the intrinsic or the extrinsic apoptosis pathways as shown by absence of an effect on terminal deoxynucleotide transferase dUTP nick end labeling (TUNEL), DNA laddering, and activated CASP3 or CASP8 and CASP9 expression versus controls (Tuttle et al., 2009). Our results diverge from those of prior studies (Jurisicova et al., 2007; Matikainen et al., 2001) using profoundly higher concentrations of BaP than are found in CS. In addition, treatment of 4-day-old mouse ovaries *in vitro* with BaP decreased BCL2 protein expression while BAX remained unchanged, suggesting a concentration-dependent effect of CS and BaP exposure on ovarian follicle loss and apoptosis (Tuttle et al., 2009). We

suggest that prior studies showing evidence of PAH-induced follicle destruction via BAX activation are phenomenological and not relevant to human health because of the high concentrations of BaP and DMBA used. Finally, mice lacking both the proapoptosis members *Bax* and the *Bak* are completely resistant to apoptosis; yet cell death proceeded normally with the appearance of autophagosomes and autolysosomes (Shimizu et al., 2004). Nonapoptotic cell death in these mice was dependent on the autophagic proteins ATG5 and BECN1. Disassociation of BECN1 from BCL2/BCL2L1 in the endoplasmic reticulum (ER) but not the mitochondria is a key driver of autophagy (Atg) (Maiuri et al., 2010).

Atg is an evolutionarily conserved process in eukaryotes, which translates to ‘‘self-eating,’’ and involves the cytoplasmic sequestering of cellular debris and organelles inside a double-membrane vesicle, termed an autophagosome, which is delivered to the lysosome for degradation (Mizushima and Levine, 2010; Szegezdi et al., 2009; Yang and Klionsky, 2010). Atg is a fundamental cellular process that removes long-lived proteins and damaged organelles (mitochondria and ER) through lysosomal degradation. Key regulatory steps involve induction of Atg via nutrient starvation, genotoxic agents, or oxidative stress (Bursch, 2001; Vilser et al., 2010), which leads to activation of Beclin 1 and membrane nucleation. Beclin 1 is part of the class III phosphoinositide 3-kinase complex and is crucial for Atg but is inhibited by BCL2 (Liang et al., 1999, 2001; Pattingre et al., 2005). During the autophagic process, microtubule-associated protein light chain 3 (LC3), the mammalian homologue of yeast Atg8, is processed from LC3-I

to LC3-II and is involved in the sequestration of organelles in the autophagosome and can be found in the membrane of the autophagosome. Mechanisms regulating cross talk between the apoptosis and Atg pathways are unclear; however, we note that BCL2 is at the interface between both pathways and emerging studies have identified Atg as an important alternative pathway of cell death in mammalian cells including human and rodent granulosa cells (Choi et al., 2010; Gawriluk et al., 2011; Vilser et al., 2010). However, the relevance of Atg to granulosa cell death and toxicant-induced changes in ovarian function are completely unexplored. Hence, we hypothesized that CS exposure would induce ovarian follicle loss via Atg rather than apoptosis. Therefore, the present study was designed to elucidate the mechanism(s) underlying follicle loss following CS exposure. The exposure protocol used in our prior study (Tuttle et al., 2009) delivers a dose of CS that results in a serum cotinine (the metabolite of nicotine) concentration that is representative of that seen in women who smoke a pack of cigarettes per day.

3.3 Materials and Methods

3.3.1 Ethics statement

All animal work described in this study was conducted using protocols approved by the McMaster University Animal Research Ethics Board and is in accordance with the Canadian Council for Animal Care guidelines for the use of animals in research.

3.3.2 Animals

The ovarian effects of CS exposure were studied in female C57BL/6 mice (8 weeks old at the start of exposure) obtained from Charles River Laboratories (Montreal, PQ, Canada). Mice were maintained in groups of three to five mice per cage in polycarbonate cages at 22 ± 2^{o}C and 50 ± 10% relative humidity on a 12-h light-dark cycle and were provided with food (LabDiet; PMI Nutrition International, Saint Louis, MO) and tap water *ad libitum* throughout the experiment.

3.3.3 CS exposure

Mice were exposed to CS twice daily, 5 days/week for 4, 8, 9, or 17 weeks using a whole-body smoke exposure system (SIU-48; Promech Lab AB, Vintrie, Sweden). Details of the exposure protocol have been described previously (Botelho et al., 2010) and in Supplementary materials and methods.

3.3.4 Histology and follicle counts

One ovary from each mouse in each treatment group was collected for histology. Ovaries were processed as described in Supplementary materials and methods. Follicles were identified and classified under light microscopy using a modification of Pedersen and Peters' classification system (Pedersen and Peters, 1968) and as described in Supplementary materials and methods.

3.3.5 Immunohistochemistry

Immunohistochemical staining was conducted using sections from the same ovaries as above but not needed for follicle counts as described previously (Tuttle et al., 2009) and in Supplementary materials and methods.

3.3.6 TUNEL labeling

TUNEL was conducted using sections from the same ovaries as above but not needed for either follicle counts or immunohistochemistry. Apoptotic cells in the ovary were labeled using the ApopTag Fluorescein *In Situ* Apoptosis Detection Kit (Chemicon International S7110, Temecula, CA) as per manufacturer's instructions and outlined briefly in Supplementary materials and methods.

3.3.7 DNA damage

DNA was extracted from smoke-exposed and control samples using a QIAmp DNA Mini Kit (Qiagen, Mississauga, ON) and quantified using a spectrophotometer. For procedure on conversion of DNA to single-stranded DNA, see Supplementary materials and methods.

3.3.8 Protein carbonyl ELISA

Samples (10 µg/ml) in 1× PBS were assayed in triplicate using the OxiSelect Protein Carbonyl ELISA Kit (Cell Biolabs) as per manufacturer's instructions. See Supplementary materials and methods.

3.3.9 Glutathione assay

Ovaries from smoke-exposed and control mice were prepared for use with the Glutathione Assay Kit (Cayman Chemical Company, Ann Arbor, MI) as described in Supplementary materials and methods.

3.3.10 Western blot

Protein expression was measured in whole-ovarian homogenates of smoke-exposed and control animals. Details of the protocol have been previously described (Tuttle et al., 2009) and are summarized in Supplementary materials and methods. Antibodies used for this study are summarized in Supplementary materials and methods.

3.3.11 Electron microscopy

Ovaries were fixed for transmission electron microscopy (TEM) and summarized in Supplementary materials and methods. Autophagosomes in granulosa cells were counted in seven fields of view per ovary at 7500× magnification and the average number of autophagosomes per female per treatment group was calculated. Only granulosa cells with a visible nucleus were counted. Autophagosomes were counted independently by two observers blinded to treatment.

3.3.12 Quantitative real-time PCR

Total RNA was isolated from ovaries using a Qiagen RNeasy mini kit with on-column DNase digestion (Qiagen) as per manufacturer's instructions. Specifics of the procedure are summarized in Supplementary materials and methods and primer sequences can be

found in Supplementary table 1. Analysis of gene expression changes were calculated according to the method of Livak and Schmittgen (2001) using the $2^{-\Delta\Delta Ct}$ method.

3.3.13 Statistical analysis

All statistical analyses were performed using Sigma-Stat (v.3.1, SPSS, Chicago, IL), see Supplementary materials and methods.

3.4 Results

3.4.1 General Health of Animals Exposed to CS

Treatment with CS had no effect on the general health of the mice, as shown by absence of stereotypical behaviors, hunched back and signs of lacrimation, porphyria, or ruffled coat. CS exposure for 8 weeks resulted in whole body and relative ovarian weights that were significantly lower compared with sham controls (Supplementary fig. 1 A–D). CS exposure also resulted in significant reductions in the number of follicles in different stages of development in ovaries of mice exposed to CS for 4, 8, 9, and 17 weeks compared with the sham exposed mice (Supplementary fig. 1 E–H and fig. 2).

Based on the above data, it was decided that an exposure of 8 weeks was sufficient to induce significant total and primordial follicle loss. Subsequently, all other experiments were performed on ovaries from mice exposed for this time period.

3.4.2 CS Exposure Results in a Stress Response and in Reactive Oxygen Species Damage

Whole ovary homogenates from mice exposed to CS for 8 weeks were examined to determine if there was a stress response in these animals compared with sham controls. Expression of the small heat shock protein Hsp25 was significantly induced ($p < 0.001$) in the ovaries of mice exposed to CS (Fig. 1A).

Protein expression of intracellular copper, zinc superoxide dismutase (SOD) 1, and mitochondrial manganese (Mn) SOD2 were measured. Although there was no significant change in SOD1 expression (Fig. 1B), expression of SOD2 was significantly lower ($p < 0.001$) in the ovaries of smoke-exposed mice (Fig. 1C), indicating a decreased ability to deal with reactive oxygen species (ROS). Treatment had no effect on 8-hydroxydeoxyguanosine (8-OHdG) (Fig. 1D), protein carbonyl formation (Fig. 1E), or total glutathione levels (Fig. 1F).

3.4.3 CS Exposure Does Not Affect the Apoptotic Response in the Ovary

There was no difference in the number of TUNEL-positive cells between the two groups (Figs. 2A and B). Immunohistochemical staining of sham and smoke-exposed ovaries using antibodies directed against BCL2 and BAX showed a marked decrease in the expression of the antiapoptotic BCL2 in exposed ovaries with no change in the expression of the proapoptotic BAX (Fig. 2C), which was quantified and confirmed by Western blot (Fig. 2D). Despite a significant decrease in the expression of BCL2, there was no increase in the expression of BAX (Fig. 2E), a proapoptotic protein, which is

directly regulated by BCL2. Although the BAX:BCL2 ratio was shifted in favor of apoptosis (Fig. 2F), there was no other evidence of increased apoptosis.

3.4.4 CS Exposure Induces Atg

Ovaries from sham and smoke-exposed mice were processed for TEM to determine whether treatment with CS-induced Atg-mediated cell death. TEM micrographs of granulosa cells from the ovaries of sham and smoke-exposed mice showed normal mitochondria and ER (Figs. 3A and 3B). In contrast, granulosa cells from CS-exposed animals contained large lysosomes and pleomorphic nuclei and an abundance of autophagosomes (Fig. 3B). Events of the Atg cascade beginning at phagophore formation through to autophagolysosome development were evident in the granulosa cells of smoke-exposed ovaries (Figs. 3C–F). Although the same number of granulosa cells were examined in each treatment group (Fig. 3G), the mean number (±SEM) of autophagosomes per ovary was significantly greater ($p < 0.001$; Fig. 3H) in smoke-exposed mice compared with controls. Real-time PCR of *Becn1* and *Lc3* gene expression was upregulated 1.46-fold ($p < 0.018$; Fig. 3I) and 1.49-fold ($p < 0.001$; Fig. 3J), respectively, confirming activation of the Atg pathway.

3.5 Discussion

Cigarette smoking is a well-documented health hazard and is potentially the most toxic and preventable hazard for reproductive function in women. Although CS exposure has been linked with earlier menopause and loss of ovarian follicles, the mechanisms underlying this phenomenon are unknown. Our results show that exposure to CS causes

primordial follicle loss and decreased numbers of all follicle populations together with markers of oxidative stress in the ovary but failed to induce apoptosis as shown by absence of an effect on TUNEL staining. Our previous study also showed that expression of activated CASP3, the common executioner in apoptosis, was not changed (Tuttle et al., 2009). However, a profound increase in the number of autophagosomes in granulosa cells was found in ovarian sections from mice exposed to CS together with increased expression of *Becn1* and *Lc3*, key regulatory proteins in the Atg cascade. Taken together, our results suggest that CS exposure, at exposures representative of average smokers, induces granulosa cell Atg and ultimately depletion of the ovarian reserve of primordial follicles. Our results expand the literature by demonstrating that Atg is a novel alternative mechanism of follicle loss in the ovary that can potentially be activated by toxicant exposure. The primordial follicle pool in mice was significantly lower as early as 4 weeks of exposure to CS. By 8 weeks, CS exposure was sufficient to induce a significant reduction in ovarian weight and primordial follicle numbers, which was extended to other follicle populations with continued exposure.

In women, premature onset of menopause is characterized by the exhaustion of the resting pool of follicles, known as primordial follicles, resulting in anovulation, changes in circulating hormone levels, and cessation of menses. In the mouse, premature ovarian failure and primordial follicle loss can be seen in animals exposed to environmental toxicants (Li et al., 1995; Miller et al., 1992), including CS (Tuttle et al., 2009); however, as in humans, the molecular mechanisms are unknown. In the present study, CS exposure

had no effect on the number of apoptotic granulosa cells, a finding that is consistent with our previous study (Tuttle et al., 2009). Mice exposed to CS for 8 weeks had significantly fewer follicles, notably in the primordial follicle pool, in the absence of differences in the expression of active CASP3, the terminal effector enzyme of the apoptosis cascade (Tuttle et al., 2009).

Our findings are contrary to previous studies, which show that exposure to a number of different ovarian toxicants result in follicle loss via apoptosis (Stacchiotti et al., 2009; Tabuchi et al., 2003). In one such study, BaP upregulated the expression of *Hrk*, a cell death gene activated downstream of the AhR which is involved in the regulation of the follicle pool in mice (Jurisicova et al., 2007). *Hrk* functions by facilitating apoptosis via sequestration of BCL2 thereby leaving BAX free to form pores in the outer mitochondrial membrane causing the release of additional apoptotic factors stored within (Jurisicova et al., 2007). We propose that the divergent results are potentially due to differences in the concentration of BaP used in the previous study and that present in CS, which is significantly lower than doses of toxicants administered in previous studies (Devine et al., 2002; Devine et al., 2004; Jurisicova et al., 2007). Furthermore, CS is a complex mixture of chemical toxicants including nicotine, carbon monoxide, polyhalogenated hydrocarbons, and metals such as cadmium (Hoffmann and Wynder, 1986). Hence, the potential interactions among these chemicals at low concentrations cannot be excluded by the current study.

Experiments designed to characterize the toxic chemicals underlying activation of Atg are currently underway using chemical fractionation of CS. It has been previously shown that the mechanism, stage of follicle affected, and speed at which follicle loss occurs is both compound and dose specific (Hoyer et al., 2009; Pandini et al., 2009; Shirota et al., 2007). Exposure to CS condensate, the particulate phase of CS, resulted in delayed follicle development and premature luteinization of follicles (Sadeu and Foster, 2011), whereas BaP exposure, at concentrations representative of human exposure, decreased steroidogenesis and anti-Müllerian hormone output of follicles (Sadeu and Foster, 2010).

In the present study, CS exposure induced oxidative stress, as shown by a threefold increased expression of HSP25, a small heat shock protein that is upregulated under oxidative stress conditions (Stacchiotti et al., 2009). Moreover, SOD2 protein expression was decreased in exposed mice, which is in line with others who found that a loss of antioxidant activity, specifically SOD2 and glutathione, leads to oxidative damage in neuronal cells (Tabuchi et al., 2003). Of note, HeLa cells transfected with SOD2 siRNA and subsequently treated with thenoyl trifluoroacetone had elevated ROS production, Atg, and cell death, whereas SOD2-overexpressing cells had reduced levels of cell death by 45% compared with controls (Chen et al., 2007). Mice exposed to CS for 16 and 32 weeks showed a marked increase in ROS generation in leukocytes (Talukder et al., 2011). In human neutrophils, exposure to CS extract resulted in tissue damage mediated by oxidative stress (Matthews et al., 2011). Circulating progenitor cells taken from smokers had a higher incidence of ROS production, lower plasma antioxidant concentration, and higher MnSOD protein expression and enzyme activity than those isolated from

nonsmoking control animals (Talukder et al., 2011). CS contains more than 4000 chemical compounds, many of which are oxidants or free radicals that are inducers of oxidative stress. Many of these are also AhR agonists, the activation of which leads to induction of cytochrome P450, which is involved in the generation of ROS (Tagawa et al., 2008), which can lead to apoptosis and Atg (Tagawa et al., 2008).

Several distinct lines of evidence lead us to believe that CS exposure induce oxidative/ER stress leading to activation of the autophagic pathway to play an important role in ovarian follicle loss. Oxidative stress can trigger ER stress (Borradaile et al., 2006; Brookheart et al., 2009; Sorensen et al., 2006), which results in activation of the unfolded protein response (UPR). The UPR functions to maintain cellular homeostasis and several ER chaperone proteins including calreticulin, glucose regulated protein 78/immunoglobulin binding protein, those proteins containing the amino acid sequence KDEL (Lys-Asp-Glu-Leu), and protein disulfide isomerase mediate protein folding to stabilize nascent proteins and restore homeostasis (Sage et al., 2010). The inability of chaperone proteins to restore homeostasis leads to increased expression of CCAAT-enhancer binding protein homologous protein, an indicator of ER stress and a potent inhibitor of BCL2 expression (Sage et al., 2010; Tagawa et al., 2008). Furthermore, induction of ER stress leads to phosphorylation of BCL2 by c-Jun N-terminal kinase, which targets BCL2 for proteasomal degradation (Szegezdi et al., 2009). Specifically, we found that CS exposure results in a significant decrease in BCL2 expression together with a significant increase in the number of autophagosomes in the granulosa cells of ovarian follicles and an increase

in the gene expression of two key Atg cascade mediators, *Becn1* and *Lc3*. Although BCL2 is a known inhibitor of apoptosis, it is also implicated in preventing the progression of Atg. In the Atg pathway, BCL2 interacts with BECN1, preventing it from facilitating membrane nucleation of the autophagosome (Glick et al., 2010; Kaushik et al., 2010). In addition to serving as a mechanism to rid the cell of misfolded, long-lived proteins, and superfluous or damaged organelles, Atg functions as an adaptive response to various stresses, including oxidative stress.

Mice lacking both *Bax* and *Bak*, proapoptosis members, are completely resistant to apoptosis; yet cell death proceeds in a normal manner with the appearance of autophagosomes and autolysosomes (Shimizu et al., 2004). Nonapoptotic cell death in these mice was dependent on the autophagic proteins ATG5 and BECN1. Disassociation of BECN1 from BCL2/BCL2L1 in the ER but not mitochondria is a key driver of Atg (Fig. 4). Taken together, we postulate that CS exposure–induced decreased expression of BCL2 leads to follicle loss via Atg ultimately resulting in depletion of the primordial follicle pool. This finding is in keeping with and extends the literature by inculpating Atg as a novel alternative cell death pathway in granulosa cells that can be activated by CS exposure. Mechanisms regulating cross talk between apoptosis and Atg are unclear; however, emerging studies have identified Atg as an important alternative cell death pathway in mammalian cells, including human and rodent granulosa cells (Choi et al., 2010; Vilser et al., 2010). In human granulosa cells, unchecked oxidative stress led to increased expression of lectin-like oxidized low-density receptor1, a scavenger receptor

and membrane glycoprotein that is activated by oxidized low-density lipoprotein (Vilser et al., 2010). Furthermore, CS extract increased conversion of LC3-I to LC3-II and increased Atg in cultures of human bronchial epithelial cells (Kim et al., 2008). Similarly, CS extract treatment induced Atg in lung epithelial cells, macrophages, and fibroblasts (Hwang et al., 2010). Therefore, we postulate that CS exposure can induce oxidative/ER stress leading to Atg in granulosa cells and that this nonapoptotic cell death pathway is central to follicle depletion as previously demonstrated.

In summary, CS exposure resulted in decreased ovarian weight and follicle numbers, increased oxidative stress as measured by HSP25 and SOD2 expression, and profoundly increased the number of autophagosomes in granulosa cells of ovarian follicles but did not increase granulosa cell apoptosis. Moreover, CS-induced increased expression of *Becn1* and *Lc3* further supports the hypothesis that Atg is the central underlying mechanism of CS-induced ovarian follicle loss. We further postulate that Atg is a novel pathway of follicle destruction activated by CS and potentially other environmental toxicants.

3.6 Funding

Canadian Institutes of Health Research (MOP 81178); salary support was provided from the Canadian Institutes of Health Research and Ontario Women's Health Council to W.G.F.

3.7 Acknowledgements

A.M.G. received scholarships from Canadian Institutes of Health Research (CIHR), the Ontario Tobacco Research Council, CIHR/IHDCYH Training Program in Reproduction, Early Development, and the Impact on Health (REDIH) and the Government of Ontario. The authors gratefully acknowledge Dr Jean-Clair Sadeu for his critical review of the manuscript. The authors declare that they do not have any conflict of interest to report. The paper was presented at the 50th Society of Toxicology Meeting, Washington DC, March 2011 and the 44th Society for the Study of Reproduction Meeting, Portland, OR, August 2011.

3.8 References

1. Baird, W. M., Hooven, L. A., and Mahadevan, B. (2005). Carcinogenic polycyclic aromatic hydrocarbon-DNA adducts and mechanism of action. Environ. Mol. Mutagen. 45, 106–114.

2. Borradaile,N.M., Han, X., Harp, J. D., Gale, S. E., Ory, D. S., and Schaffer, J. E.

3. (2006). Disruption of endoplasmic reticulum structure and integrity in lipotoxic cell death. J. Lipid Res. 47, 2726–2737.

4. Botelho, F. M., Gaschler, G. J., Kianpour, S., Zavitz, C. C., Trimble, N. J.,

5. Nikota, J. K., Bauer, C. M., and Stämpfli, M. R. (2010). Innate immune processes are sufficient for driving cigarette smoke-induced inflammation in mice. Am. J. Respir. Cell Mol. Biol. 42, 394–403.

6. Brookheart, R. T., Michel, C. I., Listenberger, L. L., Ory, D. S., and Schaffer, J. E. (2009). The non-coding RNA gadd7 is a regulator of lipid-induced oxidative and endoplasmic reticulum stress. J. Biol. Chem. 284, 7446–7454.

7. Bursch, W. (2001). The autophagosomal-lysosomal compartment in programmed cell death. Cell Death Differ. 8, 569–581.

8. Chen, Y., Millan-Ward, E., Kong, J., Israels, S. J., and Gibson, S. B. (2007). Mitochondrial electron-transport-chain inhibitors of complexes I and II induce autophagic cell death mediated by reactive oxygen species. J. Cell Sci. 120(Pt 23), 4155–4166.

9. Choi, J. Y., Jo, M. W., Lee, E. Y., Yoon, B. K., and Choi, D. S. (2010). The role of autophagy in follicular development and atresia in rat granulosa cells. Fertil. Steril. 93, 2532–2537.

10. Cohen, B., Evers, S., Manske, S., Bercovitz, K., and Edward, H. G. (2003). Smoking, physical activity and breakfast consumption among secondary school students in a southwestern Ontario community. Can. J. Public Health 94, 41–44.

11. Cortvrindt, R. G., and Smitz, J. E. (2002). Follicle culture in reproductive toxicology: A tool for in-vitro testing of ovarian function? Hum. Reprod. Update 8, 243–254.

12. Crha, I., Hruba´, D., Fiala, J., Ventruba, P., Za´kova´, J., and Petrenko, M. (2001). The outcome of infertility treatment by in-vitro fertilisation in smoking and non-smoking women. Cent. Eur. J. Public Health 9, 64–68.

13. Curtis, K. M., Savitz, D. A., and Arbuckle, T. E. (1997). Effects of cigarette smoking, caffeine consumption, and alcohol intake on fecundability. Am. J. Epidemiol. 146, 32–41.

14. Dechanet, C., Anahory, T., Mathieu Daude, J. C., Quantin, X., Reyftmann, L., Hamamah, S., Hedon, B., and Dechaud, H. (2011). Effects of cigarette smoking on reproduction. Hum. Reprod. Update 17, 76–95.

15. Desmeules, P., and Devine, P. J. (2006). Characterizing the ovotoxicity of cyclophosphamide metabolites on cultured mouse ovaries. Toxicol. Sci. 90, 500–509.

16. Detmar, J., Rennie, M. Y., Whiteley, K. J., Qu, D., Taniuchi, Y., Shang, X., Casper, R. F., Adamson, S. L., Sled, J. G., and Jurisicova, A. (2008). Fetal growth restriction triggered by polycyclic aromatic hydrocarbons is associated with altered placental vasculature and AhR-dependent changes in cell death. Am. J. Physiol. Endocrinol. Metab. 295, E519–E530.

17. Devine, P. J., Sipes, I. G., and Hoyer, P. B. (2001). Effect of 4-vinylcyclohexene diepoxide dosing in rats on GSH levels in liver and ovaries. Toxicol. Sci. 62, 315–320.

18. Devine, P. J., Sipes, I. G., and Hoyer, P. B. (2004). Initiation of delayed ovotoxicity by in vitro and in vivo exposures of rat ovaries to 4-vinylcyclohexene diepoxide. Reprod. Toxicol. 19, 71–77.

19. Devine, P. J., Sipes, I.G., Skinner, M.K., and Hoyer, P. B. (2002). Characterization of a rat in vitro ovarian culture system to study the ovarian toxicant 4-vinylcyclohexene diepoxide. Toxicol. Appl. Pharmacol. 184, 107–115.

20. El-Nemr, A., Al-Shawaf, T., Sabatini, L., Wilson, C., Lower, A. M., and Grudzinskas, J. G. (1998). Effect of smoking on ovarian reserve and ovarian stimulation in in-vitro fertilization and embryo transfer. Hum. Reprod. 13, 2192–2198.

21. Flaws, J. A., Hirshfield, A. N., Hewitt, J. A., Babus, J. K., and Furth, P. A. (2001). Effect of bcl-2 on the primordial follicle endowment in the mouse ovary. Biol. Reprod. 64, 1153–1159.

22. Freour, T., Masson, D., Mirallie, S., Jean, M., Bach, K., Dejoie, T., and Barriere, P. (2008). Active smoking compromises IVF outcome and affects ovarian reserve. Reprod. Biomed. Online 16, 96–102.

23. Fuentes, A., Munoz, A., Barnhart, K., Arguello, B., Diaz, M., and Pommer, R. (2010). Recent cigarette smoking and assisted reproductive technologies outcome. Fertil. Steril. 93, 89–95.

24. Gawriluk, T. R., Hale, A. N., Flaws, J. A., Dillon, C. P., Green, D. R., and Rucker, E. B., III. (2011). Autophagy is a cell survival program for female germ cells in the murine ovary. Reproduction 141, 759–765.

25. Glick, D., Barth, S., and Macleod, K. F. (2010). Autophagy: Cellular and molecular mechanisms. J. Pathol. 221, 3–12.

26. Gray, L. E., Jr., and Ostby, J. S. (1995). In utero 2,3,7,8-tetrachlorodibenzo-p-dioxin (TCDD) alters reproductive morphology and function in female rat offspring. Toxicol. Appl. Pharmacol. 133, 285–294.

27. Health Canada (2003). Canadian Tobacco Use Monitoring Survey. Health Canada, Ottawa, ON.

28. Health Canada (2009). Canadian Tobacco Use Monitoring Survey. Health Canada, Ottawa, ON.

29. Hillier, S. G. (2001). Gonadotropic control of ovarian follicular growth and development. Mol. Cell Endocrinol. 179, 39–46.

30. Hoffmann, D., and Wynder, E. L. (1986). Chemical constituents and bioactivity of tobacco smoke. IARC Sci. Publ. 74, 145–165.

31. Hoyer, P. B., Davis, J. R., Bedrnicek, J. B., Marion, S. L., Christian, P. J., Barton, J. K., and Brewer, M. A. (2009). Ovarian neoplasm development by 7,12-dimethylbenz[a]anthracene (DMBA) in a chemically-induced rat model of ovarian failure. Gynecol. Oncol. 112, 610–615.

32. Hughes, E. G., and Brennan, B. G. (1996). Does cigarette smoking impair natural or assisted fecundity? Fertil. Steril. 66, 679–689.

33. Hughes, E. G., Yeo, J., Claman, P., YoungLai, E. V., Sagle, M. A., Daya, S., and Collins, J. A. (1994). Cigarette smoking and the outcomes of in vitro fertilization: Measurement of effect size and levels of action. Fertil. Steril. 62, 807–814.

34. Hwang, J. W., Chung, S., Sundar, I. K., Yao, H., Arunachalam, G., McBurney, M. W., and Rahman, I. (2010). Cigarette smoke-induced autophagy is regulated by SIRT1-PARP-1-dependent mechanism: Implication in pathogenesis of COPD. Arch. Biochem. Biophys. 500, 203–209.

35. Jick, H., and Porter, J. (1977). Relation between smoking and age of natural menopause. Report from the Boston Collaborative Drug Surveillance Program, Boston University Medical Center. Lancet 1, 1354–1355.

36. Jurisicova, A., Taniuchi, A., Li, H., Shang, Y., Antenos, M., Detmar, J., Xu, J., Matikainen, T., Benito, H. A., Nunez, G., et al. (2007). Maternal exposure to polycyclic aromatic hydrocarbons diminishes murine ovarian reserve via induction of Harakiri. J. Clin. Invest. 117, 3971–3978.

37. Kaushik, S., Singh, R., and Cuervo, A. M. (2010). Autophagic pathways and metabolic stress. Diabetes Obes. Metab. 12(Suppl. 2), 4–14.

38. Kim, H. P., Wang, X., Chen, Z. H., Lee, S. J., Huang, M. H., Wang, Y., Ryter, S. W., and Choi, A. M. (2008). Autophagic proteins regulate cigarette smoke-induced apoptosis: Protective role of heme oxygenase-1. Autophagy 4, 887–895.

39. Knight, P. G., and Glister, C. (2006). TGF-beta superfamily members and ovarian follicle development. Reproduction 132, 191–206.

40. Li, X., Johnson, D. C., and Rozman, K. K. (1995). Reproductive effects of 2,3,7,8-tetrachlorodibenzo-p-dioxin (TCDD) in female rats: Ovulation, hormonal regulation, and possible mechanism(s). Toxicol. Appl. Pharmacol. 133, 321–327.

41. Liang, X. H., Jackson, S., Seaman, M., Brown, K., Kempkes, B., Hibshoosh, H., and Levine, B. (1999). Induction of autophagy and inhibition of tumorigenesis by beclin 1. Nature 402, 672–676.

42. Liang, X. H., Yu, J., Brown, K., and Levine, B. (2001). Beclin 1 contains a leucine-rich nuclear export signal that is required for its autophagy and tumor suppressor function. Cancer Res. 61, 3443–3449.

43. Livak, K. J., and Schmittgen, T. D. (2001). Analysis of relative gene expression data using real-time quantitative PCR and the 2(-Delta Delta C(T)) Method. Methods 25, 402–408.

44. Maiuri, M. C., Criollo, A., and Kroemer, G. (2010). Crosstalk between apoptosis and autophagy within the Beclin 1 interactome. EMBO J. 29, 515–516.

45. Matikainen, T., Perez, G. I., Jurisicova, A., Pru, J. K., Schlezinger, J. J., Ryu, H. Y., Laine, J., Sakai, T., Korsmeyer, S. J., Casper, R. F., et al. (2001). Aromatic hydrocarbon receptor-driven Bax gene expression is required for premature ovarian failure caused by biohazardous environmental chemicals. Nat. Genet. 28, 355–360.

46. Matthews, J. B., Chen, F. M., Milward, M. R., Wright, H. J., Carter, K., McDonagh, A., and Chapple, I. L. (2011). Effect of nicotine, cotinine and cigarette smoke extract on the neutrophil respiratory burst. J. Clin. Periodontol 38, 208–218.

47. Mattison, D. R., and Nightingale, M. S. (1982). Oocyte destruction by polycyclic aromatic hydrocarbons is not linked to the inducibility of ovarian aryl hydrocarbon benzo(a)pyrene hydroxylase activity in (DBA/2N X C57BL/6N) F1 X DBA/2N backcross mice. Pediatr. Pharmacol. (New York) 2, 11–21.

48. Mattison, D. R., and Thorgeirsson, S. S. (1978). Smoking and industrial pollution, and their effects on menopause and ovarian cancer. Lancet 1, 187–188.

49. Mattison, D. R., White, N. B., and Nightingale, M. R. (1980). The effect of benzo(a)pyrene on fertility, primordial oocyte number, and ovarian response to pregnant mare's serum gonadotropin. Pediatr. Pharmacol. (New York) 1, 143–151.

50. Mayer, L. P., Pearsall, N. A., Christian, P. J., Devine, P. J., Payne, C. M., McCuskey, M. K., Marion, S. L., Sipes, I. G., and Hoyer, P. B. (2002). Long-term effects of ovarian follicular depletion in rats by 4-vinylcyclohexene diepoxide. Reprod. Toxicol. 16, 775–781.

51. Miller, M. M., Plowchalk, D. R., Weitzman, G. A., London, S. N., and Mattison, D. R. (1992). The effect of benzo(a)pyrene on murine ovarian and corpora lutea volumes. Am. J. Obstet. Gynecol. 166, 1535–1541.

52. Mizushima, N., and Levine, B. (2010). Autophagy in mammalian development and differentiation. Nat. Cell Biol. 12, 823–830.

53. Muller, W. F., Hobson, W., Fuller, G. B., Knauf, W., Coulston, F., and Korte, F. (1978). Endocrine effects of chlorinated hydrocarbons in rhesus monkeys. Ecotoxicol. Environ. Saf. 2, 161–172.

54. Neal, M. S., Hughes, E. G., Holloway, A. C., and Foster, W. G. (2005). Sidestream smoking is equally as damaging as mainstream smoking on IVF outcomes. Hum. Reprod. 20, 2531–2535.

55. Neal, M. S., Zhu, J., and Foster, W. G. (2008). Quantification of benzo[a]pyrene and other PAHs in the serum and follicular fluid of smokers versus non-smokers. Reprod. Toxicol. 25, 100–106.

56. Pandini, A., Soshilov, A. A., Song, Y., Zhao, J., Bonati, L., and Denison, M. S. (2009). Detection of the TCDD binding-fingerprint within the Ah receptor ligand

binding domain by structurally driven mutagenesis and functional analysis. Biochemistry 48, 5972–5983.

57. Pattingre, S., Tassa, A., Qu, X., Garuti, R., Liang, X. H., Mizushima, N., Packer, M., Schneider, M. D., and Levine, B. (2005). Bcl-2 antiapoptotic proteins inhibit Beclin 1-dependent autophagy. Cell 122, 927–939.

58. Pedersen, T., and Peters, H. (1968). Proposal for a classification of oocytes and follicles in the mouse ovary. J. Reprod. Fertil. 17, 555–557.

59. Pocar, P., Brevini, T. A., Antonini, S., and Gandolfi, F. (2006). Cellular and molecular mechanisms mediating the effect of polychlorinated biphenyls on oocyte in vitro maturation. Reprod. Toxicol. 22, 242–249.

60. Rosevear, S. K., Holt, D. W., Lee, T. D., Ford, W. C., Wardle, P. G., and Hull, M. G. (1992). Smoking and decreased fertilisation rates in vitro. Lancet 340, 1195–1196.

61. Roth, L. K., and Taylor, H. S. (2001). Risks of smoking to reproductive health: Assessment of women's knowledge. Am. J. Obstet. Gynecol. 184, 934–939.

62. Rowlands, D. J., McDermott, A., and Hull, M. G. (1992). Smoking and decreased fertilisation rates in vitro. Lancet 340, 1409–1410.

63. Sadeu, J. C., and Foster, W. G. (2011). Effect of in vitro exposure to benzo[a]pyrene, a component of cigarette smoke, on folliculogenesis, steroidogenesis and oocyte nuclear maturation. Reprod. Toxicol. 31, 402–408.

64. Sadeu, J. C., and Foster, W. G. (2011). Cigarette smoke condensate exposure delays follicular development and function in a stage-dependent manner. Fertil. Steril. 95, 2410–2417.

65. Sadeu, J. C., Hughes, C. L., Agarwal, S., and Foster, W. G. (2010). Alcohol, drugs, caffeine, tobacco, and environmental contaminant exposure: Reproductive health consequences and clinical implications. Crit. Rev. Toxicol. 40, 633–652.

66. Sage, A. T., Walter, L. A., Shi, Y., Khan, M. I., Kaneto, H., Capretta, A., and Werstuck, G. H. (2010). Hexosamine biosynthesis pathway flux promotes endoplasmic reticulum stress, lipid accumulation, and inflammatory gene expression in hepatic cells. Am. J. Physiol. Endocrinol. Metab. 298, E499–E511.

67. Sharara, F. I., Beatse, S. N., Leonardi, M. R., Navot, D., and Scott, R. T., Jr. (1994). Cigarette smoking accelerates the development of diminished ovarian reserve as evidenced by the clomiphene citrate challenge test. Fertil. Steril. 62, 257–262.

68. Shimizu, S., Kanaseki, T., Mizushima, N., Mizuta, T., Arakawa-Kobayashi, S., Thompson, C. B., and Tsujimoto, Y. (2004). Role of Bcl-2 family proteins in a non-apoptotic programmed cell death dependent on autophagy genes. Nat.Cell Biol. 6, 1221–1228.

69. Shirota, M., Kaneko, T., Okuyama, M., Sakurada, Y., Shirota, K., and Matsuki, Y. (2007). Internal dose-effects of 2,3,7,8-tetrachlorodibenzo-p-dioxin (TCDD) in gonadotropin-primed weanling rat model. Arch. Toxicol. 81, 261–269.

70. Soares, S. R., Simon, C., Remohi, J., and Pellicer, A. (2007). Cigarette smoking affects uterine receptiveness. Hum. Reprod. 22, 543–547.

71. Sorensen, S., Ranheim, T., Bakken, K. S., Leren, T. P., and Kulseth, M. A. (2006). Retention of mutant low density lipoprotein receptor in endoplasmic reticulum (ER) leads to ER stress. J. Biol. Chem. 281, 468–476.

72. Stacchiotti, A., Morandini, F., Bettoni, F., Schena, I., Lavazza, A., Grigolato, P. G., Apostoli, P., Rezzani, R., and Aleo, M. F. (2009). Stress proteins and oxidative damage in a renal derived cell line exposed to inorganic mercury and lead. Toxicology 264, 215–224.

73. Sterzik, K., Strehler, E., De, S. M., Trumpp, N., Abt, M., Rosenbusch, B., and Schneider, A. (1996). Influence of smoking on fertility in women attending an in vitro fertilization program. Fertil. Steril. 65, 810–814.

74. Szegezdi, E., Macdonald, D. C., Ni, C. T., Gupta, S., and Samali, A. (2009). Bcl-2 family on guard at the ER. Am. J. Physiol. Cell Physiol. 296, C941–C953.

75. Tabuchi, A., Funaji, K., Nakatsubo, J., Fukuchi, M., Tsuchiya, T., and Tsuda, M. (2003). Inactivation of aconitase during the apoptosis of mouse cerebellar granule neurons induced by a deprivation of membrane depolarization. J. Neurosci. Res. 71, 504–515.

76. Tagawa, Y., Hiramatsu, N., Kasai, A., Hayakawa, K., Okamura, M., Yao, J., and Kitamura, M. (2008). Induction of apoptosis by cigarette smoke via ROS-dependent endoplasmic reticulum stress and CCAAT/enhancer binding protein-homologous protein (CHOP). Free Radic. Biol. Med. 45, 50–59.

77. Takai, Y., Canning, J., Perez, G. I., Pru, J. K., Schlezinger, J. J., Sherr, D. H., Kolesnick, R. N., Yuan, J., Flavell, R. A., Korsmeyer, S. J., et al. (2003). Bax, caspase-2, and caspase-3 are required for ovarian follicle loss caused by 4-vinylcyclohexene diepoxide exposure of female mice in vivo. Endocrinology 144, 69–74.

78. Talukder, M. A., Johnson, W. M., Varadharaj, S., Lian, J., Kearns, P. N., El-Mahdy, M. A., Liu, X., and Zweier, J. L. (2011). Chronic cigarette smoking causes hypertension, increased oxidative stress, impaired NO bioavailability, endothelial dysfunction, and cardiac remodeling in mice. Am. J. Physiol. Heart Circ. Physiol. 300, H388–H396.

79. Themmen, A. P. (2005). Anti-Müllerian hormone: Its role in follicular growth initiation and survival and as an ovarian reserve marker. J. Natl. Cancer Inst. Monogr. 34, 18–21.

80. Tilly, J. L. (1998). Molecular and genetic basis of normal and toxicant-induced apoptosis in female germ cells. Toxicol. Lett. 102-103, 497–501.

81. Tuttle, A. M., Stämpfli, M., and Foster, W. G. (2009). Cigarette smoke causes follicle loss in mice ovaries at concentrations representative of human exposure. Hum. Reprod. 24, 1452–1459.

82. van Beek, R. D., van den Heuvel-Eibrink, M. M., Laven, J. S., de Jong, F. H., Themmen, A. P., Hakvoort-Cammel, F. G., van den Bos, C., van den Berg, H., Pieters, R., and de Muinck Keizer-Schrama, S. M. (2007). Anti-Müllerian hormone is a sensitive serum marker for gonadal function in women treated for Hodgkin's lymphoma during childhood. J. Clin. Endocrinol. Metab. 92, 3869–3874.

83. Van Voorhis, B. J., Dawson, J. D., Stovall, D. W., Sparks, A. E., and Syrop, C. H. (1996). The effects of smoking on ovarian function and fertility during assisted reproduction cycles. Obstet. Gynecol. 88, 785–791.

84. Vilser, C., Hueller, H., Nowicki, M., Hmeidan, F. A., Blumenauer, V., and Spanel-Borowski, K. (2010). The variable expression of lectin-like oxidized low-density lipoprotein receptor (LOX-1) and signs of autophagy and apoptosis in freshly harvested human granulosa cells depend on gonadotropin dose, age, and body weight. Fertil. Steril. 93, 2706–2715.

85. Waylen, A. L., Metwally, M., Jones, G. L., Wilkinson, A. J., and Ledger, W. L. (2009). Effects of cigarette smoking upon clinical outcomes of assisted reproduction: A meta-analysis. Hum. Reprod. Update 15, 31–44.

86. Weigert, M., Hofstetter, G., Kaipl, D., Gottlich, H., Krischker, U., Bichler, K., Poehl, M., and Feichtinger, W. (1999). The effect of smoking on oocyte quality and hormonal parameters of patients undergoing in vitro fertilization embryo transfer. J. Assist. Reprod. Genet. 16, 287–293.

87. Westhoff, C., Murphy, P., and Heller, D. (2000). Predictors of ovarian follicle number. Fertil. Steril. 74, 624–628.

88. Woodruff, T. J., Zota, A. R., and Schwartz, J. M. (2011). Environmental Chemicals in pregnant women in the U.S.: NHANES 2003-2004. Environ. Health Perspect 119, 878–885.

89. World Health Organization (2007). The European Tobacco Control Report 2007. World Health Organization Report 2007. WHO Regional Office for Europe, Copenhagen, Denmark.

90. World Health Organization (2008). WHO Report on the Global Tobacco Epidemic. MPOWER package, Geneva, Switzerland.

91. Yang, Z., and Klionsky, D. J. (2010). Eaten alive: A history of macroautophagy. Nat. Cell Biol. 12, 814–822.

92. Zenzes, M. T. (2000). Smoking and reproduction: Gene damage to human gametes and embryos. Hum. Reprod. Update 6, 122–131.

93. Zenzes, M. T., Reed, T. E., and Casper, R. F. (1997). Effects of cigarette smoking and age on the maturation of human oocytes. Hum. Reprod. 12, 1736–1741.

94. Zenzes, M. T., Wang, P., and Casper, R. F. (1995). Cigarette smoking may affect meiotic maturation of human oocytes. Hum. Reprod. 10, 3213–3217.

3.9 Figures

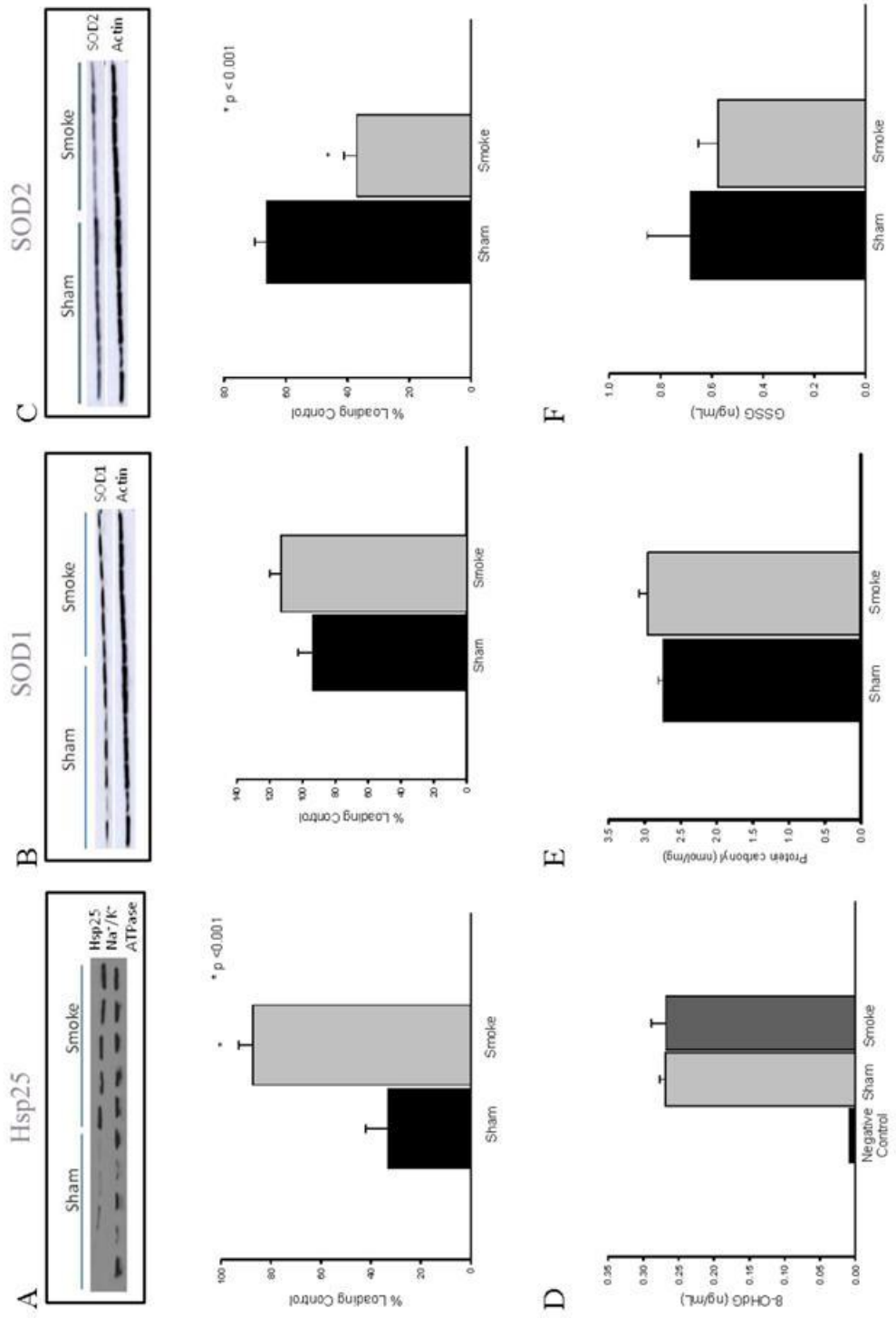
A
Hsp25
Sham
Smoke
Hsp25
Na+/K+
ATPase
% Loading Control
* p <0.001
Sham
Smoke
B
SOD1
Sham
Smoke
SOD1
Actin
% Loading Control
Sham
Smoke
C
SOD2
Sham
Smoke
SOD2
Actin
% Loading Control
* p < 0.001
Sham
Smoke
D
8-OHdG (ng/mL)
Negative Control
Sham
Smoke
E
Protein carbonyl (nmol/mg)
Sham
Smoke
F
GSSG (ng/mL)
Sham
Smoke

Figure 1. Oxidative stress is evident in CS-exposed ovaries.

Western blot analysis of proteins involved in stress response and ROS mediation was performed on whole ovary homogenates from 8-week sham and smoke-exposed mice. Expression of: (A) Hsp25 protein expression; (B) SOD1 protein expression; and (C) SOD2 protein expression in smoke-exposed ovaries compared with sham controls. Densitometric analysis of Hsp25, SOD1, and SOD2 protein expression levels were quantified relative to the Na^+/K^+ ATPase (Hsp25) and b-actin (SOD1 and SOD2) loading controls and are shown in the graph below each corresponding blot. Sham (n = 5) and smoke-exposed ovaries for Hsp25 and n = 6 sham and smoke-exposed ovaries per SOD1 and SOD2 experiment. (D) DNA damage was measured by 8-OHdG in whole ovaries of sham and smoke-exposed mice. (E) Protein carbonyl formation, an indication of ROS damage. (F) Total glutathione levels in the ovaries of sham and smoke-exposed ovaries. Values are expressed as the mean (± SEM). * $p < 0.001$.

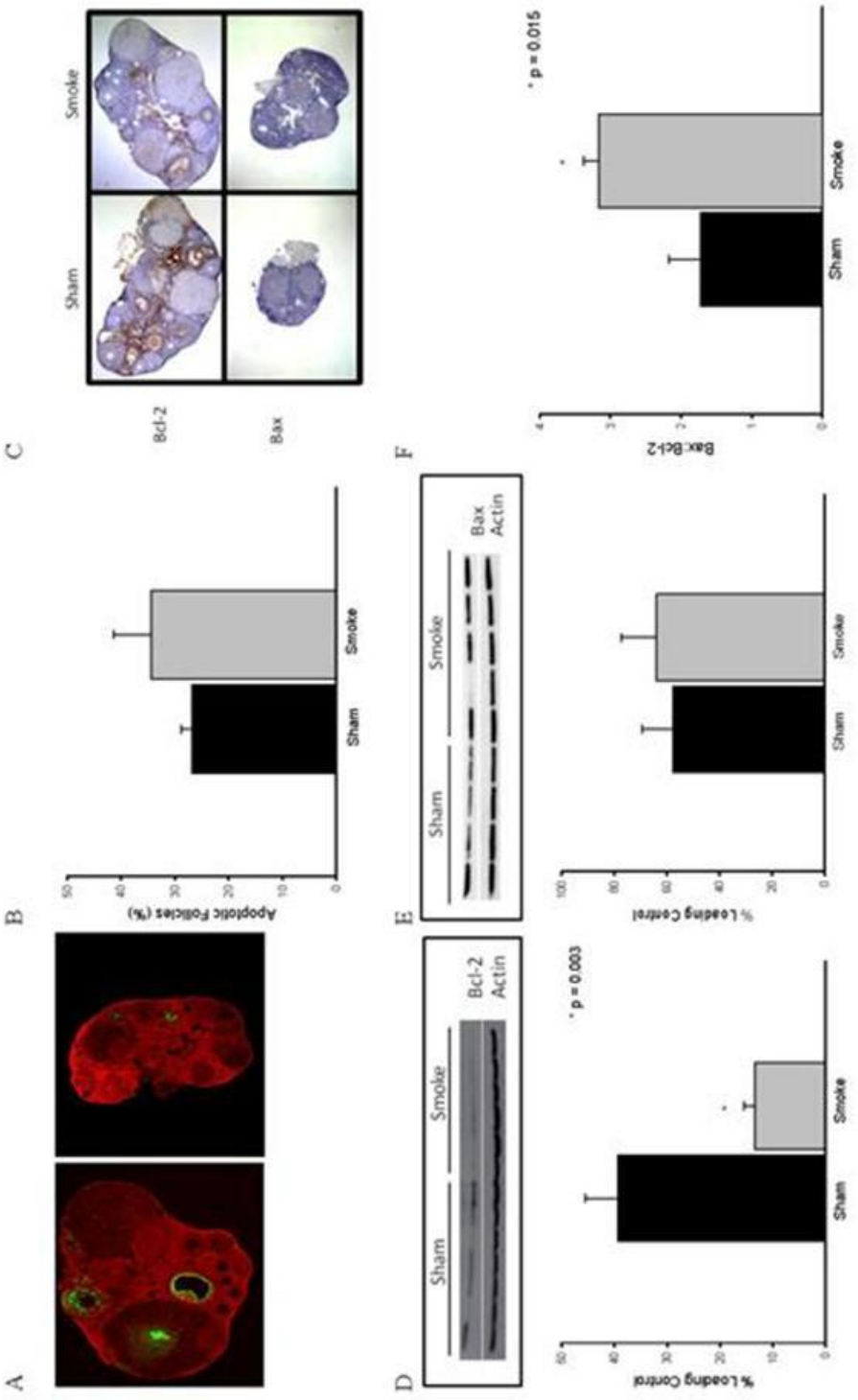
A
B
C
D
E
F
Sham
Smoke
Bcl-2
Bax
Actin
Apoptotic Follicles (%)
% Loading Control
Bax:Bcl-2
* p = 0.003
* p = 0.015

Figure 2. CS exposure does not result in increased apoptosis of ovarian follicles. TUNEL labeling was undertaken to determine whether smoke exposure results in a higher incidence of apoptotic cells. (A) Representative photomicrographs of TUNEL-labeled sham (left panel) and smoke (right panel)-exposed ovaries. TUNEL-positive cells appear green (fluorescein), whereas negative cells appear red (propidium iodide). (B) The percentage of follicles with three or more TUNEL-positive cells in smoke-exposed ovaries compared with sham ovaries. Follicles (n = 100) from five sham ovaries and 94 follicles from five smoke ovaries. (C) Immunohistochemical staining of sham and smoke-exposed ovaries showing the relative expression of BCL2 protein. Western blot analyses of (D) BCL2 (n = 7 sham and 6 smoke) and (E) BAX (n = 4 sham and 5 smoke) protein expression was performed on whole ovary homogenates from 8-week sham and smoke-exposed mice. (E) Densitometric analyses of protein expression levels of BCL2 (D) and BAX (E) were quantified relative to the β-actin loading control are shown in the graph below each corresponding blot. * $p = 0.003$. (F) The ratio of BAX:BCL2 expression in the ovaries of sham and smoke-exposed mice. * $p = 0.015$. All values are expressed as the mean (± SEM).

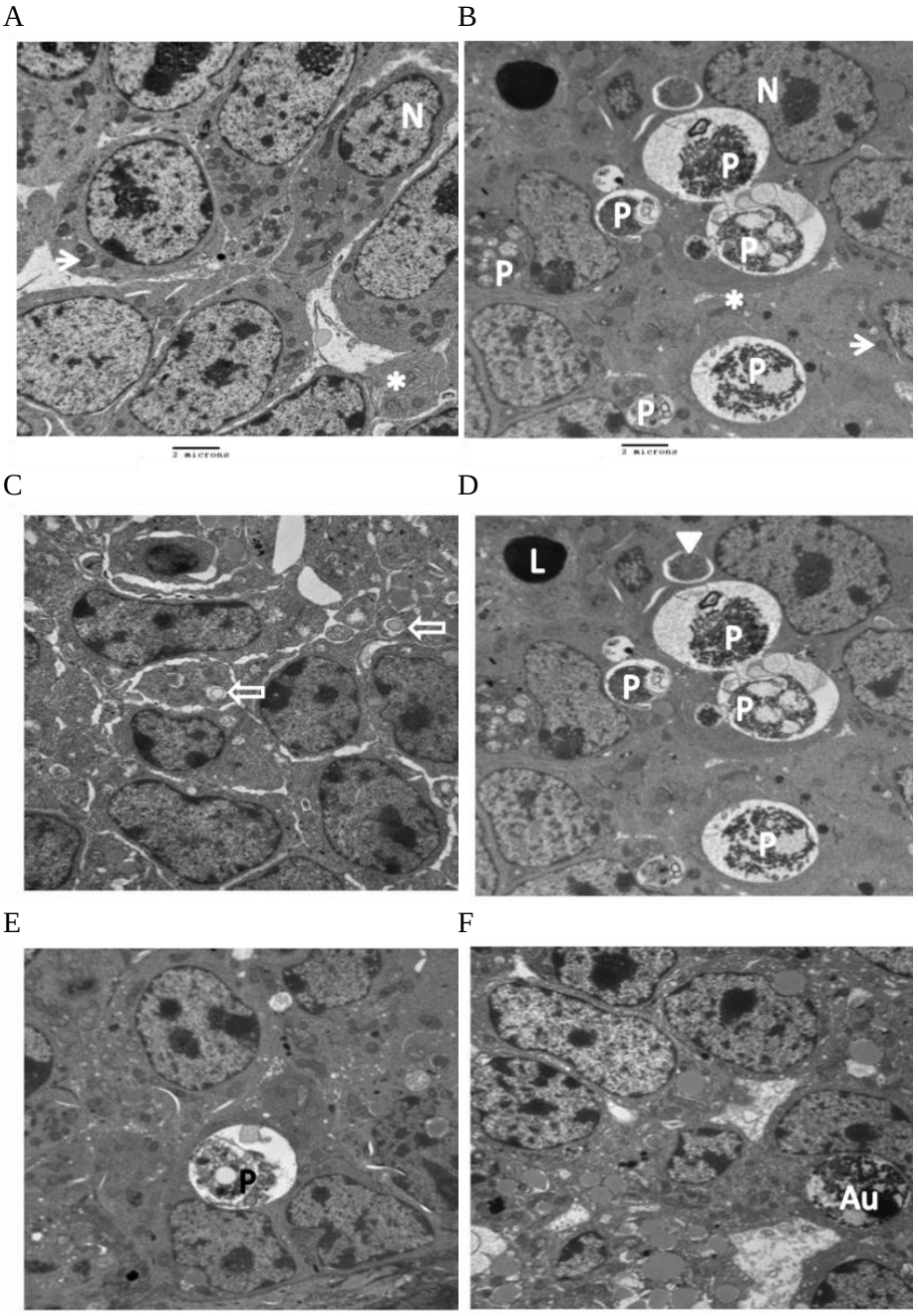
A
B
N
P
P
P
P
P
P
C
D
L
P
P
P
P
E
F
P
Au

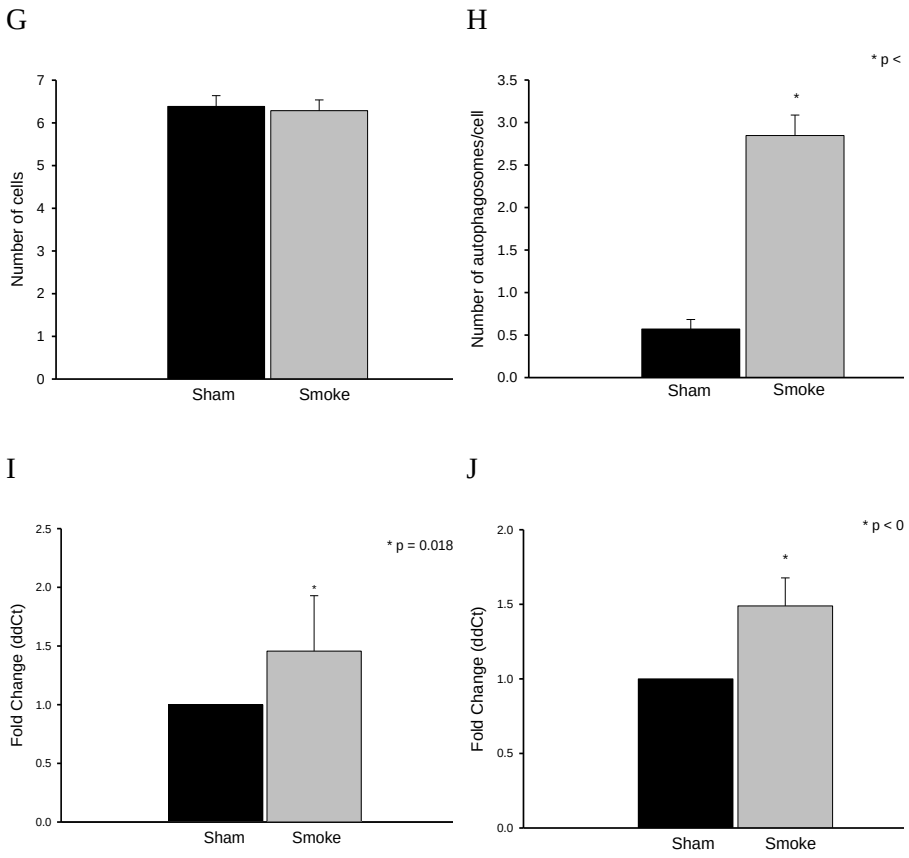
G
H
I
J
Number of cells
Number of autophagosomes/cell
Fold Change (ddCt)
Fold Change (ddCt)
Sham
Smoke
* p = 0.018
* p < 0

Figure 3. Autophagosomes are present in the granulosa cells of CS-exposed ovaries. TEM micrographs of granulosa cells of (A) sham and (B) CS-exposed ovaries. Nuclei (N), mitochondria (arrows), ER (*), and autophagosomes (P) are visible within the cells of both treatment groups. Autophagolysosome formation in the granulosa cells of CS-exposed ovaries can be visualized at all stages of development in the granulosa cells of CS-exposed ovaries. (C) Developing phagophores (open arrows). (D) Sequestering of organelles and cytoplasmic materials within the developing autophagosome (arrowhead) and autophagosomes (P). (E) An autophagosome (P). (F) An autophagolysosome (Au). Original magnification: 7500×. (G) The number of cells counted in each treatment group was not different. (H) The incidence of autophagosomes in the granulosa cells of smoke-exposed ovaries compared with that in sham ovaries. Sham and smoke-exposed ovaries (n = 5). Real-time PCR of (I) *Becn1* and (J) *Lc3* gene expression in smoke-exposed ovaries compared with sham controls. Fold change relative to β-actin (*Becn1*) and glyceraldehyde 3-phosphate dehydrogenase (*Lc3*). Sham and smoke-exposed ovaries (n = 6). Values are expressed as the mean (± SEM).

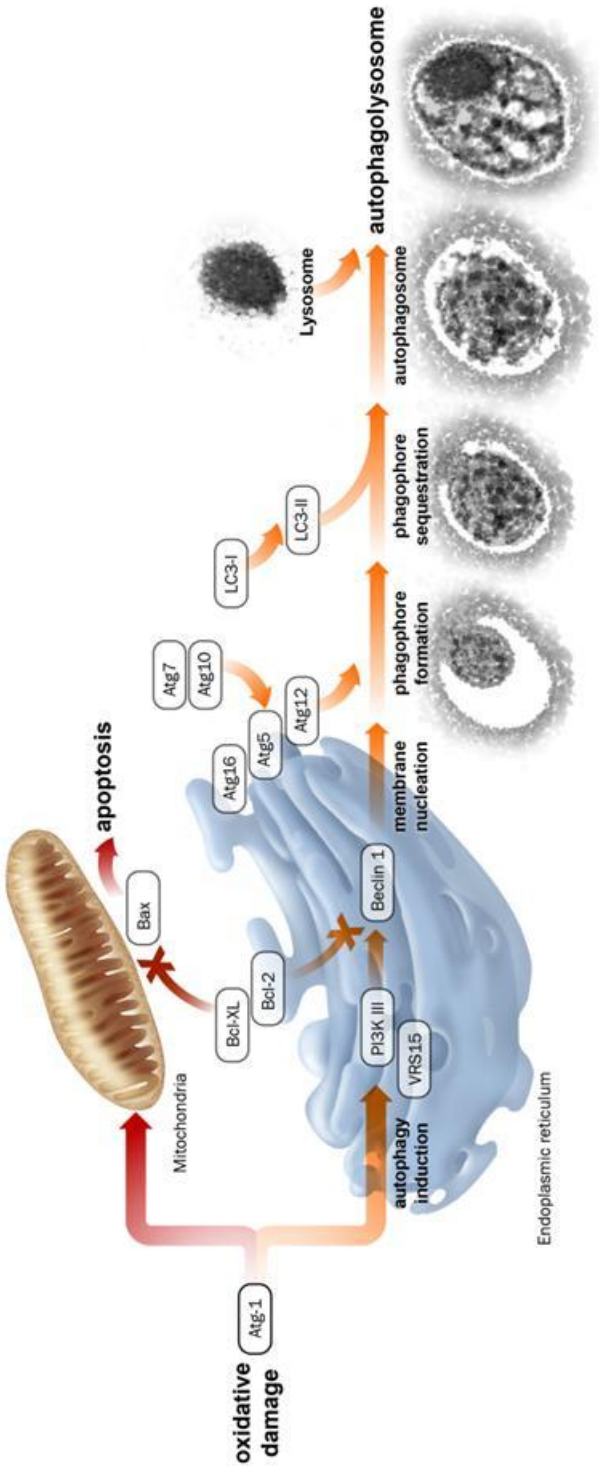
oxidative damage
Atg-1
autophagy induction
PI3K III
VRS15
Beclin 1
membrane nucleation
Bcl-XL
Bcl-2
Bax
apoptosis
Mitochondria
Endoplasmic reticulum
Atg16
Atg5
Atg12
Atg7
Atg10
phagophore formation
LC3-I
LC3-II
phagophore sequestration
Lysosome
autophagosome
autophagolysosome

Figure 4. The Atg cascade.
Emerging evidence suggests that Atg is a potentially important mechanism of cell death in the mammalian ovary. BCL2 plays a pivotal role in regulating both apoptosis and Atg, two distinct pathways of programmed cell death. It is an inhibitor of Beclin-1, a central protein in the Atg cascade. Beclin-1 expression drives membrane nucleation and leading to the formation of the phagophore and autophagosome. Cytoplasmic processing of LC3-I to LC3-II regulates sequestration of damaged organelles (e.g., mitochondria and endoplasmic reticulum) and long-lived proteins into the autophagosome for degradation. LC3-II is then localized to the membrane of the fully formed autophagosomes. Fusion of the autophagosome with lysosomes containing digestive enzymes results in autophagolysosomes, which can be detected by electron microscopy. Artwork by G. Oomen, Glen Oomen Medical & Scientific Graphics, Guelph, ON.

3.10 Supplementary Data

3.10.1 Supplementary Materials and Methods

3.10.1.1 Cigarette smoke exposure

3R4F reference cigarettes (Tobacco and Health Research Institute, University of Kentucky, Lexington, KY, USA) were utilized with filters removed. Control animals were placed in the restrainer for 50 minutes twice daily, 5 days a week and exposed to room air only. Mice were euthanized within 2 hours of the last cigarette smoke exposure by anaesthetization with isoflurane and exsanguination and ovaries were collected and weighed prior to processing. One ovary from each mouse was collected and fixed for histology, while the remaining ovary was snap frozen and used for protein and RNA isolation.

3.10.1.2 Histology and Follicle Counts

Ovaries were fixed in 10% (v/v) formaldehyde, washed in cold water and transferred to 70% ethanol 24 h later. Following fixation, ovaries were dehydrated in graded ethanol solutions, cleared in xylene and embedded in paraffin. Serial sections (4 micron thickness) were prepared and mounted on glass slides, deparaffinized in xylene and rehydrated in graded ethanol solutions, stained with haematoxylin and eosin and follicle counts were carried out. Briefly, primordial follicles were defined as having a single squamous cell layer surrounding the oocyte; transitional follicles as having a single cell layer of granulosa cells surrounding the oocyte whereby half the cells were squamous and

half were cuboidal; primary follicles contained a single layer of cuboidal granulosa cells surrounding the oocyte; secondary follicles were any oocyte surrounded by two or more complete layers of granulosa cells but lacking an antrum; and antral follicles were any oocyte surrounded by two or more complete layers of granulosa cells and having an antrum. Only follicles with a visible nucleus in the oocyte were counted in every tenth section.

3.10.1.3 Immunohistochemistry

Following rehydration, endogenous peroxidase activity was quenched and antigen retrieval was carried out using citrate buffer (pH 3.0) at 37^{o}C for 30 minutes. Sections were blocked with horse serum. Avidin/biotin blocking was carried out prior to incubation with primary antibody (BCL2 1:100; Santa Cruz Biotechnology, Inc., Santa Cruz, CA, USA and BAX 1:100; Cell Signaling Technology, Danvers, MA, USA) was carried out on 4 micron thick ovarian slices for 16 hours at 4^{o}C. Immunohistochemical targets were localized using diaminobenzidine (DAB; 0.25 mg/mL w/v; Sigma Aldrich, Oakville, ON) in PBS and counterstained using Harris haematoxylin (Sigma Aldrich). Sections were dehydrated and cover slips were mounted using Permount. Slides were examined using an Olympus IX81 microscope at 20X and 40X magnification and images were captured using Image Pro AMS (Media Cybernetics, Silver Spring, MD, USA).

3.10.1.4 TUNEL Labelling

Following the labelling of apoptotic cells using the ApopTag® Fluorescein *In Situ* Apoptosis Detection Kit (Chemicon International), slides were counterstained using

propidium iodide. Labelled slides were stored in the dark at -20^{o}C prior to being analysed by fluorescent microscopy using the standard Fluorescein and propidium iodide excitation and emission filter cubes. Ovarian follicles were randomly selected and all cells in the field (20× magnification) were counted. The number of healthy (red nuclei) and apoptotic (green nuclei) cells were counted in 90-100 follicles per treatment group by an observer blinded to treatment group.

3.10.1.5 DNA Damage

Following isolation and quantification, DNA was converted to single-stranded DNA by denaturing the samples at 95^{o}C for 5 min followed immediately by rapidly chilling on ice. Samples were then digested to nucelosides by incubating the denatured DNA with nuclease P1 for 2 h at 37^{o}C in 20 mM sodium acetate (pH 5.2) followed by 1 h incubation at 37^{o}C with alkaline phosphatase in 100 mM Tris (pH 7.5). Samples were centrifuged for 5 min at 6000 x g and the supernatant used to measure DNA damage. A standard curve was generated and the concentration of 8-hydroxydeoxyguanosine (OHdG; ng/mL) was determined for each sample using the equation of the line of best fit from the standard curve. Oxidative DNA damage was measured using the OxiSelect^{TM} Oxidative DNA Damage enzyme linked immunosorbent assay (ELISA) Kit (Cell Biolabs, Inc., San Diego, CA) as per manufacturer's instructions.

3.10.1.6 Protein Carbonyl ELISA

Protein homogenates from the ovaries of smoke-exposed and control mice were used to measure the quantity of protein carbonyls present as a measure of protein oxidation

resulting from the presence of reactive oxygen species (ROS) or secondary by-products of oxidative stress. Absorbance was read on a plate reader using 450 nm as the primary wavelength. Protein carbonyl levels (nmol/mg) were determined using the standard curve generated using reduced and oxidized bovine serum albumin (BSA; provided).

3.10.1.7 Glutathione Assay

Ovaries were homogenized in cold 50 mM MES buffer (0.4 M 2-(N-morpholino)ethanesulphonic acid, 0.1 M phosphate, 2 mM EDTA; pH 6.0) and centrifuged at 10000 x g for 15 min at 4^{o}C and the supernatant kept for analysis. The samples were deproteinated by adding an equal volume of metaphosphoric acid (MPA; 5 g in 50 mL H_2O) reagent and vortexing. Samples were left to stand at room temperature (RT) for 5 min followed by centrifugation at 2000 x g for 2 min. The supernatant was collected and 50 μL of triethanolamine (TEAM; 4 M) per mL of sample was added to the supernatant and vortexed. Following preparation of samples using the Glutathione Assay Kit, absorbance was read at 405 nm using a plate reader at 5 min intervals for 30 min. Total glutathione concentration was determined by plotting the average absorbance of each sample as a function of time, determining the slope of the line and then plotting the slopes as a function of the concentration of total glutathione in the standard curve. The value of total glutathione for each sample was then calculated from their respective slopes using the slope vs. glutathione standard curve. Samples were assayed in triplicate for glutathione concentration using as per manufacturer's instructions.

3.10.1.8 Western Blot

Protein was extracted from whole ovaries using RIPA lysis buffer (2 mM v/v EDTA, 1% v/v Triton X-100, 0.1% w/v SDS, 150 mM NaCl, 0.5% w/v sodium deoxycholate), with phenylmethanesulphonyl fluoride (PMSF; 1mM; Sigma Aldrich) and Complete Mini EDTA-free protease inhibitors (Roche Applied Science, Laval, PQ). For Western blots, 10-20 μg of protein was loaded. SDS-PAGE was carried out with 12% acrylamide gels using a Mini-Protean II system (BioRad, Mississauga, ON) and then electro-transferred to polyvinylidene difluoride (PVDF) blotting membrane (BioRad Laboratories, Hercules, CA). Membranes were blocked with 5% w/v skim milk in tris-buffered saline (TBS, 0.5% v/v Tween-20) at 4^{o}C overnight and incubated for 1 h at RT in primary antibody on a rocking platform. A loading control antibody was used. Following washing with TBS-T, blots were incubated with horseradish peroxidase-conjugated secondary anti-rabbit IgG (1:5000; Amersham Biosciences, Piscataway, NJ) or anti-mouse IgG (1:5000; Amersham Biosciences) antibodies for 1 h at RT on a rocking platform. Blots were washed thoroughly in TBS-T, followed by TBS whereupon reactive protein was detected using ECL-plus chemiluminescence substrate (Amersham Biosciences) and Bioflex X-ray film (Clonex Corporation, Markham, ON). Densitometric analysis of immunoblots was performed using ImageJ 1.37v software. Density was corrected for background and normalized to the density of the corresponding band for β-Actin or Na^{+}/K^{+} ATPase. The data were expressed as a ratio of the optical densities of target protein to β-Actin or Na^{+}/K^{+} ATPase (whose expression was unaffected by treatment). Antibodies used for this study were: intracellular copper, zinc SOD (SOD1; 17 kDa; Abcam, Cambridge, MA,

USA), mitochondrial manganese SOD (SOD2; 25 kDa; Abcam), Hsp27 (23 kDa; Abcam), Na^+/K^+ ATPase (1:5000; Abcam) and β-Actin (1:5000; 43 kDa). Densitometric analysis of immunoblots was performed using ImageJ 1.37v software. Density was corrected for background and normalized to the density of the corresponding band for β-Actin or Na^+/K^+ ATPase. The data were expressed as a ratio of the optical densities of target protein to β-Actin or Na^+/K^+ ATPase (whose expression was unaffected by treatment).

3.10.1.9 Electron Microscopy

Ovaries were excised from sham and smoke exposed mice and fixed with 2% glutaraldehyde buffered in 0.1 M sodium cacodylate buffer containing 0.05% calcium chloride (pH 7.4) at 4^oC. The tissue was then washed overnight in 0.1 M sodium cacodylate buffer containing 4% sucrose and kept in the same buffer at 4^oC. The tissue blocks from six mice/treatment group were sectioned at 75 μm with a Sorvall TC-2 tissue sectioner. The sections were postfixed in 1.5% ferrocyanide reduced osmium tetroxide and then dehydrated in ethanol, followed by infiltration in propylene oxide and embedding in Epon. Sections were analysed for the presence of autophagosomes in the granulosa cells.

3.10.1.10 Quantitative Real Time PCR

Following confirmation of RNA integrity by gel electrophoresis and spectrophotometric quantification, cDNA was reverse transcribed using an iScript kit (BioRad). Real time

PCR was performed with murine specific primers using an Applied Biosystems 7900HT Fast Real Time PCR System (Applied BioSystems, Foster City, CA). Control reactions without cDNA and a no RT control were run to verify the absence of primer dimerization and genomic DNA contamination, respectively. PCR amplification was carried out in a 20 μL reaction volume containing 1-5 ng of cDNA, 0.5 μM each of forward and reverse primers and 10 μL of Fast SYBR Green Master Mix (Applied Biosystems). Gene- and species-specific primers were designed for autophagy markers *Becn1* and *Lc3* using Primer3 and OligoAnalyzer. See Table S1 for the sequence of the forward and reverse primers, and amplicon lengths of the genes analysed. The PCR reactions were initiated with denaturation at 95^{o}C for 10 min; followed by 40 amplification cycles at 95^{o}C for 15 sec and 60^{o}C for 1 min. Following amplification, to confirm the presence of a single amplification product, PCR products were subjected to a dissociation stage and derivative curve analysis as well as product separation on a 4% agarose gel stained with ethidium bromide. Samples were run in triplicate and results were averaged. CT was calculated by analysis software SDS 2.2.1 (Applied Biosystems). Analysis of gene expression changes were calculated according to the method of Livak *et al.* using the $2^{-\Delta\Delta Ct}$ method. The normalized expression ratio (fold induction) was calculated by $2^{-\Delta\Delta Ct}$ = fold induction. Statistical analyses were performed using the $\Delta Ct \pm SD$ values.

3.10.1.11 Statistical Analysis

Results are expressed as mean ± standard error of the mean (SEM) unless otherwise stated. Data were checked for normality and equal variance by Kolmogorov-Smirnov test

and treatment effects were tested using a two-tailed t-test. A $p \leq 0.05$ was considered significant.

3.10.2 Supplementary Figures

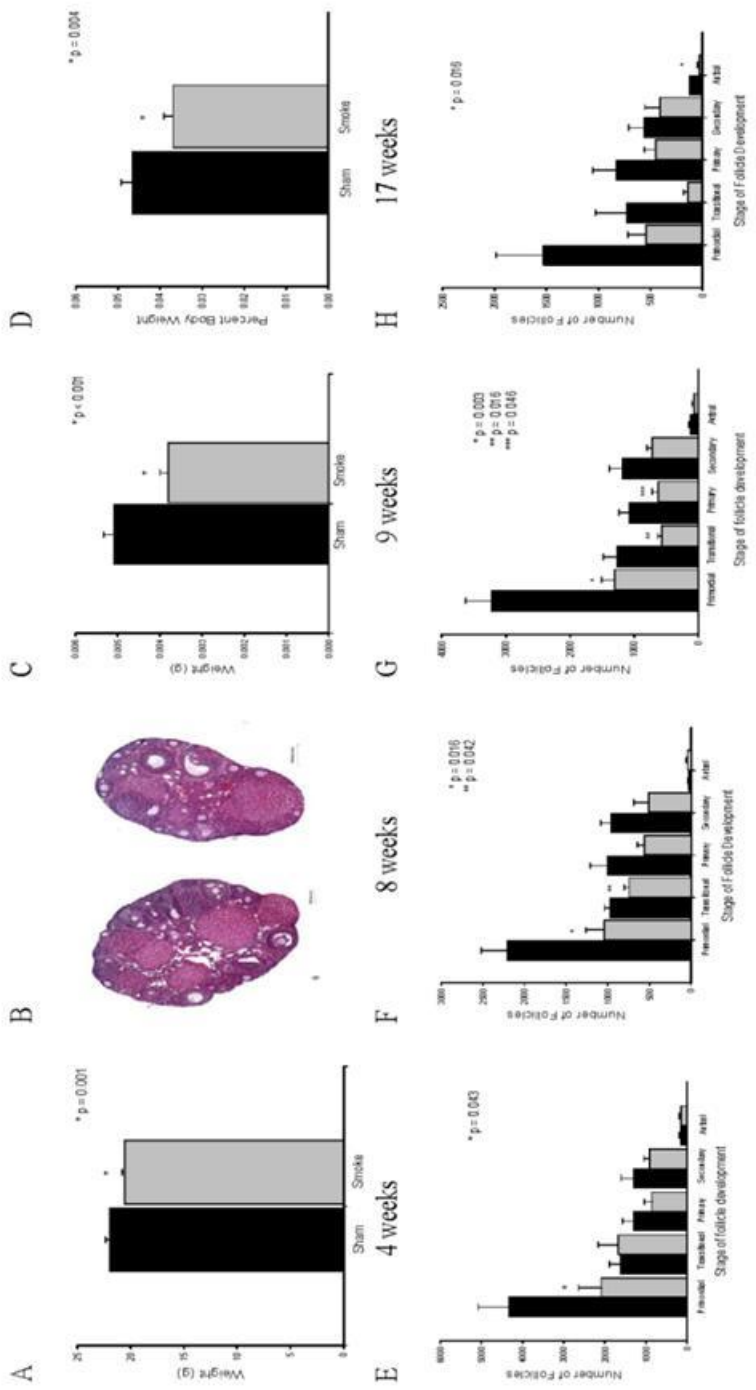

Figure S1: Cigarette smoke exposure results in smaller ovaries with fewer follicles. A) Smoke exposed mice were significantly smaller than sham controls ($p = 0.001$). B) Representative photomicrographs of H & E-stained ovaries of sham and smoke exposed mice. C) Mice exposed to sham or cigarette smoke for 8 weeks were weighed at sacrifice to determine whether treatment affected body weight. Ovaries from smoke exposed mice were significantly smaller than sham controls ($p < 0.001$). D) Relative ovarian weights of smoke exposed and sham control mice indicate that smoke exposed mice have smaller ovaries relative to body size ($p = 0.004$). n = 20 sham and 21 smoke exposed mice (A-D). E-H) The number of follicles was determined in serial sections of ovaries from sham and cigarette smoke in E) 4, F) 8, G) 9 and H) 17 week exposed mice. E) Ovaries from smoke exposed mice had significantly fewer primordial ($p = 0.043$) follicles than sham mice. F) Ovaries from smoke exposed mice had a significantly fewer primordial (*$p = 0.016$) and transitional (**$p = 0.042$) follicles than sham mice. G) Ovaries from smoke exposed mice had significantly fewer primordial (*$p = 0.003$), transitional (**$p = 0.016$) and primary (***$p = 0.046$) follicles than sham mice. H) Although there was a strong trend towards fewer primordial ($p = 0.078$), transitional ($p = 0.087$), and primary ($p = 0.1$) follicles, only the number of antral follicles present in smoke exposed mice was significantly lower ($p = 0.016$) than that found in sham mice. n = 5 mice per treatment group. All values are expressed as the mean (± SEM).

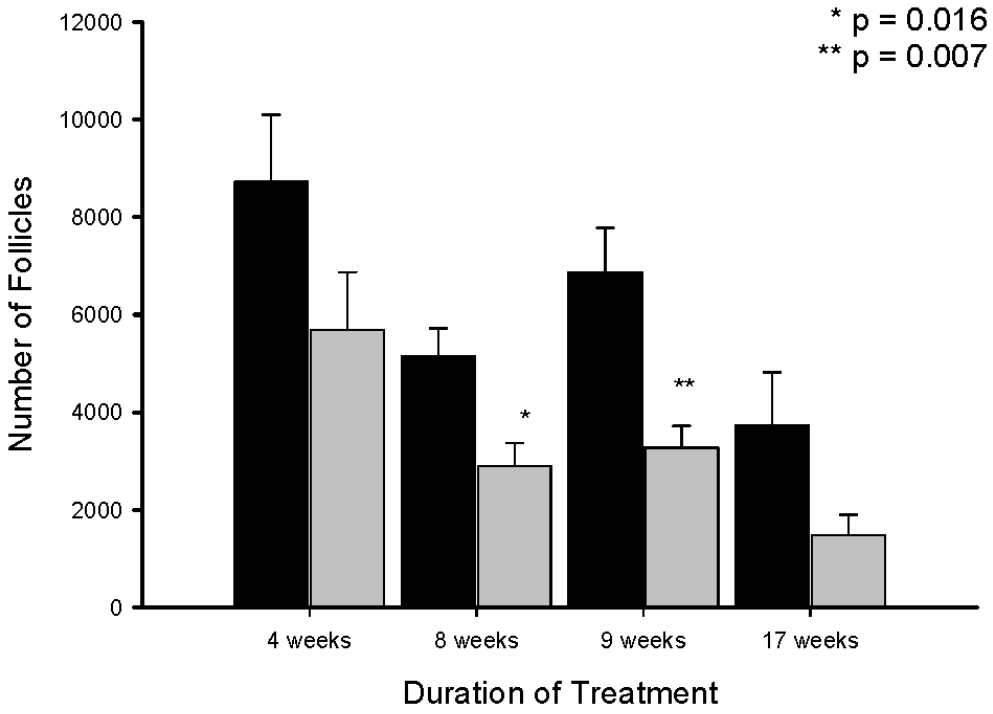
* p = 0.016
** p = 0.007
12000
10000
8000
6000
4000
2000
0
Number of Follicles
*
**
4 weeks
8 weeks
9 weeks
17 weeks
Duration of Treatment

Figure S2.
The total number of follicles contained within the ovary was significantly lower in ovaries exposed to cigarette smoke for 8 or 9 weeks compared to sham exposed ovaries ($p = 0.016$ and 0.007, respectively). $n = 5$ mice per treatment group. All values are expressed as the mean (± SEM).

Table S1.
PCR primer pairs for semi-quantitative RT-PCR, annealing temperatures, and amplicon sizes.

Gene	Left Primer	Right Primer	Product Size	% GC content	Melting Point
Beclin-1	CCAGCCAGGATGATGTCTAC	CCCGATCAGAGTGAAGCTATT	51	55/47.2	58.1/58.42
LC3	CACTCCCATCTCCGAAGTGTA	TGCGAGGCATAAACCATGTA	72	52.38/45	60.12/60.1

Chapter 4

Cigarette smoke exposure elicits increased autophagy and dysregulation of mitochondrial dynamics in murine granulosa cells

Gannon, AM., Stämpfli, MR., and Foster, WG.

This article appeared in Biology of Reproduction, 2013; 88(3):63, 1-11.

4.1 Abstract

Cigarette smoking is a lifestyle behavior associated with significant adverse health effects including subfertility and premature ovarian failure. Cigarette smoke contains a number of chemicals, many of which are involved in the generation of reactive oxygen species, which can lead to apoptosis and autophagy. Autophagy is a fundamental process that removes damaged organelles and proteins through lysosomal degradation. The relevance of autophagy to toxicant-induced changes in ovarian function is largely unexplored. Previously, we reported that exposure to cigarette smoke causes follicle loss, oxidative stress, activation of the autophagy pathway, and a decrease in manganese superoxide dismutase expression (which points to altered mitochondrial function). Therefore, our objective was to test whether cigarette smoke exposure results in the dysregulation of mitochondrial repair mechanisms leading to loss of follicles via autophagy-mediated granulosa cell death. In this study, mice were exposed to cigarette smoke or room air for 8 weeks. The expression of genes and proteins of autophagy and mitochondrial repair factors were measured using quantitative real time PCR and Western blot,

immunohistochemistry and ELISA. Increased expression of parkin and decreased expression of the mitofusins suggest that cigarette smoke exposure triggers mitochondrial damage. Moreover, the autophagy cascade proteins, BECN1 and LC3, were up-regulated, while the antagonist BCL2 was down-regulated following treatment. Taken together, our results suggest cigarette smoke exposure induces dysfunction of mitochondrial repair mechanisms, leading to autophagy-mediated follicle death.

4.2 Introduction

Although numerous sources of infertility have been identified, many otherwise healthy couples of childbearing age experience infertility for unknown reasons. Premature exhaustion of the ovarian follicle reserve has been identified as a possible causative factor for infertility. Several studies have shown that exposure to environmental toxicants results in the destruction of the follicle population, often in a stage-specific manner [1-9]. Of the numerous environmental toxicants and lifestyle factors known to affect fertility and ovarian function studied to date, cigarette smoking may perhaps be the single most clinically-relevant and preventable toxic exposure in women, making it an ideal target for infertility prevention [10]. Cigarette smoke and its relationship to female fertility has been strongly associated. That smoking depletes ovarian follicle reserve and impairs uterine receptivity is well documented [11]. Studies conducted in our laboratory have revealed that women exposed to cigarette smoke had greatly decreased implantation and pregnancy rates [12]. We also found that benzo(a)pyrene (BaP), a polycyclic aromatic hydrocarbon (PAH) present in cigarette smoke and known agonist of the aryl

hydrocarbon receptor (AhR), is detectable in the serum and follicular fluid of women who smoke or are exposed to cigarette smoke and that treatment with BaP impairs cumulus expansion in isolated rat follicle culture experiments [5;13]. More recently, we reported that mice exposed to cigarette smoke have smaller ovaries and significantly fewer primordial follicles compared to sham controls [14].

Cigarette smoke contains more than 4,000 chemical compounds, many of which are oxidants or free radicals that are inducers of oxidative stress. Previous studies have revealed that of the chemicals present in cigarette smoke, levels of PAHs, most notably BaP, are present in levels that are 10-fold higher in sidestream than mainstream smoke [15], and have been shown to lead to the production of free radicals, reactive oxygen species (ROS) and oxidative stress. Cigarette smoke contains a number of AhR agonists, the activation of which leads to induction of cytochrome P450 enzymes CYP1A1, 1A2, and 1B1, which are involved in the generation of ROS [16]. Oxidative stress and the production of ROS can lead to both apoptosis and autophagy. Several studies point to BCL2-associated X protein (BAX) activation as the central pathway regulating follicle numbers; however, emerging evidence challenges this belief and our data support an alternative cell death pathway as being important in regulating follicle demise. Destruction of developing fetal ovarian germ cells and induction of premature ovarian failure has been achieved in mice treated with AhR ligands which activated the intrinsic pathway leading to enhanced *Bax* expression [17-19]. However, although *in vivo* exposure to cigarette smoke decreased B cell leukemia/lymphoma 2 (BCL2) protein

expression, BAX protein expression remained unchanged, enhanced apoptosis was not evident in treated ovaries suggesting a concentration-dependent effect of cigarette smoke exposure on ovarian follicle loss and apoptosis [14]. Cigarette smoke exposure instead resulted in activation of the autophagy cascade, as evidenced by an increase in the number of autophagosomes and expression of key regulatory genes in the ovaries of exposed mice [20].

Autophagy is a fundamental cellular process that was first described nearly six decades ago by Clark in mammalian cells by electron microscopy and later systemically characterized by de Duve [21-24]. Derived from the Greek for "self-eating", autophagy is evolutionarily conserved from yeast to mammals. To date, approximately 35 autophagy genes have been identified in yeast, a number of which have mammalian homologues identified. These genes have been established as important regulators of both bulk and selective autophagy [25-27], including Beclin 1 (*Becn1*), microtubule-associated protein 1 light chain 3 (*Lc3*) and *Bcl2*. Traditionally considered a stress adaptation to avoid cell death (as in starvation conditions), autophagy has also been implicated as an alternative pathway to cell demise in recent years [28-31]. Programmed cell death (PCD) type I demonstrates the hallmarks of apoptosis while PCD type II has been coined to describe cell death that demonstrates hallmarks of autophagy, namely the accumulation of autophagosomes. While this classification has generated considerable controversy, due primarily to debate over whether autophagy actually promotes cell death or if it is simply a reactive process upstream of PCD type I, numerous studies have shown that autophagy

acts independently of apoptosis to elicit cell death during development [32-34] as well as in response to cytotoxic [35-37] and metabolic stressors [38].

Mitophagy is the selective degradation of mitochondria via autophagy. Mitochondria are essential energy-producing organelles that exist in a dynamic interconnected network that is constantly reshaped by a strictly regulated balance between fission and fusion to maintain proper mitochondrial content in daughter cells and allow repair of damaged mitochondria [39-43]. During fission, mitochondria become fragmented and are targeted for autophagosomal degradation by parkin (PARK2), while at the same time, the ubiquitination and degradation of central fusion proteins, mitofusin 1 (MFN1) and mitofusin 2 (MFN2) is occurring [44-46]. During apoptosis, mitochondrial cristae are remodeled opening their tubular junctions leading to release of pro-apoptotic factors such as cytochrome *c*, and activation of the apoptosis cascade [47;48], a process that we have consistently shown is not upregulated by cigarette smoke exposure [14;20]. In contrast to fission, key regulatory proteins in mitochondrial fusion drive mitochondrial elongation, increased cristae density, and maintenance of ATP output [49] to sustain cell viability. Thus, unopposed mitophagy results in an energy-deficient state in the affected cells culminating in the death of those cells.

Although cigarette smoke exposure increases the number of autophagosomes [20], it is not known if the adverse effects are primarily mitochondrial-specific (mitophagy) or if multiple organelles undergo autophagy (bulk autophagy). Therefore, the objective of our

current study was to explore the mechanistic pathway linking cigarette smoke exposure to mitochondrial dysfunction and autophagy, a novel alternative cell death pathway important in follicle development and demise. Decreased superoxide dismutase 2 (SOD2) expression suggests mitochondrial damage in cigarette smoke exposed ovaries [20]. Fusion and elongation provides a mechanism for mitochondrial repair, a process that opposes autophagy [49;50]. Taken together, we postulate that cigarette smoke exposure-induced mitochondrial dysfunction in granulosa cells leads to autophagy-mediated cell death, a novel alternative ovarian cell death pathway.

4.3 Materials and Methods

4.3.1 Ethics Statement

All animal work described in this study was conducted using protocols approved by the McMaster University Animal Research Ethics Board and is in accordance with the Canadian Council for Animal Care guidelines for the use of animals in research.

4.3.2 Animals

The ovarian effects of cigarette smoke exposure was studied in female C57BL/6 mice (8 weeks old at the start of exposure) obtained from Charles River Laboratories (Montreal, PQ, Canada). Mice were maintained in polycarbonate cages at 22 ± 2oC and 50 ± 10% relative humidity on a 12-hour light-dark cycle and were provided with food (LabDiet, PMI Nutrition International, Saint Louis, MO, USA) and tap water *ad libitum* throughout the experiment.

4.3.3 Cigarette Smoke Exposure

Mice were exposed to cigarette smoke twice daily, 5 days a week for 8 weeks using a whole body smoke exposure system (SIU-48, Promech Lab AB, Vintrie, Sweden). Details of the exposure protocol have been described previously [51]. Briefly, cigarette smoke from twelve 3R4F reference cigarettes (Tobacco and Health Research Institute, University of Kentucky, Lexington, KY, USA) with filter removed was mixed with room air and delivered into the exposure chamber over a 50 minute period twice daily. Animals were placed in the restrainer, which was then placed in the smoke exposure box. There was no lead-up period required for smoke exposure; however, mice were acclimatized to the restrainer over a three-day period prior to commencement of the experiment. This acclimatization was accomplished by placing mice in the restrainer for 20 minutes on Day 1, for 30 minutes on Day 2, and for 50 minutes on Day 3. Following the acclimatization period, mice were exposed to cigarette smoke for 50 minutes twice daily, 5 days a week for 8 weeks prior to sacrifice. Control animals were placed in the restrainer for 50 minutes twice daily, 5 days a week and exposed to room air only. Mice were euthanized at the end of the exposure by exsanguination and ovaries were collected and weighed prior to processing.

4.3.4 Electron Microscopy

Ovaries were collected and processed for electron microscopy as described previously [20]. Briefly, ovaries were excised and fixed with 2% glutaraldehyde buffered in 0.1M sodium cacodylate buffer containing 0.05% calcium chloride (pH 7.4) at 4^{o}C. The tissue was washed in 0.1M sodium cacodylate buffer with 4% sucrose and stored at 4^{o}C. Tissue

blocks from six mice/treatment group were sectioned at 75 µm with a Sorvall TC-2 tissue sectioner and postfixed in 1.5% ferrocyanide reduced osmium tetroxide, dehydrated in ethanol, followed by infiltration in propylene oxide and embedded in Epon. Sections were analyzed for the presence of autophagosomes in the granulosa cells.

4.3.5 Immunohistochemistry

Ovaries were fixed in 10% (v/v) formaldehyde, washed in cold water and transferred to 70% ethanol 24 h later. Following fixation, ovaries were dehydrated in graded ethanol solutions, cleared in xylene and embedded in paraffin. Serial sections (4 µm thickness) were prepared and mounted on glass slides, deparaffinized in xylene and rehydrated in graded ethanol solutions. Following rehydration, endogenous peroxidase activity was quenched and antigen retrieval was carried out using citrate buffer (pH 3.0) at 37^{o}C for 30 minutes. Sections were blocked with horse serum. Avidin/biotin blocking was carried out prior to incubation with primary antibody (BECN1 1:100; Cell Signaling, Danvers, MA, USA) was carried out on 4 µm thick ovarian slices for 16 hours at 4^{o}C. Immunohistochemical targets were localized using diaminobenzidine (DAB; 0.25 mg/mL w/v; Sigma Aldrich, Oakville, ON, Canada) in phosphate buffered saline (PBS; 8 g/L NaCl w/v, 0.2 g/L w/v KCl, 1.44 g/L w/v Na_3PO_4, 0.24 g/L w/v KH_2PO_4, pH 7.4) and counterstained using Harris haematoxylin (Sigma Aldrich). Sections were dehydrated and cover slips were mounted using Permount. Slides were examined by a reader blinded to treatment group using an Olympus IX81 microscope and images were captured using Image Pro AMS (Media Cybernetics, Silver Spring, MD, USA). Positive staining cells

were counted using Image Pro software to identify cells within each follicle stained with DAB and were expressed as a percentage of granulosa cells per follicle that were positive for BECN1.

4.3.6 RNA Isolation and cDNA Synthesis

Total RNA was isolated from ovaries using a Qiagen RNeasy mini kit with on-column DNase digestion (Qiagen, Mississauga, ON, Canada) as per manufacturer's instructions. Potential genomic DNA contamination was removed from the samples by treatment with RNase-free DNase (Invitrogen, Life Technologies, Burlington, ON, Canada) for 15 min at 37°C. Following confirmation of RNA integrity by gel electrophoresis and spectrophotometric quantification, cDNA was reverse transcribed using an iScript kit (BioRad, Mississauga, ON, Canada).

4.3.7 Quantitative Real Time PCR

Gene- and species-specific primers for pro-survival factor *Bcl2*, mitochondrial repair mechanism markers *Parkin*, *Mfn1* and *Mfn2* obtained from SA Biosciences (SA Biosciences, Qiagen, Mississauga, ON, Canada). Control reactions without cDNA and a no RT control were run to verify the absence of primer dimerization and genomic DNA contamination, respectively. PCR amplification was carried out in a 20 µL reaction volume containing 1-5 ng of cDNA, 0.5 µM each of forward and reverse primers and 10 µL of Fast SYBR Green Master Mix (SA Biosciences). The PCR reactions were initiated with denaturation at 95^{o}C for 10 min; followed by 40 amplification cycles at 95^{o}C for 15 sec and 60^{o}C for 1 min. Samples were run in triplicate and results were averaged. CT was

calculated using the analysis software SDS 2.2.1 (Applied Biosystems, Life Technologies, Burlington, ON, Canada). Analysis of gene expression changes was calculated according to the method described by Livak and Schmittgen [52].

4.3.8 Beclin 1 Enzyme-Linked Immunosorbent Assay

Ovaries from mice exposed for 8 weeks to either sham or cigarette smoke were homogenized in 0.02 mol/L phosphate buffered saline (PBS; pH 7-7.2) and quantified using the Bradford method of protein quantification. Beclin 1 concentrations in ovarian homogenates were assayed using a commercially available enzyme-linked immunosorbent assay (ELISA) kit (Beclin 1 ELISA; Shanghai BlueGene Biotech CO. Ltd, Shanghai, China). Sample Beclin 1 concentration was calculated using a four parameter logistic (4-PL) curve-fit using the formula: y = min + (max-min)/(1 + abs(x/EC50)^Hillslope). The sensitivity in this assay is 0.1 ng/mL. Values were calculated and expressed as mean (± SEM).

4.3.9 Western Blot

Protein expression was measured in whole ovarian homogenates sham and smoke exposed mice as described previously [20]. Following SDS-PAGE and transfer to polyvinylidene difluoride (PVDF) blotting membrane (BioRad Laboratories, Hercules, CA, USA), membranes were blocked overnight with 5% (w/v) skim milk in tris-buffered saline (TBS; 8 g/L w/v NaCl, 0.2 g/L w/v KCl, 3 g/L w/v Tris base, pH 7.4,) with Tween-20 (TBS-T; 1x TBS, 0.5% v/v Tween-20) and incubated with primary antibody. The following antibodies were used for this study: ACTB (1:5000; Abcam, Cambridge, MA,

USA), BCL2 (1:2000; Abcam), BECN1 (1:1000; Cell Signaling), GAPDH (1:5000; Abcam), LC3 (1:2000; Novus Biologicals, Littleton, CO, USA), MFN1 (1:2000; Sigma Aldrich), MFN2 (1:2000; SigmaAldrich), and PARK2 (1:1000; Cell Signaling). Following washing with TBS-T, blots were incubated with horseradish peroxidase-conjugated secondary anti-rabbit IgG (1:4000; Amersham Biosciences, Piscataway, NJ, USA) or anti-mouse IgG (1:4000; Amersham Biosciences) antibodies for 1 hour at room temperature. Blots were thoroughly washed in TBS-T, followed by TBS whereupon reactive protein was detected using ECL-plus chemiluminescence substrate (Amersham Biosciences) and Bioflex X-ray film (Clonex Corporation, Markham, ON, Canada). Densitometric analysis of immunoblots was performed using ImageJ 1.37v software; all proteins were quantified relative to the loading control.

4.3.10 Statistical analysis

All statistical analyses were performed using SigmaStat (v.3.1, SPSS, Chicago, IL, USA). Results are expressed as mean ± SEM unless otherwise stated. Data were checked for normality and equal variance and treatment effects were tested using t-test. A $p \leq 0.05$ was considered significant.

4.4 Results

4.4.1 General health of animals exposed to cigarette smoke

Treatment with cigarette smoke had no effect on the general health of the mice, as shown by absence of stereotypical behaviors, hunched back and signs of lacrimation, porphyria,

or ruffled coat. Our previous work has shown changes in whole body and relative ovarian weights following 8 weeks of cigarette smoke exposure [20] in the absence of any signs of adverse effects on the general health of the animals.

4.4.2 Autophagosome formation is evident following cigarette smoke exposure

Ovaries from sham and smoke exposed ovaries were collected and processed for transmission electron microscopy (TEM) to confirm our previous findings of autophagosomes in the granulosa cells of ovarian follicles treated with cigarette smoke. Nuclei were normal in appearance in granulosa cells from both sham and smoke exposed mice (Figure 1), although nuclei were displaced by autophagosomes in smoke exposed mice (Figure 1B). Autophagosomes were more abundant in granulosa cells of smoke exposed vs. controls, in keeping with our previous findings [20]. Additionally, though mitochondria were visible in the cytoplasm of granulosa cells from both treatment groups (Figure 1, arrowheads), autophagosomes located in smoke exposed ovaries were found to contain large, swollen organelles resembling mitochondria (Figure 1B, arrows).

4.4.3 Cigarette smoke exposure alters immunolocalization of Beclin 1 protein

Immunohistochemical analysis of ovaries sectioned and stained using the rabbit anti-BECN1 antibody revealed changes in the intensity, amount and location of staining in treated vs. sham control ovaries. BECN1 staining was seen in all stages of follicle development, including primordial follicles. Low power magnification of sham and smoke exposed ovaries (Figure 2A and B, respectively) shows BECN1 staining in both treatment groups. Primordial follicles showed evidence of staining in both sham (Figure

2C) and smoke (Figure 2D); however, localization in the smoke exposed ovaries differed from that of the sham ovaries. In smoke exposed primordial follicles, the granulosa cells stained positive for BECN1, while in sham follicles, only the oocyte stained positively. This pattern did not hold true for larger follicles, however. In primary (Figure 2E and F), pre-antral (Figure 2G and H) and antral follicles (Figure 2I and J), staining was evident in the theca, granulosa cells and the oocyte in both treatment and sham follicles. However, those follicles in the smoke exposed ovaries had a higher percentage of positively-stained cells (although only significant in pre-antral follicles; Figure 2K, $p = 0.008$) and the intensity of staining was greater. Interestingly, the pattern of staining was also different. In the sham exposed ovaries, BECN1 staining was more punctate with less cytoplasmic staining, whereas in the smoke exposed mice, staining was evident in the cytoplasm and more diffuse than punctate in nature.

4.4.4 Cigarette smoke exposure results in up-regulation of autophagy machinery

Homogenates from whole ovaries were examined to determine if the genes of the autophagy cascade and the proteins for which they code were altered following treatment. Changes in gene expression, as measured by mRNA expression changes using real time RT-PCR, were assessed for *Bcl2*. While gene expression of *Bcl2* was not changed, a trend towards down-regulation was seen (Figure 3). Protein expression of BCL2, however, was significantly lower in the ovaries of mice exposed to cigarette smoke (Figure 3, $p = 0.003$). In keeping with gene expression data from our previous experiment [20], both BECN1 and LC3 proteins were significantly up-regulated in smoke exposed mice (Figure

4A and B, p = 0.002 and 0.037, respectively). An ELISA also revealed that BECN1 was more abundant in smoke-exposed mice compared to sham controls (Figure 5, p = 0.003).

4.4.5 Mitochondrial repair mechanisms are disrupted by cigarette smoke exposure

Gene and protein expression of three important regulators of mitochondrial repair was examined in the homogenates of ovaries from cigarette smoke and sham control mice. Significant increases in the expression of both the gene (p = 0.001) and protein (p = 0.006) of the pro-fission marker parkin were seen following cigarette smoke exposure (Figure 6A and B), while expression of the genes *Mfn1* and *Mfn2*, encoding pro-fusion proteins MFN1 and MFN2, (Figure 6C and E, p = 0.003 and p = 0.052, respectively) were decreased. In line with the gene expression changes, expression of both MFN1 and MFN2 was significantly down-regulated following treatment (Figure 6D and F, p < 0.001 and p = 0.02, respectively).

4.5 Discussion

Our results show that cigarette smoke exposure causes over-expression of the autophagy proteins BECN1 and LC3 and under-expression of an autophagy inhibitor, BCL2. Coupled with induction of autophagy, mitochondrial dysfunction appears to occur following cigarette smoke exposure, as evidenced by increases in the expression of the pro-fission protein, PARK2 and the decreased expression of the pro-fusion proteins MFN1 and MFN2. These findings, together with our previous results which revealed a profound increase in autophagosomes in granulosa cells and over-expression of the pro-

autophagy genes, *Becn1* and *Lc3* [14;20], suggest that cigarette smoke exposure induces mitochondrial dysfunction culminating in mitochondrial-specific autophagy.

In the present study, cigarette smoke exposure results in changes in the localization and expression of the BECN1 protein. BECN1 was present but restricted to the oocyte in resting primordial follicles of sham exposed mice. In addition to the oocyte, BECN1 was present in both granulosa and theca cells of larger follicles. These findings are inconsistent with those of Gaytán *et al.*, who found that staining was restricted to the theca cells of secondary, antral and pre-ovulatory follicles in the human ovary [53]; however, this disparity could be explained by interspecies differences as well as variation in the sensitivity of the antibody used. To our knowledge, there are currently no published studies identifying the immunolocalization pattern of BECN1 expression in murine ovaries. Expression of BECN1 in untreated ovaries was expected however, as numerous studies have identified a basal level of expression in a variety of cells including rat pheochromocytoma cells [54], human umbilical vein endothelial cells [55], ovarian follicles [53] and melanoma cells [56] and mouse ovarian [20], cortical and hippocampal tissues [57]. BECN1 is a key protein initiator of autophagy, a fundamental cellular process that constitutively eliminates damaged organelles (mitochondria and ER) and long-lived insoluble proteins via lysosomal degradation and is essential for survival, differentiation, development, and homeostasis. BECN1, a BCL2-regulated protein, is required for normal mammalian development [53] and is at the intersection between apoptosis and autophagy, suggesting a role in the interrelationship between the two

processes. In our study, BECN1 expression is increased following cigarette smoke exposure and immunohistochemical staining reveals a shift from focal to diffuse staining throughout the cytoplasm. Activation of the autophagy cascade begins with induction of BECN1 expression and membrane nucleation. Taken together we interpret these data as evidence that cigarette smoke exposure increases BECN1 expression leading to its wider distribution in the cytoplasm to sites of membrane nucleation and induction of autophagolysosome development.

In the current study, we examined the effect of cigarette smoke exposure on the expression of genes and their respective proteins involved in the autophagy cascade. Of these, we found a significant increase in both the gene and protein expression of two pro-autophagy cascade members, BECN1 and LC3. Moreover, while we saw no change in *Bcl2* gene expression, an autophagy antagonist, there was a significant decrease in BCL2 protein expression following cigarette smoke exposure. Our findings are consistent with those of others who have demonstrated that drugs such as etoposide and staurosporine (known apoptosis inducers), and cigarette smoke and its extract, induce autophagy in a variety of cell types and species [35;38;58-62], suggesting that although tissue and/or species differences exist, autophagy-mediated cell death can act as a substitute for apoptosis under certain conditions. Interestingly, not all treatments that elicited an autophagic response resulted in the same type of autophagy; to wit: while etoposide treatment caused death-associated autophagy in Hep3B hepatoma cells, staurosporine treatment in the same cells was cytoprotective [62]. Whereas our results are in keeping

with the above studies, Shimizu *et al.* have demonstrated that over-expression, rather than reduction in the expression of either BCL2 or BCL2-like 1 (BCL2L1; a BECN1-interacting protein), resulted in autophagy-mediated cell death similar to that seen in their double *Bax*/*Bak* mutants [35]. Once again, death-associated autophagy appeared to be regulated differently than starvation-induced autophagy (survival). For instance, BCL2L1 is required for regulation of BECN1 in death-associated but not starvation-induced autophagy and upregulation of BECN1 expression is only seen in death-associated autophagy [63].

Emerging evidence challenges the long-held belief that BAX activation is the central pathway regulating follicle density and our data support the view that an alternative cell death pathway is important in regulating follicle demise. Mechanisms regulating cross-talk between the apoptosis and autophagy pathways are unclear; however, we note that BCL2 is at the interface between both pathways and several studies have identified autophagy as an important alternative pathway of cell death in mammalian cells including human and rodent granulosa cells. We and others have shown stress-induced cell death often proceeds in an apoptosis-independent manner. Specifically, mice lacking both *Bax* and BCL2-antagonist/killer 1 (*Bak*) are completely resistant to apoptosis yet cell death progresses normally, the execution of which was dependent upon the induction of autophagy [35]. Similarly, human granulosa cells with unopposed oxidative stress demonstrated increased autophagy following increased expression of lectin-like oxidized low-density receptor (LOX-I), a scavenger receptor and membrane glycoprotein that is

activated by oxidized low-density lipoprotein [61;64]. During yolk removal in some fish species, autophagosomes containing degenerating mitochondria and other material were evident in follicular cells [29]. Finally, our lab reported a significant loss of follicles at all stages of development in mice exposed to cigarette smoke without activating either the intrinsic or extrinsic apoptosis pathways despite a significant reduction in the expression of BCL2 [14;20].

We have previously shown that both cigarette smoke condensate and BaP delayed follicle development, decreased E_2 and AMH output of follicles in isolated follicle cultures [13;65;66]; while cigarette smoke exposure induced oxidative stress as shown by increased HSP25 and decreased SOD2 expression [20] but did not induce apoptosis in mice [14;20] via no changes in active Caspase 3 (CASP3) expression, TUNEL staining or DNA laddering. The observed absence of changes in active Caspase 3, the common executioner in the apoptosis cascade, coupled with a lack of increased TUNEL staining in treated ovaries lead us to conclude that apoptosis was not upregulated following cigarette smoke exposure. This conclusion was further supported by our EM experiments which showed a distinct lack of hallmarks of apoptosis and an abundance of autophagosomes in various stages of maturity [20]. These findings, coupled with our present findings, suggest that cigarette smoke induces oxidative stress via an AhR-dependent process leading to dysregulation of mitochondrial dynamics, as evidenced by the observed increase in PARK2 expression and the decrease in MFN1 and MFN2 expression, leading to mitophagy and ultimately follicle demise. Overall, our findings suggest that cigarette

smoke exposure, representative of exposure in women who smoke a pack a day, does not activate the apoptosis machinery of ovarian follicles [14;20], but instead induces autophagy (present study and [20]), which leads to death of the granulosa cells and ultimately death of the follicle. Numerous studies have shown that treatment with ovarian toxicants results in apoptosis in the ovary [2;7;67-77]. We propose that the concentrations of chemicals used in those studies were significantly higher than the concentrations achieved in women who smoke and thus resulted in activation of the canonical apoptosis cell death pathway whereas our treatment initiated autophagy which in all likelihood was initially an adaptive response to protect follicle development and mediate oxidative stress caused by the cigarette smoke but which ultimately was overcome due to the chronic activation of the cascade and led to autophagy-mediated cell death. This hypothesis is not without precedent. Previous studies have shown that prolonged activation of the autophagy cascade, particularly non-physiological assaults (i.e.: chemotherapy), lead to autophagy-mediated cell death without the activation of apoptosis [78;79].

Mitochondrial homeostasis is vital to the survival of cells. Mitochondria are responsible for the execution of a number of processes upon which cells depend to maintain appropriate energy levels, reduce ROS accumulation, and carry out programmed cell death [39]. In mouse pancreatic beta cells, metabolically stressed mitochondria, in the form of free fatty acids and high glucose levels, displayed elevated levels of membrane potential heterogeneity and increased autophagy [43;80;81]. Prior to mitophagy, mitochondria have been shown to depolarize and are sequestered in a pre-autophagy pool

[42]. These mitochondria no longer contribute to the pool of mitochondria capable of fusing. Mitofusins play an important role in maintaining mitochondrial integrity. In mouse embryonic fibroblasts, the absence of either MFN1 or MFN2 resulted in reduced fusion and increased numbers of fragmented mitochondria [82] and also resulted in the cells' increased sensitivity to various apoptotic stimuli [83]. Interestingly, inhibition of autophagy (by deletion of *Atg5* or silencing of *Becn1*) or induction of mitophagy (starvation-induced) both resulted in mitochondrial membrane depolarization [42], suggesting that changes in membrane potential are indicative of perturbations in the delicate balance between mitochondrial survival and elimination.

Finally, in the newly fertilized oocyte, selective mitophagy has been documented whereby sperm mitochondria are selectively targeted for mitophagy immediately following fertilization [84]. The oocyte requires a large amount of energy to produce a mature oocyte containing the appropriate number of chromosomes and as such contains the most mitochondria of all the cells in the body, making the maintenance of mtDNA integrity and repair paramount. Hence, the proper balance between mitochondrial fission and fusion and its core proteins is essential to producing a viable oocyte. Numerous studies have also shown that in order to produce a viable oocyte, healthy granulosa cells are required [85-98]. Thus our findings showing increased autophagy and mitochondrial dysfunction in granulosa cells suggest that cigarette smoke decreases granulosa cell numbers via autophagy and in so doing decreasing follicle survival.

In summary, we have shown here that cigarette smoke exposure results in mitochondrial dysfunction as supported by increased expression of the pro-fission PARK2 and the subsequent decreased expression of its targets, pro-fusion proteins MFN1 and MFN2. Enhanced autophagy activity was also apparent as evidenced by the increased presence of autophagosomes in treated ovaries and via increases in gene and protein expression of BECN1, a key initiator of autophagy, and of LC3, which is responsible for sequestration of organelles within the autophagosome, as well as the decreased expression of the autophagy antagonist, BCL2. Taken together, our results suggest that cigarette smoke, in doses relevant to human exposure, causes mitochondrial damage and dysfunction, leading to enhanced autophagy activity in the granulosa cells of ovarian follicles. Although our results show that cigarette smoke exposure induces changes in the expression of several mitochondrial-specific proteins we cannot rule out potential adverse effects on other organelles following cigarette smoke exposure. Given that all smokers do not suffer from infertility, we postulate that reparative autophagy is inadequate to manage cigarette smoke-induced oxidative stress; the threshold needed to support follicle growth and oocyte development is exceeded resulting in follicle loss and sub-fertility. The number of young women starting smoking is growing [99], suggesting that prevention strategies are not effective deterrents in this population. This coupled with the addictive quality of nicotine, often requiring multiple attempts to quit smoking [100], implies that counseling women to quit is not an effective strategy when managing smoking-related infertility. Moreover, it is unknown if cigarette smoke-induced ovarian damage is reversible by smoking cessation. Therefore, the mechanistic pathway elucidated in this study is

important in identifying the potential targets for anti-oxidant therapies for fertility preservation. With mitochondrial dysfunction being implicated in a broad spectrum of diseases covering every aspect of medicine, our results may have far-reaching implications in both reproductive medicine and throughout medicine in general.

4.6 Acknowledgements

AG received scholarships from CIHR, the Ontario Tobacco Research Council, CIHR/IHDCYH Training Program in Reproduction, Early Development, and the Impact on Health (REDIH) and the Government of Ontario. Salary support was provided to WGF from the Canadian Institutes of Health Research and the Ontario Women's Health Council. The authors declare that they do not have any conflict of interest to report.

4.7 Reference List

1. van Beek RD, van den Heuvel-Eibrink MM, Laven JS, de Jong FH, Themmen AP, Hakvoort-Cammel FG, van den BC, van den BH, Pieters R, de Muinck Keizer-Schrama SM. Anti-Müllerian hormone is a sensitive serum marker for gonadal function in women treated for Hodgkin's lymphoma during childhood. J Clin Endocrinol Metab 2007; 92: 3869-3874.

2. Devine PJ, Sipes IG, Hoyer PB. Initiation of delayed ovotoxicity by in vitro and in vivo exposures of rat ovaries to 4-vinylcyclohexene diepoxide. Reprod Toxicol 2004; 19: 71-77.

3. Devine PJ, Sipes IG, Skinner MK, Hoyer PB. Characterization of a rat in vitro ovarian culture system to study the ovarian toxicant 4-vinylcyclohexene diepoxide. Toxicol Appl Pharmacol 2002; 184: 107-115.

4. Mayer LP, Pearsall NA, Christian PJ, Devine PJ, Payne CM, McCuskey MK, Marion SL, Sipes IG, Hoyer PB. Long-term effects of ovarian follicular depletion in rats by 4-vinylcyclohexene diepoxide. Reprod Toxicol 2002; 16: 775-781.

5. Neal MS, Zhu J, Foster WG. Quantification of benzo[a]pyrene and other PAHs in the serum and follicular fluid of smokers versus non-smokers. Reprod Toxicol 2008; 25: 100-106.

6. Desmeules P, Devine PJ. Characterizing the ovotoxicity of cyclophosphamide metabolites on cultured mouse ovaries. Toxicol Sci 2006; 90: 500-509.

7. Jurisicova A, Taniuchi A, Li H, Shang Y, Antenos M, Detmar J, Xu J, Matikainen T, Benito HA, Nunez G, Casper RF. Maternal exposure to polycyclic aromatic hydrocarbons diminishes murine ovarian reserve via induction of Harakiri. J Clin Invest 2007; 117: 3971-3978.

8. La Marca A., Volpe A. The Anti-Müllerian hormone and ovarian cancer. Hum Reprod Update 2007; 13: 265-273.

9. Lie FS, Lugtenburg PJ, Schipper I, Themmen AP, de Jong FH, Sonneveld P, Laven JS. Anti-Müllerian hormone as a marker of ovarian function in women after chemotherapy and radiotherapy for haematological malignancies. Hum Reprod 2008; 23: 674-678.

10. Sadeu JC, Hughes CL, Agarwal S, Foster WG. Alcohol, drugs, caffeine, tobacco, and environmental contaminant exposure: reproductive health consequences and clinical implications. Crit Rev Toxicol 2010; 40: 633-652.

11. Soares SR, Simon C, Remohi J, Pellicer A. Cigarette smoking affects uterine receptiveness. Hum Reprod 2007; 22: 543-547.

12. Neal MS, Hughes EG, Holloway AC, Foster WG. Sidestream smoking is equally as damaging as mainstream smoking on IVF outcomes. Hum Reprod 2005; 20: 2531-2535.

13. Neal MS, Zhu J, Holloway AC, Foster WG. Follicle growth is inhibited by benzo-[a]-pyrene, at concentrations representative of human exposure, in an isolated rat follicle culture assay. Hum Reprod 2007; 22: 961-967.

14. Tuttle AM, Stampfli M, Foster WG. Cigarette smoke causes follicle loss in mice ovaries at concentrations representative of human exposure. Hum Reprod 2009; 24: 1452-1459.

15. Lodovici M, Akpan V, Evangelisti C, Dolara P. Sidestream tobacco smoke as the main predictor of exposure to polycyclic aromatic hydrocarbons. J Appl Toxicol 2004; 24: 277-281.

16. Tagawa Y, Hiramatsu N, Kasai A, Hayakawa K, Okamura M, Yao J, Kitamura M. Induction of apoptosis by cigarette smoke via ROS-dependent endoplasmic reticulum stress and CCAAT/enhancer-binding protein-homologous protein (CHOP). Free Radic Biol Med 2008; 45: 50-59.

17. Matikainen T, Perez GI, Jurisicova A, Pru JK, Schlezinger JJ, Ryu HY, Laine J, Sakai T, Korsmeyer SJ, Casper RF, Sherr DH, Tilly JL. Aromatic hydrocarbon receptor-driven Bax gene expression is required for premature ovarian failure caused by biohazardous environmental chemicals. Nat Genet 2001; 28: 355-360.

18. Matikainen TM, Moriyama T, Morita Y, Perez GI, Korsmeyer SJ, Sherr DH, Tilly JL. Ligand activation of the aromatic hydrocarbon receptor transcription factor drives Bax-dependent apoptosis in developing fetal ovarian germ cells. Endocrinology 2002; 143: 615-620.

19. Kee K, Flores M, Cedars MI, Reijo Pera RA. Human primordial germ cell formation is diminished by exposure to environmental toxicants acting through the AHR signaling pathway. Toxicol Sci 2010; 117: 218-224.

20. Gannon AM, Stampfli MR, Foster WG. Cigarette smoke exposure leads to follicle loss via an alternative ovarian cell death pathway in a mouse model. Toxicol Sci 2012; 125: 274-284.

21. De DC. Lysosomes and phagosomes. The vacuolar apparatus. Protoplasma 1967; 63: 95-98.

22. Deter RL, Baudhuin P, De DC. Participation of lysosomes in cellular autophagy induced in rat liver by glucagon. J Cell Biol 1967; 35: C11-C16.

23. Deter RL, De DC. Influence of glucagon, an inducer of cellular autophagy, on some physical properties of rat liver lysosomes. J Cell Biol 1967; 33: 437-449.

24. CLARK SL, Jr. Cellular differentiation in the kidneys of newborn mice studies with the electron microscope. J Biophys Biochem Cytol 1957; 3: 349-362.

25. Reggiori F, Klionsky DJ. Autophagosomes: biogenesis from scratch? Curr Opin Cell Biol 2005; 17: 415-422.

26. Reggiori F, Klionsky DJ. Autophagy in the eukaryotic cell. Eukaryot Cell 2002; 1: 11-21.

27. Muller M, Reichert AS. Mitophagy, mitochondrial dynamics and the general stress response in yeast. Biochem Soc Trans 2011; 39: 1514-1519.

28. Mizushima N, Levine B, Cuervo AM, Klionsky DJ. Autophagy fights disease through cellular self-digestion. Nature 2008; 451: 1069-1075.

29. Thome RG, Santos HB, Arantes FP, Domingos FF, Bazzoli N, Rizzo E. Dual roles for autophagy during follicular atresia in fish ovary. Autophagy 2009; 5: 117-119.

30. Bolt AM, Klimecki WT. Autophagy in toxicology: self-consumption in times of stress and plenty. J Appl Toxicol 2012; 32: 465-479.

31. Bolt AM, Byrd RM, Klimecki WT. Autophagy is the predominant process induced by arsenite in human lymphoblastoid cell lines. Toxicol Appl Pharmacol 2010; 244: 366-373.

32. Hashimoto D, Ohmuraya M, Hirota M, Yamamoto A, Suyama K, Ida S, Okumura Y, Takahashi E, Kido H, Araki K, Baba H, Mizushima N, Yamamura K. Involvement of autophagy in trypsinogen activation within the pancreatic acinar cells. J Cell Biol 2008; 181: 1065-1072.

33. Schiaffino S, Mammucari C, Sandri M. The role of autophagy in neonatal tissues: just a response to amino acid starvation? Autophagy 2008; 4: 727-730.

34. Kuma A, Hatano M, Matsui M, Yamamoto A, Nakaya H, Yoshimori T, Ohsumi Y, Tokuhisa T, Mizushima N. The role of autophagy during the early neonatal starvation period. Nature 2004; 432: 1032-1036.

35. Shimizu S, Kanaseki T, Mizushima N, Mizuta T, rakawa-Kobayashi S, Thompson CB, Tsujimoto Y. Role of Bcl-2 family proteins in a non-apoptotic programmed cell death dependent on autophagy genes. Nat Cell Biol 2004; 6: 1221-1228.

36. Yousefi S, Perozzo R, Schmid I, Ziemiecki A, Schaffner T, Scapozza L, Brunner T, Simon HU. Calpain-mediated cleavage of Atg5 switches autophagy to apoptosis. Nat Cell Biol 2006; 8: 1124-1132.

37. Moretti L, Attia A, Kim KW, Lu B. Crosstalk between Bak/Bax and mTOR signaling regulates radiation-induced autophagy. Autophagy 2007; 3: 142-144.

38. Azad MB, Chen Y, Henson ES, Cizeau J, Millan-Ward E, Israels SJ, Gibson SB. Hypoxia induces autophagic cell death in apoptosis-competent cells through a mechanism involving BNIP3. Autophagy 2008; 4: 195-204.

39. Braschi E, McBride HM. Mitochondria and the culture of the Borg: understanding the integration of mitochondrial function within the reticulum, the cell, and the organism. Bioessays 2010; 32: 958-966.

40. Molina AJ, Wikstrom JD, Stiles L, Las G, Mohamed H, Elorza A, Walzer G, Twig G, Katz S, Corkey BE, Shirihai OS. Mitochondrial networking protects beta-cells from nutrient-induced apoptosis. Diabetes 2009; 58: 2303-2315.

41. Twig G, Liu X, Liesa M, Wikstrom JD, Molina AJ, Las G, Yaniv G, Hajnoczky G, Shirihai OS. Biophysical properties of mitochondrial fusion events in pancreatic beta-cells and cardiac cells unravel potential control mechanisms of its selectivity. Am J Physiol Cell Physiol 2010; 299: C477-C487.

42. Twig G, Elorza A, Molina AJ, Mohamed H, Wikstrom JD, Walzer G, Stiles L, Haigh SE, Katz S, Las G, Alroy J, Wu M, Py BF, Yuan J, Deeney JT, Corkey BE, Shirihai OS. Fission and selective fusion govern mitochondrial segregation and elimination by autophagy. EMBO J 2008; 27: 433-446.

43. Wikstrom JD, Twig G, Shirihai OS. What can mitochondrial heterogeneity tell us about mitochondrial dynamics and autophagy? Int J Biochem Cell Biol 2009; 41: 1914-1927.

44. Glauser L, Sonnay S, Stafa K, Moore DJ. Parkin promotes the ubiquitination and degradation of the mitochondrial fusion factor mitofusin 1. J Neurochem 2011; 118: 636-645.

45. Tanaka A, Cleland MM, Xu S, Narendra DP, Suen DF, Karbowski M, Youle RJ. Proteasome and p97 mediate mitophagy and degradation of mitofusins induced by Parkin. J Cell Biol 2010; 191: 1367-1380.

46. Gegg ME, Cooper JM, Chau KY, Rojo M, Schapira AH, Taanman JW. Mitofusin 1 and mitofusin 2 are ubiquitinated in a PINK1/parkin-dependent manner upon induction of mitophagy. Hum Mol Genet 2010; 19: 4861-4870.

47. Cipolat S, Rudka T, Hartmann D, Costa V, Serneels L, Craessaerts K, Metzger K, Frezza C, Annaert W, D'Adamio L, Derks C, Dejaegere T, Pellegrini L, D'Hooge R, Scorrano L, De SB. Mitochondrial rhomboid PARL regulates cytochrome c release during apoptosis via OPA1-dependent cristae remodeling. Cell 2006; 126: 163-175.

48. Pellegrini L, Scorrano L. A cut short to death: Parl and Opa1 in the regulation of mitochondrial morphology and apoptosis. Cell Death Differ 2007; 14: 1275-1284.

49. Gomes LC, Di BG, Scorrano L. During autophagy mitochondria elongate, are spared from degradation and sustain cell viability. Nat Cell Biol 2011; 13: 589-598.

50. Gomes LC, Scorrano L. Mitochondrial elongation during autophagy: a stereotypical response to survive in difficult times. Autophagy 2011; 7: 1251-1253.

51. Botelho FM, Gaschler GJ, Kianpour S, Zavitz CC, Trimble NJ, Nikota JK, Bauer CM, Stampfli MR. Innate immune processes are sufficient for driving cigarette smoke-induced inflammation in mice. Am J Respir Cell Mol Biol 2010; 42: 394-403.

52. Livak KJ, Schmittgen TD. Analysis of relative gene expression data using real-time quantitative PCR and the 2(-Delta Delta C(T)) Method. Methods 2001; 25: 402-408.

53. Gaytan M, Morales C, Sanchez-Criado JE, Gaytan F. Immunolocalization of beclin 1, a bcl-2-binding, autophagy-related protein, in the human ovary: possible relation to life span of corpus luteum. Cell Tissue Res 2008; 331: 509-517.

54. Mo Z, Fang Y, He Y, Ke X. Change of Beclin-1 dependent on ATP, [Ca2+]i and MMP in PC12 cells following oxygen-glucose deprivation -reoxygenation injury. Cell Biol Int 2012.

55. Ding Z, Wang X, Khaidakov M, Liu S, Dai Y, Mehta JL. Degradation of heparan sulfate proteoglycans enhances oxidized-LDL-mediated autophagy and apoptosis in human endothelial cells. Biochem Biophys Res Commun 2012.

56. Smith CC, Lee KS, Li B, Laing JM, Hersl J, Shvartsbeyn M, Aurelian L. Restored expression of the atypical heat shock protein H11/HspB8 inhibits the growth of genetically diverse melanoma tumors through activation of novel TAK1-dependent death pathways. Cell Death Dis 2012; 3: e371.

57. Wang YQ, Wang L, Zhang MY, Wang T, Bao HJ, Liu WL, Dai DK, Zhang L, Chang P, Dong WW, Chen XP, Tao LY. Necrostatin-1 suppresses autophagy and apoptosis in mice traumatic brain injury model. Neurochem Res 2012; 37: 1849-1858.

58. Chen ZH, Kim HP, Sciurba FC, Lee SJ, Feghali-Bostwick C, Stolz DB, Dhir R, Landreneau RJ, Schuchert MJ, Yousem SA, Nakahira K, Pilewski JM, Lee JS, Zhang

Y, Ryter SW, Choi AM. Egr-1 regulates autophagy in cigarette smoke-induced chronic obstructive pulmonary disease. PLoS ONE 2008; 3: e3316.

59. Kim HP, Wang X, Chen ZH, Lee SJ, Huang MH, Wang Y, Ryter SW, Choi AM. Autophagic proteins regulate cigarette smoke-induced apoptosis: protective role of heme oxygenase-1. Autophagy 2008; 4: 887-895.

60. Hwang JW, Chung S, Sundar IK, Yao H, Arunachalam G, McBurney MW, Rahman I. Cigarette smoke-induced autophagy is regulated by SIRT1-PARP-1-dependent mechanism: implication in pathogenesis of COPD. Arch Biochem Biophys 2010; 500: 203-209.

61. Serke H, Vilser C, Nowicki M, Hmeidan FA, Blumenauer V, Hummitzsch K, Losche A, Spanel-Borowski K. Granulosa cell subtypes respond by autophagy or cell death to oxLDL-dependent activation of the oxidized lipoprotein receptor 1 and toll-like 4 receptor. Autophagy 2009; 5: 991-1003.

62. Yoo SH, Yoon YG, Lee JS, Song YS, Oh JS, Park BS, Kwon TK, Park C, Choi YH, Yoo YH. Etoposide induces a mixed type of programmed cell death and overcomes the resistance conferred by Bcl-2 in Hep3B hepatoma cells. Int J Oncol 2012.

63. Liang XH, Kleeman LK, Jiang HH, Gordon G, Goldman JE, Berry G, Herman B, Levine B. Protection against fatal Sindbis virus encephalitis by beclin, a novel Bcl-2-interacting protein. J Virol 1998; 72: 8586-8596.

64. Vilser C, Hueller H, Nowicki M, Hmeidan FA, Blumenauer V, Spanel-Borowski K. The variable expression of lectin-like oxidized low-density lipoprotein receptor (LOX-1) and signs of autophagy and apoptosis in freshly harvested human granulosa cells depend on gonadotropin dose, age, and body weight. Fertil Steril 2010; 93: 2706-2715.

65. Sadeu JC, Foster WG. Effect of in vitro exposure to benzo[a]pyrene, a component of cigarette smoke, on folliculogenesis, steroidogenesis and oocyte nuclear maturation. Reprod Toxicol 2010.

66. Sadeu JC, Foster WG. Cigarette smoke condensate exposure delays follicular development and function in a stage-dependent manner. Fertil Steril 2011; 95: 2410-2417.

67. Flaws JA, Doerr JK, Sipes IG, Hoyer PB. Destruction of preantral follicles in adult rats by 4-vinyl-1-cyclohexene diepoxide. Reprod Toxicol 1994; 8: 509-514.

68. Borman SM, Christian PJ, Sipes IG, Hoyer PB. Ovotoxicity in female Fischer rats and B6 mice induced by low-dose exposure to three polycyclic aromatic

hydrocarbons: comparison through calculation of an ovotoxic index. Toxicol Appl Pharmacol 2000; 167: 191-198.

69. Devine PJ, Sipes IG, Hoyer PB. Effect of 4-vinylcyclohexene diepoxide dosing in rats on GSH levels in liver and ovaries. Toxicol Sci 2001; 62: 315-320.

70. Hoyer PB, Davis JR, Bedrnicek JB, Marion SL, Christian PJ, Barton JK, Brewer MA. Ovarian neoplasm development by 7,12-dimethylbenz[a]anthracene (DMBA) in a chemically-induced rat model of ovarian failure. Gynecol Oncol 2009; 112: 610-615.

71. Hoyer PB, Devine PJ, Hu X, Thompson KE, Sipes IG. Ovarian toxicity of 4-vinylcyclohexene diepoxide: a mechanistic model. Toxicol Pathol 2001; 29: 91-99.

72. Kappeler CJ, Hoyer PB. 4-vinylcyclohexene diepoxide: a model chemical for ovotoxicity. Syst Biol Reprod Med 2012; 58: 57-62.

73. Boone DL, Carnegie JA, Rippstein PU, Tsang BK. Induction of apoptosis in equine chorionic gonadotropin (eCG)-primed rat ovaries by anti-eCG antibody. Biol Reprod 1997; 57: 420-427.

74. Boone DL, Tsang BK. Caspase-3 in the rat ovary: localization and possible role in follicular atresia and luteal regression. Biol Reprod 1998; 58: 1533-1539.

75. Dharma SJ, Kelkar RL, Nandedkar TD. Fas and Fas ligand protein and mRNA in normal and atretic mouse ovarian follicles. Reproduction 2003; 126: 783-789.

76. Hussein MR. Apoptosis in the ovary: molecular mechanisms. Hum Reprod Update 2005; 11: 162-177.

77. Kim JM, Boone DL, Auyeung A, Tsang BK. Granulosa cell apoptosis induced at the penultimate stage of follicular development is associated with increased levels of Fas and Fas ligand in the rat ovary. Biol Reprod 1998; 58: 1170-1176.

78. Kanzawa T, Kondo Y, Ito H, Kondo S, Germano I. Induction of autophagic cell death in malignant glioma cells by arsenic trioxide. Cancer Res 2003; 63: 2103-2108.

79. Kanzawa T, Zhang L, Xiao L, Germano IM, Kondo Y, Kondo S. Arsenic trioxide induces autophagic cell death in malignant glioma cells by upregulation of mitochondrial cell death protein BNIP3. Oncogene 2005; 24: 980-991.

80. Wikstrom JD, Katzman SM, Mohamed H, Twig G, Graf SA, Heart E, Molina AJ, Corkey BE, de Vargas LM, Danial NN, Collins S, Shirihai OS. beta-Cell mitochondria exhibit membrane potential heterogeneity that can be altered by stimulatory or toxic fuel levels. Diabetes 2007; 56: 2569-2578.

81. Choi SE, Lee SM, Lee YJ, Li LJ, Lee SJ, Lee JH, Kim Y, Jun HS, Lee KW, Kang Y. Protective role of autophagy in palmitate-induced INS-1 beta-cell death. Endocrinology 2009; 150: 126-134.

82. Chen H, Detmer SA, Ewald AJ, Griffin EE, Fraser SE, Chan DC. Mitofusins Mfn1 and Mfn2 coordinately regulate mitochondrial fusion and are essential for embryonic development. J Cell Biol 2003; 160: 189-200.

83. Frezza C, Cipolat S, Martins de BO, Micaroni M, Beznoussenko GV, Rudka T, Bartoli D, Polishuck RS, Danial NN, De SB, Scorrano L. OPA1 controls apoptotic cristae remodeling independently from mitochondrial fusion. Cell 2006; 126: 177-189.

84. Shitara H, Kaneda H, Sato A, Inoue K, Ogura A, Yonekawa H, Hayashi JI. Selective and continuous elimination of mitochondria microinjected into mouse eggs from spermatids, but not from liver cells, occurs throughout embryogenesis. Genetics 2000; 156: 1277-1284.

85. Gittens JE, Barr KJ, Vanderhyden BC, Kidder GM. Interplay between paracrine signaling and gap junctional communication in ovarian follicles. J Cell Sci 2005; 118: 113-122.

86. Gittens JE, Kidder GM. Differential contributions of connexin37 and connexin43 to oogenesis revealed in chimeric reaggregated mouse ovaries. J Cell Sci 2005; 118: 5071-5078.

87. Dyce PW, Norris RP, Lampe PD, Kidder GM. Phosphorylation of Serine Residues in the C-terminal Cytoplasmic Tail of Connexin43 Regulates Proliferation of Ovarian Granulosa Cells. J Membr Biol 2012; 245: 291-301.

88. Kidder GM, Vanderhyden BC. Bidirectional communication between oocytes and follicle cells: ensuring oocyte developmental competence. Can J Physiol Pharmacol 2010; 88: 399-413.

89. Li TY, Colley D, Barr KJ, Yee SP, Kidder GM. Rescue of oogenesis in Cx37-null mutant mice by oocyte-specific replacement with Cx43. J Cell Sci 2007; 120: 4117-4125.

90. Tong D, Gittens JE, Kidder GM, Bai D. Patch-clamp study reveals that the importance of connexin43-mediated gap junctional communication for ovarian folliculogenesis is strain specific in the mouse. Am J Physiol Cell Physiol 2006; 290: C290-C297.

91. Veitch GI, Gittens JE, Shao Q, Laird DW, Kidder GM. Selective assembly of connexin37 into heterocellular gap junctions at the oocyte/granulosa cell interface. J Cell Sci 2004; 117: 2699-2707.

92. Wang HX, Tekpetey FR, Kidder GM. Identification of WNT/beta-CATENIN signaling pathway components in human cumulus cells. Mol Hum Reprod 2009; 15: 11-17.

93. Wang HX, Tong D, El-Gehani F, Tekpetey FR, Kidder GM. Connexin expression and gap junctional coupling in human cumulus cells: contribution to embryo quality. J Cell Mol Med 2009; 13: 972-984.

94. Pangas SA, Matzuk MM. The art and artifact of GDF9 activity: cumulus expansion and the cumulus expansion-enabling factor. Biol Reprod 2005; 73: 582-585.

95. Silva JR, van den HR, van Tol HT, Roelen BA, Figueiredo JR. Expression of growth differentiation factor 9 (GDF9), bone morphogenetic protein 15 (BMP15), and BMP receptors in the ovaries of goats. Mol Reprod Dev 2005; 70: 11-19.

96. Liao WX, Moore RK, Otsuka F, Shimasaki S. Effect of intracellular interactions on the processing and secretion of bone morphogenetic protein-15 (BMP-15) and growth and differentiation factor-9. Implication of the aberrant ovarian phenotype of BMP-15 mutant sheep. J Biol Chem 2003; 278: 3713-3719.

97. Zhang B, Wei Q, Shi S, Dong F, Shi F, Xu Y. Immunolocalization and expression pattern of gpr3 in the ovary and its effect on proliferation of ovarian granulosa cells in pigs. J Reprod Dev 2012; 58: 410-419.

98. Bennett J, Wu YG, Gossen J, Zhou P, Stocco C. Loss of GATA-6 and GATA-4 in granulosa cells blocks folliculogenesis, ovulation, and follicle stimulating hormone receptor expression leading to female infertility. Endocrinology 2012; 153: 2474-2485.

99. Cohen B, Evers S, Manske S, Bercovitz K, Edward HG. Smoking, physical activity and breakfast consumption among secondary school students in a southwestern Ontario community. Can J Public Health 2003; 94: 41-44.

100. West R. The multiple facets of cigarette addiction and what they mean for encouraging and helping smokers to stop. COPD 2009; 6: 277-283.

4.8 Figures

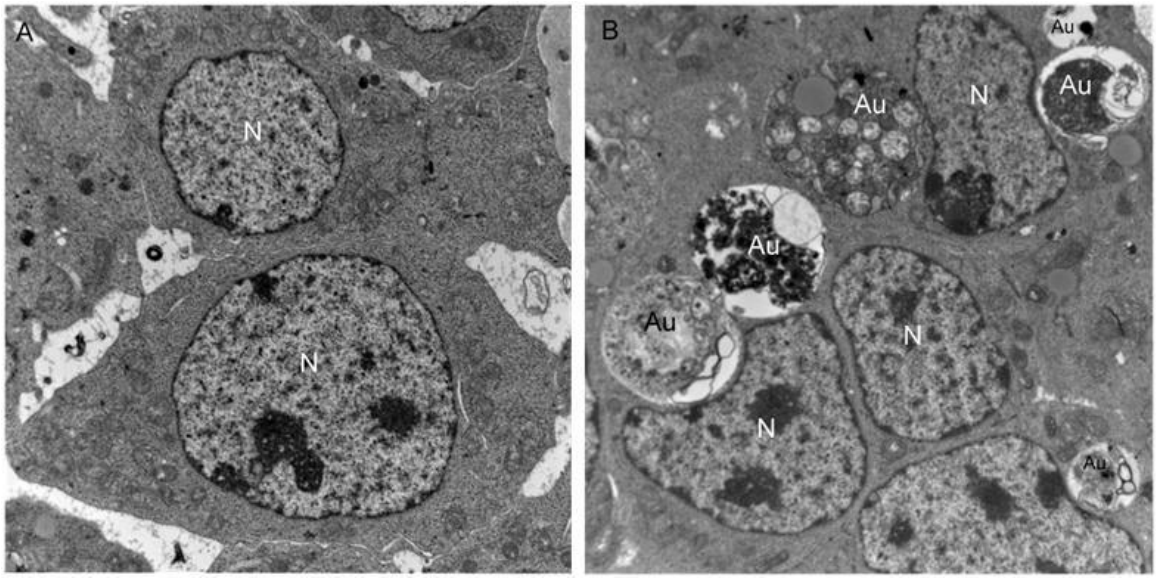

Figure 1: Autophagosomes are present in the granulosa cells of ovarian follicles exposed to cigarette smoke.
Representative TEM micrographs of granulosa cells from growing follicles in A) sham and B) cigarette smoke exposed ovaries. Nuclei (N) appear normal but are displaced by autophagosomes (Au) in cigarette smoke exposed ovaries. Mitochondria are visible in both sham and smoke exposed ovaries (arrowheads) and can be visualized within an autophagosome (arrows) in a smoke exposed ovarian follicle. Original magnification: 10000x.

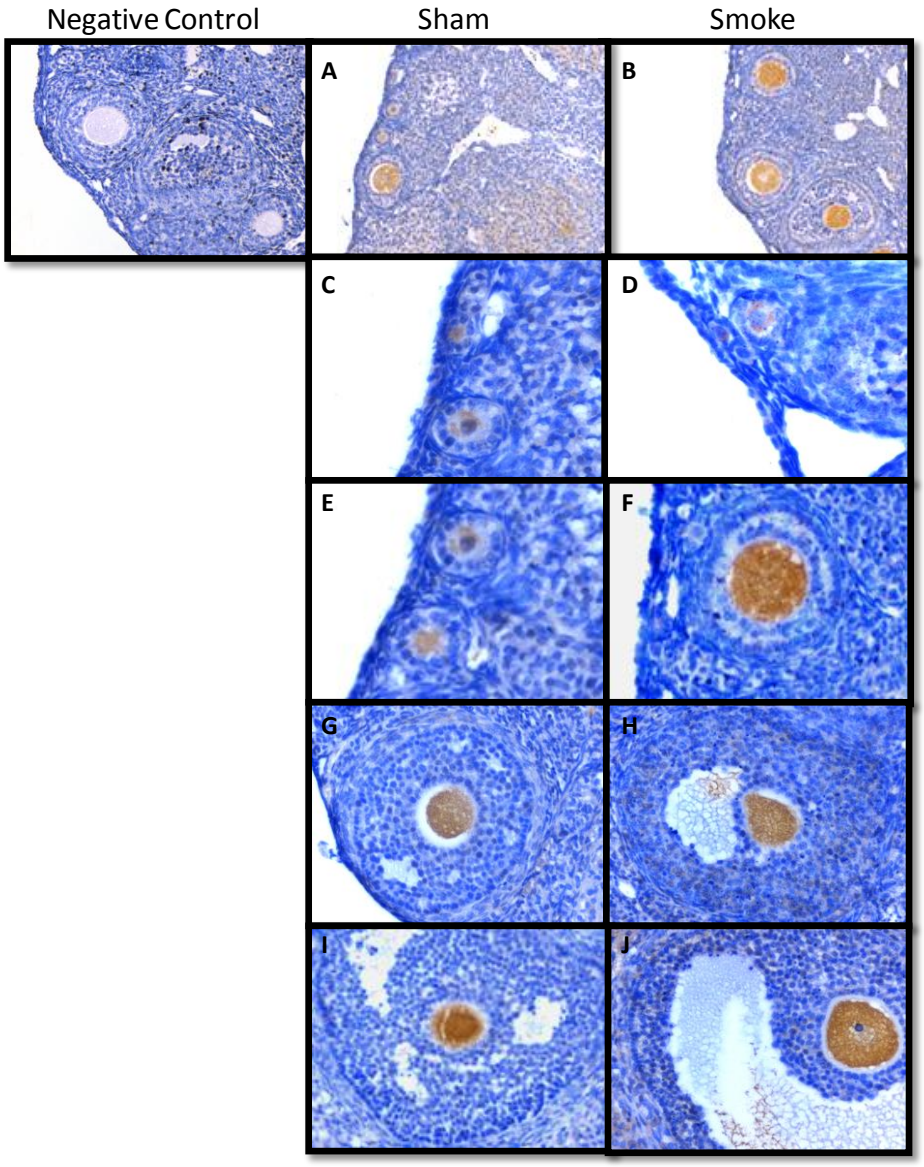
Negative Control
Sham
Smoke
A
B
C
D
E
F
G
H
I
J

K

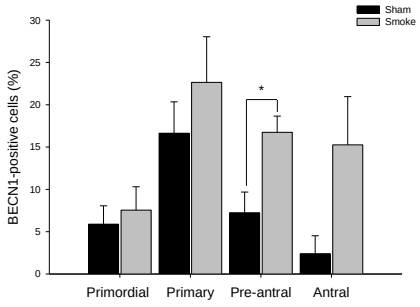
Sham
Smoke
BECN1-positive cells (%)
30
25
20
15
10
5
0
*
Primordial
Primary
Pre-antral
Antral

Figure 2: Beclin 1 protein localization.
Immunohistochemical staining for BECN1 in ovaries from sham and smoke exposed mice (A-J). Negative control, Sham (A, C, E, G and I) and Smoke (B, D, F, H and J) exposed. Follicles at all stages of maturity (C-D: primordial, E-F: primary, G-H: pre-antral/secondary, I-J: antral) expressed BECN1 protein in both sham and smoke exposed mice. The intensity of the staining as well as the localization differed between treatment groups and follicle stage. Original magnifications: Negative control: 10x, A-B: 4x, C-J: 20x. K: The percentage of BECN1 positive cells present in follicles at each stage of development is shown. Data were checked for normality and equal variance and treatment effects were tested using t-test. Values are expressed as the mean (± SEM).

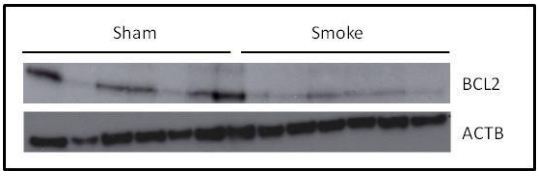
Sham
Smoke
BCL2
ACTB

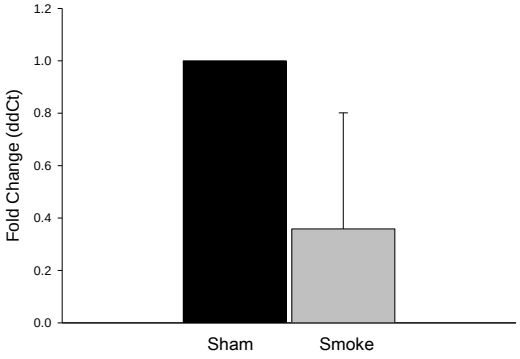
Fold Change (ddCt)
1.2
1.0
0.8
0.6
0.4
0.2
0.0
Sham
Smoke

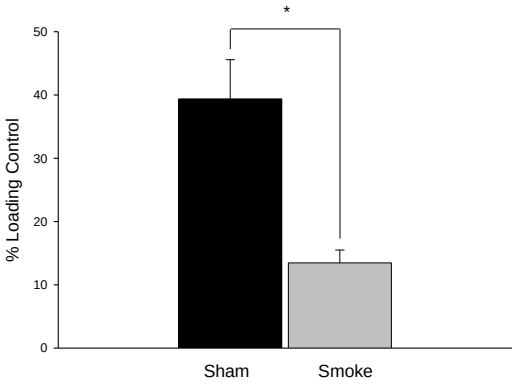
*
% Loading Control
50
40
30
20
10
0
Sham
Smoke

Figure 3: *Bcl2* gene and BCL2 protein expression changes following cigarette smoke exposure.
Analysis of *Bcl2* gene and BCL2 protein expression was performed on whole ovary homogenates from 8 week sham and smoke-exposed mice. The graph in the left column depicts gene expression changes relative to *Actb* control (n = 6/group). The graph and representative blot in the right column depict protein expression changes relative to ACTB loading control (n = 7 sham, 6 smoke). Data were checked for normality and equal variance and treatment effects were tested using t-test. Values are expressed as mean (± SEM).

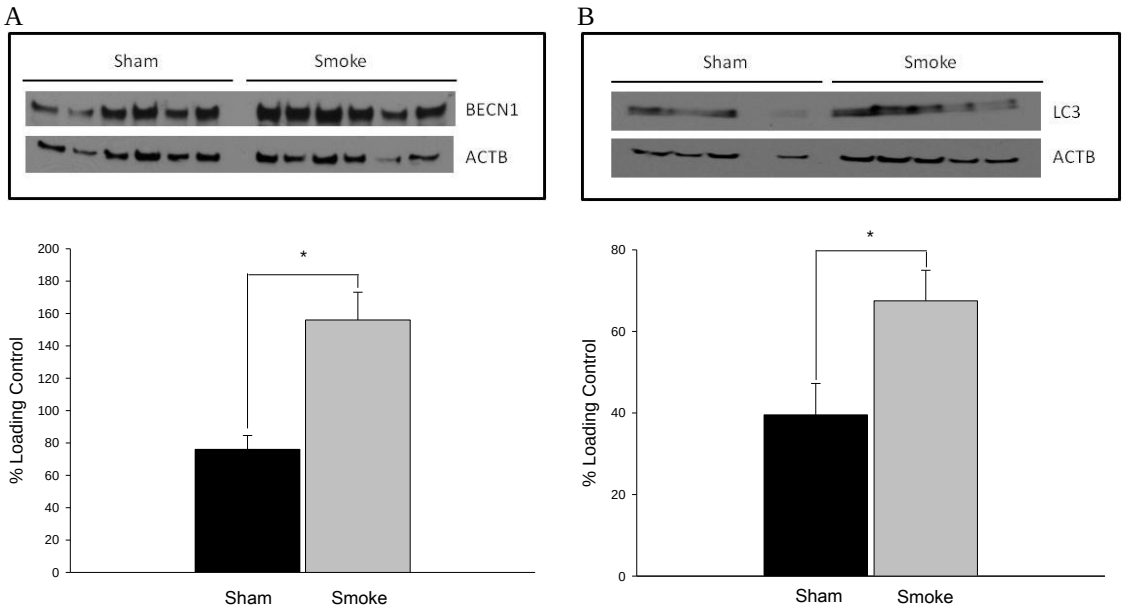
A
Sham
Smoke
BECN1
ACTB
% Loading Control
200
180
160
140
120
100
80
60
40
20
0
*
Sham
Smoke
B
Sham
Smoke
LC3
ACTB
% Loading Control
80
60
40
20
0
*
Sham
Smoke

Figure 4: Autophagy-related proteins are altered following cigarette smoke exposure.
Analysis of A) BECN1 and B) LC3 protein expression was performed on whole ovary homogenates from 8 week sham and smoke-exposed mice. Protein expression was measured relative to ACTB loading control (A: n = 6/group; B: n = 5/group). A representative blot is shown for each graph. Data were checked for normality and equal variance and treatment effects were tested using t-test. Values are expressed as mean (± SEM).


*
0.60
0.58
0.56
0.54
0.52
0.50
0.48
0.46
Concentration (ng/mL)
Sham
Smoke

Figure 5: Beclin 1 protein changes following cigarette smoke exposure.
Protein expression changes measured by Western blot analysis were confirmed using a Beclin 1 ELISA. n = 15/group. Data were checked for normality and equal variance and treatment effects were tested using t-test. Values are expressed as mean (± SEM).

Gene

Protein

A

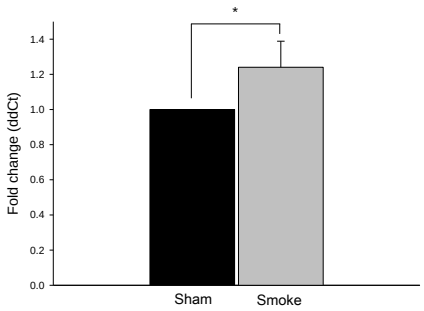

B

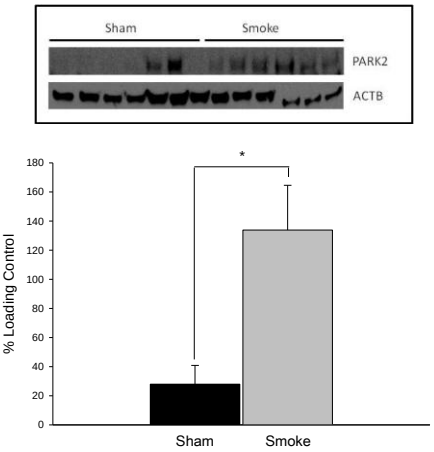

C

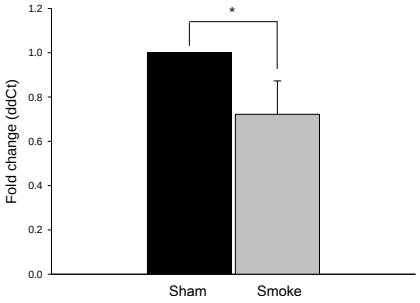

D

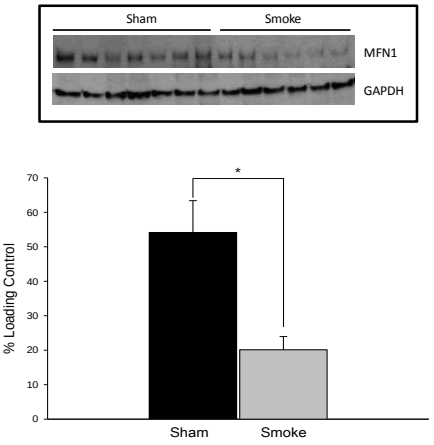

E

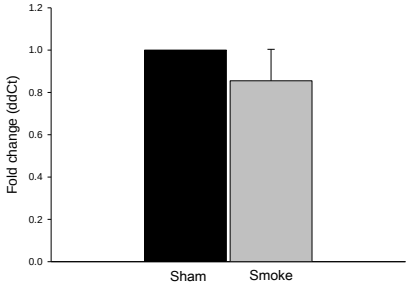

F

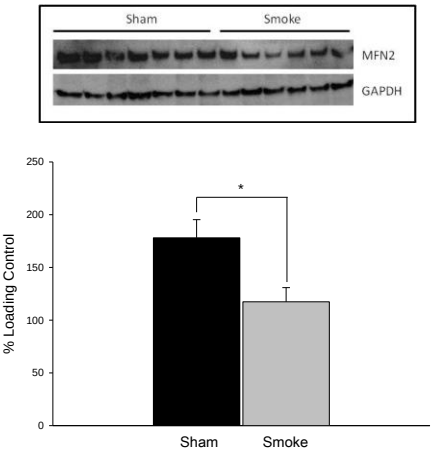

Figure 6: Dysregulation of mitochondrial repair mechanisms is evident in ovaries exposed to cigarette smoke exposure.
Analysis of PARK2 (A-B), MFN1 (C-D), and MFN2 (E-F) gene and protein expression in whole ovary homogenates from 8 week sham and smoke-exposed mice. Gene expression changes (A, C, E; n = 6/group) were measured relative to *Actb* control and protein expression changes (B, D, F; n = 7 sham, 6 smoke) were measured relative to ACTB (PARK2) or GAPDH (MFN1 and MFN2) loading controls. Data were checked for normality and equal variance and treatment effects were tested using t-test. Values are expressed as mean (± SEM).

Chapter 5

Discussion

Cigarette smoking is a serious threat to reproductive health [4;37;48;59;392]. Women who smoke have reduced fertility and undergo menopause earlier than those who have never smoked, suggesting that cigarette smoking depletes the ovarian reserve. Despite the myriad associations between smoking status and infertility, relatively little is known about the molecular mechanisms underlying its adverse effects on the ovary. As such, the purpose of this thesis was to resolve the mechanism by which cigarette smoke exhausts the ovarian follicle population in a mouse *in vivo* model of cigarette smoke-induced ovarian follicle loss. The studies herein were undertaken with the hypothesis that cigarette smoke causes primordial follicle death via apoptosis leading to shortened reproductive lifespan.

Although our original hypothesis was proven wrong, taken together, the data presented in this thesis provide a mechanism by which ovarian follicles are lost following cigarette smoke exposure. The data presented in chapter 2 illustrate in an *in vivo* model that cigarette smoke exposure does in fact diminish the ovarian follicle population and that the follicles most affected are those in the primordial stage. Although follicles are being lost, it is not through apoptosis, the canonical pathway through which follicle loss was previously thought to occur. While cigarette smoke indisputably reduced the follicle

number in mice, the mechanism through which these follicles were being lost was unknown, despite significant changes in the expression of a key anti-apoptotic protein, BCL2. The data presented in chapters 3 and 4 further support these findings and point instead to a novel alternative cell death pathway in the ovary, autophagy.

At the time of the first and second studies, it was generally accepted that follicles exposed to a chemical insult died through apoptosis. As such, we set out to show that cigarette smoke exposure, like many other reproductive toxicants, caused ovarian follicle loss through apoptosis. As expected, following exposure mice in the treatment group were found to have significantly smaller ovaries with a diminished ovarian follicle count compared to age-matched controls. Unexpectedly however, treated ovaries showed no more evidence of apoptosis than did controls. This was true despite the significantly lower expression levels of the anti-apoptotic protein BCL2 in treated ovaries. Given that BCL2 prevents BAX (a pro-apoptotic protein) from inserting itself into the mitochondrial OM and creating pores through which cytochrome *c* can pass, it was expected that BCL2 reduction would shift the balance in favour of apoptosis. Despite this, all tests for apoptosis were not different between treatment groups. In order to ensure that subtle changes in apoptosis were not being missed as a result of using whole ovaries and their homogenates for the above studies, electron microscopy was employed with hopes of finding evidence of increased apoptosis occurring at the sub-cellular level. Surprisingly, no apparent increase in apoptotic activity was taking place. Even more surprising, however, was the unmistakable presence of organelles associated with another cell death

pathway, autophagy. Autophagy has long been considered a mechanism employed by cells to maintain homeostasis in times of starvation or oxidative stress and so, although surprising, evidence of it occurring in the granulosa cells of follicles exposed to cigarette smoke was not altogether unexpected.

Cigarette smoke is comprised of a complex mixture of chemicals, many of which are oxidants themselves or have the ability to cause ROS once internalized. Knowing this, the second study included a number of outcome measures aimed at determining how much oxidative damage was occurring in the ovaries of smoke exposed mice. Although there was no significant difference between treated and control groups for some of the measures (protein carbonyl formation, DNA damage and glutathione levels), there was evidence that the cells of treated ovaries were experiencing oxidative stress, as evidenced by the increased expression of the small heat shock protein, HSP25 and by the significantly lower levels of the antioxidant enzyme SOD2, which is produced in the mitochondria. Upon closer examination, mitochondria were visible in the autophagosomes contained within the granulosa cells of treated ovaries. Future studies are needed to confirm this using mitochondrial-specific markers. Taken together, these results suggested that there was a reduced capacity for an antioxidant defense against ROS production in treated ovaries.

Having systematically ruled out apoptosis as the primary mechanism through which follicles were being lost in the first and second studies, the third study was designed to

further elucidate the molecular mechanism through which autophagy was activated, resulting in the loss of these follicles. Autophagy involves a number of different molecular mediators, each key in different stages of the cascade. Knowing this, we chose to look at Beclin 1, a key mediator involved in the initiation stage of autophagy and responsible for membrane nucleation, and LC3, which is involved in autophagosome formation and facilitation of organelle transport into autophagosomes, as markers of enhanced autophagy in smoke exposed ovaries. Given that mitochondria were evident within the autophagosomes and that SOD2 expression was significantly lower in smoke exposed ovaries, we hypothesized that mitochondria were being selectively targeted for autophagosomal degradation. These findings, coupled with the knowledge that mitochondria-specific autophagy, mitophagy, exists to rid the cell of damaged mitochondria, we set out to determine if cigarette smoke exposure was causing targeted damage of mitochondria. Upon completion of this study, it was evident that not only was cigarette smoke increasing the autophagosomal activity within the granulosa cells of smoke exposed ovaries (increased number of autophagosomes, decreased BCL2 expression and increased BECN1 and LC3 expression), but it was also resulting in the dysfunction of mitochondrial dynamics in those cells, as seen by the disruption in the balance between fission (increased PARK2 expression) and fusion (decreased MFN1 and MFN 2 expression).

5.1 Proposed model of cigarette smoke-induced ovarian follicle loss

Based on the combined studies of this thesis, I have developed a model for the mechanism through which cigarette smoke adversely affects ovarian follicle survival (Figure 9). I propose that cigarette smoke acts through one of two pathways, likely both, culminating in the death of granulosa cells in ovarian follicles. First, cigarette smoke acts directly on the mitochondria resulting in an increase in the production of ROS, which overwhelms the antioxidant capacity of the cell and leads to oxidative damage. The oxidative damage, in turn, further increases ROS production, especially in the mitochondria which are particularly susceptible to ROS-induced oxidative damage, compounding the effect. This ultimately leads to dysfunction of the mitochondria and decreased ability to fuse with others in the syncytium for repair, leading to increased fission and subsequent degradation of the mitochondria via mitophagy. In the second scenario, components contained within cigarette smoke, namely BaP, act through the AhR to activate the transcription and translation of genes involved in the metabolism of those same components. Metabolism of those components leads to an increase in intracellular ROS. An increase in ROS triggers an increase in mitochondria to produce antioxidants, which are quickly overwhelmed leading to oxidative damage. Again, this positive feedback loop leads to further enhanced ROS production and oxidative damage. Because mitochondria are both producers of ROS and targets of ROS, they are susceptible to damage and this damage leads to dysregulation of repair mechanisms in place to combat this damage. Consequently, an increase in fission and a decrease in fusion results in fewer functional mitochondria. Fewer mitochondria mean less

antioxidant production to combat ROS production and to provide much needed energy to the cell. In both scenarios, the continued exposure to cigarette smoke does not allow for the reparative mechanisms to overcome the damage induced, and ultimately as more and more mitochondria are damaged and degraded, the cell becomes energy depleted and dies. Autophagy of the mitochondria is likely an initial attempt at survival of the granulosa cells, but the system is overwhelmed by the continuous onslaught of cigarette smoke exposure and ultimately becomes the mechanism by which these cells die.

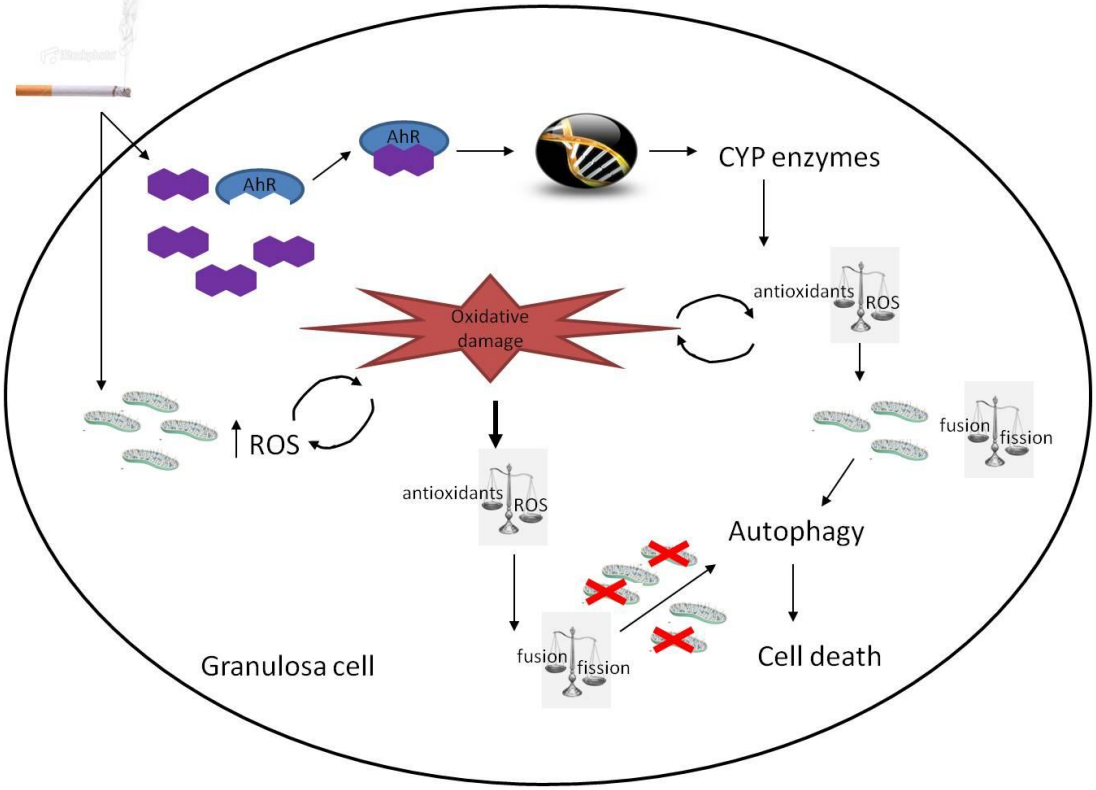

Figure 9: Proposed model of cigarette smoke-induced granulosa cell death.
Cigarette smoke acts through one of two pathways culminating in the death of granulosa cells in ovarian follicles. In the first pathway, direct action of cigarette smoke on the mitochondria results in an increase in the production of ROS, overwhelming the antioxidant capacity of the cell, leading to oxidative damage. This, in turn, further increases ROS production, especially in the mitochondria which are particularly susceptible to ROS-induced oxidative damage, compounding the effect, ultimately leading to dysfunction of the mitochondria and decreased ability to fuse with other mitochondria for repair, leading to increased fission and subsequent degradation via mitophagy. In the second pathway, compounds within cigarette smoke, namely BaP, act through the AhR to activate the transcription and translation of genes (i.e.: *Cyp1A1*) involved in the metabolism of those same components, which increases intracellular ROS, signalling mitochondria to produce antioxidants. This defense mechanism is quickly overwhelmed leading to a positive feedback loop of oxidative damage and dysregulation of repair mechanisms in place to combat this damage resulting in fewer functional mitochondria. Fewer mitochondria mean less antioxidant production to combat ROS production and to provide much needed energy to the cell. In both scenarios, the continued exposure to cigarette smoke does not allow for the reparative mechanisms to overcome the damage induced, and ultimately as more and more mitochondria are damaged and degraded, the cell becomes energy depleted and dies.

5.2 Contribution of this thesis to our understanding of toxicant-induced ovarian follicle loss

5.2.1.1 Cigarette smoke causes significant ovarian follicle loss, but not through apoptosis

In chapter 2, we sought to determine if the adverse effects associated with smoking were due, at least in part, to ovarian follicle loss. To achieve this, we exposed mice to cigarette smoke for 8 weeks, at the end of which we assessed their complement of follicles both numerically and for markers of programmed cell death type I, apoptosis. Our key findings following this study were that cigarette smoke at doses representative of human exposure causes significant follicle loss but not via the canonical apoptosis pathway. The significant follicle loss in these ovaries would effectively reduce the duration of reproductive life. This finding is in keeping with epidemiological studies conducted by Windham *et al.,* who showed that women who smoke have shorter menstrual cycles and by Hayatbakhsh *et al.,* who found that smokers enter menopause at an earlier age compared with women who do not smoke [52;393]. However, our study extends the toxicology literature, which, at the time of publication, had largely reported that reproductive toxicants caused ovarian follicle loss via apoptosis [19;53;62;63;65;66;221;227;229;233;265;268;290;394-397]. Indeed, treatment of ovaries in different species, with different toxicants and at different doses resulted in apoptosis of follicles at different stages of folliculogenesis and impacted fertility to varying degrees ranging from subfertility to sterility. Thus, reporting that apoptosis was not taking place in our model was paradoxical. However, upon in depth consideration, it became clear that the doses where apoptosis was consistently seen were significantly higher and less

environmentally relevant than those we were administering, suggesting that not only did each toxicant elicit its response upon different cohorts of follicles, but it did so at toxicological levels. Specifically, VCD, a metabolite of VCH and an effective follicle toxicant, elicits apoptosis in small pre-antral follicles in both rat and mouse ovaries, but does so via different molecular pathways [265]. Whereas rat ovaries were found to employ the AhR in VCD-induced ovotoxicity, mice did not. Similarly, the metabolism of these chemicals is often species-specific. For example, in mice, VCH exposure resulted in a decrease in small follicles by more than 50%, but the same treatment in rats resulted in no discernible follicle loss [398] a difference attributed to rats' inability to metabolize VCH to VCD in high enough quantities to elicit follicle loss. Moreover, the effects of dose and toxicant used on follicle loss was found to be essential [18;19;217]. Whereas VCH selectively destroys primordial follicles and requires repeated dosing for prolonged ovotoxicity [19], DMBA (1 mg/Kg) destroys all types of ovarian follicles in both rat and mouse ovaries [18;217].

5.2.1.2 Cigarette smoke exposure results in oxidative stress

Given that cigarette smoke constituents have been implicated in oxidative stress and its resultant pathology, we assessed the role of ROS and their consequent oxidative damage to ovarian follicle loss. While specific measures of oxidative damage (DNA measured by 8-OHdG, protein measured by protein carbonyl formation) were not significantly different, indirect markers of a response to an increase in ROS were (HSP25 expression). Specifically, expression of the small heat shock protein HSP25 was significantly

upregulated in smoke exposed ovaries, a finding consistent with several other studies investigating oxidative stress in other tissues [399-405]. One such study looked at the effect of knocking out the transcription factor partially responsible for HSP25 expression on mitochondrial oxidative stress in the kidney. They found that reduced expression of heat shock factor (HSF) 1 resulted in a down-regulation of protein expression resulting in increased ROS ($O_2^{\bullet -}$) as well as increased mitochondria-specific indicators of stress (opening of the membrane transition pore and change in membrane potential) [405]. Two studies looking at induced diabetes in mice saw increased HSP25 expression in the hippocampus [403] and retina [404] of treated mice coincident with increases in oxidative stress. Similarly, doxorubicin-induced congestive heart failure also resulted in an increase in HSP25 expression that correlated with the increase in oxidative stress [402]. Interestingly, treatment with schisandrin B, an antioxidant derived from the fruit of *Schisandra chinensis*, protects against hepatotoxicity by enhancing HSP25 expression and activating the cytochrome P450 oxidant pathway and ROS, suggesting that its role as an antioxidant is dependent upon the initial upregulation of oxidant species to trigger cellular response pathways [399]. With respect to our studies, it is entirely plausible that a similar cellular response to cigarette smoke is occurring whereby the heat shock and oxidant responses are being activated (as evidenced by increased HSP25 expression), but that their prolonged upregulation overwhelms these defense mechanisms (decreased SOD2 expression) resulting in decreased ability to reduce the effect of the ROS produced. Our findings were inconsistent, however, with one study investigating the effects of thioacetamide-induced liver injury on the stress response and ROS generation

[406]. The investigators of this study found a decrease in HSP25 expression following treatment resulting in enhanced ROS accumulation in the liver. The observed difference may be due to the chemical studied, the dose or indeed the tissue-specific response. It is important to note that this study was performed in a conditional $p38\alpha^{\Delta hep}$ knockout mouse; therefore, we cannot rule out the unanticipated effects of gene knockout on liver response to treatment.

In addition to an increase in HSP25 expression, smoke exposed ovaries had significantly reduced SOD2 expression, suggesting an increase in mitochondrial damage and a subsequent decreased capacity to combat ROS. SOD2 is the anti-super oxide enzyme produced by mitochondria. Finding its levels lower in our smoke exposed ovaries was at first surprising, having expected an enhanced level concomitant with increased ROS. However, our findings were in line with others who demonstrated that prolonged exposure to pro-oxidants resulted in a decrease in SOD2 expression despite increases in ROS and oxidative damage [276;407]. Still others reported that cigarette smoking and exposure to cigarette smoke extract (CSE) resulted in increased oxidative stress and enhanced circulating SOD2 levels [293;408], suggesting that there are differences in response to similar substances within different tissues and when comparing *in vitro* vs. *in vivo* models. Taken together, these conflicting results show that response to oxidants and ROS production differs depending on chemical tested, dose, route of exposure, model system used, tissue tested and duration of experiment. Thus, direct comparison of results is complicated and should be made with caution.

5.2.1.3 Evidence of profound autophagy in granulosa cells of cigarette smoke exposed ovaries

In chapter 3, after having effectively ruled out apoptosis as the cause of ovarian follicle loss using molecular markers, we turned to electron microscopy thinking that subtle changes in apoptosis were potentially taking place that were being masked by using whole ovary homogenates to measure gene and protein expression. To our surprise, we found evidence of an entirely different phenomenon occurring – autophagy. The presence of numerous double-membrane-bound vesicles was striking in the smoke exposed ovaries. EM is considered the gold standard for identifying autophagosomes and thus the occurrence of autophagy [409]. However, we used RNA extracted from whole ovaries in treated and control groups to assess the expression levels of two genes involved in autophagy to confirm our findings [345]. Expression of both genes, *Becn1* and *Lc3* was significantly higher in smoke vs. sham ovaries. Interestingly, a finding from our first study whose significance had perplexed us suddenly became clear. Cigarette smoke exposure resulted in significantly lower expression of BCL2. At the time, we expected its decrease to result in enhanced apoptosis owing to its association with BAX; however, BCL2 also plays a pivotal role in inhibiting the progression of autophagy [351;410;411]. These results meant that our treatment was activating a previously unreported mechanism of toxicant-induced ovarian follicle loss, thereby highlighting a novel alternative cell death pathway in the ovary.

We further investigated the change in expression of molecular markers of autophagy in chapter 4. In addition to profound autophagosome formation in the granulosa cells of

cigarette smoke exposed ovaries, the gene and protein expression of the anti-autophagic BCL2 and of the pro-autophagic BECN1 and LC3 were assessed. In keeping with our previous findings, BCL2 protein expression was significantly lower while both the gene and protein expression of both BECN1 and LC3 were significantly higher in smoke exposed ovaries. Autophagy has long been considered a survival mechanism employed by cells to maintain homeostasis in times of oxygen or nutrient deprivation. However, in recent years, numerous studies have emerged highlighting its role as a cell death mechanism. Our findings are in line with the latter role of autophagy and are in keeping with others who have also shown autophagy increases cell death irrespective of enhanced apoptosis [276;277;349;350;355;391;412-422]. Autophagy has been shown to mediate cell death most often, although not exclusively, in the event of non-physiological assaults to the cell. These include arsenite [412;414;415], arsenic trioxide [350], 2-methoxyestradiol [416], etoposide [410], H_2O_2 [416] and cigarette smoke [355;417;421]. Thus, our findings emphasize the role of autophagy as a cell death pathway, and confirm its role in ovarian follicle loss.

5.2.1.4 Mitochondrial dysfunction is evident in cigarette smoke exposed ovaries

Finally, in addition to showing that autophagy is important in cigarette smoke exposed ovaries, we demonstrated that mitochondrial dynamics were disrupted in cigarette smoke exposed ovaries, potentially leading to mitochondria-specific autophagy and granulosa cell death. Specifically, cigarette smoke exposed ovaries had significantly higher PARK2 gene and protein expression concurrent with significantly lower MFN1 gene and protein

and MFN2 protein expression. These changes in the homeostatic balance of the proteins necessary to maintain appropriate levels of mitochondrial fission and fusion occurring within the cell indicate a shift towards fission and mitochondrial loss [243;358;365;370;423;424]. Mitochondria are continually fusing with one another, elongating and undergoing fission in a tightly choreographed ballet that maintains appropriate mtDNA content, helps mitigate mitochondrial damage and increases ATP output [261;358;366;379;425]. Our findings here, coupled with the decreased SOD2 expression seen in chapter 3 point to a dysregulation of the mitochondrial dynamics in cigarette smoke exposed ovaries. Given that other laboratories have reported increased autophagy following toxicant exposure, our results may provide insight into the dysfunction within the cell precipitating autophagy [379]. To wit, mitochondria can be specifically targeted for autophagy through mitophagy and increased mitophagy ultimately results in death of the cell if left unchecked. Therefore, evaluating markers of mitochondrial dysfunction could shed light on the molecular events of cells exposed to various chemicals and potentially lead to therapeutic interventions to reduce cell death.

5.3 Strengths of the thesis

There are a number of strengths to the animal model chosen to investigate the effects of cigarette smoke exposure on the ovary in humans. Careful consideration must always be given when choosing how best to study a human phenomenon in another species.

5.3.1 *in vitro* vs. *in vivo* model

Utilizing an *in vivo* model instead of an *in vitro* model is one of the primary strengths of this thesis. While *in vitro* models lend themselves well to large sample sizes and multiple replicates at a lower cost (both monetarily and in time), they lack the complexity of multiple organ system involvement obtainable in an *in vivo* model. For example, although it has been shown that the ovary possesses the necessary enzymes to metabolize cigarette smoke constituents [426-429], we cannot rule out the involvement of liver metabolism and subsequent transport of reactive metabolites through the bloodstream to the ovary. Indeed, cigarette smoke constituents including BaP can be measured in serum and follicular fluid of smokers [56], and its metabolites are present in the ovary [429]. Consequently we chose to employ the use of an *in vivo* cigarette smoke exposure system to more closely emulate the effects of smoking on human ovaries in our animals.

5.3.2 Dose and route of exposure

In our animal model, female C57BL/6 mice received a whole body smoke exposure of 12 reference cigarettes/hour twice daily for 5 days/week. Prior to the commencement of our studies, Dr. Stämpfli and his laboratory had worked out that this protocol worked well for obtaining serum cotinine and carboxyhaemoglobin (a measure of haemoglobin CO saturation) levels within the range of an average smoker [430]. For example, levels measured in exposed mice were consistent with those of moderate to heavy smokers [430-432]. In contrast, other ovarian toxicity studies use high doses ranging from 12.5 nM - 500 mg/kg of cigarette smoke components, including BaP and DMBA, and administer these doses via injection, ingestion and in culture media in *in vitro* studies

[66;217;218;230;231;264;267;297]. These doses are not analogous to those seen by the ovary in human exposures. Additionally, the aforementioned methods of administration are not representative of human routes of ingestion of cigarette smoke and its components. Thus, we chose to employ a whole body exposure; however, we recognize that there is the potential for additional oral exposure to mice during coat grooming following exposure. To address this, we considered the potential confounding results this could cause and found that although true, humans also consume cigarette smoke components during inhalation and their metabolites can be measured in oral cells [433]. Thus, humans do have the potential to ingest cigarette smoke components as well.

5.3.3 Reproducibility

Reproducibility is fundamental to the strength of any scientific endeavour. Results from this thesis have been reliably reproduced in several animal cohorts. For instance, the observed loss of ovarian follicles in the absence of increased apoptosis were replicated in three separate treatment cohorts [434;435]. Moreover, two independent cohorts were assessed for changes in autophagy markers and oxidative stress [435;436]. In addition, similar results were obtained in other models of cigarette smoke exposure. For example, Hwang *et al.* found that *in vivo* exposure of murine lung epithelial cells to cigarette smoke resulted in autophagy that could be attenuated by pre-treatment with resveratrol [355]. Similarly, *in vitro* treatment of human lung epithelial cells with CSE produced profound autophagosome formation and upregulation of LC3 processing [391]. However, contrary to our results, *in vitro* treatment with CSE also resulted in an upregulation in

extrinsic apoptosis markers, the expression of which was partially dependent upon the autophagy proteins BECN1 and LC3 [391]. The apparent differences between these findings could be the product of the differences in species and cell type studied, *in vitro* vs. *in vivo* models (direct exposure of CSE vs. indirect exposure following systemic intake and metabolism), dose and duration of the experiment. In Chinese hamster ovary (CHO) cell cultures, autophagy was found to be protective against toxicant-induced cell death by preferentially inducing mitophagy to remove damaged mitochondria [420]. It is entirely possible that the dose and/or duration were not sufficient to induce autophagy-mediated cell death. Conversely, given that the chemical used was different, the mechanism of cell death could likewise differ. It is interesting to note though, that despite differences in activation of autophagy and apoptosis, mitochondrial damage was evident in these treated cells, suggesting that there may be a threshold for mitochondrial damage beyond which mitophagy leads to death.

5.4 Limitations of the thesis

5.4.1 Murine model of a human condition

While *in vivo* animal models are preferable to *in vitro* models for assessing the effects of a challenge on a particular system, they remain far from ideal. There are a number of challenges associated with utilizing an animal model to study the effects of a chemical on the human condition. In the case of this thesis, we endeavoured to mimic the effects of daily cigarette smoke exposure on the ovary using an *in vivo* mouse model of cigarette smoke exposure. We chose a murine model for several reasons. First, the model for

cigarette smoke exposure had been optimized for the mouse, allowing for the generation of data without the long lead-up time associated with optimizing a model system. Second, the reagents and tools have been extensively developed for this species. Third, mice have a short reproductive cycle, allowing for multiple cycles to take place over the course of the experiment, lending itself well to the recapitulation of long-term smoking over a much shorter time-frame. Lastly, from a practicality perspective, mice are relatively inexpensive to house, allowing for larger cohorts of animals to be used to increase the power of our studies. Despite the aforementioned reasons, it is important to bear in mind the limitations of employing a mouse model for the study of cigarette smoke exposure-induced follicle loss, as mice and humans display anatomic and physiologic differences in their reproductive tracts, as well as in their xenobiotic metabolism. First and foremost, mice are a litter-bearing species while humans are not, meaning that multiple follicles are selected for dominance and ovulation in mice while typically only one is in the human ovary. Second, the estrus cycle in the mouse is 4-6 days [437] in duration while humans have a highly variable menstrual cycle ranging between 26-35 days [83], meaning that growing follicles would be exposed to cigarette smoke for longer periods of time in the human than in the mouse, potentially resulting in a more pronounced phenotype in humans. Third, to control for the differences in smoking patterns – that being that each time a cigarette is puffed, the depth of inhalation, dilution of cigarette smoke with room air, rate and intensity of puffing differs – we used a cigarette smoke machine which is calibrated to ensure delivery of a controlled, consistent dose of cigarette smoke in each puff and measured serum cotinine levels, the most important mammalian metabolite of

nicotine, following treatment in our mice. However, to further confound the dose measurement, cotinine has a significantly shorter half life in mice (20.1 ± 2.3 min for C57BL/6 mice) [438] than it does in humans (10-16 hr) [438;439] due to its rapid metabolism. Thus, collection of serum had to be done immediately following treatment to ensure accurate measurements. Finally, it cannot be assumed that what happens in one species will occur to the same degree in another, thus direct comparison is not possible. While these limitations will likely restrict the degree to which we can determine how much cigarette smoking will affect human ovarian follicle survival, the model nonetheless provides significant insight into the likely mechanisms driving ovarian follicle loss following cigarette smoke exposure and may lead to the development of potential therapeutic interventions for fertility preservation in patients exposed not only to cigarette smoke, but potentially to a multitude of reproductive toxicants.

5.4.2 Technical challenges

There were numerous technical challenges that limited the depth to which certain questions could be answered in this thesis. One of the consistent challenges throughout my thesis was the issue of using whole ovarian homogenates to gain insight into follicle- and granulosa cell-specific questions. While the use of immunohistochemistry (IHC) allows for the determination of the localization of a protein of interest, it is not a sensitive enough method to use to determine the quantity of a protein. As such, I coupled IHC with real time PCR and Western blotting to determine the localization and relative abundance

of a gene and its protein compared with an appropriate loading control. However, both the real time PCR and Western blots were completed using whole ovarian homogenates, which meant that stromal tissue expression of any gene or protein was also included in the final analysis. Alternative tests using laser capture microdissection (LCM) would circumvent this issue, however, at the time of these studies, were not available to me. Future studies employing the use of LCM would be able to further illuminate the degree to which the tested genes and proteins are altered by cigarette smoke. It is possible that where we saw no significant difference between treated and control ovaries using whole ovarian homogenates (i.e.: markers of apoptosis, markers of oxidative damage), that the effects were masked by stromal cells in the ovary. Conversely, where there was a significant difference between treated and control ovaries at the whole ovary level (i.e.: SOD2, markers of autophagy signaling cascade, markers of mitochondrial repair mechanism), I propose that the observed effect is more modest than would be in an isolated follicle preparation. We do not, however, anticipate that these tests would alter our main findings; chiefly that autophagy and not apoptosis is the mechanism by which ovarian follicle loss occurs following chronic cigarette smoke exposure. This is because although we used whole ovarian homogenates for our real time PCR and Western blotting experiments, those were complimented by the use of TUNEL, IHC and EM to show that autophagy and not apoptosis was increased in treated ovaries.

Based on results from previous studies in our laboratory, the aryl hydrocarbon receptor (AhR) was identified as a probable candidate for mediating the effects of BaP on follicles

in vitro [300]. Moreover, given that similar effects were seen in CSC- and BaP-treated follicles [57;58;299;300], it is not unreasonable to postulate that BaP within cigarette smoke is largely responsible for the adverse effects seen in the CSC-treated cultures and by extension in our *in vivo* cigarette smoke exposed mice. Therefore, in an attempt to identify the pathway chiefly responsible for mediating the loss of ovarian follicles in our smoke exposure model, I designed an experiment using the aryl hydrocarbon receptor knockout (ARKO) mouse to determine the degree to which a functional AhR is required for follicle loss. The planned study was to complement the existing WT *in vivo* cigarette smoke exposure model – treating ARKO mice with cigarette smoke for 8 weeks and comparing them to age-matched ARKO sham controls. The study encountered several difficulties. Initially, the plan was to use homozygous breeding pairs and use the female offspring for the *in vivo* experiments. The heterozygous knockout mice were ordered and it took 10 months to receive four homozygous breeding pairs. Once they arrived, however, there were multiple problems: the dams produced very small litters (1-4 pups on average), were cannibalizing their young and those that weren't cannibalized were not female (the ratio of male:female was approximately 5:1); consequently I was unable to obtain sufficient numbers of mice for experimentation. Suspecting that it was the genotype of the dams that was the issue, I backcrossed the mice to a heterozygous genotype and began breeding heterozygous females with homozygous males to optimize the number of homozygous offspring. The change in genotype of the dam helped with cannibalizing tremendously, and I began genotyping the offspring. Genotyping proved successful, but the number of homozygous female mice was inevitably too small to run

experiments. The decision was made to retire the colony in favour of finishing the project with the data I had to date and attempt the ARKO study at a later date. Interestingly, with the availability of an AhR deletion mutant (*AhR*^{d}), I was able to obtain some preliminary data on BECN1 expression in WT and *AhR*^{d} following cigarette smoke exposure (Appendix II, Figure S6) and it appears that the AhR does indeed play a role in mediating the response of cigarette smoke in the ovary. Expression was significantly different between all groups ($p = 0.007$), as measured by one way analysis of variance (ANOVA). Sham WT was significantly lower than both sham *AhR*^{d} (<d>) ($p = 0.02$) and smoke WT ($p=0.001$) but not different from smoke <d>. *AhR*^{d} treated ovaries were not different from control *AhR*^{d} ovaries. These preliminary data suggest that similar levels of autophagy are occurring in WT untreated controls and *AhR*^{d} smoke exposed ovaries, potentially owing to the requirement for a functional AhR for autophagy-induced follicle loss. It is not clear at present why *AhR*^{d} controls would have greater BECN1 expression than WT controls. Future work in this vein will be necessary to further elucidate the degree to which the AhR is required.

5.5 Future directions

Although this thesis presents a strong, evidence-based theory on the mechanism regulating ovarian follicle loss following cigarette smoke exposure, a number of questions remain unanswered. In order to answer these questions, several additional studies requiring considerable work must be undertaken. Thus, the work presented here provides an excellent foundation for future directions using this model.

5.5.1 Aryl hydrocarbon receptor knockout mice

In an effort to further elucidate the mechanistic pathway through which cigarette smoke elicits its effects, it is imperative that studies be done using the aryl hydrocarbon receptor knockout mouse. The AhR has been implicated in the metabolism of a number of compounds found within cigarette smoke, including BaP. In previous studies, antagonists of the AhR have been shown to mediate the adverse effects of cigarette smoke condensate in human bronchial epithelial cells [421] and of BaP on isolated rat follicles [300] *in vitro*, making it important to be able to show that the AhR is playing a similar role in mediating the *in vivo* actions of cigarette smoke on the ovary.

5.5.1.1 The Aryl Hydrocarbon Receptor

Polycyclic aromatic hydrocarbons (PAHs) are a class of compounds formed by the incomplete combustion of fossil fuels and organic matter. Previous studies have revealed that of the more than 4,000 chemicals present in cigarette smoke, levels of PAHs (especially BaP) are present in levels that are 10-fold higher in sidestream than mainstream smoke [440]. BaP possesses mutagenic properties and is known to cause the formation of DNA adducts and is primarily activated by the cytochrome P450 (CYP) enzymes, most notably CYP1A1, CYP1A2, CYP1B1 [294], which are regulated by the aryl hydrocarbon receptor pathway. The AhR, a cytosolic ligand-activated receptor [427], is a member of a highly conserved family of transcription factors known as the basic helix-loop-helix Per-Arnt-Sim (bHLH-PAS) family. The AhR, which is localized in numerous tissues throughout the body including oocytes and granulosa cells, mediates the effects of multiple xenobiotics including a number of compounds collectively known as

PAHs, persistent environmental contaminants whose effects are widespread throughout the body [441] and are constituents in cigarette smoke. Although no endogenous ligand has been found for the AhR to date, its conservation throughout a vast number of animal species indicates a physiologic role in addition to its mediation of xenobiotics [426]. As shown in figure 10, under normal physiological conditions, the AhR resides in the cytoplasm, bound to HSP90 and XAP2 [426]. Upon binding to its ligand, the AhR translocates to the nucleus where it forms a dimer with ARNT, the aryl hydrocarbon receptor nuclear translocator, and binds to xenobiotic/dioxin response elements (XRE/DRE) in the promoter regions of xenobiotic metabolizing enzymes and genes involved in cellular function, upregulating their transcription [441]. Previous work has shown that the ovotoxic effect of PAHs appear to be compound-specific [262], likely a consequence of their diverse affinities for the AhR as well as the action of the downstream enzymes that are activated.

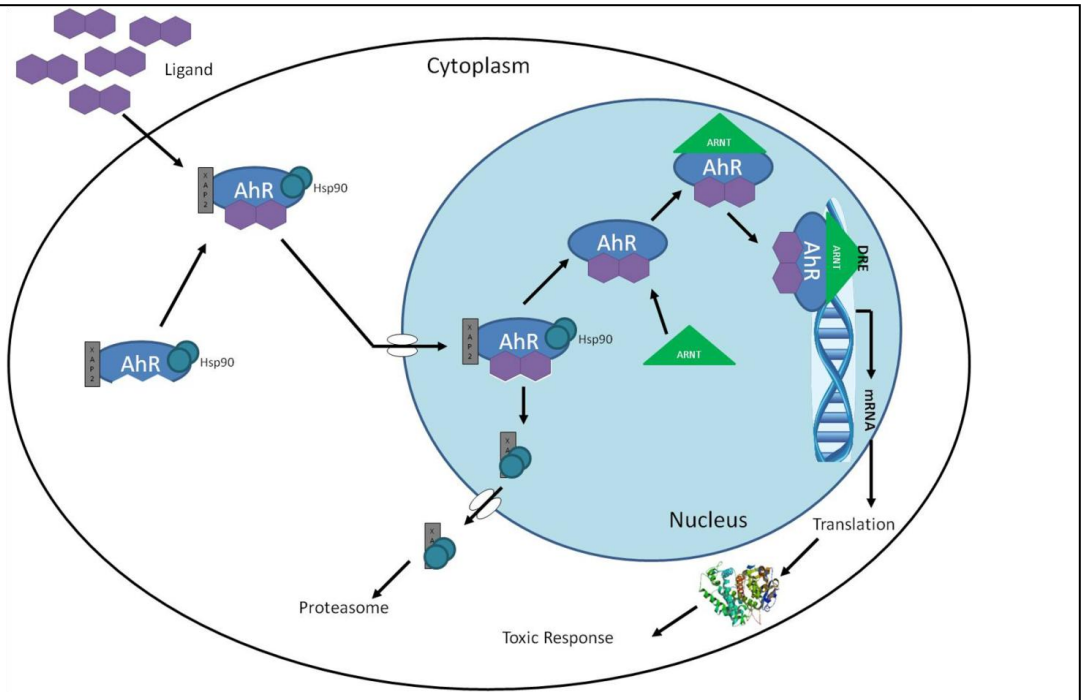

Figure 10: The aryl hydrocarbon receptor pathway.
Under physiological conditions, the AhR resides in the cytoplasm, bound to HSP90 and XAP2. Upon binding to its ligand (i.e.: BaP), the AhR translocates to the nucleus where it forms a dimer with ARNT, the aryl hydrocarbon receptor nuclear translocator. HSP90 and XAP2 are subsequently degraded in the proteasome. The AhR/ARNT/ligand complex then binds to dioxin response elements (DRE) in the promoter regions of xenobiotic metabolizing enzymes (i.e.: CYP1A1) and genes involved in cellular function, upregulating their transcription, translation and ensuing toxic response.

5.5.1.2 Benzo(a)pyrene

Cigarette smoke is composed of 4,000 chemicals including benzo(a)pyrene, a prototypical PAH. While many of the consitiutents in cigarette smoke are toxic, only BaP has been measured in the follicular fluid of women who smoke. Therefore, of the chemicals present in cigarette smoke, BaP is potentially the most relevant with respect to ovarian follicle loss. BaP is a product of incomplete combustion of fossil fuels and is found in coal tar, exhaust fumes, cereals, char-broiled foods, and cigarette smoke. High

concentrations have been measured in indoor air where wood-fired stoves are used for cooking and in homes near coal-burning plants. Consequently, BaP is a ubiquitous environmental toxicant, exposure to which is widespread and unavoidable. BaP is a five-ring polycyclic aromatic hydrocarbon that is highly mutagenic and carcinogenic and acts through the AhR. Exposure to BaP leads to the activation of the AhR pathway and subsequently to increased cytochrome P450 enzyme expression (CYP1A1, 1A2, 1B1) [265] and the metabolic breakdown of BaP into its active metabolite, benzo(a)pyrene diol epoxide (BPDE; Figure 11). BPDE then intercalates with DNA forming adducts resulting in carcinogenic mutations [442]. BaP-induced ovarian toxicity has been documented in *in vitro* studies and animal models [8;57;218;230;262;297;443;444]; however, few have investigated the effects of treatment using concentrations relevant to human exposure. Our lab found that BaP exposure, at levels representative of those measured in human follicular fluid of women exposed to smoke, results in impaired cumulus expansion and attenuated FSH-stimulated growth in a dose-dependent manner in isolated rat follicles [56;57]. Similarly, using a mouse isolated follicle culture system, follicle survival was significantly lower in 13 day cultures of follicles exposed to BaP, at concentrations equivalent to those measured in human ovarian follicular fluid of smokers, compared to control follicles [58]. In addition, follicles had significantly reduced estradiol (E_2) secretion at day 8 of culture and significantly higher relative average increase in estradiol secretion between days 8 and 12, compared to controls while progesterone levels were unchanged with respect to controls.

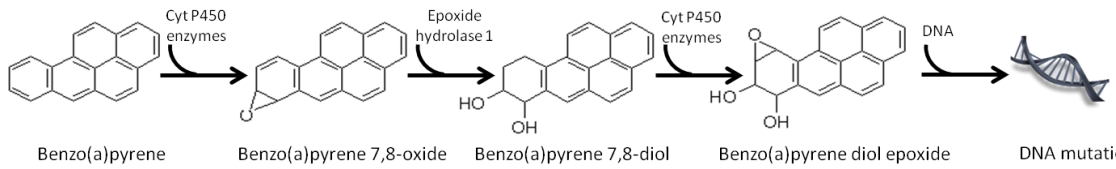

Figure 11: The metabolic pathway of benzo(a)pyrene.
Benzo(a)pyrene is metabolized in a three-step pathway. First, BaP is oxidized by cytochrome p450 enzymes to BaP 7,8-oxide. Next epoxide hydrolase 1 metabolises BaP 7,8-oxide to BaP 7,8-diol which is then converted to BaP 7,8-diol epoxide via interaction with the cytochrome p450 enzymes. BPDE is then capable of intercalating with DNA to form covalent bonds with guanine residues and inducing mutations.

5.5.1.3 Proposed studies using ARKO mice

Knowing that the effects of both CSC and BaP are attenuated following treatment with AhR antagonists [300;421], and that *in vitro* treatment with either of these compounds results in effects similar to those seen in female smokers experiencing infertility [56-58;299;300], it is important to determine if an *in vivo* model of cigarette smoke exposure in the absence of the AhR itself likewise attenuates the adverse effects of smoke exposure. Specifically, age-matched WT and ARKO mice would be randomly assigned to sham or treatment group and exposed to room air or cigarette smoke for 8 weeks (as per the established protocol). At the end of the treatment, outcome measures to be tested would include serum cotinine, AMH, E_2 and FSH levels, follicle counts and analysis of gene and protein expression for markers of mitochondrial dysfunction, apoptosis and autophagy. If the absence of the AhR results in fewer follicles lost to cigarette smoke exposure, as we believe it will, then AhR targeted therapies could be designed aimed at decreasing the downstream oxidative damage that activation of this pathway causes.

5.5.2 Autophagy blockage

In order to further verify that cigarette smoke exposure causes autophagy which in turn results in loss of follicles, attenuation experiments must be carried out. To achieve this, it would be necessary to inject mice with the specific inhibitor of autophagy, 3-methyladenine (3-MA), prior to and during cigarette smoke treatment. 3-methyladenine is a pharmacological inhibitor of autophagy. Specifically, it is a class III phosphatidylinositol 3-kinase (PI3K) inhibitor that functions by blocking the initial autophagic sequestration and autophagosome formation, thereby inhibiting autophagy [445]. Experiments previously conducted in mice indicate that a dose of 30 mg/kg of 3-MA are necessary to inhibit autophagy [445]; however, these experiments were short-term (48 hour treatments) and thus a single treatment of 3-MA would likely not be sufficient to mitigate follicle loss. Thus, continued treatment with 3-MA throughout the 8 week smoke exposure would be necessary. At the end of the 8 week exposure, ovaries would be collected and assessed for markers of autophagy, including EM analysis for visual confirmation of successful inhibition. Previous experiments using 3-MA to inhibit autophagy in lung ischemia-reperfusion injury confirm that it is effective in preventing autophagy-induced injury in tissue prone to autophagy-mediated cell death [446;447]. Alternatively, *in vitro* gene knockdown experiments utilizing small interfering RNA (siRNA) directed against *Becn1* could be employed in CSC treated whole ovary cultures to mitigate autophagy-induced follicle loss [445]. siRNA prevent the expression of the gene against which they are directed. Thus, prevention of *Becn1* expression would inhibit membrane nucleation and thereby prevent autophagosome formation.

5.5.3 Mitochondrial and ER involvement

Although we have shown that cigarette smoke exposure increases the number of autophagosomes and expression of autophagy cascade members, it is not known if the adverse effects are primarily mitochondrial specific or if multiple organelles undergo autophagy. Therefore, it would be prudent to investigate the role of mitochondria and the potential involvement of other organelles, primarily the ER, in increased autophagy following cigarette smoke exposure. Thus an experiment designed to elucidate mitochondrial (and potentially ER) involvement in cigarette smoke-induced autophagy by visualizing the change in mitochondrial membrane potential, followed by formation of autophagosomes and autophagy of damaged mitochondria would be required. An *in vitro* system would perhaps be the best method in which to initially test this, as it would permit the monitoring of the formation of autophagosomes and the incorporation of mitochondria or other organelles into them in large numbers of follicles in a relatively short time-frame (13 days) compared to an 8 week *in vivo* experiment. To achieve this, mice expressing green fluorescent protein (GFP) fused to LC3 (GFP-LC3) could be used for isolated follicle culture experiments. In these mice, GFP-LC3 is expressed in tissues throughout the body including the reproductive tract and the ovary. To maximize the number of follicles retrieved, mice would need to be treated with recombinant FSH and human chorionic gonadotropin (hCG) prior to ovary collection, a procedure previously optimized in our lab [58;299]. Each follicle would be treated with vehicle control (dimethyl sulfoxide), or with increasing concentrations of cigarette smoke condensate (0-90 μg/ml) or BaP (0-90 ng/ml) ± 5 μM of 3',4'-dimethoxy flavone (3,4-DMF), an AhR

antagonist, and cultured for 13 days. Following treatment, cells would be incubated with tetramethylrhodamine methylester (TMRM; a mitochondria membrane potential-indicating fluorophore), and MitoFluor Far Red (MFFR; a fluorophore specific for mitochondria) and visualized using confocal microscopy. Knowing that ROS have the capability of altering MMP and that both CSC and BaP produce ROS, it is expected that treated follicles would display mitochondria with altered MMP and that those mitochondria damaged by oxidative stress would be incorporated into autophagosomes labeled with GFP-LC3; a process that should be attenuated by co-treatment with 3,4-DMF. I believe that the number of mitochondria engulfed by autophagosomes would be greater in treated vs. vehicle control cultures demonstrating that mitophagy (GFP-LC3 + MFFR) and not bulk autophagy (GFP-LC3 only) is occurring preferentially in these cultures.

It is also possible that mitochondria may not prove to be the sole targets of autophagy in our treated follicles. To test this, I propose that red fluorescent protein (RFP)-labelled ER (RFP-ER) markers also be employed in the above experiment. RFP-ER molecular probes are available that incorporate both the calreticulin ER insertion and KDEL sequences for specific visualization of the ER. The ER is responsible for the synthesis and folding of secreted and membrane-bound proteins. Optimal protein folding requires an oxidative environment, the exacerbation of which can lead to the unfolded protein response (UPR). The UPR in turn induces the expression of a number of proteins including CCAAT/enhancer-binding protein-homologous protein (CHOP), an early indicator of ER stress and a potent inhibitor of BCL2 expression [294]. Additionally, BCL2 is closely

associated with promoting a lower resting state ER calcium (Ca^{2+}) content and with reducing Ca^{2+} release during stress by blocking inositol 1,4,5-triphosphate (IP_3)-mediated opening of the IP_3 receptor (IP_3R) [339]. However, this regulatory role is potentially compromised by the localization of BAX and BAK to the ER, which interact with BCL2, thereby preventing it from interacting with IP_3R. Additionally, BCL2 is phosphorylated by JNK in the UPR pathway and is thus targeted for proteasomal degradation [339]. Because we have seen a decrease in BCL2 expression in our smoke exposed ovaries, and the ER is also a site of BCL2 localization, we cannot rule out the involvement of the ER in cigarette smoke-mediated autophagy. Therefore, the inclusion of an ER marker would strengthen our findings and shed more light on the molecular mechanisms governing the loss of follicles in cigarette smoke-exposed ovaries.

5.5.4 Reversibility/cessation studies

Cigarette smoking reduces fertility [37]. As such, it is common practice for physicians to advise women attending their clinics to discontinue smoking prior to conception attempts. However, it is not known whether and if smoking cessation improves fertility or the time interval required. Therefore, studies investigating the potential for fertility improvement and the timeline required for that improvement are needed. I believe that although not reversible, cigarette smoke-induced damage can be mitigated by decreasing exposure to toxic chemicals in cigarette smoke which will decrease oxidative stress and return autophagy to normal reparative levels in the ovary leading to improved fertility. To achieve this, mice would be exposed to the established 8 week protocol (this exposure

period is ≈ 1 year of cigarette smoke exposure in a woman, based on a 4-6 day cycle in mice and a 28-35 day cycle in women) and then subsets allowed to recover for varying periods of time, representing months (4 weeks ≈ 6 months) to several years (10 months ≈ 5 years) in women. Blood and tissue would be collected from a subset from each treatment group for analysis of oxidative stress, mitochondrial dysfunction, and autophagy. The remaining subset would be housed with proven male breeders to determine the effect of smoking cessation on fertility. Outcome measures for this experiment would be time to pregnancy, number of pups/litter, number of implantation sites (uterus) vs. number of corpora lutea (ovary). Results from these studies would enhance physician counselling regarding duration of smoking cessation and potentially increase the successful pregnancy rates among female smokers.

5.6 Summary

Collectively, the data presented in this thesis provide greater insight into the mechanism of ovarian follicle loss following exposure to cigarette smoke. Our data expand the literature by challenging the long-held belief that ovarian follicle destruction is mediated by apoptosis following chemical exposure and highlighting a novel alternative cell death pathway employed by ovarian follicles when exposed to chronic, low doses of cigarette smoke. Our findings further highlight the importance of mitochondria and of autophagy in the health and maintenance of the ovarian follicles and ultimately fertility preservation. Our results could be important in a number of other pathways including loss of ovarian follicles exposed to other environmental toxicants, particularly chemotherapeutic drugs or

chronic occupational exposure to ovarian toxicants, other causes of infertility that have been linked to the production of ROS and/or mitochondrial dysfunction. Autophagy has been correlated with increased oxidative stress in older age and obese women [448], and autophagy disruption has been observed in women receiving assisted reproductive therapy; thus, dysregulation of mitochondrial dynamics and mitophagy in granulosa cells may be central to obesity and age-related decreased fertility as well as the response to environmental stressors.

5.6 References

Reference List

[1] Galhardo A, Pinto-Gouveia J, Cunha M, Matos M. The impact of shame and self-judgment on psychopathology in infertile patients. Hum Reprod 2011; 26: 2408-2414.

[2] Poppe K, Velkeniers B. Female infertility and the thyroid. Best Pract Res Clin Endocrinol Metab 2004; 18: 153-165.

[3] Soares SR, Simon C, Remohi J, Pellicer A. Cigarette smoking affects uterine receptiveness. Hum Reprod 2007; 22: 543-547.

[4] Jick H, Porter J. Relation between smoking and age of natural menopause. Report from the Boston Collaborative Drug Surveillance Program, Boston University Medical Center. Lancet 1977; 1: 1354-1355.

[5] Hughes EG, Brennan BG. Does cigarette smoking impair natural or assisted fecundity? Fertil Steril 1996; 66: 679-689.

[6] Klonoff-Cohen H. Female and male lifestyle habits and IVF: what is known and unknown. Hum Reprod Update 2005; 11: 179-203.

[7] Neal MS, Hughes EG, Holloway AC, Foster WG. Sidestream smoking is equally as damaging as mainstream smoking on IVF outcomes. Hum Reprod 2005; 20: 2531-2535.

[8] Baird WM, Hooven LA, Mahadevan B. Carcinogenic polycyclic aromatic hydrocarbon-DNA adducts and mechanism of action. Environ Mol Mutagen 2005; 45: 106-114.

[9] Infections, pregnancies, and infertility: perspectives on prevention. World Health Organization. Fertil Steril 1987; 47: 964-968.

[10] Bushnik T, Cook JL, Yuzpe AA, Tough S, Collins J. Estimating the prevalence of infertility in Canada. Hum Reprod 2012; 27: 738-746.

[11] The psychological impact of infertility and its treatment. Medical interventions may exacerbate anxiety, depression, and stress. Harv Ment Health Lett 2009; 25: 1-3.

[12] Chambers GM, Sullivan EA, Ishihara O, Chapman MG, Adamson GD. The economic impact of assisted reproductive technology: a review of selected developed countries. Fertil Steril 2009; 91: 2281-2294.

[13] Costello MF, Misso ML, Wong J, Hart R, Rombauts L, Melder A, Norman RJ, Teede HJ. The treatment of infertility in polycystic ovary syndrome: a brief update. Aust N Z J Obstet Gynaecol 2012; 52: 400-403.

[14] Wallace WH, Kelsey TW. Human ovarian reserve from conception to the menopause. PLoS One 2010; 5: e8772.

[15] Monget P, Bobe J, Gougeon A, Fabre S, Monniaux D, bies-Tran R. The ovarian reserve in mammals: a functional and evolutionary perspective. Mol Cell Endocrinol 2012; 356: 2-12.

[16] Shelling AN. Premature ovarian failure. Reproduction 2010; 140: 633-641.

[17] Kappeler CJ, Hoyer PB. 4-vinylcyclohexene diepoxide: a model chemical for ovotoxicity. Syst Biol Reprod Med 2012; 58: 57-62.

[18] Bhattacharya P, Keating AF. Ovarian metabolism of xenobiotics. Exp Biol Med (Maywood) 2011; 236: 765-771.

[19] Hoyer PB, Devine PJ, Hu X, Thompson KE, Sipes IG. Ovarian toxicity of 4-vinylcyclohexene diepoxide: a mechanistic model. Toxicol Pathol 2001; 29: 91-99.

[20] Broer SL, Mol BW, Hendriks D, Broekmans FJ. The role of antimullerian hormone in prediction of outcome after IVF: comparison with the antral follicle count. Fertil Steril 2009; 91: 705-714.

[21] Frisch RE. Body composition in amenorrheic athletic women. Ann Intern Med 1985; 103: 153.

[22] Frisch RE. Fatness, menarche, and female fertility. Perspect Biol Med 1985; 28: 611-633.

[23] Frisch RE. The right weight: body fat, menarche and ovulation. Baillieres Clin Obstet Gynaecol 1990; 4: 419-439.

[24] Frisch RE. Body fat, menarche, fitness and fertility. Hum Reprod 1987; 2: 521-533.

[25] Baker ER. Body weight and the initiation of puberty. Clin Obstet Gynecol 1985; 28: 573-579.

[26] amanti-Kandarakis E, Bergiele A. The influence of obesity on hyperandrogenism and infertility in the female. Obes Rev 2001; 2: 231-238.

[27] Sadeu JC, Hughes CL, Agarwal S, Foster WG. Alcohol, drugs, caffeine, tobacco, and environmental contaminant exposure: reproductive health consequences and clinical implications. Crit Rev Toxicol 2010; 40: 633-652.

[28] Neal MS, Hughes EG, Holloway AC, Foster WG. Sidestream smoking is equally as damaging as mainstream smoking on IVF outcomes. Hum Reprod 2005; 20: 2531-2535.

[29] World Health Organization (WHO). The Top 10 Causes of Death. In, FactSheet No. 310 ed. 2011.

[30] Hoyert DL, Xu J. National Vital Statistics Report. In Deaths: Preliminary for 2011, 61(6) ed. 2013.

[31] Statistics Canada. Leading Causes of Death, by sex. In. 2009.

[32] Health Canada. Canadian Tobacco Use Monitoring Survey. In. 2006.

[33] Statistics Canada. Current Smoking Trends. In, 82-624-x ed. 2012.

[34] Cohen B, Evers S, Manske S, Bercovitz K, Edward HG. Smoking, physical activity and breakfast consumption among secondary school students in a southwestern Ontario community. Can J Public Health 2003; 94: 41-44.

[35] Bouyer J, Rouxel A, Job-Spira N. Smoking cessation or reduction in women attempting to conceive after ectopic pregnancy. Eur J Epidemiol 2001; 17: 1063-1066.

[36] Dorfman SF. Tobacco and fertility: our responsibilities. Fertil Steril 2008; 89: 502-504.

[37] Smoking and infertility. Fertil Steril 2006; 86: S172-S177.

[38] Howe G, Westhoff C, Vessey M, Yeates D. Effects of age, cigarette smoking, and other factors on fertility: findings in a large prospective study. Br Med J (Clin Res Ed) 1985; 290: 1697-1700.

[39] Fuentes A, Munoz A, Barnhart K, Arguello B, Diaz M, Pommer R. Recent cigarette smoking and assisted reproductive technologies outcome. Fertil Steril 2010; 93: 89-95.

[40] Zenzes MT, Reed TE, Casper RF. Effects of cigarette smoking and age on the maturation of human oocytes. Hum Reprod 1997; 12: 1736-1741.

[41] Zenzes MT, Wang P, Casper RF. Cigarette smoking may affect meiotic maturation of human oocytes. Hum Reprod 1995; 10: 3213-3217.

[42] Curtis KM, Savitz DA, Arbuckle TE. Effects of cigarette smoking, caffeine consumption, and alcohol intake on fecundability. Am J Epidemiol 1997; 146: 32-41.

[43] Petanovski Z, Dimitrov G, Aydin B, Hadzi-Lega M, Sotirovska V, Susleski D, Saltirovski S, Matevski V, Stojkovska S, Petanovska E, Savic M, Balkanov T. Impact of active female smoking on controlled ovarian stimulation in intracytoplasmic sperm insemination cycles. Med Glas Ljek komore Zenicko - doboj kantona 2012; 9: 273-280.

[44] Sharara FI, Beatse SN, Leonardi MR, Navot D, Scott RT, Jr. Cigarette smoking accelerates the development of diminished ovarian reserve as evidenced by the clomiphene citrate challenge test. Fertil Steril 1994; 62: 257-262.

[45] Freour T, Masson D, Mirallie S, Jean M, Bach K, Dejoie T, Barriere P. Active smoking compromises IVF outcome and affects ovarian reserve. Reprod Biomed Online 2008; 16: 96-102.

[46] Rogers JM. Tobacco and pregnancy. Reprod Toxicol 2009; 28: 152-160.

[47] Waylen AL, Metwally M, Jones GL, Wilkinson AJ, Ledger WL. Effects of cigarette smoking upon clinical outcomes of assisted reproduction: a meta-analysis. Hum Reprod Update 2009; 15: 31-44.

[48] Dechanet C, Anahory T, Mathieu Daude JC, Quantin X, Reyftmann L, Hamamah S, Hedon B, Dechaud H. Effects of cigarette smoking on reproduction. Hum Reprod Update 2011; 17: 76-95.

[49] Stejskalova L, Pavek P. The function of cytochrome P450 1A1 enzyme (CYP1A1) and aryl hydrocarbon receptor (AhR) in the placenta. Curr Pharm Biotechnol 2011; 12: 715-730.

[50] Bizon A, Milnerowicz-Nabzdyk E, Zalewska M, Zimmer M, Milnerowicz H. Changes in pro/antioxidant balance in smoking and non-smoking pregnant women with intrauterine growth restriction. Reprod Toxicol 2011; 32: 360-367.

[51] Rogers JM. Tobacco and pregnancy: overview of exposures and effects. Birth Defects Res C Embryo Today 2008; 84: 1-15.

[52] Windham GC, Elkin EP, Swan SH, Waller KO, Fenster L. Cigarette smoking and effects on menstrual function. Obstet Gynecol 1999; 93: 59-65.

[53] Matikainen T, Perez GI, Jurisicova A, Pru JK, Schlezinger JJ, Ryu HY, Laine J, Sakai T, Korsmeyer SJ, Casper RF, Sherr DH, Tilly JL. Aromatic hydrocarbon receptor-driven Bax gene expression is required for premature ovarian failure

caused by biohazardous environmental chemicals. Nat Genet 2001; 28: 355-360.

[54] Broer S, Mol B, Hendriks D, Broekmans F. The role of antimullerian hormone in prediction of outcome after IVF: comparison with the antral follicle count. In. 2008.

[55] Westhoff C, Murphy P, Heller D. Predictors of ovarian follicle number. Fertil Steril 2000; 74: 624-628.

[56] Neal MS, Zhu J, Foster WG. Quantification of benzo[a]pyrene and other PAHs in the serum and follicular fluid of smokers versus non-smokers. Reprod Toxicol 2008; 25: 100-106.

[57] Neal MS, Zhu J, Holloway AC, Foster WG. Follicle growth is inhibited by benzo-[a]-pyrene, at concentrations representative of human exposure, in an isolated rat follicle culture assay. Hum Reprod 2007; 22: 961-967.

[58] Sadeu JC, Foster WG. Effect of in vitro exposure to benzo[a]pyrene, a component of cigarette smoke, on folliculogenesis, steroidogenesis and oocyte nuclear maturation. Reprod Toxicol 2010.

[59] El-Nemr A, Al-Shawaf T, Sabatini L, Wilson C, Lower AM, Grudzinskas JG. Effect of smoking on ovarian reserve and ovarian stimulation in in-vitro fertilization and embryo transfer. Hum Reprod 1998; 13: 2192-2198.

[60] Cortvrindt RG, Smitz JE. Follicle culture in reproductive toxicology: a tool for in-vitro testing of ovarian function? Hum Reprod Update 2002; 8: 243-254.

[61] van Beek RD, van den Heuvel-Eibrink MM, Laven JS, de Jong FH, Themmen AP, Hakvoort-Cammel FG, van den BC, van den BH, Pieters R, de Muinck Keizer-Schrama SM. Anti-Mullerian hormone is a sensitive serum marker for gonadal function in women treated for Hodgkin's lymphoma during childhood. J Clin Endocrinol Metab 2007; 92: 3869-3874.

[62] Devine PJ, Sipes IG, Skinner MK, Hoyer PB. Characterization of a rat in vitro ovarian culture system to study the ovarian toxicant 4-vinylcyclohexene diepoxide. Toxicol Appl Pharmacol 2002; 184: 107-115.

[63] Devine PJ, Sipes IG, Hoyer PB. Initiation of delayed ovotoxicity by in vitro and in vivo exposures of rat ovaries to 4-vinylcyclohexene diepoxide. Reprod Toxicol 2004; 19: 71-77.

[64] Mayer LP, Pearsall NA, Christian PJ, Devine PJ, Payne CM, McCuskey MK, Marion SL, Sipes IG, Hoyer PB. Long-term effects of ovarian follicular

depletion in rats by 4-vinylcyclohexene diepoxide. Reprod Toxicol 2002; 16: 775-781.

[65] Desmeules P, Devine PJ. Characterizing the ovotoxicity of cyclophosphamide metabolites on cultured mouse ovaries. Toxicol Sci 2006; 90: 500-509.

[66] Jurisicova A, Taniuchi A, Li H, Shang Y, Antenos M, Detmar J, Xu J, Matikainen T, Benito HA, Nunez G, Casper RF. Maternal exposure to polycyclic aromatic hydrocarbons diminishes murine ovarian reserve via induction of Harakiri. J Clin Invest 2007; 117: 3971-3978.

[67] La Marca A., Volpe A. The Anti-Mullerian hormone and ovarian cancer. Hum Reprod Update 2007; 13: 265-273.

[68] Lie FS, Lugtenburg PJ, Schipper I, Themmen AP, de Jong FH, Sonneveld P, Laven JS. Anti-mullerian hormone as a marker of ovarian function in women after chemotherapy and radiotherapy for haematological malignancies. Hum Reprod 2008; 23: 674-678.

[69] Themmen AP. Anti-Mullerian hormone: its role in follicular growth initiation and survival and as an ovarian reserve marker. J Natl Cancer Inst Monogr 2005; 18-21.

[70] Knight PG, Glister C. TGF-beta superfamily members and ovarian follicle development. Reproduction 2006; 132: 191-206.

[71] Gong SP, Lee ST, Lee EJ, Kim DY, Lee G, Chi SG, Ryu BK, Lee CH, Yum KE, Lee HJ, Han JY, Tilly JL, Lim JM. Embryonic stem cell-like cells established by culture of adult ovarian cells in mice. Fertil Steril 2010; 93: 2594-601, 2601.

[72] Johnson J, Canning J, Kaneko T, Pru JK, Tilly JL. Germline stem cells and follicular renewal in the postnatal mammalian ovary. Nature 2004; 428: 145-150.

[73] Niikura Y, Niikura T, Tilly JL. Aged mouse ovaries possess rare premeiotic germ cells that can generate oocytes following transplantation into a young host environment. Aging (Albany NY) 2009; 1: 971-978.

[74] Skaznik-Wikiel M, Tilly JC, Lee HJ, Niikura Y, Kaneko-Tarui T, Johnson J, Tilly JL. Serious doubts over "Eggs forever?". Differentiation 2007; 75: 93-99.

[75] Tilly JL, Telfer EE. Purification of germline stem cells from adult mammalian ovaries: a step closer towards control of the female biological clock? Mol Hum Reprod 2009; 15: 393-398.

[76] Tilly JL, Niikura Y, Rueda BR. The current status of evidence for and against postnatal oogenesis in mammals: a case of ovarian optimism versus pessimism? Biol Reprod 2009; 80: 2-12.

[77] Tilly JL, Rueda BR. Minireview: stem cell contribution to ovarian development, function, and disease. Endocrinology 2008; 149: 4307-4311.

[78] White YA, Woods DC, Takai Y, Ishihara O, Seki H, Tilly JL. Oocyte formation by mitotically active germ cells purified from ovaries of reproductive-age women. Nat Med 2012; 18: 413-421.

[79] Woods DC, Tilly JL. The next (re)generation of ovarian biology and fertility in women: is current science tomorrow's practice? Fertil Steril 2012; 98: 3-10.

[80] Visser JA, de Jong FH, Laven JS, Themmen AP. Anti-Mullerian hormone: a new marker for ovarian function. Reproduction 2006; 131: 1-9.

[81] Hillier SG. Gonadotropic control of ovarian follicular growth and development. Mol Cell Endocrinol 2001; 179: 39-46.

[82] Yeh J, Kim B, Peresie J, Liang YJ, Arroyo A. Serum and ovarian Mullerian inhibiting substance, and their decline in reproductive aging. Fertil Steril 2007; 87: 1227-1230.

[83] Mihm M, Gangooly S, Muttukrishna S. The normal menstrual cycle in women. Anim Reprod Sci 2011; 124: 229-236.

[84] Lutchman SK, Muttukrishna S, Stein RC, McGarrigle HH, Patel A, Parikh B, Groome NP, Davies MC, Chatterjee R. Predictors of ovarian reserve in young women with breast cancer. Br J Cancer 2007; 96: 1808-1816.

[85] Lee JR, Kim SH, Kim SM, Jee BC, Ku SY, Suh CS, Choi YM, Kim JG, Moon SY. Follicular fluid anti-Mullerian hormone and inhibin B concentrations: comparison between gonadotropin-releasing hormone (GnRH) agonist and GnRH antagonist cycles. Fertil Steril 2008; 89: 860-867.

[86] Shin SY, Lee JR, Noh GW, Kim HJ, Kang WJ, Kim SH, Chung JK. Analysis of serum levels of anti-Mullerian hormone, inhibin B, insulin-like growth factor-I, insulin-like growth factor binding protein-3, and follicle-stimulating hormone with respect to age and menopausal status. J Korean Med Sci 2008; 23: 104-110.

[87] Massin N, Meduri G, Bachelot A, Misrahi M, Kuttenn F, Touraine P. Evaluation of different markers of the ovarian reserve in patients presenting with premature ovarian failure. Mol Cell Endocrinol 2008; 282: 95-100.

[88] Tsepelidis S, Devreker F, Demeestere I, Flahaut A, Gervy C, Englert Y. Stable serum levels of anti-Mullerian hormone during the menstrual cycle: a prospective study in normo-ovulatory women. Hum Reprod 2007; 22: 1837-1840.

[89] Gnoth C, Schuring AN, Friol K, Tigges J, Mallmann P, Godehardt E. Relevance of anti-Mullerian hormone measurement in a routine IVF program. Hum Reprod 2008; 23: 1359-1365.

[90] Kwee J, Schats R, McDonnell J, Themmen A, de JF, Lambalk C. Evaluation of anti-Mullerian hormone as a test for the prediction of ovarian reserve. Fertil Steril 2008; 90: 737-743.

[91] La Marca A., Volpe A. Anti-Mullerian hormone (AMH) in female reproduction: is measurement of circulating AMH a useful tool? Clin Endocrinol (Oxf) 2006; 64: 603-610.

[92] La Marca A., Giulini S, Tirelli A, Bertucci E, Marsella T, Xella S, Volpe A. Anti-Mullerian hormone measurement on any day of the menstrual cycle strongly predicts ovarian response in assisted reproductive technology. Hum Reprod 2007; 22: 766-771.

[93] Visser JA, Themmen AP. Anti-Mullerian hormone and folliculogenesis. Mol Cell Endocrinol 2005; 234: 81-86.

[94] Orisaka M, Tajima K, Tsang BK, Kotsuji F. Oocyte-granulosa-theca cell interactions during preantral follicular development. J Ovarian Res 2009; 2: 9.

[95] Campbell BK. The endocrine and local control of ovarian follicle development in the ewe. In, 6 (1) ed. 2009: 159-171.

[96] Nilsson E, Rogers N, Skinner MK. Actions of anti-Mullerian hormone on the ovarian transcriptome to inhibit primordial to primary follicle transition. Reproduction 2007; 134: 209-221.

[97] Durlinger AL, Gruijters MJ, Kramer P, Karels B, Ingraham HA, Nachtigal MW, Uilenbroek JT, Grootegoed JA, Themmen AP. Anti-Mullerian hormone inhibits initiation of primordial follicle growth in the mouse ovary. Endocrinology 2002; 143: 1076-1084.

[98] Salmon NA, Handyside AH, Joyce IM. Oocyte regulation of anti-Mullerian hormone expression in granulosa cells during ovarian follicle development in mice. Dev Biol 2004; 266: 201-208.

[99] Thomas FH, Telfer EE, Fraser HM. Expression of anti-Mullerian hormone protein during early follicular development in the primate ovary in vivo is influenced by suppression of gonadotropin secretion and inhibition of vascular endothelial growth factor. Endocrinology 2007; 148: 2273-2281.

[100] Durlinger AL, Gruijters MJ, Kramer P, Karels B, Kumar TR, Matzuk MM, Rose UM, de Jong FH, Uilenbroek JT, Grootegoed JA, Themmen AP. Anti-Mullerian hormone attenuates the effects of FSH on follicle development in the mouse ovary. Endocrinology 2001; 142: 4891-4899.

[101] Durlinger AL, Kramer P, Karels B, de Jong FH, Uilenbroek JT, Grootegoed JA, Themmen AP. Control of primordial follicle recruitment by anti-Mullerian hormone in the mouse ovary. Endocrinology 1999; 140: 5789-5796.

[102] Vitt UA, Hayashi M, Klein C, Hsueh AJ. Growth differentiation factor-9 stimulates proliferation but suppresses the follicle-stimulating hormone-induced differentiation of cultured granulosa cells from small antral and preovulatory rat follicles. Biol Reprod 2000; 62: 370-377.

[103] McGrath SA, Esquela AF, Lee SJ. Oocyte-specific expression of growth/differentiation factor-9. Mol Endocrinol 1995; 9: 131-136.

[104] Vitt UA, Mazerbourg S, Klein C, Hsueh AJ. Bone morphogenetic protein receptor type II is a receptor for growth differentiation factor-9. Biol Reprod 2002; 67: 473-480.

[105] Silva JR, van den HR, van Tol HT, Roelen BA, Figueiredo JR. Expression of growth differentiation factor 9 (GDF9), bone morphogenetic protein 15 (BMP15), and BMP receptors in the ovaries of goats. Mol Reprod Dev 2005; 70: 11-19.

[106] Pangas SA, Matzuk MM. Genetic models for transforming growth factor beta superfamily signaling in ovarian follicle development. Mol Cell Endocrinol 2004; 225: 83-91.

[107] Orisaka M, Orisaka S, Jiang JY, Craig J, Wang Y, Kotsuji F, Tsang BK. Growth differentiation factor 9 is antiapoptotic during follicular development from preantral to early antral stage. Mol Endocrinol 2006; 20: 2456-2468.

[108] Pangas SA, Matzuk MM. The art and artifact of GDF9 activity: cumulus expansion and the cumulus expansion-enabling factor. Biol Reprod 2005; 73: 582-585.

[109] Gittens JE, Barr KJ, Vanderhyden BC, Kidder GM. Interplay between paracrine signaling and gap junctional communication in ovarian follicles. J Cell Sci 2005; 118: 113-122.

[110] Liao WX, Moore RK, Otsuka F, Shimasaki S. Effect of intracellular interactions on the processing and secretion of bone morphogenetic protein-15 (BMP-15) and growth and differentiation factor-9. Implication of the aberrant ovarian phenotype of BMP-15 mutant sheep. J Biol Chem 2003; 278: 3713-3719.

[111] Mazaud GS, Guigon CJ, Coudouel N, Magre S. Consequences of fetal irradiation on follicle histogenesis and early follicle development in rat ovaries. Biol Reprod 2006; 75: 749-759.

[112] Otsuka F, Yao Z, Lee T, Yamamoto S, Erickson GF, Shimasaki S. Bone morphogenetic protein-15. Identification of target cells and biological functions. J Biol Chem 2000; 275: 39523-39528.

[113] Moore RK, Otsuka F, Shimasaki S. Molecular basis of bone morphogenetic protein-15 signaling in granulosa cells. J Biol Chem 2003; 278: 304-310.

[114] Juengel JL, Bodensteiner KJ, Heath DA, Hudson NL, Moeller CL, Smith P, Galloway SM, Davis GH, Sawyer HR, McNatty KP. Physiology of GDF9 and BMP15 signalling molecules. Anim Reprod Sci 2004; 82-83: 447-460.

[115] Hanrahan JP, Gregan SM, Mulsant P, Mullen M, Davis GH, Powell R, Galloway SM. Mutations in the genes for oocyte-derived growth factors GDF9 and BMP15 are associated with both increased ovulation rate and sterility in Cambridge and Belclare sheep (Ovis aries). Biol Reprod 2004; 70: 900-909.

[116] Yan C, Wang P, DeMayo J, DeMayo FJ, Elvin JA, Carino C, Prasad SV, Skinner SS, Dunbar BS, Dube JL, Celeste AJ, Matzuk MM. Synergistic roles of bone morphogenetic protein 15 and growth differentiation factor 9 in ovarian function. Mol Endocrinol 2001; 15: 854-866.

[117] Galloway SM, Gregan SM, Wilson T, McNatty KP, Juengel JL, Ritvos O, Davis GH. Bmp15 mutations and ovarian function. Mol Cell Endocrinol 2002; 191: 15-18.

[118] Davis GH, McEwan JC, Fennessy PF, Dodds KG, McNatty KP, WS O. Infertility due to bilateral ovarian hypoplasia in sheep homozygous (FecXI FecXI) for the Inverdale prolificacy gene located on the X chromosome. Biol Reprod 1992; 46: 636-640.

[119] Nilsson EE, Skinner MK. Growth and differentiation factor-9 stimulates progression of early primary but not primordial rat ovarian follicle development. Biol Reprod 2002; 67: 1018-1024.

[120] Otsuka F, Yamamoto S, Erickson GF, Shimasaki S. Bone morphogenetic protein-15 inhibits follicle-stimulating hormone (FSH) action by suppressing FSH receptor expression. J Biol Chem 2001; 276: 11387-11392.

[121] McNatty KP, Heath DA, Lundy T, Fidler AE, Quirke L, O'Connell A, Smith P, Groome N, Tisdall DJ. Control of early ovarian follicular development. J Reprod Fertil Suppl 1999; 54: 3-16.

[122] Webb R, Campbell BK, Garverick HA, Gong JG, Gutierrez CG, Armstrong DG. Molecular mechanisms regulating follicular recruitment and selection. J Reprod Fertil Suppl 1999; 54: 33-48.

[123] Richards JS. Hormonal control of gene expression in the ovary. Endocr Rev 1994; 15: 725-751.

[124] Picton HM, Danfour MA, Harris SE, Chambers EL, Huntriss J. Growth and maturation of oocytes in vitro. Reprod Suppl 2003; 61: 445-462.

[125] Su YQ, Wu X, O'Brien MJ, Pendola FL, Denegre JN, Matzuk MM, Eppig JJ. Synergistic roles of BMP15 and GDF9 in the development and function of the oocyte-cumulus cell complex in mice: genetic evidence for an oocyte-granulosa cell regulatory loop. Dev Biol 2004; 276: 64-73.

[126] Baird DT, Campbell BK, McNeilly AS. Ovine follicular fluid suppresses the ovarian secretion of androgens, oestradiol and inhibin. J Endocrinol 1990; 127: 23-32.

[127] Campbell BK, Dobson H, Baird DT, Scaramuzzi RJ. Examination of the relative role of FSH and LH in the mechanism of ovulatory follicle selection in sheep. J Reprod Fertil 1999; 117: 355-367.

[128] Campbell BK, Scaramuzzi RJ. The effect of ovarian arterial infusion of human recombinant inhibin and bovine follicular fluid on ovarian hormone secretion by ewes with an autotransplanted ovary. J Endocrinol 1996; 149: 531-540.

[129] Ma X, Dong Y, Matzuk MM, Kumar TR. Targeted disruption of luteinizing hormone beta-subunit leads to hypogonadism, defects in gonadal steroidogenesis, and infertility. Proc Natl Acad Sci U S A 2004; 101: 17294-17299.

[130] Hillier SG. Current concepts of the roles of follicle stimulating hormone and luteinizing hormone in folliculogenesis. Hum Reprod 1994; 9: 188-191.

[131] Peng C, Mukai ST. Activins and their receptors in female reproduction. Biochem Cell Biol 2000; 78: 261-279.

[132] Dyce PW, Norris RP, Lampe PD, Kidder GM. Phosphorylation of Serine Residues in the C-terminal Cytoplasmic Tail of Connexin43 Regulates Proliferation of Ovarian Granulosa Cells. J Membr Biol 2012; 245: 291-301.

[133] Gittens JE, Kidder GM. Differential contributions of connexin37 and connexin43 to oogenesis revealed in chimeric reaggregated mouse ovaries. J Cell Sci 2005; 118: 5071-5078.

[134] Kidder GM, Vanderhyden BC. Bidirectional communication between oocytes and follicle cells: ensuring oocyte developmental competence. Can J Physiol Pharmacol 2010; 88: 399-413.

[135] Li TY, Colley D, Barr KJ, Yee SP, Kidder GM. Rescue of oogenesis in Cx37-null mutant mice by oocyte-specific replacement with Cx43. J Cell Sci 2007; 120: 4117-4125.

[136] Tong D, Gittens JE, Kidder GM, Bai D. Patch-clamp study reveals that the importance of connexin43-mediated gap junctional communication for ovarian folliculogenesis is strain specific in the mouse. Am J Physiol Cell Physiol 2006; 290: C290-C297.

[137] Veitch GI, Gittens JE, Shao Q, Laird DW, Kidder GM. Selective assembly of connexin37 into heterocellular gap junctions at the oocyte/granulosa cell interface. J Cell Sci 2004; 117: 2699-2707.

[138] Wang HX, Tong D, El-Gehani F, Tekpetey FR, Kidder GM. Connexin expression and gap junctional coupling in human cumulus cells: contribution to embryo quality. J Cell Mol Med 2009; 13: 972-984.

[139] Pangas SA, Jorgez CJ, Tran M, Agno J, Li X, Brown CW, Kumar TR, Matzuk MM. Intraovarian activins are required for female fertility. Mol Endocrinol 2007; 21: 2458-2471.

[140] Lovell TM, Gladwell RT, Groome NP, Knight PG. Ovarian follicle development in the laying hen is accompanied by divergent changes in inhibin A, inhibin B, activin A and follistatin production in granulosa and theca layers. J Endocrinol 2003; 177: 45-55.

[141] Ge W. Roles of the activin regulatory system in fish reproduction. Can J Physiol Pharmacol 2000; 78: 1077-1085.

[142] Young JM, Henderson S, Souza C, Ludlow H, Groome N, McNeilly AS. Activin B is produced early in antral follicular development and suppresses thecal androgen production. Reproduction 2012; 143: 637-650.

[143] Young JM, McNeilly AS. Inhibin removes the inhibitory effects of activin on steroid enzyme expression and androgen production by normal ovarian thecal cells. J Mol Endocrinol 2012; 48: 49-60.

[144] Andreone L, Velasquez EV, Abramovich D, Ambao V, Loreti N, Croxatto HB, Parborell F, Tesone M, Campo S. Regulation of inhibin/activin expression in rat early antral follicles. Mol Cell Endocrinol 2009; 309: 48-54.

[145] Shidaifat F. Effect of activin-a on goat granulosa cell steroidogenesis. Theriogenology 2001; 56: 591-599.

[146] Silva JR, Tharasanit T, Taverne MA, van der Weijden GC, Santos RR, Figueiredo JR, van den HR. The activin-follistatin system and in vitro early follicle development in goats. J Endocrinol 2006; 189: 113-125.

[147] di Clemente N, Josso N, Gouedard L, Belville C. Components of the anti-Mullerian hormone signaling pathway in gonads. Mol Cell Endocrinol 2003; 211: 9-14.

[148] Rey R, Lukas-Croisier C, Lasala C, Bedecarras P. AMH/MIS: what we know already about the gene, the protein and its regulation. Mol Cell Endocrinol 2003; 211: 21-31.

[149] Uzumcu M, Kuhn PE, Marano JE, Armenti AE, Passantino L. Early postnatal methoxychlor exposure inhibits folliculogenesis and stimulates anti-Mullerian hormone production in the rat ovary. J Endocrinol 2006; 191: 549-558.

[150] Kevenaar ME, Meerasahib MF, Kramer P, van de Lang-Born BM, de Jong FH, Groome NP, Themmen AP, Visser JA. Serum anti-mullerian hormone levels reflect the size of the primordial follicle pool in mice. Endocrinology 2006; 147: 3228-3234.

[151] Fortune JE, Yang MY, Muruvi W. In vitro and in vivo regulation of follicular formation and activation in cattle. Reprod Fertil Dev 2011; 23: 15-22.

[152] Thomas FH, Vanderhyden BC. Oocyte-granulosa cell interactions during mouse follicular development: regulation of kit ligand expression and its role in oocyte growth. Reprod Biol Endocrinol 2006; 4: 19.

[153] Hunter MG, Paradis F. Intra-follicular regulatory mechanisms in the porcine ovary. Soc Reprod Fertil Suppl 2009; 66: 149-164.

[154] Shimasaki S, Moore RK, Erickson GF, Otsuka F. The role of bone morphogenetic proteins in ovarian function. Reprod Suppl 2003; 61: 323-337.

[155] Juengel JL, Hudson NL, Heath DA, Smith P, Reader KL, Lawrence SB, O'Connell AR, Laitinen MP, Cranfield M, Groome NP, Ritvos O, McNatty KP. Growth differentiation factor 9 and bone morphogenetic protein 15 are essential for ovarian follicular development in sheep. Biol Reprod 2002; 67: 1777-1789.

[156] Juengel JL, Hudson NL, Berg M, Hamel K, Smith P, Lawrence SB, Whiting L, McNatty KP. Effects of active immunization against growth differentiation factor 9 and/or bone morphogenetic protein 15 on ovarian function in cattle. Reproduction 2009; 138: 107-114.

[157] McIntosh CJ, Lawrence S, Smith P, Juengel JL, McNatty KP. Active immunization against the proregions of GDF9 or BMP15 alters ovulation rate and litter size in mice. Reproduction 2012; 143: 195-201.

[158] McNatty KP, Juengel JL, Reader KL, Lun S, Myllymaa S, Lawrence SB, Western A, Meerasahib MF, Mottershead DG, Groome NP, Ritvos O, Laitinen MP. Bone morphogenetic protein 15 and growth differentiation factor 9 co-operate to regulate granulosa cell function in ruminants. Reproduction 2005; 129: 481-487.

[159] McNatty KP, Juengel JL, Reader KL, Lun S, Myllymaa S, Lawrence SB, Western A, Meerasahib MF, Mottershead DG, Groome NP, Ritvos O, Laitinen MP. Bone morphogenetic protein 15 and growth differentiation factor 9 co-operate to regulate granulosa cell function. Reproduction 2005; 129: 473-480.

[160] Young JM, Juengel JL, Dodds KG, Laird M, Dearden PK, McNeilly AS, McNatty KP, Wilson T. The activin receptor-like kinase 6 Booroola mutation enhances suppressive effects of bone morphogenetic protein 2 (BMP2), BMP4, BMP6 and growth and differentiation factor-9 on FSH release from ovine primary pituitary cell cultures. J Endocrinol 2008; 196: 251-261.

[161] Juengel JL, Reader KL, Bibby AH, Lun S, Ross I, Haydon LJ, McNatty KP. The role of bone morphogenetic proteins 2, 4, 6 and 7 during ovarian follicular development in sheep: contrast to rat. Reproduction 2006; 131: 501-513.

[162] Souza CJ, Campbell BK, McNeilly AS, Baird DT. Effect of bone morphogenetic protein 2 (BMP2) on oestradiol and inhibin A production by sheep granulosa cells, and localization of BMP receptors in the ovary by immunohistochemistry. Reproduction 2002; 123: 363-369.

[163] Brankin V, Quinn RL, Webb R, Hunter MG. BMP-2 and -6 modulate porcine theca cell function alone and co-cultured with granulosa cells. Domest Anim Endocrinol 2005; 29: 593-604.

[164] Kashimada K, Pelosi E, Chen H, Schlessinger D, Wilhelm D, Koopman P. FOXL2 and BMP2 act cooperatively to regulate follistatin gene expression during ovarian development. Endocrinology 2011; 152: 272-280.

[165] Kayani AR, Glister C, Knight PG. Evidence for an inhibitory role of bone morphogenetic protein(s) in the follicular-luteal transition in cattle. Reproduction 2009; 137: 67-78.

[166] Shi J, Yoshino O, Osuga Y, Koga K, Hirota Y, Nose E, Nishii O, Yano T, Taketani Y. Bone morphogenetic protein-2 (BMP-2) increases gene expression of FSH receptor and aromatase and decreases gene expression of LH receptor and StAR in human granulosa cells. Am J Reprod Immunol 2011; 65: 421-427.

[167] Haugen MJ, Johnson AL. Bone morphogenetic protein 2 inhibits FSH responsiveness in hen granulosa cells. Reproduction 2010; 140: 551-558.

[168] Pierre A, Pisselet C, Dupont J, Mandon-Pepin B, Monniaux D, Monget P, Fabre S. Molecular basis of bone morphogenetic protein-4 inhibitory action on progesterone secretion by ovine granulosa cells. J Mol Endocrinol 2004; 33: 805-817.

[169] Yamashita H, Murayama C, Takasugi R, Miyamoto A, Shimizu T. BMP-4 suppresses progesterone production by inhibiting histone H3 acetylation of StAR in bovine granulosa cells in vitro. Mol Cell Biochem 2011; 348: 183-190.

[170] Abir R, Ben-Haroush A, Melamed N, Felz C, Krissi H, Fisch B. Expression of bone morphogenetic proteins 4 and 7 and their receptors IA, IB, and II in human ovaries from fetuses and adults. Fertil Steril 2008; 89: 1430-1440.

[171] Tanwar PS, O'Shea T, McFarlane JR. In vivo evidence of role of bone morphogenetic protein-4 in the mouse ovary. Anim Reprod Sci 2008; 106: 232-240.

[172] Li CW, Zhou R, Ge W. Differential regulation of gonadotropin receptors by bone morphogenetic proteins in the zebrafish ovary. Gen Comp Endocrinol 2012; 176: 420-425.

[173] Pierre A, Pisselet C, Dupont J, Bontoux M, Monget P. Bone morphogenetic protein 5 expression in the rat ovary: biological effects on granulosa cell proliferation and steroidogenesis. Biol Reprod 2005; 73: 1102-1108.

[174] Otsuka F, Moore RK, Shimasaki S. Biological function and cellular mechanism of bone morphogenetic protein-6 in the ovary. J Biol Chem 2001; 276: 32889-32895.

[175] Li CW, Ge W. Spatiotemporal expression of bone morphogenetic protein family ligands and receptors in the zebrafish ovary: a potential paracrine-signaling mechanism for oocyte-follicle cell communication. Biol Reprod 2011; 85: 977-986.

[176] Sugiura K, Su YQ, Eppig JJ. Does bone morphogenetic protein 6 (BMP6) affect female fertility in the mouse? Biol Reprod 2010; 83: 997-1004.

[177] Ocon-Grove OM, Poole DH, Johnson AL. Bone morphogenetic protein 6 promotes FSH receptor and anti-Mullerian hormone mRNA expression in granulosa cells from hen prehierarchal follicles. Reproduction 2012; 143: 825-833.

[178] Shi J, Yoshino O, Osuga Y, Akiyama I, Harada M, Koga K, Fujimoto A, Yano T, Taketani Y. Growth differentiation factor 3 is induced by bone morphogenetic protein 6 (BMP-6) and BMP-7 and increases luteinizing hormone receptor messenger RNA expression in human granulosa cells. Fertil Steril 2012; 97: 979-983.

[179] Lee WS, Otsuka F, Moore RK, Shimasaki S. Effect of bone morphogenetic protein-7 on folliculogenesis and ovulation in the rat. Biol Reprod 2001; 65: 994-999.

[180] Glister C, Satchell L, Knight PG. Changes in expression of bone morphogenetic proteins (BMPs), their receptors and inhibin co-receptor betaglycan during bovine antral follicle development: inhibin can antagonize the suppressive effect of BMPs on thecal androgen production. Reproduction 2010; 140: 699-712.

[181] Huang HJ, Wu JC, Su P, Zhirnov O, Miller WL. A novel role for bone morphogenetic proteins in the synthesis of follicle-stimulating hormone. Endocrinology 2001; 142: 2275-2283.

[182] Grynberg M, Pierre A, Rey R, Leclerc A, Arouche N, Hesters L, Catteau-Jonard S, Frydman R, Picard JY, Fanchin R, Veitia R, di CN, Taieb J. Differential regulation of ovarian anti-mullerian hormone (AMH) by estradiol through alpha- and beta-estrogen receptors. J Clin Endocrinol Metab 2012; 97: E1649-E1657.

[183] Quirk SM, Cowan RG, Harman RM, Hu CL, Porter DA. Ovarian follicular growth and atresia: the relationship between cell proliferation and survival. J Anim Sci 2004; 82 E-Suppl: E40-E52.

[184] Richards JS, Russell DL, Ochsner S, Hsieh M, Doyle KH, Falender AE, Lo YK, Sharma SC. Novel signaling pathways that control ovarian follicular development, ovulation, and luteinization. Recent Prog Horm Res 2002; 57: 195-220.

[185] Findlay JK, Britt K, Kerr JB, O'Donnell L, Jones ME, Drummond AE, Simpson ER. The road to ovulation: the role of oestrogens. Reprod Fertil Dev 2001; 13: 543-547.

[186] Bahr JM, Johnson AL. Regulation of the follicular hierarchy and ovulation. J Exp Zool 1984; 232: 495-500.

[187] Etches RJ, Petitte JN. Reptilian and avian follicular hierarchies: models for the study of ovarian development. J Exp Zool Suppl 1990; 4: 112-122.

[188] Yu J, Thomson TC, Johnson J. Cross talk between estradiol and mTOR kinase in the regulation of ovarian granulosa proliferation. Reprod Sci 2012; 19: 143-151.

[189] Nakamura E, Otsuka F, Inagaki K, Miyoshi T, Matsumoto Y, Ogura K, Tsukamoto N, Takeda M, Makino H. Mutual regulation of growth hormone and bone morphogenetic protein system in steroidogenesis by rat granulosa cells. Endocrinology 2012; 153: 469-480.

[190] Cummins SB, Lonergan P, Evans AC, Butler ST. Genetic merit for fertility traits in Holstein cows: II. Ovarian follicular and corpus luteum dynamics, reproductive hormones, and estrus behavior. J Dairy Sci 2012; 95: 3698-3710.

[191] Forde N, Beltman ME, Lonergan P, Diskin M, Roche JF, Crowe MA. Oestrous cycles in Bos taurus cattle. Anim Reprod Sci 2011; 124: 163-169.

[192] Fortune JE. Ovarian follicular growth and development in mammals. Biol Reprod 1994; 50: 225-232.

[193] Schwarz T, Kopyra M, Nowicki J. Physiological mechanisms of ovarian follicular growth in pigs--a review. Acta Vet Hung 2008; 56: 369-378.

[194] Wu X, Chen L, Brown CA, Yan C, Matzuk MM. Interrelationship of growth differentiation factor 9 and inhibin in early folliculogenesis and ovarian tumorigenesis in mice. Mol Endocrinol 2004; 18: 1509-1519.

[195] Nath A, Sharma V, Dubey PK, M D P, Gade NE, Saikumar G, Sharma GT. Impact of gonadotropin supplementation on the expression of germ cell marker genes (MATER, ZAR1, GDF9, and BMP15) during in vitro maturation of buffalo (Bubalus bubalis) oocyte. In Vitro Cell Dev Biol Anim 2012.

[196] Wang XL, El-Gayar M, Knight PG, Holtz W. The long-term effect of active immunization against inhibin in goats. Theriogenology 2009; 71: 318-322.

[197] Holtz W, Wang X, El-Gayar M, Knight PG. The effect of exogenous gonadotropins on ovarian function in goats actively immunized against inhibin. Theriogenology 2012; 77: 253-259.

[198] Merkwitz C, Lochhead P, Tsikolia N, Koch D, Sygnecka K, Sakurai M, Spanel-Borowski K, Ricken AM. Expression of KIT in the ovary, and the role of somatic precursor cells. Prog Histochem Cytochem 2011; 46: 131-184.

[199] Hutt KJ, McLaughlin EA, Holland MK. KIT/KIT ligand in mammalian oogenesis and folliculogenesis: roles in rabbit and murine ovarian follicle activation and oocyte growth. Biol Reprod 2006; 75: 421-433.

[200] Moniruzzaman M, Miyano T. KIT-KIT ligand in the growth of porcine oocytes in primordial follicles. J Reprod Dev 2007; 53: 1273-1281.

[201] Moniruzzaman M, Sakamaki K, Akazawa Y, Miyano T. Oocyte growth and follicular development in KIT-deficient Fas-knockout mice. Reproduction 2007; 133: 117-125.

[202] Miyoshi T, Otsuka F, Nakamura E, Inagaki K, Ogura-Ochi K, Tsukamoto N, Takeda M, Makino H. Regulatory role of kit ligand-c-kit interaction and oocyte factors in steroidogenesis by rat granulosa cells. Mol Cell Endocrinol 2012; 358: 18-26.

[203] Parrott JA, Skinner MK. Kit-ligand/stem cell factor induces primordial follicle development and initiates folliculogenesis. Endocrinology 1999; 140: 4262-4271.

[204] Parrott JA, Skinner MK. Direct actions of kit-ligand on theca cell growth and differentiation during follicle development. Endocrinology 1997; 138: 3819-3827.

[205] Jagarlamudi K, Rajkovic A. Oogenesis: transcriptional regulators and mouse models. Mol Cell Endocrinol 2012; 356: 31-39.

[206] Bouilly J, Bachelot A, Broutin I, Touraine P, Binart N. Novel NOBOX loss-of-function mutations account for 6.2% of cases in a large primary ovarian insufficiency cohort. Hum Mutat 2011; 32: 1108-1113.

[207] Lechowska A, Bilinski S, Choi Y, Shin Y, Kloc M, Rajkovic A. Premature ovarian failure in nobox-deficient mice is caused by defects in somatic cell

invasion and germ cell cyst breakdown. J Assist Reprod Genet 2011; 28: 583-589.

[208] Tripurani SK, Lee KB, Wang L, Wee G, Smith GW, Lee YS, Latham KE, Yao J. A novel functional role for the oocyte-specific transcription factor newborn ovary homeobox (NOBOX) during early embryonic development in cattle. Endocrinology 2011; 152: 1013-1023.

[209] Novak B, Sible J, Tyson J. Checkpoints in the Cell Cycle. In. Macmillan Publishers Ltd, Nature Publishing Group; 2002: 1-8.

[210] Thyberg J, Moskalewski S. Role of microtubules in the organization of the Golgi complex. Exp Cell Res 1999; 246: 263-279.

[211] Thyberg J, Moskalewski S. Microtubules and the organization of the Golgi complex. Exp Cell Res 1985; 159: 1-16.

[212] Craig ZR, Hannon PR, Wang W, Ziv-Gal A, Flaws JA. Di-n-butyl Phthalate Disrupts the Expression of Genes Involved in Cell Cycle and Apoptotic Pathways in Mouse Ovarian Antral Follicles. Biol Reprod 2012.

[213] Muller WF, Hobson W, Fuller GB, Knauf W, Coulston F, Korte F. Endocrine effects of chlorinated hydrocarbons in rhesus monkeys. Ecotoxicol Environ Saf 1978; 2: 161-172.

[214] Pocar P, Brevini TA, Antonini S, Gandolfi F. Cellular and molecular mechanisms mediating the effect of polychlorinated biphenyls on oocyte in vitro maturation. Reprod Toxicol 2006; 22: 242-249.

[215] Davis BJ, Maronpot RR, Heindel JJ. Di-(2-ethylhexyl) phthalate suppresses estradiol and ovulation in cycling rats. Toxicol Appl Pharmacol 1994; 128: 216-223.

[216] Wu KL, Berger T. Reduction in rat oocyte fertilizability mediated by S-(1, 2-dichlorovinyl)-L-cysteine: a trichloroethylene metabolite produced by the glutathione conjugation pathway. Bull Environ Contam Toxicol 2008; 81: 490-493.

[217] Igawa Y, Keating AF, Rajapaksa KS, Sipes IG, Hoyer PB. Evaluation of ovotoxicity induced by 7, 12-dimethylbenz[a]anthracene and its 3,4-diol metabolite utilizing a rat in vitro ovarian culture system. Toxicol Appl Pharmacol 2009; 234: 361-369.

[218] Mattison DR, White NB, Nightingale MR. The effect of benzo(a)pyrene on fertility, primordial oocyte number, and ovarian response to pregnant mare's serum gonadotropin. Pediatr Pharmacol (New York) 1980; 1: 143-151.

[219] Mattison DR, Nightingale MS. Oocyte destruction by polycyclic aromatic hydrocarbons is not linked to the inducibility of ovarian aryl hydrocarbon (benzo(a)pyrene) hydroxylase activity in (DBA/2N X C57BL/6N) F1 X DBA/2N backcross mice. Pediatr Pharmacol (New York) 1982; 2: 11-21.

[220] Devine PJ, Sipes IG, Hoyer PB. Effect of 4-vinylcyclohexene diepoxide dosing in rats on GSH levels in liver and ovaries. Toxicol Sci 2001; 62: 315-320.

[221] Takai Y, Canning J, Perez GI, Pru JK, Schlezinger JJ, Sherr DH, Kolesnick RN, Yuan J, Flavell RA, Korsmeyer SJ, Tilly JL. Bax, caspase-2, and caspase-3 are required for ovarian follicle loss caused by 4-vinylcyclohexene diepoxide exposure of female mice in vivo. Endocrinology 2003; 144: 69-74.

[222] Boone DL, Carnegie JA, Rippstein PU, Tsang BK. Induction of apoptosis in equine chorionic gonadotropin (eCG)-primed rats ovaries by anti-eCG antibody. Biology of Reproduction 1997; 57: 420-427.

[223] Boone DL, Tsang BK. Identification and localization of deoxyribonuclease I in the rat ovary. Biology of Reproduction 1997; 57: 813-821.

[224] Boone DL, Tsang BK. Caspase-3 in the rat ovary: Localization and possible role in follicular atresia and luteal regression. Biology of Reproduction 1998; 58: 1533-1539.

[225] Dharma SJ, Kelkar RL, Nandedkar TD. Fas and Fas ligand protein and mRNA in normal and atretic mouse ovarian follicles. Reproduction 2003; 126: 783-789.

[226] Flaws JA, Hirshfield AN, Hewitt JA, Babus JK, Furth PA. Effect of Bcl-2 on primordial follicle endowment in the mouse ovary. Biology of Reproduction 2001; 64: 1153-1159.

[227] Kim J-M, Boone DL, Auyeung A, Tsang BK. Granulosa cell apoptosis induced at the penultimate stage of follicular development is associated with increased levels of Fas and Fas ligand in the rat ovary. Biology of Reproduction 1998; 58: 1170-1176.

[228] Tilly JL. Molecular and genetic basis of normal and toxicant-induced apoptosis in female germ cells. Toxicol Lett 1998; 102-103: 497-501.

[229] Matikainen TM, Moriyama T, Morita Y, Perez GI, Korsmeyer SJ, Sherr DH, Tilly JL. Ligand activation of the aromatic hydrocarbon receptor transcription

factor drives Bax-dependent apoptosis in developing fetal ovarian germ cells. Endocrinology 2002; 143: 615-620.

[230] Mattison DR, Singh H, Takizawa K, Thomford PJ. Ovarian toxicity of benzo(a)pyrene and metabolites in mice. Reprod Toxicol 1989; 3: 115-125.

[231] Shiromizu K, Mattison DR. Murine oocyte destruction following intraovarian treatment with 3-methylcholanthrene or 7,12-dimethylbenz(a)anthracene: protection by alpha-naphthoflavone. Teratog Carcinog Mutagen 1985; 5: 463-472.

[232] Chiong M, Wang ZV, Pedrozo Z, Cao DJ, Troncoso R, Ibacache M, Criollo A, Nemchenko A, Hill JA, Lavandero S. Cardiomyocyte death: mechanisms and translational implications. Cell Death Dis 2011; 2: e244.

[233] Hussein MR. Apoptosis in the ovary: molecular mechanisms. Hum Reprod Update 2005; 11: 162-177.

[234] Burlacu A. Regulation of apoptosis by Bcl-2 family proteins. J Cell Mol Med 2003; 7: 249-257.

[235] Gross A, McDonnell JM, Korsmeyer SJ. BCL-2 family members and the mitochondria in apoptosis. Genes Dev 1999; 13: 1899-1911.

[236] Blaineau SV, Aouacheria A. BCL2DB: moving 'helix-bundled' BCL-2 family members to their database. Apoptosis 2009; 14: 923-925.

[237] Gross A, McDonnell JM, Korsmeyer SJ. BCL-2 family members and the mitochondria in apoptosis. Genes Dev 1999; 13: 1899-1911.

[238] Burlacu A. Regulation of apoptosis by Bcl-2 family proteins. J Cell Mol Med 2003; 7: 249-257.

[239] Burlacu A. Regulation of apoptosis by Bcl-2 family proteins. J Cell Mol Med 2003; 7: 249-257.

[240] Blaineau SV, Aouacheria A. BCL2DB: moving 'helix-bundled' BCL-2 family members to their database. Apoptosis 2009; 14: 923-925.

[241] Gross A, McDonnell JM, Korsmeyer SJ. BCL-2 family members and the mitochondria in apoptosis. Genes Dev 1999; 13: 1899-1911.

[242] Burlacu A. Regulation of apoptosis by Bcl-2 family proteins. J Cell Mol Med 2003; 7: 249-257.

[243] Bellance N, Lestienne P, Rossignol R. Mitochondria: from bioenergetics to the metabolic regulation of carcinogenesis. Front Biosci 2009; 14: 4015-4034.

[244] Samuel T, Okada K, Hyer M, Welsh K, Zapata JM, Reed JC. cIAP1 Localizes to the nuclear compartment and modulates the cell cycle. Cancer Res 2005; 65: 210-218.

[245] Silke J, Kratina T, Chu D, Ekert PG, Day CL, Pakusch M, Huang DC, Vaux DL. Determination of cell survival by RING-mediated regulation of inhibitor of apoptosis (IAP) protein abundance. Proc Natl Acad Sci U S A 2005; 102: 16182-16187.

[246] Cheng Y, Maeda A, Goto Y, Matsuda F, Miyano T, Inoue N, Sakamaki K, Manabe N. Changes in expression and localization of X-linked inhibitor of apoptosis protein (XIAP) in follicular granulosa cells during atresia in porcine ovaries. J Reprod Dev 2008; 54: 454-459.

[247] Schimmer AD, Dalili S. Targeting the IAP family of caspase inhibitors as an emerging therapeutic strategy. Hematology Am Soc Hematol Educ Program 2005; 215-219.

[248] Deveraux QL, Reed JC. IAP family proteins--suppressors of apoptosis. Genes Dev 1999; 13: 239-252.

[249] Yang YL, Li XM. The IAP family: endogenous caspase inhibitors with multiple biological activities. Cell Res 2000; 10: 169-177.

[250] Johnson AL, Langer JS, Bridgham JT. Survivin as a cell cycle-related and antiapoptotic protein in granulosa cells. Endocrinology 2002; 143: 3405-3413.

[251] Deveraux QL, Takahashi R, Salvesen GS, Reed JC. X-linked IAP is a direct inhibitor of cell-death proteases. Nature 1997; 388: 300-304.

[252] Mazoochi T, Salehnia M, Pourbeiranvand S, Forouzandeh M, Mowla SJ, Hajizadeh E. Analysis of apoptosis and expression of genes related to apoptosis in cultures of follicles derived from vitrified and non-vitrified ovaries. Mol Hum Reprod 2009; 15: 155-164.

[253] Athanassiadou P, Grapsa D, Athanassiades P, Gonidi M, Athanassiadou AM, Tsipis A, Patsouris E. The prognostic significance of COX-2 and survivin expression in ovarian cancer. Pathol Res Pract 2008; 204: 241-249.

[254] Runnebaum IB, Bruning A. Glucocorticoids inhibit cell death in ovarian cancer and up-regulate caspase inhibitor cIAP2. Clin Cancer Res 2005; 11: 6325-6332.

[255] Das M, Djahanbakhch O, Hacihanefioglu B, Saridogan E, Ikram M, Ghali L, Raveendran M, Storey A. Granulosa cell survival and proliferation are altered in polycystic ovary syndrome. J Clin Endocrinol Metab 2008; 93: 881-887.

[256] Zimmermann KC, Bonzon C, Green DR. The machinery of programmed cell death. Pharmacol Ther 2001; 92: 57-70.

[257] Zimmermann KC, Green DR. How cells die: apoptosis pathways. J Allergy Clin Immunol 2001; 108: S99-103.

[258] Muzio M, Chinnaiyan AM, Kischkel FC, O'Rourke K, Shevchenko A, Ni J, Scaffidi C, Bretz JD, Zhang M, Gentz R, Mann M, Krammer PH, Peter ME, Dixit VM. FLICE, a novel FADD-homologous ICE/CED-3-like protease, is recruited to the CD95 (Fas/APO-1) death--inducing signaling complex. Cell 1996; 85: 817-827.

[259] Gulbins E. Regulation of death receptor signaling and apoptosis by ceramide. Pharmacol Res 2003; 47: 393-399.

[260] Green DR, Kroemer G. The pathophysiology of mitochondrial cell death. Science 2004; 305: 626-629.

[261] Wikstrom JD, Twig G, Shirihai OS. What can mitochondrial heterogeneity tell us about mitochondrial dynamics and autophagy? Int J Biochem Cell Biol 2009; 41: 1914-1927.

[262] Borman SM, Christian PJ, Sipes IG, Hoyer PB. Ovotoxicity in female Fischer rats and B6 mice induced by low-dose exposure to three polycyclic aromatic hydrocarbons: comparison through calculation of an ovotoxic index. Toxicol Appl Pharmacol 2000; 167: 191-198.

[263] Flaws JA, Doerr JK, Sipes IG, Hoyer PB. Destruction of preantral follicles in adult rats by 4-vinyl-1-cyclohexene diepoxide. Reprod Toxicol 1994; 8: 509-514.

[264] Hoyer PB, Davis JR, Bedrnicek JB, Marion SL, Christian PJ, Barton JK, Brewer MA. Ovarian neoplasm development by 7,12-dimethylbenz[a]anthracene (DMBA) in a chemically-induced rat model of ovarian failure. Gynecol Oncol 2009; 112: 610-615.

[265] Thompson KE, Bourguet SM, Christian PJ, Benedict JC, Sipes IG, Flaws JA, Hoyer PB. Differences between rats and mice in the involvement of the aryl hydrocarbon receptor in 4-vinylcyclohexene diepoxide-induced ovarian follicle loss. Toxicol Appl Pharmacol 2005; 203: 114-123.

[266] Greenfeld CR, Pepling ME, Babus JK, Furth PA, Flaws JA. BAX regulates follicular endowment in mice. Reproduction 2007; 133: 865-876.

[267] Weitzman GA, Miller MM, London SN, Mattison DR. Morphometric assessment of the murine ovarian toxicity of 7,12-dimethylbenz(a)anthracene. Reprod Toxicol 1992; 6: 137-141.

[268] Matikainen T, Perez GI, Zheng TS, Kluzak TR, Rueda BR, Flavell RA, Tilly JL. Caspase-3 gene knockout defines cell lineage specificity for programmed cell death signaling in the ovary. Endocrinology 2001; 142: 2468-2480.

[269] Jurisicova A, Taniuchi A, Li H, Shang Y, Antenos M, Detmar J, Xu J, Matikainen T, Benito HA, Nunez G, Casper RF. Maternal exposure to polycyclic aromatic hydrocarbons diminishes murine ovarian reserve via induction of Harakiri. J Clin Invest 2007; 117: 3971-3978.

[270] Detmar J, Rennie MY, Whiteley KJ, Qu D, Taniuchi Y, Shang X, Casper RF, Adamson SL, Sled JG, Jurisicova A. Fetal growth restriction triggered by polycyclic aromatic hydrocarbons is associated with altered placental vasculature and AhR-dependent changes in cell death. Am J Physiol Endocrinol Metab 2008; 295: E519-E530.

[271] Kang MY, Kim HB, Piao C, Lee KH, Hyun JW, Chang IY, You HJ. The critical role of catalase in prooxidant and antioxidant function of p53. Cell Death Differ 2013; 20: 117-129.

[272] Rizzo A, Roscino MT, Binetti F, Sciorsci RL. Roles of reactive oxygen species in female reproduction. Reprod Domest Anim 2012; 47: 344-352.

[273] Fujii J, Iuchi Y, Okada F. Fundamental roles of reactive oxygen species and protective mechanisms in the female reproductive system. Reprod Biol Endocrinol 2005; 3: 43.

[274] Schnabel D, Salas-Vidal E, Narvaez V, Sanchez-Carbente MR, Hernandez-Garcia D, Cuervo R, Covarrubias L. Expression and regulation of antioxidant enzymes in the developing limb support a function of ROS in interdigital cell death. Dev Biol 2006; 291: 291-299.

[275] Bentov Y, Yavorska T, Esfandiari N, Jurisicova A, Casper RF. The contribution of mitochondrial function to reproductive aging. J Assist Reprod Genet 2011; 28: 773-783.

[276] Chen Y, Millan-Ward E, Kong J, Israels SJ, Gibson SB. Mitochondrial electron-transport-chain inhibitors of complexes I and II induce autophagic cell death mediated by reactive oxygen species. J Cell Sci 2007; 120: 4155-4166.

[277] Yu L, Wan F, Dutta S, Welsh S, Liu Z, Freundt E, Baehrecke EH, Lenardo M. Autophagic programmed cell death by selective catalase degradation. Proc Natl Acad Sci U S A 2006; 103: 4952-4957.

[278] Scherz-Shouval R, Shvets E, Fass E, Shorer H, Gil L, Elazar Z. Reactive oxygen species are essential for autophagy and specifically regulate the activity of Atg4. EMBO J 2007; 26: 1749-1760.

[279] Gaytan M, Morales C, Sanchez-Criado JE, Gaytan F. Immunolocalization of beclin 1, a bcl-2-binding, autophagy-related protein, in the human ovary: possible relation to life span of corpus luteum. Cell Tissue Res 2008; 331: 509-517.

[280] Whitworth AJ, Pallanck LJ. The PINK1/Parkin pathway: a mitochondrial quality control system? J Bioenerg Biomembr 2009; 41: 499-503.

[281] Molina AJ, Wikstrom JD, Stiles L, Las G, Mohamed H, Elorza A, Walzer G, Twig G, Katz S, Corkey BE, Shirihai OS. Mitochondrial networking protects beta-cells from nutrient-induced apoptosis. Diabetes 2009; 58: 2303-2315.

[282] Twig G, Liu X, Liesa M, Wikstrom JD, Molina AJ, Las G, Yaniv G, Hajnoczky G, Shirihai OS. Biophysical properties of mitochondrial fusion events in pancreatic beta-cells and cardiac cells unravel potential control mechanisms of its selectivity. Am J Physiol Cell Physiol 2010; 299: C477-C487.

[283] Wikstrom JD, Katzman SM, Mohamed H, Twig G, Graf SA, Heart E, Molina AJ, Corkey BE, de Vargas LM, Danial NN, Collins S, Shirihai OS. beta-Cell mitochondria exhibit membrane potential heterogeneity that can be altered by stimulatory or toxic fuel levels. Diabetes 2007; 56: 2569-2578.

[284] Choi SE, Lee SM, Lee YJ, Li LJ, Lee SJ, Lee JH, Kim Y, Jun HS, Lee KW, Kang Y. Protective role of autophagy in palmitate-induced INS-1 beta-cell death. Endocrinology 2009; 150: 126-134.

[285] Choi YK, Por ED, Kwon YG, Kim YM. Regulation of ROS production and vascular function by carbon monoxide. Oxid Med Cell Longev 2012; 2012: 794237.

[286] Alfadda AA, Sallam RM. Reactive oxygen species in health and disease. J Biomed Biotechnol 2012; 2012: 936486.

[287] Mena S, Ortega A, Estrela JM. Oxidative stress in environmental-induced carcinogenesis. Mutat Res 2009; 674: 36-44.

[288] Mates JM, Segura JA, Alonso FJ, Marquez J. Roles of dioxins and heavy metals in cancer and neurological diseases using ROS-mediated mechanisms. Free Radic Biol Med 2010; 49: 1328-1341.

[289] Flora SJ. Arsenic-induced oxidative stress and its reversibility. Free Radic Biol Med 2011; 51: 257-281.

[290] Hoyer PB, Sipes IG. Development of an animal model for ovotoxicity using 4-vinylcyclohexene: a case study. Birth Defects Res B Dev Reprod Toxicol 2007; 80: 113-125.

[291] Ciftci O, Disli OM, Timurkaan N. Protective effects of protocatechuic acid on TCDD-induced oxidative and histopathological damage in the heart tissue of rats. Toxicol Ind Health 2012.

[292] Zhu Z, Xu W, Dai J, Chen X, Zhao X, Fang P, Yang F, Tang M, Wang Z, Wang L, Ma D, Qaio Z. The alteration of protein profile induced by cigarette smoking via oxidative stress in mice epididymis. Int J Biochem Cell Biol 2012.

[293] Talukder MA, Johnson WM, Varadharaj S, Lian J, Kearns PN, El-Mahdy MA, Liu X, Zweier JL. Chronic cigarette smoking causes hypertension, increased oxidative stress, impaired NO bioavailability, endothelial dysfunction, and cardiac remodeling in mice. Am J Physiol Heart Circ Physiol 2011; 300: H388-H396.

[294] Tagawa Y, Hiramatsu N, Kasai A, Hayakawa K, Okamura M, Yao J, Kitamura M. Induction of apoptosis by cigarette smoke via ROS-dependent endoplasmic reticulum stress and CCAAT/enhancer-binding protein-homologous protein (CHOP). Free Radic Biol Med 2008; 45: 50-59.

[295] Shimada T, Hiramatsu N, Hayakawa K, Takahashi S, Kasai A, Tagawa Y, Mukai M, Yao J, Fujii-Kuriyama Y, Kitamura M. Dual suppression of adipogenesis by cigarette smoke through activation of the aryl hydrocarbon receptor and induction of endoplasmic reticulum stress. Am J Physiol Endocrinol Metab 2009; 296: E721-E730.

[296] Kitamura M, Kasai A. Cigarette smoke as a trigger for the dioxin receptor-mediated signaling pathway. Cancer Lett 2007; 252: 184-194.

[297] Miller MM, Plowchalk DR, Weitzman GA, London SN, Mattison DR. The effect of benzo(a)pyrene on murine ovarian and corpora lutea volumes. Am J Obstet Gynecol 1992; 166: 1535-1541.

[298] Huang J, Okuka M, McLean M, Keefe DL, Liu L. Effects of cigarette smoke on fertilization and embryo development in vivo. Fertil Steril 2009; 92: 1456-1465.

[299] Sadeu JC, Foster WG. Cigarette smoke condensate exposure delays follicular development and function in a stage-dependent manner. Fertil Steril 2011; 95: 2410-2417.

[300] Neal MS, Mulligan Tuttle AM, Casper RF, Lagunov A, Foster WG. Aryl hydrocarbon receptor antagonists attenuate the deleterious effects of benzo[a]pyrene on isolated rat follicle development. Reprod Biomed Online 2010; 21: 100-108.

[301] Franco R, Sanchez-Olea R, Reyes-Reyes EM, Panayiotidis MI. Environmental toxicity, oxidative stress and apoptosis: menage a trois. Mutat Res 2009; 674: 3-22.

[302] Katschinski DM. On heat and cells and proteins. News Physiol Sci 2004; 19: 11-15.

[303] Robert J. Evolution of heat shock protein and immunity. Dev Comp Immunol 2003; 27: 449-464.

[304] Stromer T, Ehrnsperger M, Gaestel M, Buchner J. Analysis of the interaction of small heat shock proteins with unfolding proteins. J Biol Chem 2003; 278: 18015-18021.

[305] Azzoni AR, Tada SF, Rosselli LK, Paula DP, Catani CF, Sabino AA, Barbosa JA, Guimaraes BG, Eberlin MN, Medrano FJ, Souza AP. Expression and purification of a small heat shock protein from the plant pathogen Xylella fastidiosa. Protein Expr Purif 2004; 33: 297-303.

[306] Agashe VR, Hartl FU. Roles of molecular chaperones in cytoplasmic protein folding. Semin Cell Dev Biol 2000; 11: 15-25.

[307] Heikkila JJ, Ohan N, Tam Y, Ali A. Heat shock protein gene expression during Xenopus development. Cell Mol Life Sci 1997; 53: 114-121.

[308] Tam Y, Heikkila JJ. Identification of members of the HSP30 small heat shock protein family and characterization of their developmental regulation in heat-shocked Xenopus laevis embryos. Dev Genet 1995; 17: 331-339.

[309] Morimoto RI, Kroeger PE, Cotto JJ. The transcriptional regulation of heat shock genes: a plethora of heat shock factors and regulatory conditions. EXS 1996; 77: 139-163.

[310] Morimoto RI, Kline MP, Bimston DN, Cotto JJ. The heat-shock response: regulation and function of heat-shock proteins and molecular chaperones. Essays Biochem 1997; 32: 17-29.

[311] Aldonyte R, Hutchinson TE, Jin B, Brantly M, Block E, Patel J, Zhang J. Endothelial alpha-1-antitrypsin attenuates cigarette smoke induced apoptosis in vitro. COPD 2008; 5: 153-162.

[312] Mulligan-Tuttle A, Heikkila JJ. Expression of the small heat shock protein gene, hsp30, in Rana catesbeiana fibroblasts. Comp Biochem Physiol A Mol Integr Physiol 2007; 148: 308-316.

[313] Tuttle AM, Gauley J, Chan N, Heikkila JJ. Analysis of the expression and function of the small heat shock protein gene, hsp27, in Xenopus laevis embryos. Comp Biochem Physiol A Mol Integr Physiol 2007; 147: 112-121.

[314] Arrigo AP. Small stress proteins: chaperones that act as regulators of intracellular redox state and programmed cell death. Biol Chem 1998; 379: 19-26.

[315] Ehrnsperger M, Hergersberg C, Wienhues U, Nichtl A, Buchner J. Stabilization of proteins and peptides in diagnostic immunological assays by the molecular chaperone Hsp25. Anal Biochem 1998; 259: 218-225.

[316] MacRae TH. Structure and function of small heat shock/alpha-crystallin proteins: established concepts and emerging ideas. Cell Mol Life Sci 2000; 57: 899-913.

[317] Van MR, Slingsby C, Vierling E. Structure and function of the small heat shock protein/alpha-crystallin family of molecular chaperones. Adv Protein Chem 2001; 59: 105-156.

[318] Young JT, Gauley J, Heikkila JJ. Simultaneous exposure of Xenopus A6 kidney epithelial cells to concurrent mild sodium arsenite and heat stress results in enhanced hsp30 and hsp70 gene expression and the acquisition of thermotolerance. Comp Biochem Physiol A Mol Integr Physiol 2009; 153: 417-424.

[319] Young JT, Heikkila JJ. Proteasome inhibition induces hsp30 and hsp70 gene expression as well as the acquisition of thermotolerance in Xenopus laevis A6 cells. Cell Stress Chaperones 2010; 15: 323-334.

[320] Wakayama T, Iseki S. Expression and cellular localization of the mRNA for the 25-kDa heat-shock protein in the mouse. Cell Biol Int 1998; 22: 295-304.

[321] Quinlan R, van d, I. Fatal attraction: when chaperone turns harlot. Nat Med 1999; 5: 25-26.

[322] Bova MP, Yaron O, Huang Q, Ding L, Haley DA, Stewart PL, Horwitz J. Mutation R120G in alphaB-crystallin, which is linked to a desmin-related myopathy, results in an irregular structure and defective chaperone-like function. Proc Natl Acad Sci U S A 1999; 96: 6137-6142.

[323] Irobi J, Van IK, Seeman P, Jordanova A, Dierick I, Verpoorten N, Michalik A, De VE, Jacobs A, Van G, V, Vennekens K, Mazanec R, Tournev I, Hilton-Jones D, Talbot K, Kremensky I, Van Den BL, Robberecht W, Van VJ, Van BC, Gettemans J, De JP, Timmerman V. Hot-spot residue in small heat-shock protein 22 causes distal motor neuropathy. Nat Genet 2004; 36: 597-601.

[324] Edwards DP, Adams DJ, McGuire WL. Estradiol stimulates synthesis of a major intracellular protein in a human breast cancer cell line (MCF-7). Breast Cancer Res Treat 1981; 1: 209-223.

[325] Ciocca DR, Adams DJ, Edwards DP, Bjercke RJ, McGuire WL. Estrogen-induced 24K protein in MCF-7 breast cancer cells is localized in granules. Breast Cancer Res Treat 1984; 4: 261-268.

[326] Gernold M, Knauf U, Gaestel M, Stahl J, Kloetzel PM. Development and tissue-specific distribution of mouse small heat shock protein hsp25. Dev Genet 1993; 14: 103-111.

[327] Klemenz R, Andres AC, Frohli E, Schafer R, Aoyama A. Expression of the murine small heat shock proteins hsp 25 and alpha B crystallin in the absence of stress. J Cell Biol 1993; 120: 639-645.

[328] Tanguay RM, Wu Y, Khandjian EW. Tissue-specific expression of heat shock proteins of the mouse in the absence of stress. Dev Genet 1993; 14: 112-118.

[329] Wilkinson JM, Pollard I. Immunohistochemical localisation of the 25 kDa heat shock protein in unstressed rats: possible functional implications. Anat Rec 1993; 237: 453-457.

[330] Wilkinson JM, Pollard I. Immunohistochemical localisation of the 90, 70 and 25 kDa heat shock proteins in control and caffeine treated rat embryos. Ann Anat 1993; 175: 561-566.

[331] Loones MT, Chang Y, Morange M. The distribution of heat shock proteins in the nervous system of the unstressed mouse embryo suggests a role in neuronal and non-neuronal differentiation. Cell Stress Chaperones 2000; 5: 291-305.

[332] Kim M, Geum D, Khang I, Park YM, Kang BM, Lee KA, Kim K. Expression pattern of HSP25 in mouse preimplantation embryo: heat shock responses during oocyte maturation. Mol Reprod Dev 2002; 61: 3-13.

[333] Arrigo AP. Tumor necrosis factor induces the rapid phosphorylation of the mammalian heat shock protein hsp28. Mol Cell Biol 1990; 10: 1276-1280.

[334] Salminen WF, Jr., Voellmy R, Roberts SM. Effect of N-acetylcysteine on heat shock protein induction by acetaminophen in mouse liver. J Pharmacol Exp Ther 1998; 286: 519-524.

[335] Gottschalg E, Moore NE, Ryan AK, Travis LC, Waller RC, Pratt S, Atmaca M, Kind CN, Fry JR. Phenotypic anchoring of arsenic and cadmium toxicity in three hepatic-related cell systems reveals compound- and cell-specific selective up-regulation of stress protein expression: implications for fingerprint profiling of cytotoxicity. Chem Biol Interact 2006; 161: 251-261.

[336] Gotthardt R, Neininger A, Gaestel M. The anti-cancer drug cisplatin induces H25 in Ehrlich ascites tumor cells by a mechanism different from transcriptional stimulation influencing predominantly H25 translation. Int J Cancer 1996; 66: 790-795.

[337] Chiu PY, Ko KM. Time-dependent enhancement in mitochondrial glutathione status and ATP generation capacity by schisandrin B treatment decreases the susceptibility of rat hearts to ischemia-reperfusion injury. Biofactors 2003; 19: 43-51.

[338] Bartosiewicz M, Penn S, Buckpitt A. Applications of gene arrays in environmental toxicology: fingerprints of gene regulation associated with cadmium chloride, benzo(a)pyrene, and trichloroethylene. Environ Health Perspect 2001; 109: 71-74.

[339] Szegezdi E, Macdonald DC, Ni CT, Gupta S, Samali A. Bcl-2 family on guard at the ER. Am J Physiol Cell Physiol 2009; 296: C941-C953.

[340] Mizushima N, Levine B. Autophagy in mammalian development and differentiation. Nat Cell Biol 2010; 12: 823-830.

[341] Yang Z, Klionsky DJ. Eaten alive: a history of macroautophagy. Nat Cell Biol 2010; 12: 814-822.

[342] Isakson P, Holland P, Simonsen A. The role of ALFY in selective autophagy. Cell Death Differ 2013; 20: 12-20.

[343] Codogno P, Mehrpour M, Proikas-Cezanne T. Canonical and non-canonical autophagy: variations on a common theme of self-eating? Nat Rev Mol Cell Biol 2012; 13: 7-12.

[344] Funderburk SF, Wang QJ, Yue Z. The Beclin 1-VPS34 complex--at the crossroads of autophagy and beyond. Trends Cell Biol 2010; 20: 355-362.

[345] Glick D, Barth S, Macleod KF. Autophagy: cellular and molecular mechanisms. J Pathol 2010; 221: 3-12.

[346] Pyo JO, Nah J, Jung YK. Molecules and their functions in autophagy. Exp Mol Med 2012; 44: 73-80.

[347] Kaushik S, Singh R, Cuervo AM. Autophagic pathways and metabolic stress. Diabetes Obes Metab 2010; 12 Suppl 2: 4-14.

[348] Hamasaki M, Yoshimori T. Where do they come from? Insights into autophagosome formation. FEBS Lett 2010; 584: 1296-1301.

[349] Kanzawa T, Kondo Y, Ito H, Kondo S, Germano I. Induction of autophagic cell death in malignant glioma cells by arsenic trioxide. Cancer Res 2003; 63: 2103-2108.

[350] Kanzawa T, Zhang L, Xiao L, Germano IM, Kondo Y, Kondo S. Arsenic trioxide induces autophagic cell death in malignant glioma cells by upregulation of mitochondrial cell death protein BNIP3. Oncogene 2005; 24: 980-991.

[351] Shimizu S, Kanaseki T, Mizushima N, Mizuta T, rakawa-Kobayashi S, Thompson CB, Tsujimoto Y. Role of Bcl-2 family proteins in a non-apoptotic programmed cell death dependent on autophagy genes. Nat Cell Biol 2004; 6: 1221-1228.

[352] Heath-Engel HM, Chang NC, Shore GC. The endoplasmic reticulum in apoptosis and autophagy: role of the BCL-2 protein family. Oncogene 2008; 27: 6419-6433.

[353] Vilser C, Hueller H, Nowicki M, Hmeidan F, Blumenauer V, Spanel-Borowski K. The variable expression of lectin-like oxidized low-density lipoprotein receptor (LOX-1) and signs of autophagy and apoptosis in freshly harvested human granulosa cells depend on gonadotropin dose, age, and body weight. In, 93 ed. 2010: 2706-2715.

[354] Choi J, Jo M, Lee E, Yoon B, Choi D. The role of autophagy in follicular development and atresia in rat granulosa cells. In, 93 ed. 2010: 2532-2537.

[355] Hwang JW, Chung S, Sundar IK, Yao H, Arunachalam G, McBurney MW, Rahman I. Cigarette smoke-induced autophagy is regulated by SIRT1-PARP-1-dependent mechanism: implication in pathogenesis of COPD. Arch Biochem Biophys 2010; 500: 203-209.

[356] Chen Z, Kim H, Sciurba F, Lee SJ, Feghali-Bostwick C, Stolz D, Dhir R, Landreneau R, Schuchert M, Yousem S, Nakahira K, Pilewski J, Lee J, Zhang Y, Ryter S, Choi A. Egr-1 regulates autophagy in cigarette smoke-induced chronic obstructive pulmonary disease. In, 3 ed. 2008: e3316.

[357] Kim H, Wang X, Chen Z, Lee SJ, Huang M, Wang Y, Ryter S, Choi A. Autophagic proteins regulate cigarette smoke-induced apoptosis: protective role of heme oxygenase-1. In, 4 ed. 2008: 887-895.

[358] Braschi E, McBride HM. Mitochondria and the culture of the Borg: understanding the integration of mitochondrial function within the reticulum, the cell, and the organism. Bioessays 2010; 32: 958-966.

[359] Nunnari J, Suomalainen A. Mitochondria: in sickness and in health. Cell 2012; 148: 1145-1159.

[360] Iglewski M, Hill JA, Lavandero S, Rothermel BA. Mitochondrial fission and autophagy in the normal and diseased heart. Curr Hypertens Rep 2010; 12: 418-425.

[361] Landes T, Martinou JC. Mitochondrial outer membrane permeabilization during apoptosis: the role of mitochondrial fission. Biochim Biophys Acta 2011; 1813: 540-545.

[362] Detmer SA, Chan DC. Functions and dysfunctions of mitochondrial dynamics. Nat Rev Mol Cell Biol 2007; 8: 870-879.

[363] Westermann B. Mitochondrial fusion and fission in cell life and death. Nat Rev Mol Cell Biol 2010; 11: 872-884.

[364] Stiles L, Ferree A, Shirihai OS. Mitochondrial dynamics and autophagy. In: Lu B (ed.), Mitochondrial Dynamics and Neurodegeneration. Springer Science and Business Media; 2011: 69-108.

[365] Ashrafi G, Schwarz TL. The pathways of mitophagy for quality control and clearance of mitochondria. Cell Death Differ 2013; 20: 31-42.

[366] Twig G, Elorza A, Molina AJ, Mohamed H, Wikstrom JD, Walzer G, Stiles L, Haigh SE, Katz S, Las G, Alroy J, Wu M, Py BF, Yuan J, Deeney JT, Corkey BE, Shirihai OS. Fission and selective fusion govern mitochondrial segregation and elimination by autophagy. EMBO J 2008; 27: 433-446.

[367] Grimm S. The ER-mitochondria interface: the social network of cell death. Biochim Biophys Acta 2012; 1823: 327-334.

[368] Eura Y, Ishihara N, Yokota S, Mihara K. Two mitofusin proteins, mammalian homologues of FZO, with distinct functions are both required for mitochondrial fusion. J Biochem 2003; 134: 333-344.

[369] Ishihara N, Eura Y, Mihara K. Mitofusin 1 and 2 play distinct roles in mitochondrial fusion reactions via GTPase activity. J Cell Sci 2004; 117: 6535-6546.

[370] Chu CT. Tickled PINK1: mitochondrial homeostasis and autophagy in recessive Parkinsonism. Biochim Biophys Acta 2010; 1802: 20-28.

[371] Glauser L, Sonnay S, Stafa K, Moore DJ. Parkin promotes the ubiquitination and degradation of the mitochondrial fusion factor mitofusin 1. J Neurochem 2011; 118: 636-645.

[372] Tanaka A, Cleland MM, Xu S, Narendra DP, Suen DF, Karbowski M, Youle RJ. Proteasome and p97 mediate mitophagy and degradation of mitofusins induced by Parkin. J Cell Biol 2010; 191: 1367-1380.

[373] Gegg ME, Cooper JM, Chau KY, Rojo M, Schapira AH, Taanman JW. Mitofusin 1 and mitofusin 2 are ubiquitinated in a PINK1/parkin-dependent manner upon induction of mitophagy. Hum Mol Genet 2010; 19: 4861-4870.

[374] Narendra D, Tanaka A, Suen DF, Youle RJ. Parkin is recruited selectively to impaired mitochondria and promotes their autophagy. J Cell Biol 2008; 183: 795-803.

[375] Goldberg MS, Fleming SM, Palacino JJ, Cepeda C, Lam HA, Bhatnagar A, Meloni EG, Wu N, Ackerson LC, Klapstein GJ, Gajendiran M, Roth BL, Chesselet MF, Maidment NT, Levine MS, Shen J. Parkin-deficient mice exhibit nigrostriatal deficits but not loss of dopaminergic neurons. J Biol Chem 2003; 278: 43628-43635.

[376] Cereghetti GM, Stangherlin A, Martins de BO, Chang CR, Blackstone C, Bernardi P, Scorrano L. Dephosphorylation by calcineurin regulates translocation of Drp1 to mitochondria. Proc Natl Acad Sci U S A 2008; 105: 15803-15808.

[377] Gomes LC, Di BG, Scorrano L. During autophagy mitochondria elongate, are spared from degradation and sustain cell viability. Nat Cell Biol 2011; 13: 589-598.

[378] Gomes LC, Scorrano L. Mitochondrial elongation during autophagy: A stereotypical response to survive in difficult times. Autophagy 2011; 7.

[379] Twig G, Shirihai OS. The interplay between mitochondrial dynamics and mitophagy. Antioxid Redox Signal 2011; 14: 1939-1951.

[380] Chen H, Chan DC. Emerging functions of mammalian mitochondrial fusion and fission. Hum Mol Genet 2005; 14 Spec No. 2: R283-R289.

[381] Chen H, Chomyn A, Chan DC. Disruption of fusion results in mitochondrial heterogeneity and dysfunction. J Biol Chem 2005; 280: 26185-26192.

[382] Nicholson GA, Magdelaine C, Zhu D, Grew S, Ryan MM, Sturtz F, Vallat JM, Ouvrier RA. Severe early-onset axonal neuropathy with homozygous and compound heterozygous MFN2 mutations. Neurology 2008; 70: 1678-1681.

[383] Alexander C, Votruba M, Pesch UE, Thiselton DL, Mayer S, Moore A, Rodriguez M, Kellner U, Leo-Kottler B, Auburger G, Bhattacharya SS, Wissinger B. OPA1, encoding a dynamin-related GTPase, is mutated in autosomal dominant optic atrophy linked to chromosome 3q28. Nat Genet 2000; 26: 211-215.

[384] Thiselton DL, Alexander C, Morris A, Brooks S, Rosenberg T, Eiberg H, Kjer B, Kjer P, Bhattacharya SS, Votruba M. A frameshift mutation in exon 28 of the OPA1 gene explains the high prevalence of dominant optic atrophy in the Danish population: evidence for a founder effect. Hum Genet 2001; 109: 498-502.

[385] Delettre C, Lenaers G, Griffoin JM, Gigarel N, Lorenzo C, Belenguer P, Pelloquin L, Grosgeorge J, Turc-Carel C, Perret E, starie-Dequeker C, Lasquellec L, Arnaud B, Ducommun B, Kaplan J, Hamel CP. Nuclear gene OPA1, encoding a mitochondrial dynamin-related protein, is mutated in dominant optic atrophy. Nat Genet 2000; 26: 207-210.

[386] Zuchner S, Mersiyanova IV, Muglia M, Bissar-Tadmouri N, Rochelle J, Dadali EL, Zappia M, Nelis E, Patitucci A, Senderek J, Parman Y, Evgrafov O, Jonghe PD, Takahashi Y, Tsuji S, Pericak-Vance MA, Quattrone A, Battaloglu E, Polyakov AV, Timmerman V, Schroder JM, Vance JM. Mutations in the mitochondrial GTPase mitofusin 2 cause Charcot-Marie-Tooth neuropathy type 2A. Nat Genet 2004; 36: 449-451.

[387] Nicholson GA, Magdelaine C, Zhu D, Grew S, Ryan MM, Sturtz F, Vallat JM, Ouvrier RA. Severe early-onset axonal neuropathy with homozygous and compound heterozygous MFN2 mutations. Neurology 2008; 70: 1678-1681.

[388] Glauser L, Sonnay S, Stafa K, Moore DJ. Parkin promotes the ubiquitination and degradation of the mitochondrial fusion factor mitofusin 1. J Neurochem 2011; 118: 636-645.

[389] Tanaka A, Cleland MM, Xu S, Narendra DP, Suen DF, Karbowski M, Youle RJ. Proteasome and p97 mediate mitophagy and degradation of mitofusins induced by Parkin. J Cell Biol 2010; 191: 1367-1380.

[390] Gegg ME, Cooper JM, Chau KY, Rojo M, Schapira AH, Taanman JW. Mitofusin 1 and mitofusin 2 are ubiquitinated in a PINK1/parkin-dependent manner upon induction of mitophagy. Hum Mol Genet 2010; 19: 4861-4870.

[391] Kim HP, Wang X, Chen ZH, Lee SJ, Huang MH, Wang Y, Ryter SW, Choi AM. Autophagic proteins regulate cigarette smoke-induced apoptosis: protective role of heme oxygenase-1. Autophagy 2008; 4: 887-895.

[392] Augood C, Duckitt K, Templeton AA. Smoking and female infertility: a systematic review and meta-analysis. Hum Reprod 1998; 13: 1532-1539.

[393] Hayatbakhsh MR, Clavarino A, Williams GM, Sina M, Najman JM. Cigarette smoking and age of menopause: a large prospective study. Maturitas 2012; 72: 346-352.

[394] Boone DL, Tsang BK. Caspase-3 in the rat ovary: localization and possible role in follicular atresia and luteal regression. Biol Reprod 1998; 58: 1533-1539.

[395] Dharma SJ, Kelkar RL, Nandedkar TD. Fas and Fas ligand protein and mRNA in normal and atretic mouse ovarian follicles. Reproduction 2003; 126: 783-789.

[396] Gregoraszczuk EL, Sowa M, Kajta M, Ptak A, Wojtowicz A. Effect of PCB 126 and PCB 153 on incidence of apoptosis in cultured theca and granulosa cells collected from small, medium and large preovulatory follicles. Reprod Toxicol 2003; 17: 465-471.

[397] Tilly JL. Molecular and genetic basis of normal and toxicant-induced apoptosis in female germ cells. Toxicol Lett 1998; 102-103: 497-501.

[398] Smith BJ, Mattison DR, Sipes IG. The role of epoxidation in 4-vinylcyclohexene-induced ovarian toxicity. Toxicol Appl Pharmacol 1990; 105: 372-381.

[399] Chiu PY, Mak DH, Poon MK, Ko KM. Role of cytochrome P-450 in schisandrin B-induced antioxidant and heat shock responses in mouse liver. Life Sci 2005; 77: 2887-2895.

[400] Pons M, Cousins SW, Csaky KG, Striker G, Marin-Castano ME. Cigarette smoke-related hydroquinone induces filamentous actin reorganization and heat shock protein 27 phosphorylation through p38 and extracellular signal-regulated

kinase 1/2 in retinal pigment epithelium: implications for age-related macular degeneration. Am J Pathol 2010; 177: 1198-1213.

[401] Stacchiotti A, Morandini F, Bettoni F, Schena I, Lavazza A, Grigolato PG, Apostoli P, Rezzani R, Aleo MF. Stress proteins and oxidative damage in a renal derived cell line exposed to inorganic mercury and lead. Toxicology 2009; 264: 215-224.

[402] Vedam K, Nishijima Y, Druhan LJ, Khan M, Moldovan NI, Zweier JL, Ilangovan G. Role of heat shock factor-1 activation in the doxorubicin-induced heart failure in mice. Am J Physiol Heart Circ Physiol 2010; 298: H1832-H1841.

[403] Mastrocola R, Barutta F, Pinach S, Bruno G, Perin PC, Gruden G. Hippocampal heat shock protein 25 expression in streptozotocin-induced diabetic mice. Neuroscience 2012; 227: 154-162.

[404] Pinach S, Burt D, Berrone E, Barutta F, Bruno G, Porta M, Perin PC, Gruden G. Retinal heat shock protein 25 in early experimental diabetes. Acta Diabetol 2011.

[405] Yan LJ, Rajasekaran NS, Sathyanarayanan S, Benjamin IJ. Mouse HSF1 disruption perturbs redox state and increases mitochondrial oxidative stress in kidney. Antioxid Redox Signal 2005; 7: 465-471.

[406] Sakurai T, Kudo M, Umemura A, He G, Elsharkawy AM, Seki E, Karin M. p38alpha Inhibits Liver Fibrogenesis and Consequent Hepatocarcinogenesis by Curtailing Accumulation of Reactive Oxygen Species. Cancer Res 2013; 73: 215-224.

[407] Tabuchi A, Funaji K, Nakatsubo J, Fukuchi M, Tsuchiya T, Tsuda M. Inactivation of aconitase during the apoptosis of mouse cerebellar granule neurons induced by a deprivation of membrane depolarization. J Neurosci Res 2003; 71: 504-515.

[408] Matthews JB, Chen FM, Milward MR, Wright HJ, Carter K, McDonagh A, Chapple IL. Effect of nicotine, cotinine and cigarette smoke extract on the neutrophil respiratory burst. J Clin Periodontol 2011.

[409] Barth S, Glick D, Macleod KF. Autophagy: assays and artifacts. J Pathol 2010; 221: 117-124.

[410] Yoo SH, Yoon YG, Lee JS, Song YS, Oh JS, Park BS, Kwon TK, Park C, Choi YH, Yoo YH. Etoposide induces a mixed type of programmed cell death and

overcomes the resistance conferred by Bcl-2 in Hep3B hepatoma cells. Int J Oncol 2012.

[411] Pattingre S, Tassa A, Qu X, Garuti R, Liang XH, Mizushima N, Packer M, Schneider MD, Levine B. Bcl-2 antiapoptotic proteins inhibit Beclin 1-dependent autophagy. Cell 2005; 122: 927-939.

[412] Bolt AM, Zhao F, Pacheco S, Klimecki WT. Arsenite-induced autophagy is associated with proteotoxicity in human lymphoblastoid cells. Toxicol Appl Pharmacol 2012.

[413] Bolt AM, Klimecki WT. Autophagy in toxicology: self-consumption in times of stress and plenty. J Appl Toxicol 2012; 32: 465-479.

[414] Bolt AM, Douglas RM, Klimecki WT. Arsenite exposure in human lymphoblastoid cell lines induces autophagy and coordinated induction of lysosomal genes. Toxicol Lett 2010; 199: 153-159.

[415] Bolt AM, Byrd RM, Klimecki WT. Autophagy is the predominant process induced by arsenite in human lymphoblastoid cell lines. Toxicol Appl Pharmacol 2010; 244: 366-373.

[416] Chen Y, Millan-Ward E, Kong J, Israels SJ, Gibson SB. Oxidative stress induces autophagic cell death independent of apoptosis in transformed and cancer cells. Cell Death Differ 2008; 15: 171-182.

[417] Chen ZH, Kim HP, Sciurba FC, Lee SJ, Feghali-Bostwick C, Stolz DB, Dhir R, Landreneau RJ, Schuchert MJ, Yousem SA, Nakahira K, Pilewski JM, Lee JS, Zhang Y, Ryter SW, Choi AM. Egr-1 regulates autophagy in cigarette smoke-induced chronic obstructive pulmonary disease. PLoS ONE 2008; 3: e3316.

[418] Ding Z, Wang X, Khaidakov M, Liu S, Dai Y, Mehta JL. Degradation of heparan sulfate proteoglycans enhances oxidized-LDL-mediated autophagy and apoptosis in human endothelial cells. Biochem Biophys Res Commun 2012.

[419] Gao W, Kang J-H, Liao Y, Li M, Yin XM. Autophagy and Cell Death. In: Yin XM, Dong Z (eds.), Essentials of Apoptosis. Humana Press; 2009: 671-688.

[420] Lee JS, Lee GM. Effect of sodium butyrate on autophagy and apoptosis in Chinese hamster ovary cells. Biotechnol Prog 2012; 28: 349-357.

[421] Shi J, Yin N, Xuan LL, Yao CS, Meng AM, Hou Q. Vam3, a derivative of resveratrol, attenuates cigarette smoke-induced autophagy. Acta Pharmacol Sin 2012; 33: 888-896.

[422] Thome RG, Santos HB, Arantes FP, Domingos FF, Bazzoli N, Rizzo E. Dual roles for autophagy during follicular atresia in fish ovary. Autophagy 2009; 5: 117-119.

[423] Chen H, Chan DC. Emerging functions of mammalian mitochondrial fusion and fission. Hum Mol Genet 2005; 14 Spec No. 2: R283-R289.

[424] Detmer SA, Chan DC. Functions and dysfunctions of mitochondrial dynamics. Nat Rev Mol Cell Biol 2007; 8: 870-879.

[425] Twig G, Hyde B, Shirihai OS. Mitochondrial fusion, fission and autophagy as a quality control axis: the bioenergetic view. Biochim Biophys Acta 2008; 1777: 1092-1097.

[426] Baba T, Mimura J, Nakamura N, Harada N, Yamamoto M, Morohashi K, Fujii-Kuriyama Y. Intrinsic function of the aryl hydrocarbon (dioxin) receptor as a key factor in female reproduction. Mol Cell Biol 2005; 25: 10040-10051.

[427] Benedict JC, Miller KP, Lin TM, Greenfeld C, Babus JK, Peterson RE, Flaws JA. Aryl hydrocarbon receptor regulates growth, but not atresia, of mouse preantral and antral follicles. Biol Reprod 2003; 68: 1511-1517.

[428] Bernshausen T, Jux B, Esser C, Abel J, Fritsche E. Tissue distribution and function of the Aryl hydrocarbon receptor repressor (AhRR) in C57BL/6 and Aryl hydrocarbon receptor deficient mice. Arch Toxicol 2006; 80: 206-211.

[429] Zenzes MT, Puy LA, Bielecki R. Immunodetection of benzo[a]pyrene adducts in ovarian cells of women exposed to cigarette smoke. Mol Hum Reprod 1998; 4: 159-165.

[430] Botelho FM, Gaschler GJ, Kianpour S, Zavitz CC, Trimble NJ, Nikota JK, Bauer CM, Stampfli MR. Innate immune processes are sufficient for driving cigarette smoke-induced inflammation in mice. Am J Respir Cell Mol Biol 2010; 42: 394-403.

[431] Sen S, Peltz C, Beard J, Zeno B. Recurrent carbon monoxide poisoning from cigarette smoking. Am J Med Sci 2010; 340: 427-428.

[432] Dulger H, Donder A, Sekeroglu MR, Erkoc R, Ozbay B. Investigation of the relationship between serum levels of cotinine and the renal function in active and passive smokers. Ren Fail 2011; 33: 475-479.

[433] Greenspan EJ, Lee H, Dyba M, Pan J, Mekambi K, Johnson T, Blancato J, Mueller S, Berry DL, Chung FL. High-throughput, quantitative analysis of

acrolein-derived DNA adducts in human oral cells by immunohistochemistry. J Histochem Cytochem 2012; 60: 844-853.

[434] Tuttle AM, Stampfli M, Foster WG. Cigarette smoke causes follicle loss in mice ovaries at concentrations representative of human exposure. Hum Reprod 2009; 24: 1452-1459.

[435] Gannon AM, Stampfli MR, Foster WG. Cigarette smoke exposure leads to follicle loss via an alternative ovarian cell death pathway in a mouse model. Toxicol Sci 2012; 125: 274-284.

[436] Gannon AM, Stampfli MR, Foster WG. Cigarette Smoke Exposure Elicits Increased Autophagy and Dysregulation of Mitochondrial Dynamics in Murine Granulosa Cells. Biol Reprod 2013.

[437] Nelson JF, Felicio LS, Randall PK, Sims C, Finch CE. A longitudinal study of estrous cyclicity in aging C57BL/6J mice: I. Cycle frequency, length and vaginal cytology. Biol Reprod 1982; 27: 327-339.

[438] Petersen DR, Norris KJ, Thompson JA. A comparative study of the disposition of nicotine and its metabolites in three inbred strains of mice. Drug Metab Dispos 1984; 12: 725-731.

[439] Hukkanen J, Jacob P, III, Benowitz NL. Metabolism and disposition kinetics of nicotine. Pharmacol Rev 2005; 57: 79-115.

[440] Lodovici M, Akpan V, Evangelisti C, Dolara P. Sidestream tobacco smoke as the main predictor of exposure to polycyclic aromatic hydrocarbons. In, 24 ed. 2004: 277-281.

[441] Bussmann UA, Baranao JL. Regulation of aryl hydrocarbon receptor expression in rat granulosa cells. Biol Reprod 2006; 75: 360-369.

[442] Lodovici M, Luceri C, Guglielmi F, Bacci C, Akpan V, Fonnesu ML, Boddi V, Dolara P. Benzo(a)pyrene diolepoxide (BPDE)-DNA adduct levels in leukocytes of smokers in relation to polymorphism of CYP1A1, GSTM1, GSTP1, GSTT1, and mEH. Cancer Epidemiol Biomarkers Prev 2004; 13: 1342-1348.

[443] Kim JY, Chung JY, Park JE, Lee SG, Kim YJ, Cha MS, Han MS, Lee HJ, Yoo YH, Kim JM. Benzo[a]pyrene induces apoptosis in RL95-2 human endometrial cancer cells by cytochrome P450 1A1 activation. Endocrinology 2007; 148: 5112-5122.

[444] Sadeu JC, Foster WG. Effect of in vitro exposure to Benzo[a]pyrene, a component of cigarette smoke, on folliculogenesis, steroidogenesis, and oocyte maturation. Reprod Toxicol 2011; 31: 402-408.

[445] Jiang M, Liu K, Luo J, Dong Z. Autophagy is a renoprotective mechanism during in vitro hypoxia and in vivo ischemia-reperfusion injury. Am J Pathol 2010; 176: 1181-1192.

[446] Zhang J, Wang JS, Zheng ZK, Tang J, Fan K, Guo H, Wang JJ. Participation of autophagy in lung ischemia-reperfusion injury in vivo. J Surg Res 2012.

[447] Suzuki C, Isaka Y, Takabatake Y, Tanaka H, Koike M, Shibata M, Uchiyama Y, Takahara S, Imai E. Participation of autophagy in renal ischemia/reperfusion injury. Biochem Biophys Res Commun 2008; 368: 100-106.

[448] Vilser C, Hueller H, Nowicki M, Hmeidan FA, Blumenauer V, Spanel-Borowski K. The variable expression of lectin-like oxidized low-density lipoprotein receptor (LOX-1) and signs of autophagy and apoptosis in freshly harvested human granulosa cells depend on gonadotropin dose, age, and body weight. Fertil Steril 2010; 93: 2706-2715.

Appendix I

Supplemental Information for Paper 2

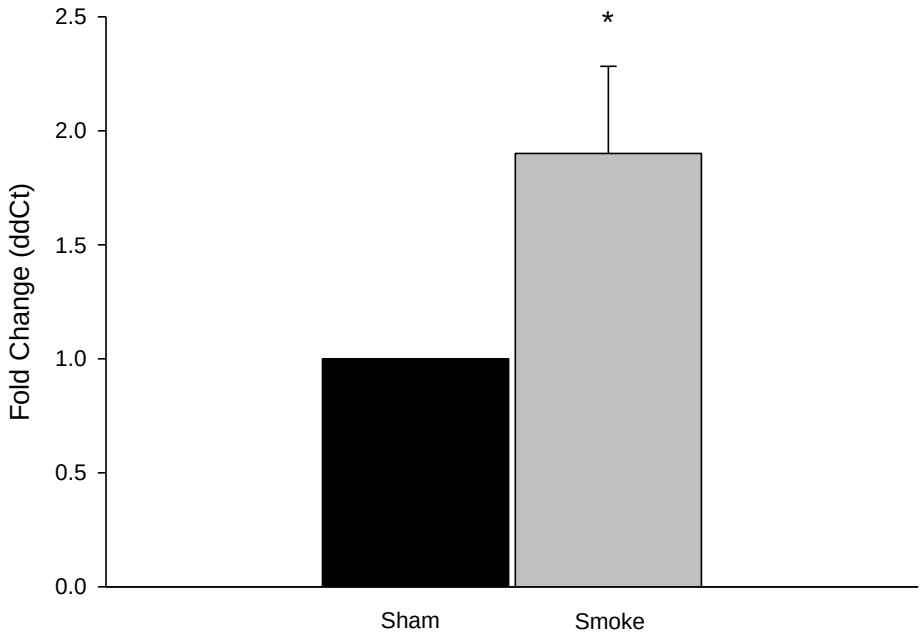

Figure S1: AhR gene expression.
Cigarette smoke exposure results in an upregulation of the *Ahr* gene following 8 weeks of treatment compared with age-matched controls. $p < 0.001$, $n = 6$.

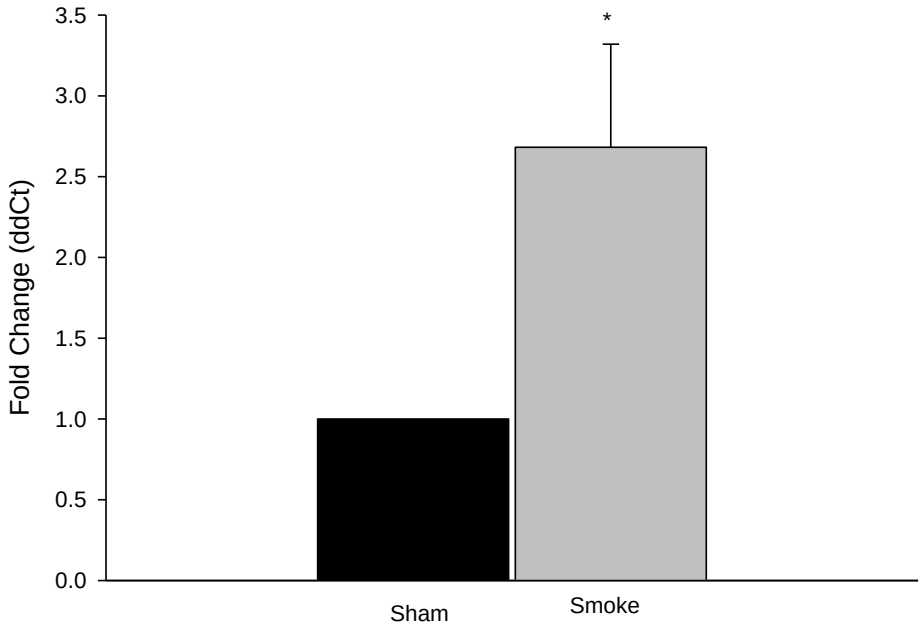

Figure S2: *Cyp1A1* gene expression.
An 8 week exposure to cigarette smoke leads to upregulated *Cyp1A1* expression, a downstream target of the AhR, compared to sham controls. $p < 0.001$, $n = 6$.

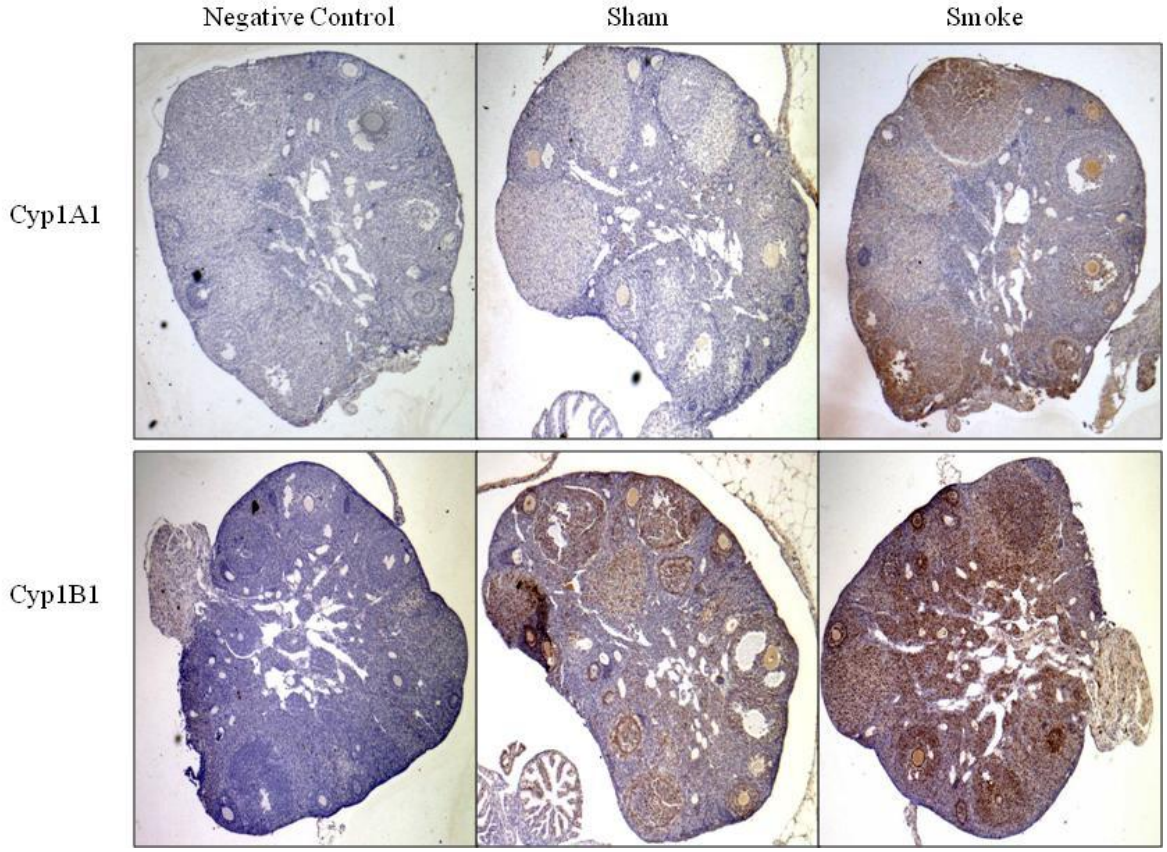

Figure S3: Cyp1A1 and Cyp1B1 protein expression.
Immunohistochemical staining of sham and smoke exposed ovaries show an increase in cytochrome P450 enzymes regulated by activation of the AhR.

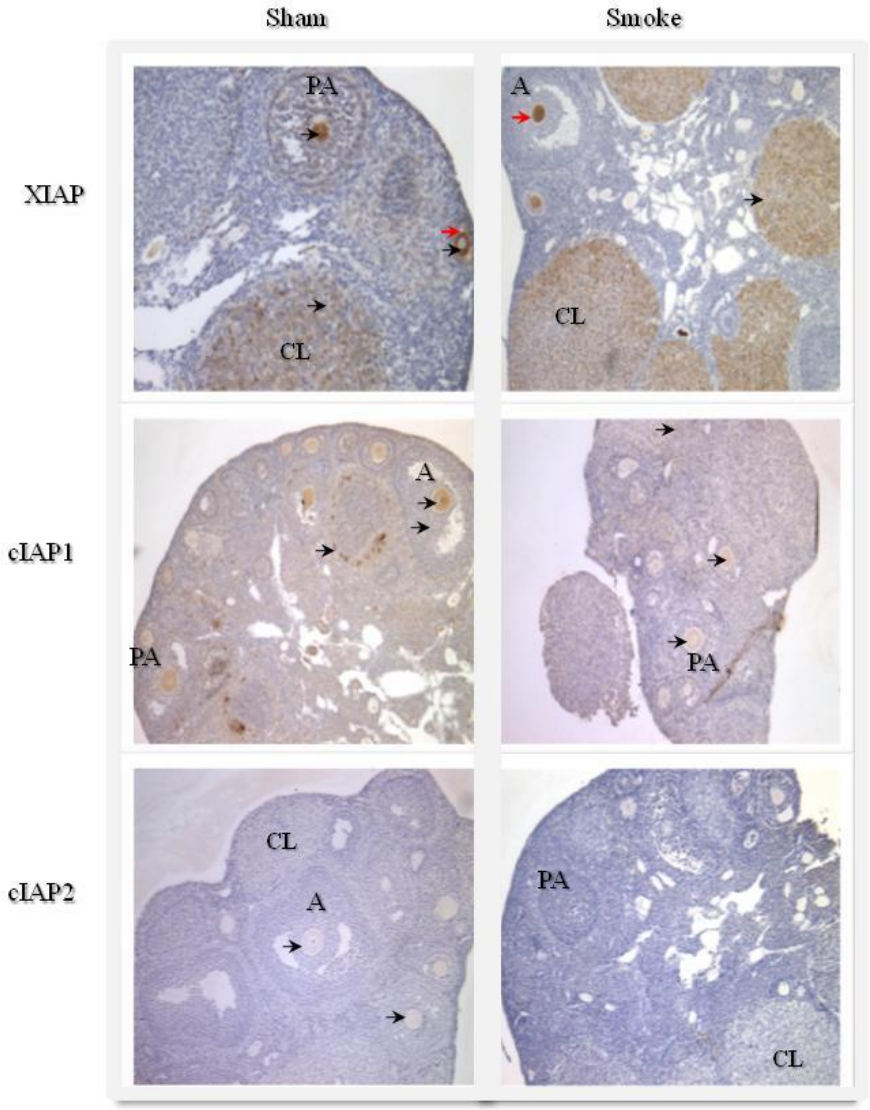

Figure S4: Inhibitors of apoptosis protein expression.
Several IAPs were studied using IHC to determine localization and potential changes in expression following cigarette smoke exposure. All IAPs were present in sham ovaries, although cIAP2 expression was very low. XIAP and cIAP1 were present in the oocyte and granulosa cells of follicles at all stages of development and in the corpora lutea (CL) and some stromal cells of sham ovaries, but appeared to be primarily present in the oocytes and CL of smoke exposed ovaries. cIAP1 also stained positively in granulosa cells of smoke exposed ovaries. cIAP2 was very lowly expressed in sham ovaries, with only faint staining apparent in some oocytes and few cells of the CL and was absent in smoke exposed ovaries. PA = preantral follicle, A = antral follicle, arrow = positively staining cells.

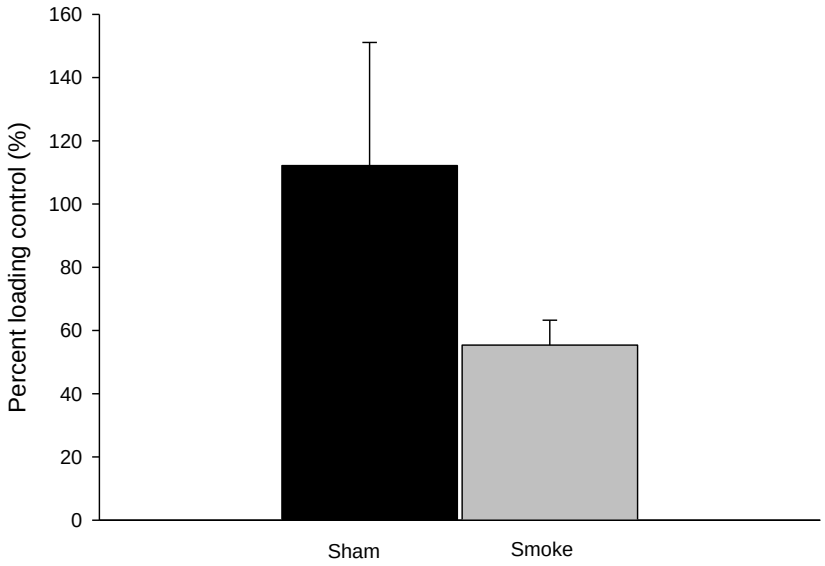

Figure S5: cIAP2 protein expression.
Protein expression of the inhibitor of apoptosis cIAP2 was not different in sham versus treated ovaries following an 8 week exposure.

Appendix II

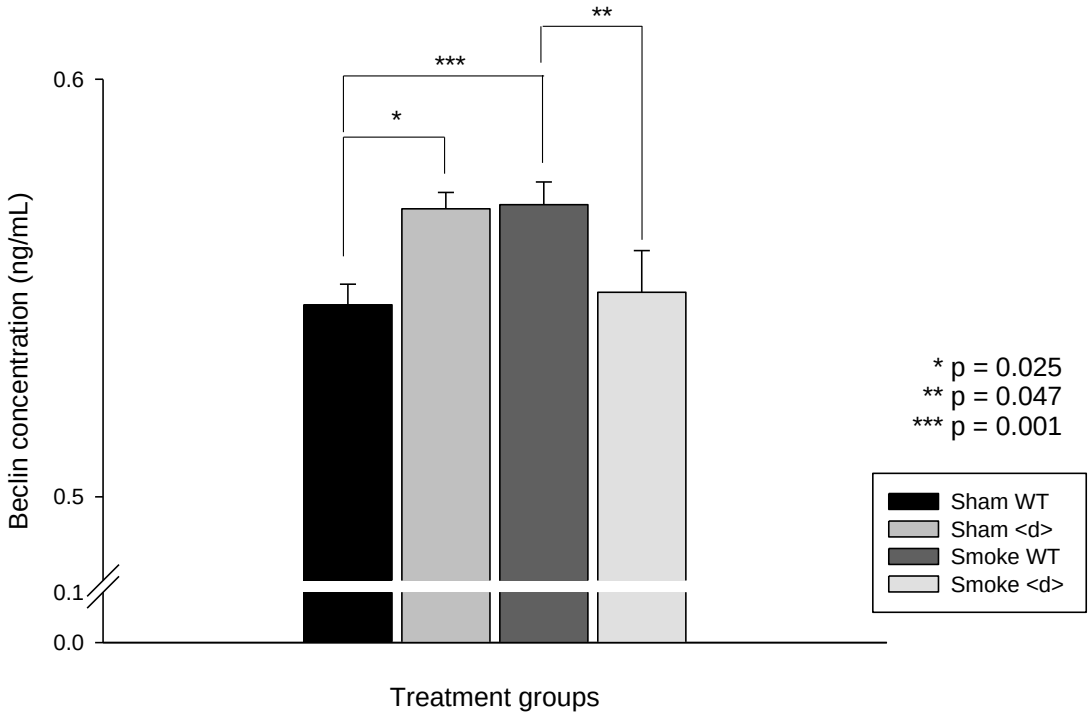

Figure S6: Beclin 1 ELISA.
Changes in BECN1 expression following 8 weeks of sham or cigarette smoke exposure in WT and *AhR*^{d} (<d>) mouse ovaries. There was a significant treatment effect (p = 0.007). Sham WT was significantly lower than both sham <d> (p = 0.02) and smoke WT (p=0.001) but not different from smoke <d>. Smoke WT was different from smoke <d> (p = 0.047). *AhR*^{d} treated ovaries were not different from control *AhR*^{d} ovaries. One-way ANOVA was performed with a Holm-Sidak post hoc test and a p value of less than or equal to 0.05 being considered significant. n = 15 WT, 5 <d> per treatment group.

Appendix III

Figure Permissions

Figure 1: The Wallace-Kelsey model of ovarian reserve
This figure originally appeared in the publication Wallace WH, Kelsey TW. Human ovarian reserve from conception to the menopause. *PLoS One* 2010; 356: 2-12 and is being used herein with the permission of the publisher as outlined in their Creative Commons Attributions License, which can be found at: http://www.plos.org/about/open-access/license/

Figure 4: Folliculogenesis
This figure was adapted and modified from Su,YQ., Wu, X., O'Brien, MJ., Pendola, FL., Denegre, JN., Matzuk, MM. and Eppig, JJ. Synergistic roles of BMP15 and GDF9 in the development and function of the oocyte-cumulus cell complex in mice: genetic evidence for an oocyte-granulosa cell regulatory loop. *Developmental Biology* 2004; 276(1): 64-73 with permission from Elsevier.

ELSEVIER LICENSE
TERMS AND CONDITIONS

Jan 10, 2013

This is a License Agreement between Anne M Gannon ("You") and Elsevier ("Elsevier") provided by Copyright Clearance Center ("CCC"). The license consists of your order details, the terms and conditions provided by Elsevier, and the payment terms and conditions.

All payments must be made in full to CCC. For payment instructions, please see information listed at the bottom of this form.

Supplier	Elsevier Limited The Boulevard,Langford Lane Kidlington,Oxford,OX5 1GB,UK
Registered Company Number	1982084
Customer name	Anne M Gannon
Customer address	27-95 Wendover Drive Hamilton, ON L9C2S8
License number	3065451339344
License date	Jan 10, 2013
Licensed content publisher	Elsevier
Licensed content publication	Developmental Biology

Licensed content title	Synergistic roles of BMP15 and GDF9 in the development and function of the oocyte–cumulus cell complex in mi genetic evidence for an oocyte–granulosa cell regulatory loop
Licensed content author	You-Qiang Su,Xuemei Wu,Marilyn J. O'Brien,Frank L. Pendola,James N. Denegre,Martin M. Matzuk,John J. Eppig
Licensed content date	1 December 2004
Licensed content volume number	276
Licensed content issue number	1
Number of pages	10
Start Page	64
End Page	73
Type of Use	reuse in a thesis/dissertation
Portion	figures/tables/illustrations
Number of figures/tables/illustrations	1
Format	both print and electronic
Are you the author of this Elsevier article?	No
Will you be translating?	No
Order reference number	
Title of your thesis/dissertation	EXPOSURE TO CIGARETTE SMOKE AND ITS IMPACT ON THE OVARIAN FOLLICLE POPULATION: MECHANISMS OF FOLLICLE LOSS
Expected completion date	Feb 2013
Estimated size (number of pages)	250
Elsevier VAT number	GB 494 6272 12
Permissions price	0.00 USD
VAT/Local Sales Tax	0.0 USD / 0.0 GBP
Total	0.00 USD
Terms and Conditions	

INTRODUCTION

1. The publisher for this copyrighted material is Elsevier. By clicking "accept" in connection with completing this licensing transaction, you agree that the following terms and conditions apply to this transaction (along with the Billing and Payment terms and conditions established by Copyright Clearance Center, Inc. ("CCC"), at the time that you opened your Rightslink account and that are available at any time at http://myaccount.copyright.com).

GENERAL TERMS

2. Elsevier hereby grants you permission to reproduce the aforementioned material subject to the terms and conditions indicated.
3. Acknowledgement: If any part of the material to be used (for example, figures) has appeared in our publication with credit or acknowledgement to another source, permission must also be sought from that source. If such permission is not obtained then that material may not be included in your publication/copies. Suitable acknowledgement to the source must be made, either as a footnote or in a reference list at the end of your publication, as follows:
"Reprinted from Publication title, Vol /edition number, Author(s), Title of article / title of chapter, Pages No., Copyright (Year), with permission from Elsevier [OR APPLICABLE SOCIETY COPYRIGHT OWNER]." Also Lancet special credit - "Reprinted from The Lancet, Vol. number, Author(s), Title of article, Pages No., Copyright (Year), with permission from Elsevier."
4. Reproduction of this material is confined to the purpose and/or media for which permission is hereby given.
5. Altering/Modifying Material: Not Permitted. However figures and illustrations may be altered/adapted minimally to serve your work. Any other abbreviations, additions, deletions and/or any other alterations shall be made only with prior written authorization of Elsevier Ltd. (Please contact Elsevier at permissions@elsevier.com)
6. If the permission fee for the requested use of our material is waived in this instance, please be advised that your future requests for Elsevier materials may attract a fee.
7. Reservation of Rights: Publisher reserves all rights not specifically granted in the combination of (i) the license details provided by you and accepted in the course of this licensing transaction, (ii) these terms and conditions and (iii) CCC's Billing and Payment terms and conditions.
8. License Contingent Upon Payment: While you may exercise the rights licensed immediately upon issuance of the license at the end of the licensing process for the transaction, provided that you have disclosed complete and accurate details of your proposed use, no license is finally effective unless and until full payment is received from you (either by publisher or by CCC) as provided in CCC's Billing and Payment terms and conditions. If full payment is not received on a timely basis, then any license preliminarily granted shall be deemed automatically revoked and shall be void as if never granted. Further, in the event that you breach any of these terms and conditions or any of CCC's Billing and Payment terms and conditions, the license is automatically revoked and shall be void as if never granted. Use of materials as described in a revoked license, as well as any use of the materials beyond the scope of an unrevoked license, may constitute copyright infringement and publisher reserves the right to take any and all action to protect its copyright in the materials.
9. Warranties: Publisher makes no representations or warranties with respect to the licensed material.
10. Indemnity: You hereby indemnify and agree to hold harmless publisher and CCC, and their respective officers, directors, employees and agents, from and against any and all

claims arising out of your use of the licensed material other than as specifically authorized pursuant to this license.
11. No Transfer of License: This license is personal to you and may not be sublicensed, assigned, or transferred by you to any other person without publisher's written permission.
12. No Amendment Except in Writing: This license may not be amended except in a writing signed by both parties (or, in the case of publisher, by CCC on publisher's behalf).
13. Objection to Contrary Terms: Publisher hereby objects to any terms contained in any purchase order, acknowledgment, check endorsement or other writing prepared by you, which terms are inconsistent with these terms and conditions or CCC's Billing and Payment terms and conditions. These terms and conditions, together with CCC's Billing and Payment terms and conditions (which are incorporated herein), comprise the entire agreement between you and publisher (and CCC) concerning this licensing transaction. In the event of any conflict between your obligations established by these terms and conditions and those established by CCC's Billing and Payment terms and conditions, these terms and conditions shall control.
14. Revocation: Elsevier or Copyright Clearance Center may deny the permissions described in this License at their sole discretion, for any reason or no reason, with a full refund payable to you. Notice of such denial will be made using the contact information provided by you. Failure to receive such notice will not alter or invalidate the denial. In no event will Elsevier or Copyright Clearance Center be responsible or liable for any costs, expenses or damage incurred by you as a result of a denial of your permission request, other than a refund of the amount(s) paid by you to Elsevier and/or Copyright Clearance Center for denied permissions.

LIMITED LICENSE

The following terms and conditions apply only to specific license types:
15. **Translation**: This permission is granted for non-exclusive world **English** rights only unless your license was granted for translation rights. If you licensed translation rights you may only translate this content into the languages you requested. A professional translator must perform all translations and reproduce the content word for word preserving the integrity of the article. If this license is to re-use 1 or 2 figures then permission is granted for non-exclusive world rights in all languages.
16. **Website**: The following terms and conditions apply to electronic reserve and author websites:
Electronic reserve: If licensed material is to be posted to website, the web site is to be password-protected and made available only to bona fide students registered on a relevant course if:
This license was made in connection with a course,
This permission is granted for 1 year only. You may obtain a license for future website posting,
All content posted to the web site must maintain the copyright information line on the bottom of each image,
A hyper-text must be included to the Homepage of the journal from which you are licensing at http://www.sciencedirect.com/science/journal/xxxxx or the Elsevier homepage

for books at http://www.elsevier.com , and
Central Storage: This license does not include permission for a scanned version of the material to be stored in a central repository such as that provided by Heron/XanEdu.
17. **Author website** for journals with the following additional clauses:
All content posted to the web site must maintain the copyright information line on the bottom of each image, and the permission granted is limited to the personal version of your paper. You are not allowed to download and post the published electronic version of your article (whether PDF or HTML, proof or final version), nor may you scan the printed edition to create an electronic version. A hyper-text must be included to the Homepage of the journal from which you are licensing at
http://www.sciencedirect.com/science/journal/xxxxx . As part of our normal production process, you will receive an e-mail notice when your article appears on Elsevier's online service ScienceDirect (www.sciencedirect.com). That e-mail will include the article's Digital Object Identifier (DOI). This number provides the electronic link to the published article and should be included in the posting of your personal version. We ask that you wait until you receive this e-mail and have the DOI to do any posting.
Central Storage: This license does not include permission for a scanned version of the material to be stored in a central repository such as that provided by Heron/XanEdu.
18. **Author website** for books with the following additional clauses:
Authors are permitted to place a brief summary of their work online only.
A hyper-text must be included to the Elsevier homepage at http://www.elsevier.com . All content posted to the web site must maintain the copyright information line on the bottom of each image. You are not allowed to download and post the published electronic version of your chapter, nor may you scan the printed edition to create an electronic version.
Central Storage: This license does not include permission for a scanned version of the material to be stored in a central repository such as that provided by Heron/XanEdu.
19. **Website** (regular and for author): A hyper-text must be included to the Homepage of the journal from which you are licensing at
http://www.sciencedirect.com/science/journal/xxxxx. or for books to the Elsevier homepage at http://www.elsevier.com
20. **Thesis/Dissertation**: If your license is for use in a thesis/dissertation your thesis may be submitted to your institution in either print or electronic form. Should your thesis be published commercially, please reapply for permission. These requirements include permission for the Library and Archives of Canada to supply single copies, on demand, of the complete thesis and include permission for UMI to supply single copies, on demand, of the complete thesis. Should your thesis be published commercially, please reapply for permission.
21. **Other Conditions**:

If you would like to pay for this license now, please remit this license along with your payment made payable to "COPYRIGHT CLEARANCE CENTER" otherwise you will be invoiced within 48 hours of the license date. Payment should be in the form of a check or money order referencing your account number and this invoice number RLNK500931747.

Once you receive your invoice for this order, you may pay your invoice by credit card. Please follow instructions provided at that time.
Make Payment To:
Copyright Clearance Center
Dept 001
P.O. Box 843006
Boston, MA 02284-3006
For suggestions or comments regarding this order, contact RightsLink Customer Support: customercare@copyright.com or +1-877-622-5543 (toll free in the US) or +1-978-646-2777.

Figure 6: The Apoptosis Pathway.
This figure originally appeared in the publication Bellance, N., Lestienne, P., and Rossignol, R. Mitochondria: from bioenergetics to the metabolic regulation of carcinogenesis. *Frontiers in Bioscience* 2009; 14: 4015-34 and is being used herein with the permission of the publisher as outlined in their Rights and Permissions for Educational Use, which can be found at: http://www.frontbiosci.org/rights-and-permissions

Figure 8: Mechanisms of ROS production by environmental contaminants.
This figure was adapted from Franco, R., Sanchez-Olea, R., Reyes-Reyes, EM., and Panayiotidis, MI. Environmental toxicity, oxidative stress and apoptosis: Ménage à Trois. *Oxidative Stress and Mechanisms of Environmental Toxicity* 2009; 674 (1-2):3-22 with permission from Elsevier.

ELSEVIER LICENSE
TERMS AND CONDITIONS

Jan 17, 2013

This is a License Agreement between Anne M Gannon ("You") and Elsevier ("Elsevier") provided by Copyright Clearance Center ("CCC"). The license consists of your order details, the terms and conditions provided by Elsevier, and the payment terms and conditions.

All payments must be made in full to CCC. For payment instructions, please see information listed at the bottom of this form.

Supplier	Elsevier Limited The Boulevard,Langford Lane Kidlington,Oxford,OX5 1GB,UK
Registered Company Number	1982084
Customer name	Anne M Gannon
Customer address	27-95 Wendover Drive Hamilton, ON L9C2S8
License number	3071510753137

License date	Jan 17, 2013
Licensed content publisher	Elsevier
Licensed content publication	Mutation Research/Genetic Toxicology and Environmental Mutagenesis
Licensed content title	Environmental toxicity, oxidative stress and apoptosis: Ménage à Trois
Licensed content author	Rodrigo Franco,Roberto Sánchez-Olea,Elsa M. Reyes-Reyes,Mihalis I. Panayiotidis
Licensed content date	31 March 2009
Licensed content volume number	674
Licensed content issue number	1–2
Number of pages	20
Start Page	3
End Page	22
Type of Use	reuse in a thesis/dissertation
Portion	figures/tables/illustrations
Number of figures/tables/illustrations	1
Format	both print and electronic
Are you the author of this Elsevier article?	No
Will you be translating?	No
Order reference number	
Title of your thesis/dissertation	EXPOSURE TO CIGARETTE SMOKE AND ITS IMPACT ON THE OVARIAN FOLLICLE POPULATION: MECHANISMS OF FOLLICLE LOSS
Expected completion date	Feb 2013
Estimated size (number of pages)	250
Elsevier VAT number	GB 494 6272 12
Permissions price	0.00 USD
VAT/Local Sales Tax	0.0 USD / 0.0 GBP
Total	0.00 USD
Terms and Conditions	

INTRODUCTION

1. The publisher for this copyrighted material is Elsevier. By clicking "accept" in connection with completing this licensing transaction, you agree that the following terms and conditions apply to this transaction (along with the Billing and Payment terms and conditions established by Copyright Clearance Center, Inc. ("CCC"), at the time that you

opened your Rightslink account and that are available at any time at http://myaccount.copyright.com).

GENERAL TERMS

2. Elsevier hereby grants you permission to reproduce the aforementioned material subject to the terms and conditions indicated.
3. Acknowledgement: If any part of the material to be used (for example, figures) has appeared in our publication with credit or acknowledgement to another source, permission must also be sought from that source. If such permission is not obtained then that material may not be included in your publication/copies. Suitable acknowledgement to the source must be made, either as a footnote or in a reference list at the end of your publication, as follows:
"Reprinted from Publication title, Vol /edition number, Author(s), Title of article / title of chapter, Pages No., Copyright (Year), with permission from Elsevier [OR APPLICABLE SOCIETY COPYRIGHT OWNER]." Also Lancet special credit - "Reprinted from The Lancet, Vol. number, Author(s), Title of article, Pages No., Copyright (Year), with permission from Elsevier."
4. Reproduction of this material is confined to the purpose and/or media for which permission is hereby given.
5. Altering/Modifying Material: Not Permitted. However figures and illustrations may be altered/adapted minimally to serve your work. Any other abbreviations, additions, deletions and/or any other alterations shall be made only with prior written authorization of Elsevier Ltd. (Please contact Elsevier at permissions@elsevier.com)
6. If the permission fee for the requested use of our material is waived in this instance, please be advised that your future requests for Elsevier materials may attract a fee.
7. Reservation of Rights: Publisher reserves all rights not specifically granted in the combination of (i) the license details provided by you and accepted in the course of this licensing transaction, (ii) these terms and conditions and (iii) CCC's Billing and Payment terms and conditions.
8. License Contingent Upon Payment: While you may exercise the rights licensed immediately upon issuance of the license at the end of the licensing process for the transaction, provided that you have disclosed complete and accurate details of your proposed use, no license is finally effective unless and until full payment is received from you (either by publisher or by CCC) as provided in CCC's Billing and Payment terms and conditions. If full payment is not received on a timely basis, then any license preliminarily granted shall be deemed automatically revoked and shall be void as if never granted. Further, in the event that you breach any of these terms and conditions or any of CCC's Billing and Payment terms and conditions, the license is automatically revoked and shall be void as if never granted. Use of materials as described in a revoked license, as well as any use of the materials beyond the scope of an unrevoked license, may constitute copyright infringement and publisher reserves the right to take any and all action to protect its copyright in the materials.
9. Warranties: Publisher makes no representations or warranties with respect to the licensed material.

10. Indemnity: You hereby indemnify and agree to hold harmless publisher and CCC, and their respective officers, directors, employees and agents, from and against any and all claims arising out of your use of the licensed material other than as specifically authorized pursuant to this license.
11. No Transfer of License: This license is personal to you and may not be sublicensed, assigned, or transferred by you to any other person without publisher's written permission.
12. No Amendment Except in Writing: This license may not be amended except in a writing signed by both parties (or, in the case of publisher, by CCC on publisher's behalf).
13. Objection to Contrary Terms: Publisher hereby objects to any terms contained in any purchase order, acknowledgment, check endorsement or other writing prepared by you, which terms are inconsistent with these terms and conditions or CCC's Billing and Payment terms and conditions. These terms and conditions, together with CCC's Billing and Payment terms and conditions (which are incorporated herein), comprise the entire agreement between you and publisher (and CCC) concerning this licensing transaction. In the event of any conflict between your obligations established by these terms and conditions and those established by CCC's Billing and Payment terms and conditions, these terms and conditions shall control.
14. Revocation: Elsevier or Copyright Clearance Center may deny the permissions described in this License at their sole discretion, for any reason or no reason, with a full refund payable to you. Notice of such denial will be made using the contact information provided by you. Failure to receive such notice will not alter or invalidate the denial. In no event will Elsevier or Copyright Clearance Center be responsible or liable for any costs, expenses or damage incurred by you as a result of a denial of your permission request, other than a refund of the amount(s) paid by you to Elsevier and/or Copyright Clearance Center for denied permissions.

LIMITED LICENSE

The following terms and conditions apply only to specific license types:
15. **Translation**: This permission is granted for non-exclusive world **English** rights only unless your license was granted for translation rights. If you licensed translation rights you may only translate this content into the languages you requested. A professional translator must perform all translations and reproduce the content word for word preserving the integrity of the article. If this license is to re-use 1 or 2 figures then permission is granted for non-exclusive world rights in all languages.
16. **Website**: The following terms and conditions apply to electronic reserve and author websites:
Electronic reserve: If licensed material is to be posted to website, the web site is to be password-protected and made available only to bona fide students registered on a relevant course if:
This license was made in connection with a course,
This permission is granted for 1 year only. You may obtain a license for future website posting,
All content posted to the web site must maintain the copyright information line on the bottom of each image,

A hyper-text must be included to the Homepage of the journal from which you are licensing at http://www.sciencedirect.com/science/journal/xxxxx or the Elsevier homepage for books at http://www.elsevier.com , and
Central Storage: This license does not include permission for a scanned version of the material to be stored in a central repository such as that provided by Heron/XanEdu.
17. **Author website** for journals with the following additional clauses:
All content posted to the web site must maintain the copyright information line on the bottom of each image, and the permission granted is limited to the personal version of your paper. You are not allowed to download and post the published electronic version of your article (whether PDF or HTML, proof or final version), nor may you scan the printed edition to create an electronic version. A hyper-text must be included to the Homepage of the journal from which you are licensing at
http://www.sciencedirect.com/science/journal/xxxxx . As part of our normal production process, you will receive an e-mail notice when your article appears on Elsevier's online service ScienceDirect (www.sciencedirect.com). That e-mail will include the article's Digital Object Identifier (DOI). This number provides the electronic link to the published article and should be included in the posting of your personal version. We ask that you wait until you receive this e-mail and have the DOI to do any posting.
Central Storage: This license does not include permission for a scanned version of the material to be stored in a central repository such as that provided by Heron/XanEdu.
18. **Author website** for books with the following additional clauses:
Authors are permitted to place a brief summary of their work online only.
A hyper-text must be included to the Elsevier homepage at http://www.elsevier.com . All content posted to the web site must maintain the copyright information line on the bottom of each image. You are not allowed to download and post the published electronic version of your chapter, nor may you scan the printed edition to create an electronic version.
Central Storage: This license does not include permission for a scanned version of the material to be stored in a central repository such as that provided by Heron/XanEdu.
19. **Website** (regular and for author): A hyper-text must be included to the Homepage of the journal from which you are licensing at
http://www.sciencedirect.com/science/journal/xxxxx. or for books to the Elsevier homepage at http://www.elsevier.com
20. **Thesis/Dissertation**: If your license is for use in a thesis/dissertation your thesis may be submitted to your institution in either print or electronic form. Should your thesis be published commercially, please reapply for permission. These requirements include permission for the Library and Archives of Canada to supply single copies, on demand, of the complete thesis and include permission for UMI to supply single copies, on demand, of the complete thesis. Should your thesis be published commercially, please reapply for permission.
21. **Other Conditions**:

If you would like to pay for this license now, please remit this license along with your payment made payable to "COPYRIGHT CLEARANCE CENTER" otherwise you will be invoiced within 48 hours of the license date. Payment should be in the form of a check

Figure 9: The Autophagy Pathway.
This figure originally appeared in the publication Pyo, J-O., Nah, J., and Jung Y-K. Molecules and their functions in autophagy. *Experimental and Molecular Medicine* 2012; 44(2): 73-80 and is being used herein with the permission of the publisher as outlined in their Creative Commons License, which can be found at:
http://creativecommons.org/licenses/